The Role of Stimulus and Attentional Factors in the Human Optokinetic Response

Kirsten Williams

Thesis submitted to the University of Nottingham
for the degree of Doctor of Philosophy

April 2025

Abstract

The optokinetic response (OKR) is a type of eye movement that plays an essential role in the stabilisation of visual perception. Many studies have investigated the possibility of using the OKR as an objective 'no-report' measure of visual function in both clinical and research settings. However, a greater understanding of the OKR (and its components) and how measures are impacted by various top-down and bottom-up factors is an essential first step for the effective application of OKR as an objective tool. To this end, a series of eye movement studies were carried out to quantify the role of stimulus velocity, motion direction, stimulus eccentricity, instruction type, visual attention and the presence of incongruent motion on the OKR in response to drifting sinusoidal luminance gratings (Experiment 1) and random-dot kinematograms (Experiment 2 and Experiment 3). In Experiment 1, stimulus velocity, motion direction and instruction type (look/stare) were manipulated; results indicated that increasing stimulus velocity and direction of motion away from the horizontal axis reduced the gain of the OKR. Further, reversed OKAN direction was associated with low accuracy of the preceding OKR (low gain and directional inaccuracy), indicating that this reversal may have been caused by adaptation to visual motion during optokinetic stimulation. In Experiment 2, central and peripheral regions of the visual field were stimulated separately and simultaneously with opposing directions of motion, while visual attention was manipulated. This revealed a generalised attentional boost to OKR gain and a crucial role for foveal stimulation in driving high-fidelity OKR. In the absence of central stimulation, increasing peripheral stimulus area did not increase gain. Importantly, generating an OKR to peripheral stimulation was possible in the presence of a central stimulus moving in the opposite direction, when attention was directed to the periphery. This points to an attentional reweighting of the relative contributions of different spatial regions when generating the OKR. Finally, Experiment 3 presented discrete patches of motion stimuli to 27 different spatial locations of the visual field while varying direction of motion and manipulating attention. The results were used to develop detailed maps of OKR gain across the visual field. The data presented in this thesis highlight how OKR is influenced by a wide variety of endogenous and exogenous factors that must be carefully considered in the development of OKR-based objective measures.

Acknowledgements

First and foremost, I would like to thank my supervisors, Paul McGraw, Tim Ledgeway and Denis Schluppeck, for the invaluable support and guidance that they have provided throughout my PhD. It is because of them that completion of my PhD has been a pleasant experience rather than the endless nightmare that so many people describe.

Having completed my undergraduate degree at the University of Nottingham, the vision group have had a monumental impact on my life by fostering a passion for vision science that began in my first year of university eight years ago and that I have carried unwaverlingly ever since. For this, I am forever grateful.

Beyond my supervisory team, the support that I have received from other staff has played a huge role in my development as a researcher. I'd like to thank my internal examiner, Alan Johnston, for providing his valuable insights on my project during annual reviews. And Chris Scholes, for helping me to learn how to analyse eye tracking data and providing me with scripts that made this process easier; I shudder to think what would have happened without his assistance. Similarly, Ljubica Jovanovic patiently supported me in creating my first eye tracking experiment code by sharing her own experiments with me and directing me towards resources that I went on to use throughout my PhD. And I'd like to thank Neil Roach, who (perhaps unfortunately) had an office situated directly opposite to my lab, and as a result became a target for many of my queries.

I must also thank my fellow PhD students who have endured multiple (boring) experiments and who have provided a fulfilling social element to my time as a PhD student. Yalige, Richard, Elliot, Leanne, Matt, Ryan, and the rest of the postgrad community: you are the MVPs. (Plus, a special shoutout to Tanvi, an MSc student who volunteered as my research assistant and collected some data for the final experiment of my PhD, making my life much easier.)

Finally, I want to acknowledge my family and friends. My mum, who has always been almost misguidedly supportive; and my dad, a PhD holder himself, without whom I probably never would have considered doing a PhD (though he did advise against it! *'It's very boring, Kirsten.'*). Importantly, these acknowledgements would be remiss without giving a massive thanks to my partner Joe, who has endured eight years of me studying incessantly and working absurd hours, all while picking up my dishwashing slack and listening to me to talk about vision. Joe, without you I would have spent these years living in a swamp-like hole while eating nothing but beans on toast and cereal.

Glossary of abbreviations

AMD	Age-related macular degeneration	**OKAN-II**	Secondary optokinetic after-nystagmus
AOS	Accessory optic system	**OKR**	Optokinetic response
CEF	Cingulate eye field	**PEF**	Parietal eye field
CI	Confidence interval	**PRN**	Post-rotational nystagmus
C/S	Centre-surround	**RF**	Receptive field
CSF	Contrast sensitivity function	**SD**	Standard deviation
CSP	Cumulative smooth pursuit	**SF**	Spatial frequency
DVM	Delayed visual maturation	**SEF**	Supplementary eye field
EOG	Electro-oculography	**SEM**	Standard error of the mean
EOKR	Early optokinetic response	**SPEM**	Smooth pursuit eye movement
FEF	Frontal eye field	**STS**	Superior temporal sulcus
fMRI	Functional magnetic resonance imaging	**SVFL**	Simulated visual field loss
HOKR	Horizontal optokinetic response	**TN**	Temporonasal
LOKR	Late optokinetic response	**UFOV**	Useful field of view
M	Mean	**V1**	Primary visual cortex / Striate cortex
MAE	Motion after-effect	**V2**	Secondary visual cortex / Prestriate cortex
MRI	Magnetic resonance imaging	**V4**	Visual area four / Extrastriate cortex
MST	Medial superior temporal area	**V5/MT**	Middle temporal area
NOT	Nucleus of the optic tract	**V6**	Medial motion area / Dorsomedial area
NT	Nasotemporal	**VFL**	Visual field loss
OFR	Ocular following response	**VOKR**	Vertical optokinetic response
OKAN	Optokinetic after-nystagmus	**VOR**	Vestibular-ocular reflex
OKAN-I	Primary optokinetic after-nystagmus	**VSM**	Velocity storage mechanism

Table of Contents

Chapter 1

General Introduction

1.1 What is an optokinetic response?

As we move in an environment, full field visual motion is induced. Such motion poses a challenge for the visual system, as visual quality is impaired by the presence of retinal motion. For example, retinal motion is associated with motion smear due to the temporal window over which visual signals are integrated (Bedell et al., 2010; Burr, 1980), with the length of this temporal window varying based on stimulus size and light intensity (Barlow, 1958). Consequently, there are several mechanisms for stabilising retinal motion. In humans, this is

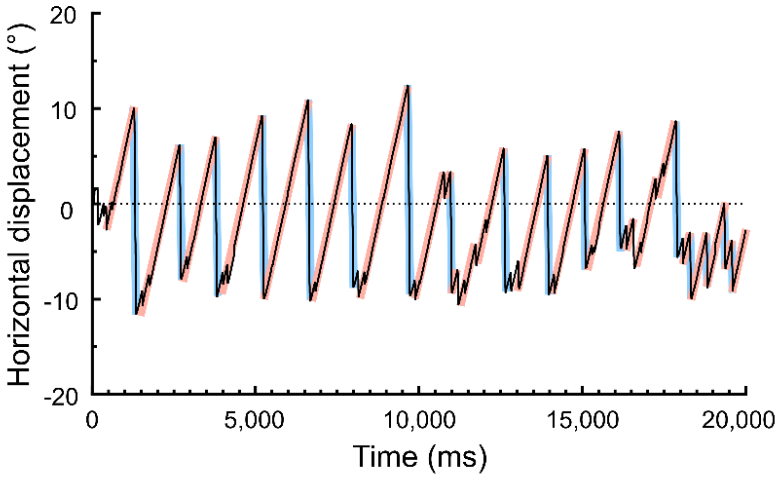

Figure 1.1: Example OKR trace showing horizontal gaze displacement over time, with slow phases highlighted in red and fast phases highlighted in blue. On the Y axis, positive degrees represent the right side of the display while negative degrees represent the left side of the display. The dashed line represents the midline of the display. This trace shows an OKR in response to a rightward drifting black and white sinusoidal grating stimulus during Experiment 1, under 'Look OKR' conditions.

achieved through a combination of vestibular-ocular reflex (VOR), smooth pursuit eye movements (SPEM) and optokinetic response (OKR) (Collewijn, 1985).

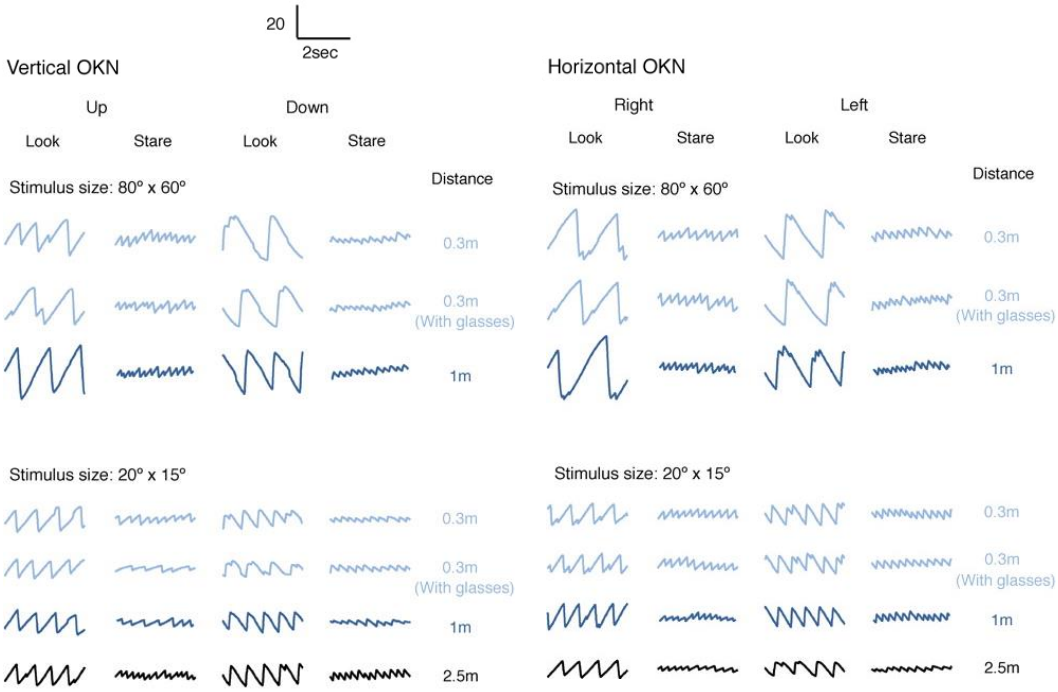

Figure 1.2: Adapted from Knapp et al. (2009). OKR eye movement traces in response to vertical (left) and horizontal (right) stimulus motion and two different stimulus sizes, illustrating the dramatic difference in amplitude and frequency between look and stare OKR, as well as between different motion directions and stimulus sizes. 'Distance' refers to the viewing distance of the stimulus. Note the dramatic difference in frequency and amplitude between look and stare OKR, which varies across motion direction, stimulus size and viewing distance conditions.

OKR typically involves a series of back-and-forth binocular eye movements known as optokinetic nystagmus, which alternate between a 'slow' phase and a 'fast' phase to produce a sawtooth waveform (Figure 1.1). The slow phase is a pursuit eye movement, during which gaze attempts to match the speed and direction of the stimulus to hold the image relatively still on the retina. The fast phase is a saccade-like eye movement moving in the opposite direction to the

slow phase; this prevents the slow phase from driving the eye to its mechanical limit (Garbutt & Harris, 1999). Each slow phase and following fast phase together constitute one nystagmus 'beat'. In research, OKR is generally characterised by its slow phase gain (ratio of slow phase velocity to stimulus velocity), amplitude (physical length of the slow phase) and frequency (number of nystagmus beats within a given timeframe) (Collewijn, 1985; Frattini & Wibble, 2021; Garbutt & Harris, 1999). While OKR is generally described as being reflexive (Carpenter, 1988, p. 39), OKR in humans is known to be affected by top-down influences such as attention (Kanari et al., 2017) and task instruction (Pola & Wyatt, 1985).

There are several types of OKR which will be covered throughout this chapter. OKR has both an early and a late component: early OKR (EOKR) has a rapid build-up (Abadi et al., 1994) and dominates in humans with normal vision (Garbutt & Harris, 1999); late OKR (LOKR) has a slow build-up and dominates in animals with poor or absent foveal vision (Collewijn, 1972), though it is present in humans (Garbutt & Harris, 1999). LOKR is also associated with a slow decay of nystagmus following termination of the stimulus, known as optokinetic after-nystagmus (OKAN) (Collewijn, 1985). The task instructions provided to observers are able to affect the OKR produced. If observers are instructed to fixate and follow features of the moving stimulus, 'look' OKR will be produced, whereas instructing observers to passively gaze at the stimulus produces 'stare' OKR (Pola & Wyatt, 1985). Look OKR is associated with high amplitude, low frequency eye movements and stare OKR is associated with low amplitude, high frequency eye movements (Honrubia et al., 1968; Knapp et al., 2008; Valmaggia et al., 2005). Amplitude and frequency of OKR vary with stimulus size, direction of motion (Knapp et al., 2009) and velocity (Abadi et al., 2005; Murasugi & Howard, 1989b; Valmaggia et al., 2005), however, the amplitude of look OKR is often at least double that of stare OKR, and the frequency of stare OKR is often at least double that of look OKR (Knapp et al., 2008, 2009; Valmaggia et al., 2005) (Figure 1.2).

1.2 Neural substrates of the OKR

Early OKR research investigating afoveate animals such as the rabbit showed that, in such animals, OKR has a directional preponderance whereby it is only produced in response to stimuli drifting in a temporonasal (TN) direction. In contrast, foveate animals such as humans produce OKR in both directions (Tauber & Atkin, 1968). Such research highlights the existence of different pathways for producing OKR. Whereas the unidirectional OKR seen in afoveate animals may be mediated by a subcortical pathway, the bidirectional OKR observed in humans may be so due to involvement of an additional cortical pathway (Garbutt & Harris, 1999).

The subcortical pathway involves the accessory optic system (AOS), including the pretectal nucleus of the optic tract (NOT) (in the macaque monkey: Büttner-Ennever et al., 1996; in the mouse: Dhande et al., 2013; Leigh & Zee, 2015). In the macaque monkey, retinal slip (relative motion of the stimulus across the retina), the stimulus for producing OKR, is encoded by contralateral retinal afferents to the AOS, with different AOS nuclei responding to different directions of motion (Leigh & Zee, 2015; Mustari et al., 1994). Research conducted using macaque monkeys has shown that, in primates, the retina, V1, MT and MST input to the NOT (Distler et al., 2002; Distler & Hoffmann, 2001), which encodes retinal error position, acceleration and velocity (Das et al., 2001). In cats, the cells of the NOT have been shown to provide direction-selective signals about retinal slip during OKR (Hoffmann & Huber, 1983), and in afoveate animals, have been shown to respond only to TN stimuli (Collewijn, 1985), indicating that the asymmetrical OKR seen in such animals is driven by this subcortical pathway. However, the NOT also plays a role in generating OKR in foveate animals: in monkeys, lesions of the NOT impair smooth pursuit and OKR slow phases in the direction of the lesioned hemisphere (Cohen et al., 1990; Kato et al., 1988) and electrical stimulation of the NOT produces nystagmus with ipsilateral slow phases (Cohen et al., 1990; Fuchs & Mustari, 1993). Thus, evidence from non-human animals suggests that the AOS and NOT play an important role in the encoding of retinal slip signals and producing pursuit eye movements.

In humans, a cortical pathway forms a major contribution to the generation of pursuit eye movements. This pathway runs from the human homologues

of MT, MST (MT+) and the frontal eye fields (FEF) to the pontine nuclei and the cerebellum (Leigh & Zee, 2015). Unlike afoveate animals, humans show a rapid build-up of slow phase velocity during OKR (Abadi et al., 1994). This rapid build-up may be due to involvement of the smooth pursuit system and the ocular following response (OFR) in human OKR (Leigh & Zee, 2015). Lesion studies and single-cell recordings from monkeys show that MST neurons are important in generating this OFR (Takemura et al., 2002; Takemura & Kawano, 2002). All of the cortical eye fields have been implicated in human OKR (Ruehl et al., 2019). In an fMRI study of human look OKR, Ruehl et al. (2019) reported that during OKR, the FEF, which is involved in the allocation of spatial attention and saccade generation (Blanke et al., 2000; Dieterich et al., 2003; Everling, 2007; Pierrot-Deseilligny et al., 2004), formed a functional subcluster with the parietal eye field (PEF), which is involved in visual attention and visually-guided saccades (Brotchie et al., 2003; Büchel et al., 1998). The FEF also formed a functional subcluster with the cingulate eye field (CEF), supplementary eye field (SEF) and V6, which has a strong response to optic flow fields and peripheral motion and is involved in processing of egomotion (Cardin & Smith, 2011; Pitzalis et al., 2010), making it a region well suited to respond to optokinetic stimuli.

The cortical pathway may be responsible for producing the bidirectional OKR seen in humans. At birth, human OKR is asymmetrical, resembling that of an afoveate animal; however, by the age of six months, it is usually symmetrical (Garbutt & Harris, 1999). This initial asymmetry is thought to be a result of dominance of the subcortical pathway at birth. As the cortical pathways mature, they become dominant in OKR production, resulting in symmetrical OKR (Leigh & Zee, 2015). Development of OKR symmetry and of binocularity may be linked; disrupting the development of normal binocular function, such as by strabismus (fixational misalignment of the two eyes), is associated with persistence of OKR asymmetry (Valmaggia et al., 2005). This indicates that the subcortical pathway may have a larger contribution to the OKR in these individuals (Leigh & Zee, 2015) and points to a role of binocular cells in producing bidirectional OKR. While the NOT is still directionally selective in foveate animals, data obtained from cats has led to the suggestion that there is an indirect route to the NOT via the binocular cells of the visual cortex in such animals (Hoffmann, 1982; Montarolo et al., 1981), allowing it to respond to both NT and TN stimuli. Animals

with stereopsis (the ability to use the disparity between the inputs to two eyes with overlapping visual fields to encode depth and distance), such as monkeys and cats, have been found to have higher OKR gain than those without, which may be a result of the stereoscopic system supplementing inputs to the pretectum (Hoffmann, 1982; Hoffmann & Distler, 1986; Montarolo et al., 1981).

The retinal slip signal encoded by the AOS and NOT is thought to play a key role in determining slow phase velocity during OKR. Researchers have studied the OKR in non-human animals using open-loop conditions such as by immobilising the viewing eye while recording eye movements from the mobile non-viewing eye. The result is a slow phase that steadily increases in velocity until its speed is many times greater than that of the stimulus, an effect that has been demonstrated in both monkeys and rabbits (Koerner & Schiller, 1972; Ter Braak, 1936). This effect occurred in a stepwise manner, increasing from slow phase to slow phase rather than involving increases of velocity within phases. This indicates that, under normal viewing conditions, retinal slip is an important determinant of slow phase velocity.

1.3 Time course of the OKR

OKR has at least two components which have different time courses: early OKR (EOKR) and late OKR (LOKR) (Garbutt & Harris, 1999). OKR is also associated with an after-effect known as optokinetic after-nystagmus (OKAN) (Figure 1.3) which can be observed when an optokinetic stimulus is terminated in complete darkness (Collewijn, 1985). EOKR and LOKR are thought to be mediated by different pathways (Fuchs & Mustari, 1993; Collewijn, 1972; Garbutt & Harris, 1999), while OKAN is thought to be related to the LOKR component (Lafortune et al., 1986b; Garbutt & Harris, 1999; Fuchs & Mustari, 1993; Cohen et al., 1981). These components may optimally operate at different stimulus velocities; Lafortune et al. (1986b) reported that EOKR was most active in the 10-30 deg/s range whereas LOKR, evident via OKAN magnitude, was most active in the 40-70 deg/s range.

1.3.1 Early OKR

EOKR is associated with a rapid build-up of slow phase velocity which reaches the stimulus velocity in approximately five seconds (Abadi et al., 1994). Though humans exhibit both EOKR and LOKR, EOKR tends to dominate under photopic light levels and is associated with a rapid drop-off of slow phase velocity following termination of the stimulus (Garbutt & Harris, 1999). EOKR is not seen in afoveate animals, such as rabbits (Collewijn, 1972), whereas monkeys show well-developed EOKR and LOKR (Cohen et al., 1977). EOKR is thought to be mediated by a cortical pathway similar to that of smooth pursuit eye movements (SPEM) (Fuchs & Mustari, 1993).

1.3.2 Late OKR

Contrary to EOKR, LOKR is associated with a gradual build-up of slow phase velocity (Garbutt & Harris, 1999). LOKR dominates in animals with poor or absent foveal vision, such as the rabbit (Collewijn, 1972), and has also been found to dominate in humans with certain conditions, including maldeveloped foveae (Baloh et al., 1980a), hereditary cerebellar ataxia (Zee et al., 1976) and parietal lobe lesions (Baloh et al., 1980b, 1982). LOKR is thought to be mediated by a subcortical pathway, with the NOT playing a key role: in monkeys, LOKR does not recover following large NOT lesions and electrical stimulation of the NOT produces eye movements resembling LOKR and OKAN (Fuchs & Mustari, 1993).

1.3.3 Optokinetic after-nystagmus

When an optokinetic stimulus is terminated in a completely dark environment, there is sometimes a gradual decay of the slow phase velocity. This persistence of nystagmus after stimulus termination is known as optokinetic after-nystagmus (OKAN) (see Figure 1.3). OKAN often follows the direction of the preceding OKR (OKAN-I). After a variable amount of time, this may be replaced by a nystagmus that is reversed in direction with respect to the preceding OKR (OKAN-II) (Collewijn, 1985).

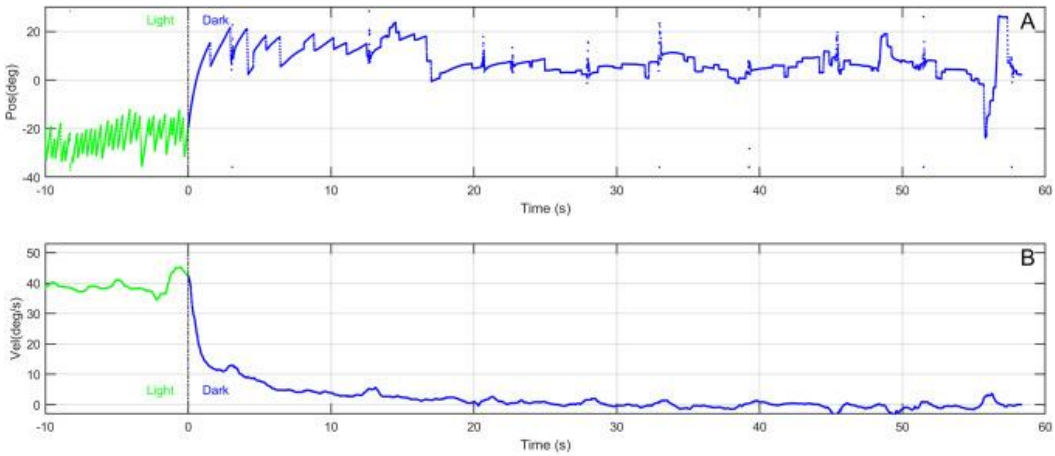

Figure 1.3: From Bertolini et al. (2021). UPPER: Eye movement trace showing gaze displacement over time, demonstrating OKR occurring during stimulation (green) followed by OKAN occurring in dark conditions (blue) before eventually decaying. LOWER: Plot showing eye velocity over time during stimulation (green) and in dark conditions (blue) showing the decay of eye movement velocity following termination of the stimulus.

OKAN is associated with the activity of the vestibular system, highlighting its functional proximity to the optokinetic system. Studies using humans and monkeys have shown that during OKR, information about velocity is stored by the velocity storage mechanism (VSM) of the vestibular nuclei of the brainstem; after OKR, the discharge of this stored activity produces OKAN (Cohen et al., 1981; Collewijn, 1985; Katz et al., 1991; Leigh & Zee, 2015). Consequently, vestibular damage affects OKR and OKAN. In humans, unilateral dysfunction of the vestibular labyrinth can cause OKAN to be diminished, whereas bilateral dysfunction can completely eradicate OKAN (Ireland & Jell, 1982). This indicates that OKAN relies on bilateral vestibular input. Further evidence of the link between OKR, OKAN and the vestibular system comes from monkey research showing that there is an adapting influence of VOR on both LOKR and OKAN (Lisberger et al., 1981) and evidence that post-rotational (vestibular) nystagmus is able to counteract OKAN in humans (Barratt & Hood, 1988). Such evidence

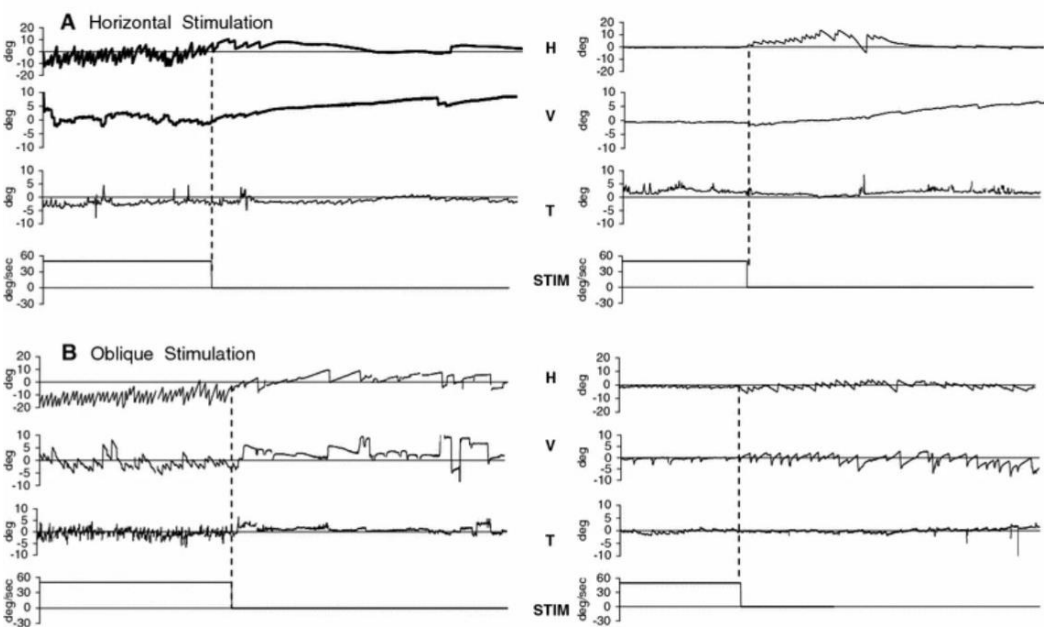

Figure 1.4: From Ventre-Dominey and Luyat (2009). Eye movement traces showing gaze displacement over time during optokinetic stimulation without a fixation cross and the following OKAN (left) compared to during fixation of a cross during optokinetic stimulation and the following OKAN (right). Stimulation is with horizontal (upper, A) and oblique (lower, B) motion. H, V and T correspond to the displaying of horizontal, vertical and torsional eye movement, respectively. Note the occurrence of OKAN-II immediately following fixation without the occurrence of OKR.

highlights that LOKR in particular is associated with OKAN, and as such, OKAN is sometimes used in research as an indicator that LOKR has occurred (e.g. Lafortune et al., 1986a).

As a feature of the LOKR component, OKAN can be seen following stimulation at a velocity which maximally stimulates the LOKR pathway. Lafortune et al. (1986b) found that OKAN magnitude in humans was highest following stimulus velocities in the 40-70 deg/s range. Using a 60 deg/s stimulus, Cohen et al. (1981) found that human OKAN has a slow phase velocity of up to 15-20 deg/s. In contrast, the OKAN of monkeys can reach velocities of 90-120 deg/s (Cohen et al., 1977), highlighting the presence of inter-species differences between the optokinetic systems of human and non-human primates; it is suggested

that activity of the LOKR component, and therefore of the VSM, is lower in humans (Cohen et al., 1981).

OKAN does not necessarily consistently follow the same direction as the preceding OKR; it can present with a reversed slow phase direction with respect to the stimulus. There are many speculated causes of these reversals. There may be a relationship between stimulus velocity and OKAN direction, with low stimulus velocities producing OKAN-I and high stimulus velocities producing the reversed OKAN-II (Collewijn, 1985). Stimulus duration has also been reported to contribute. Gygli et al. (2021) used a range of stimulus durations, finding that five of their 11 observers showed OKAN-II in 70% of trials that used prolonged (3, 5 and 10 minutes) stimulation, but only in 10% of trials that used briefer 30-second stimuli. Brandt et al. (1974) also reported OKAN-II following prolonged stimulation (3 and 15 minutes), which they explained as being a form of motion habituation. They suggested that if the 'habituative countercharge' from the stimulus outweighs the remaining 'optokinetic charge', the OKAN direction will reverse. Similarly, suppression of OKR during full-field stimulation has been reported to produce OKAN-II. Ventre-Dominey and Luyat (2009) used a fixation cross to suppress OKR, observing OKAN-II immediately afterwards (Figure 1.4). They speculated that this may have resulted from the suppression of pursuit signals and asymmetrical activity of the VSM. The occurrence of OKAN following OKR suppression indicates that an optokinetic response may not be necessary for OKAN to occur; information relating to visual input, without an oculomotor output, is sufficient to produce OKAN. This suggests that the visual input may be responsible for velocity storage rather than the OKR itself. However, it may be the case that OKAN-II is caused by a different mechanism to OKAN-I; it has been suggested that rather than being associated with VSM activity, as is the case in OKAN-I, OKAN-II may be independent of OKAN-I, instead being caused by motion adaptation (Chen et al., 2014; Gygli et al., 2021).

Studying OKAN, particularly OKAN-II, is very challenging in humans due to their weak and inconsistent OKAN (Gygli et al., 2021). Gygli et al. (2021) obtained OKAN-II data from five of their 11 participants; six of their participants did not produce OKAN-II. Koenig and Dichgans (1981) used one minute of stimulation at 30, 60, 90, 120 and 180 deg/s, reporting that four participants showed no OKAN-II. Brantberg (1992) also used one minute of stimulation with two

stimulus velocities, reporting OKAN-II during three trials in one out of 16 participants. Nooij et al. (2018) reported OKAN-II in 24% of trials that followed 60 deg/s stimulation; however, these trials were all accounted for by just four of their 13 participants. Clearly, there are large individual differences in the occurrence of OKAN-II, with many experiments reporting it in less than half of observers, making it a very challenging area of research. As a result, OKAN reversal is not fully understood.

1.4 The role of the vestibular system

Though OKR is produced by visual input, the vestibular system is known to be involved in the response. The importance of the vestibular system in OKR is exemplified by the effects of labyrinthectomy, which has been shown to reduce both the gain and frequency of OKR and to reduce or eradicate OKAN (Cohen et al., 1973). This is thought to be due to the activity of the VSM, which stores activity related to velocity during optokinetic stimulation (Cohen et al., 1981).

There is behavioural evidence of the link between OKR and the vestibular system. While vestibular stimulation produces post-rotational nystagmus (PRN), OKAN is able to counteract it (Barratt & Hood, 1988). Further, optokinetic stimuli can be used to predictably modulate PRN (Cohen et al., 1981). This evidence suggests that visual and vestibular inputs are integrated in producing these nystagmic responses. The vestibular influence on OKR appears to be greater in the LOKR system compared to the EOKR system. Lisberger et al. (1981) found that adapting monkeys towards a VOR gain of zero affected LOKR gain in parallel, as well as affecting the OKAN charging time constant, but it did not affect EOKR gain. They argued that this shows that the signals responsible for producing OKAN access the VOR pathways prior to reaching the variable gain elements responsible for VOR adaptation, with these variable gain elements located between the sites at which LOKR and EOKR mechanisms access the oculomotor pathways.

There is also neurophysiological evidence of this relationship obtained from non-human primate studies. Neurons of the vestibular nuclei of monkeys have been shown to respond to both head rotation and optokinetic stimulation

(Henn et al., 1974; Waespe & Henn, 1977). When optokinetic stimulation is terminated in a dark environment, these vestibular nucleus neurons continue to discharge for a brief time (Waespe & Schwarz, 1986), producing OKAN. Such evidence provides confirmation of the influence of optokinetic visual input upon vestibular nucleus output. However, it should be noted that the VSM of the vestibular nuclei is thought to play less of a role in human OKR compared to that of monkeys, with human OKR being driven primarily by the EOKR system (Cohen et al., 1981).

1.5 Effect of stimulus eccentricity

Many aspects of visual performance are superior in the central visual field, with increasing eccentricity having a detrimental effect. These eccentricity effects in vision are generally attributed to physiological differences between the central and peripheral visual field. Central vision has superior acuity (Anstis, 1998), contrast sensitivity (Virsu & Rovamo, 1979) and colour sensitivity (Hansen et al., 2009). More eccentric regions of the retina have lower ganglion cell density (Curcio & Allen, 1990) and photoreceptor density (Curcio et al., 1990). These differences are reflected at higher levels of visual processing; for example, the fovea is significantly over-represented in V1, as shown by Azzopardi and Cowey (1996) in the macaque monkey. Eccentricity effects also impact motion perception, with past research showing that increasing stimulus eccentricity is associated with lower perceived speed (Johnston & Wright, 1986; Tynan & Sekuler, 1982). By extension, one might expect to see eccentricity effects in the OKR.

Past research has generally confirmed central superiority in driving the OKR and a detrimental effect on gain resulting from occlusion of the centre. Howard and Ohmi (1984) equated central and peripheral sinusoidal luminance grating stimuli for visibility and contrast, finding that central superiority in driving OKR remained. From this, they concluded that this central superiority is not a consequence of lower visibility in the visual periphery. However, the periphery was able to drive the OKR by itself. With the centre occluded, the peripheral stimulus was able to produce an OKR, even when participants were instructed to attend to the central occlusion (Howard & Ohmi, 1984). Consequently, Howard and Ohmi (1984) concluded that attention to the periphery is not required for an

OKR in response to the periphery, but OKR in response to the centre has higher gain. Similarly, other studies have reported that central occlusion reduced the gain of OKR (Abadi & Pascal, 1991; Cheng & Outerbridge, 1975; Murasugi et al., 1986; van Die & Collewijn, 1982). Though attention is not required to produce a peripheral OKR (Howard & Ohmi, 1984), it has been reported to facilitate it (Dubois & Collewijn, 1979). Collewijn (1985) argued that this is a result of attention reweighting the relative contributions of different retinal locations towards oculomotor responses. Unfortunately, attention was not precisely manipulated in these studies; participants have instead simply been instructed to direct attention towards the peripheral stimulus (Dubois & Collewijn, 1979; Howard & Gonzalez, 1987).

Some studies have reported a velocity-based effect of occluding the centre. Howard and Ohmi (1984) and Valmaggia et al. (2001) both reported that the detrimental effects on gain of central occlusion only occurred in response to stimulus velocities above 30 deg/s. However, others have reported responses to velocities both above and below 30 deg/s being affected (van Die and Collewijn, 1982, 1986).

Several methodological issues have been identified by studies attempting to mask the central visual field for OKR research. A central patch surrounded by motion can appear to move in opposition to the peripheral motion, resulting in an OKR with a reversed direction with respect to the stimulus (Wyatt & Pola, 1984). A mask may also act as a stationary object within the moving field, which

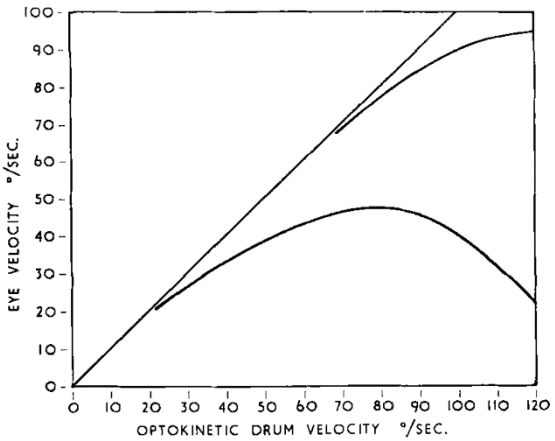

Figure 1.5: From Hood (1967). Curves showing the relationship between stimulus velocity and slow phase eye velocity. The upper curve shows the response from a participant with unilateral central scotoma; the lower curve shows the response from a participant with normal vision.

can suppress OKR by providing a fixation point (Murasugi et al., 1986). As a result, the proximity of the stationary edge of the mask to the fovea may have a larger effect on the OKR than the area of the stimulus or the mask (Carpenter, 1988). These factors make investigating peripheral OKR by using central masking challenging. Howard and Ohmi (1984) noted that the use of clear, stationary edges in central masks may cause them to suppress OKR; they created a mask with blurred edges and adjusted the peripheral stimulus in terms of contrast and spatial frequency to match central and peripheral stimulus visibility. Despite these modifications, they still reported lower gain in response to peripheral stimuli moving at speeds greater than 30 deg/s.

In contrast to the findings obtained via central masking, early reports of OKR in central scotoma patients yielded very different results, with Hood (1967, 1975) reporting high gain OKR up to a stimulus velocity far exceeding that seen in normal observers (Figure 1.5), successfully tracking stimuli at 90 deg/s. Gresty and Halmagyi (1979) were later able to replicate this result using an artificial scotoma. Hood (1967) attributed this effect to the role of LOKR in peripheral OKR, arguing that the observed high-gain OKR was mediated by the subcortical pathway as the OKR had been released of the constraints of central (and thus cortical) influence. However, this finding has not been consistently replicated, with both real and artificial scotoma studies reporting a reduction in gain (Cheng & Outerbridge, 1975; Dubois & Collewijn, 1979; Valmaggia et al., 2001; van Die & Collewijn, 1982) and van Die and Collewijn (1982) reporting that the effect on gain was similar in both central scotoma patients and central masking in visually normal observers.

The size of an occluder required to affect OKR is also contested. Valmaggia et al. (2001) investigated central scotoma patients, reporting that OKR gain was only affected in observers with central scotomas larger than 20 deg whereas observers with smaller scotomas were not different to controls. In contrast, van Die and Collewijn (1982) reported than removing even the central 5 deg was sufficient to lower gain. Valmaggia and Gottlob (2002) noted that we might expect to see differences in performance as a result of artificial masking and real scotoma, as patients with scotoma may experience 'filling in' of the optokinetic stimulus. However, van Die and Collewijn (1982) reported that, whether

the scotoma was real or artificial, the effect of central occlusion on gain was comparable.

Overall, the available evidence suggests that removal of central stimulation, either by artificial masking or by scotoma, has a detrimental effect on OKR gain.

1.6 Top-down influences on the OKR

1.6.1 Effect of task instruction: Look and stare OKR

OKR in humans appears to have both voluntary and reflexive components which can be brought out by varying the instructions given to observers. When an observer is told to actively pursue features of the moving stimulus, look OKR is produced; when an observer is told to passively gaze towards the stimulus,

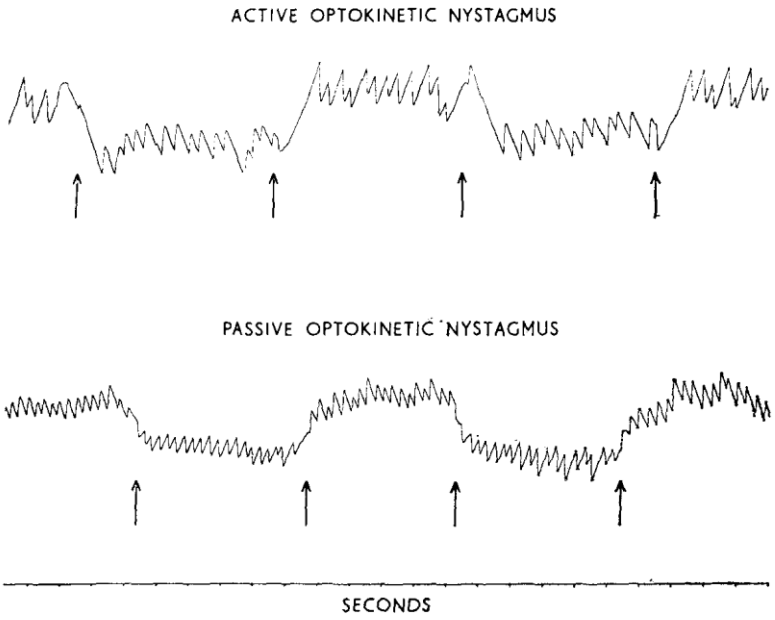

Figure 1.6: From Hood and Leech (1974). Traces showing gaze displacement during look ('active') OKR and stare ('passive') OKR, with arrows indicating the location of a reversal of stimulus motion (striped optokinetic drum) direction. Note the difference in OKR frequency and amplitude between the two conditions, and the difference in phase type leading the direction changes.

stare OKR is produced (Pola & Wyatt, 1985). Look OKR is generally described as having high amplitude, low frequency movements, whereas stare OKR is described as having low amplitude, high frequency movements (Honrubia et al., 1968; Knapp et al., 2008; Valmaggia et al., 2005).

Pola and Wyatt (1985) reported that 'active' (look) OKR had higher amplitude, gain and phase lag compared to 'passive' (stare) OKR. Increasing the stimulated area resulted in higher gain for both look and stare OKR, which they argued implicates shared oculomotor systems. They described a foveal tracking system which responds to target position and is under voluntary control and an optokinetic system which responds to target velocity and is reflexive. As stare OKR could be induced using peripheral stimuli, they suggested that this must represent a response to target velocity; in contrast, they suggested that look OKR is more related to the foveal tracking system. By their account, these two systems run in parallel and converge prior to a common integrator.

Hood and Leech (1974) showed that look and stare OKR differ in their response to a change of stimulus motion direction as well as in their tendency to produce a perception of self-motion. During look OKR, a change of motion direction enacted by reversing the direction of a striped optokinetic drum resulted in a deviation of the eyes towards the direction of drum rotation followed by a re-centring by the fast phase. In contrast, a direction change during stare OKR was associated with a deviation of the eyes away from the direction of drum rotation followed by a re-centring by the slow phase (Figure 1.6). They argued that this may reflect a difference in the function of the fast phase between look and stare OKR. Additionally, it was reported that the illusion of self-motion induced by the optokinetic stimulus was reduced during look OKR conditions. This finding implies that stare OKR is associated with more vestibular activity than look OKR, which may be due to the higher frequency of stare OKR causing greater activity of the VSM (Frattini & Wibble, 2021).

Look OKR may allow for tracking of stimuli to a higher velocity. Honrubia et al. (1968) found that during look OKR, observers had a large slow phase amplitude which remained relatively constant as stimulus velocity increased, though eye movement frequency increased linearly with stimulus velocity. During this condition, observers were capable of closely pursuing striped optokinetic drum stimuli up to a velocity of 60 deg/s. In contrast, when stimulus velocity

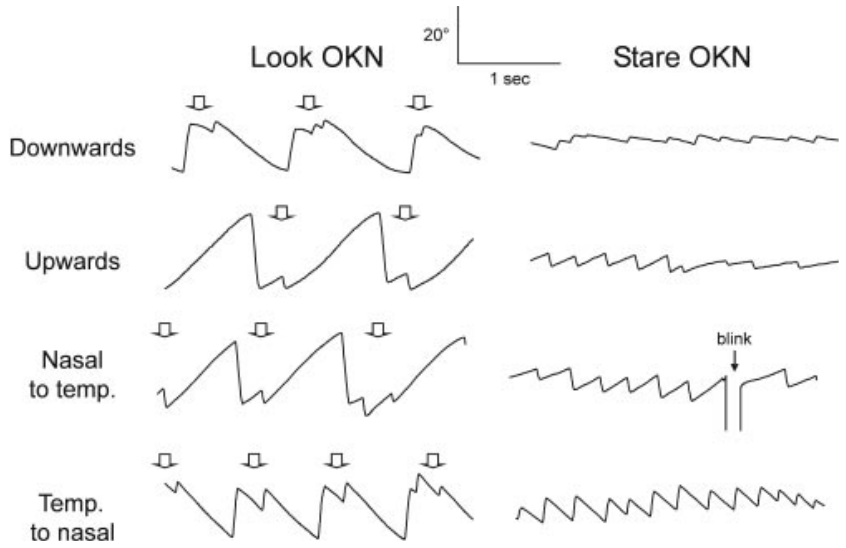

Figure 1.7: From Knapp et al. (2008). Look (left) and stare (right) OKR traces showing displacement of gaze in response to upward, downward, NT and TN motion. White arrows on look OKR traces indicate the location of stare OKR breakthrough within the look OKR trace.

was increased during stare OKR, OKR frequency increased in a non-linear fashion, reaching asymptote at a stimulus velocity of 40 deg/s. Consequently, look OKR was associated with high gain OKR up to a higher stimulus velocity compared to stare OKR. From this, Honrubia et al. (1968) argued that look and stare OKR should be considered to be mediated by separate mechanisms.

Like Honrubia et al. (1968), Valmaggia et al. (2005) reported velocity-based differences between look and stare OKR in response to striped stimuli. They showed that look OKR gain was higher than that of stare OKR in response to horizontally moving stimuli at 45 deg/s and 60 deg/s, and in response to vertically moving stimuli at 30 deg/s, 45 deg/s and 60 deg/s. This result demonstrates that stare OKR gain is able to match that of look OKR up to a higher velocity in response to horizontal compared to vertical motion. Increasing stimulus velocity decreased gain for both look and stare OKR, an effect that was largest for vertical stare OKR and smallest for horizontal look OKR, showing that stare OKR in response to vertically moving stimuli is particularly impacted by high stimulus velocity. The data of both Valmaggia et al. (2005) and Honrubia

et al. (1968) highlight that as stimulus velocity increases, the differences between look and stare OKR become more apparent. Valmaggia et al. (2005) suggested that these differences may be a consequence of different contributions from cortical and subcortical systems in look and stare OKR, as look OKR may involve the smooth pursuit system. Similarly, Garbutt and Harris (1999) posited that the differences between look and stare OKR may be caused by involvement of SPEM in look OKR.

fMRI has been used to investigate differences between look and stare OKR. Kashou et al. (2010) reported that look OKR was associated with higher levels of cortical activation compared to stare OKR, particularly in limbic, occipital and parietal lobes. They concluded that look OKR instructions are associated with a response that has more activation sites compared to stare OKR. Konen et al. (2005) also reported higher cortical activation during look OKR. They described the strength of the BOLD response as being reflective of the degree to which the eye movements were voluntary.

Maintaining look OKR requires more active effort on part of the observer compared to stare OKR, and as a result, lapses in look OKR are often reported. Stare OKR occurs during these lapses, highlighting its more reflexive nature (Figure 1.7). This stare OKR breakthrough during look OKR conditions has been reported by many researchers (Hood & Leech, 1974; Knapp et al., 2008; Pola & Wyatt, 1985). Hood and Leech (1974) suggested that the effort required for the observer to continually select and fixate features of the moving stimulus makes look OKR difficult to sustain for long periods of time, causing stare OKR to occur due to lapses in the observer's ability to maintain it. Additionally, any residual retinal motion resulting from imperfect gain may act as a trigger for stare OKR to occur. Hood and Leech (1974) argued that the tendency for stare OKR breakthrough to occur during look OKR conditions is indicative of look and stare OKR involving different underlying mechanisms. Knapp et al. (2008) also reported stare OKR breakthrough during look OKR conditions, noting that these lapses tend to occur immediately after the fast phase, a possible consequence of the observer being unable to instantly select a new feature of the stimulus to track; the result is stare OKR occurring reflexively until a new target is selected. These accounts suggest that failures of look OKR, leading to increased retinal slip, trigger a reflexive stare OKR to occur until voluntary target tracking is re-initiated.

The impact of task instruction upon the OKR has wider implications for OKR research, beyond that which looks specifically at look and stare OKR. Many existing studies do not specify what instructions were given to participants, if at all, or whether look or stare OKR has been recorded. As a result, it is sometimes unclear whether the data presented has come from look or stare OKR, which may be a source of inconsistencies both between and within studies.

1.6.2 Effect of attention on the OKR

Attention can generally be described as the focussing of cognitive resources onto certain aspects of the environment and is conceptually split into several types. Visual attention allows an observer to focus resources onto a particular visual feature, object or location (Souto & Kerzel, 2021; Sperling & Melchner, 1978) and as such, can be further divided into visual spatial attention and visual feature attention (Lindsay, 2020). Both forms of covert selective attention, visual spatial attention allows an individual to deploy attention to a particular region of the visual field whereas visual feature attention allows an individual to focus attention on a particular stimulus feature such as colour or shape (Lindsay, 2020). Attention is a limited resource, and allocating attention towards processing certain information can be a voluntary or involuntary process. The mechanisms that underlie this process are driven by both endogenous and exogenous factors, such as the intentions of the observer or the salience of the stimulus, respectively (Souto & Kerzel, 2021). Research has shown that eye movements and attention are closely related (for a review, see Souto & Kerzel, 2021).

As seen in the look and stare OKR literature, the instructions given to participants during OKR experiments impact the resulting eye movement behaviour, which may be a consequence of differences in the allocation of attention between look and stare conditions. This is because actively tracking features of the stimulus during look OKR conditions may make the task more attentionally demanding (Magnusson et al., 1985). Similarly, Pola and Wyatt (1985) suggested that the attention involved in voluntary tracking during look OKR may modulate the response to the target's position and velocity. They described attention as being the 'third component' of the OKR, after what they described as

the 'target position system' and the 'target velocity system' which they related to look and stare OKR, respectively.

Outside of the look and stare OKR literature, OKR is known to be affected by attention. Frattini and Wibble (2021) reported that OKR gain was higher during a 'focussed attention' condition compared with a 'neutral attention' condition. Focussed attention was also associated with higher VSM activity, indicating that the activity of the LOKR or vestibular system may have been increased by the attention to the stimulus. Similarly, Kanari et al. (2017) manipulated both

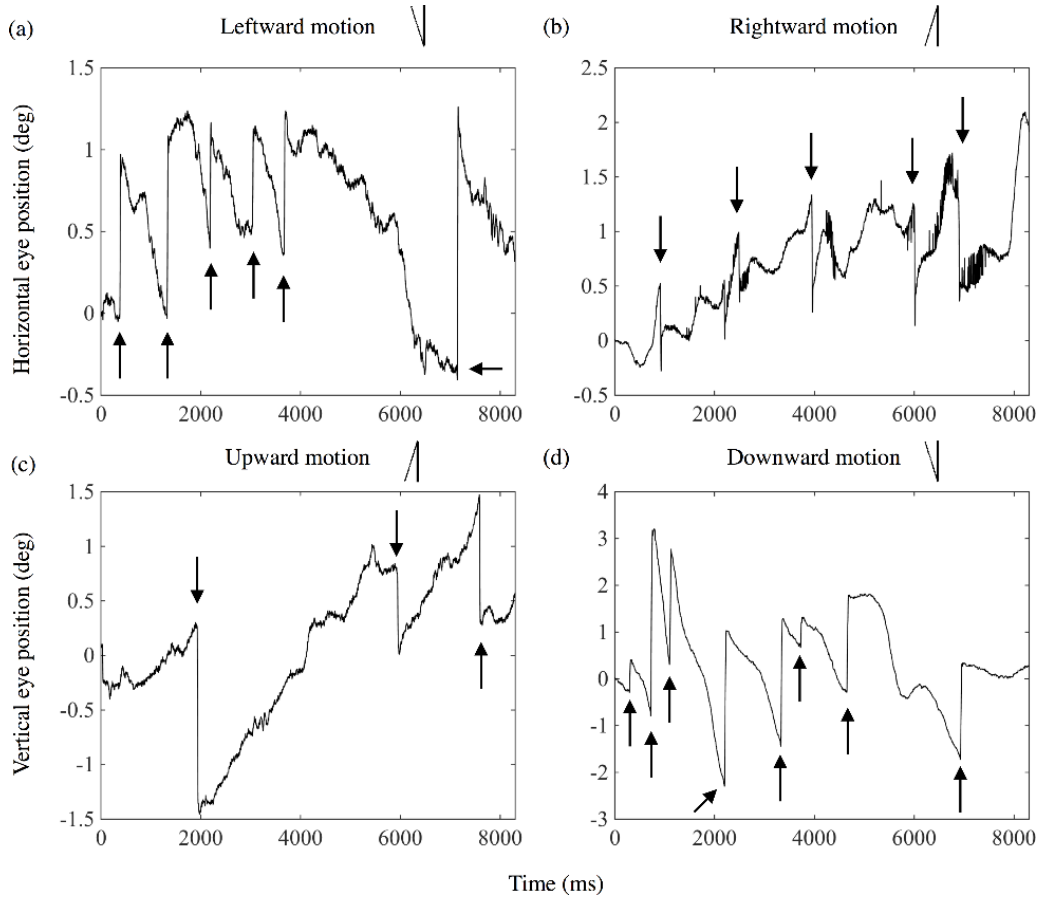

Figure 1.8: From Kanari et al. (2017). Eye movement traces from a single participant showing response to attended peripheral motion in the presence of opposing central motion. Upper plots show horizontal gaze displacement in response to leftward (a) and rightward (b) motion; lower plots show vertical gaze displacement in response to upward (c) and downward (d) motion. Solid black arrows indicate the points in the OKR trace corresponding to attended peripheral motion.

attention and stimulated visual field region, reporting that gain was highest when a task was used to increase attention toward the stimulus and when locus of attention and gaze were congruent. Given the influence of attention upon OKR, some researchers have also attempted to use OKR suppression and breakthrough as a proxy measure of attention (Rubinstein & Abel, 2011; Williams et al., 2006, 2016).

While many eccentricity effects can be attributed to physiological differences between the central and peripheral visual field regions, the anatomical explanation cannot always fully account for the effects of eccentricity. For example, M-scaling does not always compensate for eccentricity effects (Bao et al., 2013; Staugaard et al., 2016; Valsecchi et al., 2013; Wolfe et al., 1998), and training can be used to improve peripheral responses (Hubert-Wallander et al., 2011). Attention has been proposed as an additional explanation for eccentricity effects. Increasing attention towards the visual periphery has been shown to reduce some eccentricity effects during visual tasks (Kirsch et al., 2020; Staugaard et al., 2016), indicating that these eccentricity effects may be partially caused by attention. OKR has been shown to be affected by stimulus eccentricity (e.g. Abadi et al., 1999, 2005; Howard & Ohmi, 1984; Murasugi & Howard, 1989b); attention may be able to account for some of these effects.

Experiments have been carried out using optokinetic stimuli with different directions of motion presented simultaneously to assess the effect of attention on the driving stimulus for OKR. Maruyama et al. (2003) presented two patterns moving in different directions within the same plane, finding that OKR was driven by the pattern that the observer attended to. This demonstrates that within the same visual field region and depth plane the OKR will be driven by the attended stimulus. However, whether this is the case regarding stimuli presented at different eccentricities is of interest, as researchers have sought to understand whether the OKR is preferentially driven by attended motion or central motion. Howard and Gonzalez (1987) simultaneously presented stimuli with different motion directions to the centre and to the periphery, asking participants to attend to the peripheral motion; they reported that slow phase direction was determined by the direction of motion in the centre. This result is thus the same as that achieved without any manipulation of attention: using a similar stimulus, Abadi and Pascal (1991) reported that in the presence of opposing central and

peripheral motion, the centre drove the response. However, they used a square central stimulus surrounded by peripheral motion, so it is possible that the edges of the central stimulus that were perpendicular to the direction of motion had a suppressive effect on the OKR in response to the periphery (Murasugi et al., 1986). From their results, Howard and Gonzalez (1987) concluded that attention towards the periphery was not sufficient to induce a peripheral OKR in the presence of central motion. However, the periphery itself is able to drive an OKR, and Howard and Ohmi (1984) showed that in the absence of central motion, attention to the peripheral stimulus is not required for it to drive the OKR. Taken together, this evidence suggests that although the periphery can drive the OKR, and attention is not required to do so, central motion, when present, will drive the OKR regardless of attention. From this, it appears that central motion rather than attended motion preferentially drives the OKR.

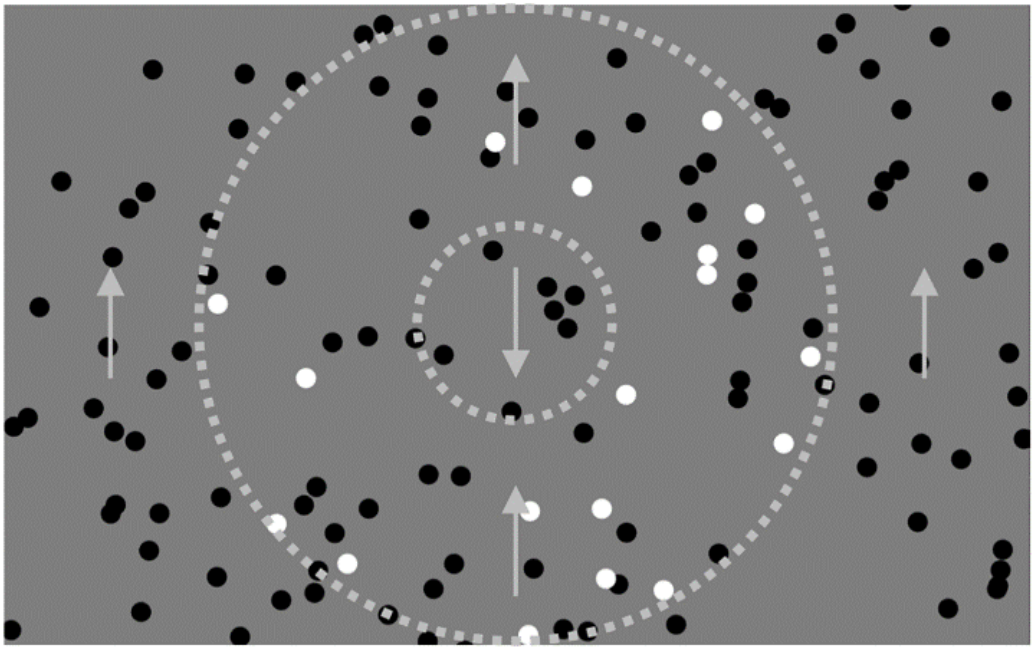

Figure 1.9: From Kanari et al. (2017). Stimulus configuration used in Kanari et al. (2017) Experiment 2. Circles with dotted lines were not presented; they are included to illustrate the borders of areas where targets were presented, and where a different direction of motion is presented to the centre. To direct attention towards the peripheral stimulus, participants were asked to count the number of white target dots.

Kanari et al. (2017) dispute the conclusion that central motion preferentially drives the OKR, arguing that past studies (e.g. Howard and Gonzalez, 1987) failed to precisely manipulate attention. Rather than controlling attention by using a task, these methods have involved instructing observers to attend to a particular region of the visual field. Consequently, Kanari et al. (2017) suggested that these results may have been caused by insufficient attention towards the peripheral stimulus, as separating gaze and attention can be challenging. To address these concerns, they presented different directions of motion to different regions of the visual field and asked participants to complete a counting task presented in one region of the stimulus (Figure 1.9). The result was an OKR that followed the direction of attended motion (Figure 1.8), and they found that gain was enhanced through the use of the counting task. They reported that the presence of an incongruent central stimulus had little effect on the gain and frequency of the peripherally driven OKR. From this, they argued that it is attended motion, not central motion, which drives the OKR, and that past research (e.g. Abadi & Pascal, 1991; Howard & Gonzalez, 1987) has reflected an attentional bias in favour of central vision. In a later study (Kanari & Kaneko, 2019) they again reported that attended motion drove the OKR, regardless of whether that motion was central or peripheral.

The available evidence suggests that attention impacts the OKR: it is able to increase gain across the visual field and manipulate the driving region of the OKR, allowing peripheral motion to be prioritised over central motion if sufficient attention can be directed to the periphery. In the absence of appropriate attentional control, central motion appears to take precedent, which may be a result of an attentional bias in favour of the locus of gaze. Overall, this evidence indicates that lower attention towards the visual periphery under normal viewing conditions may contribute to the eccentricity effects seen in the OKR.

1.6.3 How does attention influence visual performance?

Attention modulates the perception of visual stimuli. For example, it affects the perception of stimulus features such as by increasing apparent spatial frequency and contrast (Carrasco et al., 2004; Carrasco & Barbot, 2019; Gobell & Carrasco, 2005). It has been shown to modulate the strength of the motion

after-effect (Chaudhuri, 1990; Lankheet & Verstraten, 1995), though the extent to which motion adaptation mechanisms are pre-attentive remains a controversial issue (Morgan, 2013) (for a review and meta-analysis, see Bartlett et al., 2019). Attention has also been found to increase perceived motion speed across a range of stimulus velocities (Turatto et al., 2007). Turatto et al. (2007) demonstrated that the effects of attention on perceived motion speed may not be consciously perceptible, as the reported perceived speed increase was less than the just noticeable difference, and observers reported not being able to perceive a difference between stimuli. However, in a forced-choice paradigm, their performance indicated a difference in perceived speed despite observers stating that they had simply guessed. This suggests that attention is able to impact visual performance without changing conscious perception. Such effects of attention on perception are reflected at a neural level, with studies of motion processing in humans and monkeys reporting that attention modulates activity in areas V5/MT and MST (Martínez-Trujillo & Treue, 2002; Rees et al., 1997; Treue & Maunsell, 1996). For example, in monkeys, Treue and Maunsell (1996) showed that responses of neurons in areas MT and MST were reduced when attention was directed to a visual stimulus outside of the cell's receptive field and were enhanced when attention was directed inside the cell's receptive field.

Many proposals have been put forward to explain how attention modulates perception, such as by shrinking receptive fields around the attended stimulus (Moran & Desimone, 1985) or by increasing contrast gain (Reynolds et al., 2000). The biased competition model of attention (Desimone, 1998; Desimone & Duncan, 1995) suggests that attention modulates the competitive interactions between the neurons that represent the available stimuli so that neurons relating to behaviourally irrelevant stimuli are suppressed (Desimone, 1998). The normalisation model of attention (Reynolds & Heeger, 2009) expands upon this idea, outlining three basic components: a 'stimulation field', which characterises the selectivity of a neuron; a 'suppression field', which characterises the spatial positions and features which contribute to suppression; an 'attention field', which acts as a multiplier for the stimulus drive. The stimulus drive represents what the neuron's response to the stimulation field would be in the absence of suppression and attention. Normalisation involves calculating the ratio between a single neuron's activity and the summed activity of a population of neurons (Carandini &

Heeger, 2011). In this model, the attention field and the stimulus drive are multiplied together before being divided by a constant plus the suppression field, which provides normalisation. It is assumed that the stimulus drive is selective whereas the suppressive drive is not specific. According to this model, the attention field alters the balance between excitation and suppression within a population of neurons. Schwartz and Coen-Cagli (2013) further expanded on this idea in their model of spatial extent to include a flexible normalisation pool whereby the surround divisively normalises the centre if the two areas are considered to be statistically dependent. Attention multiplicatively accentuates attended features and locations prior to normalisation. The models of Schwartz and Coen-Cagli (2013) and of Reynolds and Heeger (2009) thus share the role of attention as something that has its effect before normalisation, impacting both the numerator and the normalisation pool.

1.7 Effect of stimulus characteristics on the OKR

Increasing stimulus speed has a detrimental effect on OKR gain in both cats and humans (Donaghy, 1980; Valmaggia et al., 2005). Investigating both look and stare OKR in humans, Valmaggia et al. (2005) reported that increasing stimulus velocity caused gain to decrease for both OKR types in response to both horizontal and vertical stimulus motion. This effect of increasing stimulus velocity was most pronounced in vertical stare OKR and least pronounced in horizontal look OKR. Increasing stimulus velocity has also been shown to increase the slow phase amplitude (Honrubia et al., 1968).

Many studies have reported that the size of the stimulated area has an effect on the OKR. Increasing the area of an optokinetic stimulus is associated with an increase in gain (Cheng & Outerbridge, 1975). However, small stimuli are still able to induce fairly high-gain OKR. Howard and Ohmi (1984) reported that as long as any edges in the moving field that are perpendicular to the direction of motion are sufficiently blurred, a small display can induce high-gain OKR; without blurred edges, the gain was much lower. They suggested that in many experiments investigating the effect of stimulus area, low gain in response to smaller stimuli may be due to the proximity of sharp, stationary edges to the foveae rather than being due to the area of the stimulus. Increasing the area of a

stimulus also results in an increase of the upper velocity limit of the OKR; this is thought to be a consequence of the peripheral contribution to the OKR (Dichgans, 1977; Hood, 1967, 1975). The size of a stimulus required to induce an OKR may vary based on the retinal location of the stimulus. In macaque monkeys, Koerner and Schiller (1972) found that the stimulated area required to produce OKR was a function of eccentricity, with more eccentric locations requiring larger moving fields to produce a response. In addition to the effect of proximity of sharp stimulus edges to the fovea, the effect of stimulus area on the OKR may be related to the way in which the size of a moving field influences motion perception. For example, Watamaniuk and Sekuler (1992) showed psychophysically that, in humans, the thresholds for identifying global motion direction of a random-dot field increased as the size of the moving area decreased. This indicates that increasing the stimulus area results in improved accuracy of global motion integration. This may contribute to the effect of stimulus area on measures such as OKR gain. Additionally, as stimulus size is increased, so too will the need for image stabilisation to cope with the increase in retinal motion within the visual field. In this way, larger stimuli may simply provide a more potent trigger for OKR to occur.

Various other stimulus characteristics have been shown to affect the OKR. In cats, reducing stimulus contrast was shown to reduce OKR gain, and the magnitude of this effect was dependent on the spatial frequency of the stimulus (Donaghy, 1980). While first-order (luminance-defined) motion has been shown to be a highly effective driver of OKR, particularly LOKR, second-order (texture-defined) motion, which does not provide a uniform field of motion, has been shown to be extremely ineffective as an OKR stimulus in humans (Harris & Smith, 1992, 2000). However, combining first- and second-order motion stimuli has an enhancing effect on the OKR if the first-order motion stimulus has low contrast and the stimuli are moving in the same direction. If the stimuli are moving in different directions, the effect is one of suppression (Harris & Smith, 2000). From this, Harris and Smith (2000) concluded that second-order motion is able to modify the response to low-contrast first-order motion, despite being a poor driver of OKR alone. In reference to this finding, Dakin and Turnbull (2016) suggested that the OKR system may include cortical areas which are known to support the processing of second-order motion, such as V3 (Smith et al., 1998).

Finally, the presence of stationary edges perpendicular to the direction of motion (Murasugi et al., 1986) and stationary objects within the moving field (Barnes & Crombie, 1985) have both been shown to have a suppressive effect on the OKR.

1.8 Symmetry of the OKR

1.8.1 Development of OKR symmetry

OKR can be impacted by direction of motion. It is generally agreed that horizontal OKR (HOKR) in visually normal adult humans is symmetrical (Garbutt & Harris, 1999; Knapp et al., 2008; Valmaggia et al., 2005). The development of this symmetry is thought to be related to binocularity. Humans are born with an asymmetrical OKR, much like that of the rabbit (Garbutt & Harris, 1999), whereby there is a more rigorous OKR in response to TN compared to NT motion. Within the first six months of life, human OKR becomes symmetrical (Harris et al., 1994). Evidence for a role of binocularity in this process comes from studies of humans with abnormal or absent binocularity. Valmaggia et al. (2005) showed that participants with normal binocularity had no TN-NT asymmetry whereas participants without measurable binocularity had significant asymmetry, with higher gains in the TN direction. They suggested that this is evidence of dominance of the subcortical pathway in these individuals, which in monkeys has been shown to have a preference for TN motion (Hoffmann, 1989), positing that the cortical pathway has failed to mature normally. However, evidence of EOKR in human infants younger than one month old indicates that, even before OKR symmetry develops, there is some cortical mediation of OKR (Harris et al., 1994). As well as having HOKR asymmetries, individuals with early-onset strabismus have been shown to have VOKR asymmetry, whereas individuals with later onset strabismus did not have a marked VOKR asymmetry (Tychsen et al., 1984). This shows that early abnormal visual experiences affect the development of both VOKR and HOKR (Hainline et al., 1984). It may be tempting to conclude from this evidence that early monocular deprivation is responsible for these asymmetries. However, while Reed et al. (1991) found a correlation between degree of HOKR asymmetry and age at strabismus onset, this correlation was not reflected in their monocularly enucleated observers, who were not different from controls. Consequently, they suggested that persistence

of OKR asymmetry is not a result of early monocular deprivation, but rather, is a result of early abnormal competition between the eyes.

Research sectioning the interhemispheric connections such as the corpus callosum and optic chiasm in monkeys showed that VOKR asymmetry was exaggerated as a result (Pasik et al., 1971), leading to the suggestion that immaturity of the coordination between hemispheres may play a role in OKR asymmetries (Hainline et al., 1984). Similarly, removal of a cerebral hemisphere in human infants has been shown to cause no OKR, long tracking or reversed OKR in response to stimulation in the direction of the intact half field (Braddick et al., 1992), corroborating the suggestion that interhemispheric connections play a role OKR symmetry.

1.8.2 Vertical and oblique OKR and OKAN

Whereas it is generally agreed that HOKR in humans is symmetrical (Garbutt & Harris, 1999; Knapp et al., 2008, 2013; Valmaggia et al., 2005), data regarding the symmetry of VOKR are more variable. VOKR is often reported as having lower gain than HOKR (Valmaggia et al., 2005). Studies examining the up-down symmetry of VOKR have yielded mixed results. Some studies have reported that VOKR has higher gain in response to upward moving stimuli compared to downward moving stimuli, particularly at high stimulus velocities (Howard & Simpson, 1989; Murasugi & Howard, 1989b). Other studies have reported no differences in gain between upward and downward OKR (Kanari et al., 2017). Velocity of the stimulus may be the key to witnessing this asymmetry; Kanari et al. (2017) reported no VOKR asymmetry using a 13.3 deg/s stimulus, a velocity at which Murasugi and Howard (1989b) also reported no asymmetry. However, while some research (e.g. Murasugi & Howard, 1989b) has concluded that VOKR asymmetry occurs at higher (~15-20 deg/s) stimulus velocities, other studies have reported asymmetry in response to stimuli at velocities as low as 10 deg/s (Garbutt, Han, Kumar, Harwood, Harris, et al., 2003).

There may be individual differences in VOKR asymmetry. Knapp et al. (2008) reported no overall VOKR asymmetry at the group level but noted that there were idiosyncratic asymmetries when examining individual data. There may also be individual differences in vertical OKAN symmetry. Murasugi and

Howard (1989b) reported that full-field upward stimulation produced an upward OKAN, but full-field downward stimulation did not produce a downward OKAN. However, this group level asymmetry was eliminated by stimulating only the central visual field, which resulted instead in idiosyncratic vertical OKAN asymmetries. Similarly, Baloh et al. (1983) reported that some observers only produced an upward OKAN following downward stimulation (OKAN-II).

The study of oblique OKR and OKAN has been limited, particularly in humans. However, there has been some research into oblique OKR/OKAN in monkeys. Oblique OKR relies on the combined vertical and horizontal components of the eye movements, therefore it is constrained by the limitations of both. As VOKR is reported to have lower gain than HOKR (Valmaggia et al., 2005),

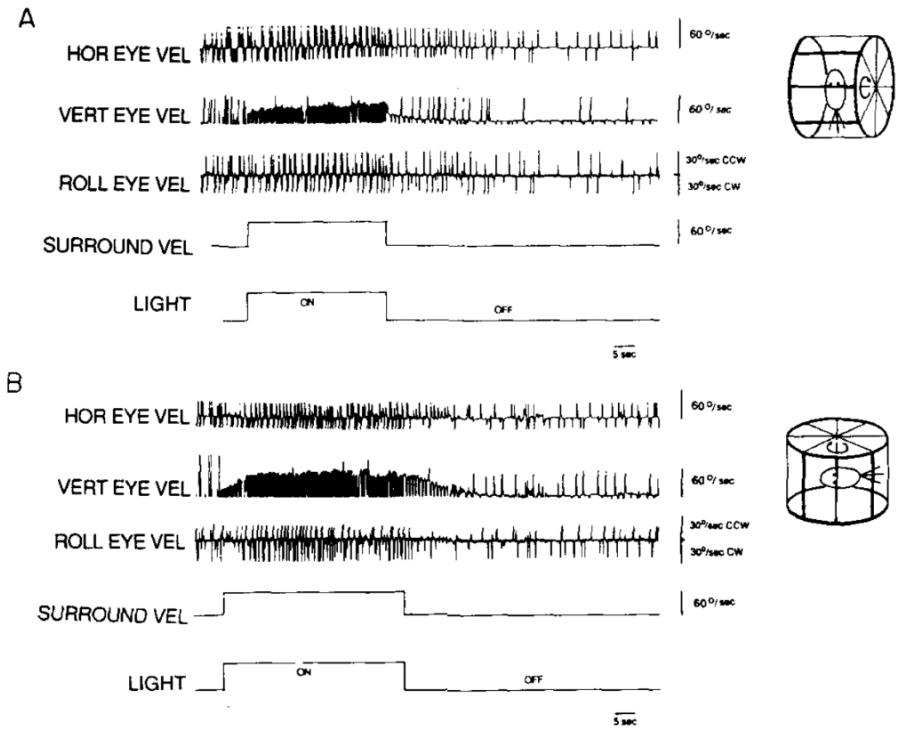

Figure 1.10: From Raphan and Cohen (1988). Horizontal, vertical and tortional eye movement velocity in the monkey in response to vertical optokinetic stimulation at 60 deg/s, and during the following OKAN, with the head upright (A) or at 90° (B). In response to this head-vertical motion, OKR and OKAN were both stronger with the head at 90° compared to with the head upright, as earth-parallel movements were facilitated.

one might expect that, as the stimulus velocity increases, the vertical component will break down first. Kröller and Behrens (1995) showed this to be the case in squirrel monkeys, as the trajectory of the slow phase shifted towards the horizontal axis when stimulus velocity exceeded 90 deg/s. They suggested that this was a result of the EOKR system struggling to produce OKR at such high velocities, with VOKR being particularly affected, resulting in a compensatory shift towards the horizontal axis to maintain gain. Similarly, they noted that the vertical component was unstable at high velocities, and no vertical OKAN was observed. This indicates that vertical velocity storage may no longer occur when the stimulus velocity is sufficiently high.

When interpreting OKR and OKAN in response to different directions of stimulus motion, it is important to consider the frame of reference being used by OKR systems. Most OKR research is conducted with the head upright, therefore head-horizontal and earth-parallel are usually congruent. Raphan and Cohen (1988) studied OKR and OKAN in rhesus and cynomolgus macaque monkeys using a variety of stimulus directions and head orientations. They reported that the OKAN slow phase direction was shifted towards an earth-parallel orientation regardless of stimulus direction or head orientation (Figure 1.10). Earth-parallel components were facilitated, which they explained in terms of the otoliths (inner ear structures that register gravity and linear acceleration) reorienting the coordinate system of the velocity storage integrator. By extension, this suggests that results such as those of Kröller and Behrens (1995) may depend on head orientation; rather than showing a breakdown of head-vertical components, their result may reflect a breakdown of earth-vertical components.

1.8.3 Pathology-induced asymmetry

OKR asymmetry can be acquired through pathology. For example, unequal visual field loss between the two eyes is sometimes associated with interocular gain differences (Dakin et al., 2019) and early-onset strabismus is associated with HOKR and VOKR asymmetry (Tychsen et al., 1984; Valmaggia et al., 2003, 2005). Lesions can produce large OKR asymmetries which can be used to make inferences about the location of the lesion (Garbutt & Harris, 1999). A unilateral lesion of the HOKR pathway can decrease the amplitude, frequency and

velocity of eye movements towards the lesioned hemisphere (Garbutt & Harris, 1999); this behaviour indicates that the lesion may be in the parietal lobe, brainstem or cerebellum (Baloh et al., 1977, 1980b). In contrast, an increase of the eye movement velocity towards the lesioned hemisphere is associated with certain acute vestibular lesions (Sasser, 1994).

1.9 Is OKR made up of smooth pursuit and saccades?

1.9.1 Slow phases as smooth pursuit eye movements

Many researchers have suggested a role of smooth pursuit eye movements (SPEM) in human OKR. The presence of OKR in animals that lack a SPEM system demonstrates that SPEM is not a prerequisite for OKR to occur, but the OKR produced by animals with and without a SPEM system does not appear to be identical (Collewijn, 1985), leaving open the possibility that SPEM contributes to the OKR in some animals. However, it is also possible that this difference is not one of having a SPEM system or not, but rather, is one of being foveate or not (Tauber & Atkin, 1968). Some researchers have suggested that the slow phase of OKR is a form of SPEM (Garbutt & Harris, 1999) and look OKR has been described as being a combination of both OKR and SPEM (Pola & Wyatt, 1985) or as a transition from OKR to SPEM (Roelofs, 1954). While both OKR slow phases and SPEM involve the smooth tracking of a stimulus, Collewijn (1985) warned against assuming that the two are the same, citing gain differences between the responses: in response to a target moving at a constant velocity, the gain of SPEM (Collewijn & Tamminga, 1984) is lower than that of OKR (Paige, 1983) and shows a more dramatic decrease as stimulus velocity increases (Collewijn, 1985); in response to drifting gratings, the gain of OKR is higher than that of SPEM (van Die & Collewijn, 1982). While SPEM typically involves foveal tracking of a target, OKR can be induced in response to peripheral motion (Kanari et al., 2017), hence some researchers have distinguished SPEM and OKR as foveation of a moving target and the stabilisation of the overall retinal image, respectively (Garbutt & Harris, 1999). By these accounts, OKR evoked by peripheral motion should not be considered as SPEM. However, it should be noted that some studies have shown evidence of eccentric smooth

pursuit in both individuals with normal vision and with central visual field loss (González et al., 2018; Steinman et al., 1969; Winterson & Steinman, 1978).

Developmental studies have provided evidence both for and against a role of SPEM in human OKR. Full-field stimuli evoke OKR in human newborn infants (Figure 1.11A) (Dayton, Jones, Aiu, et al., 1964; Gorman et al., 1957). SPEM has also been reported in human infants, though it is stimulus-dependent, inconsistent and jerky in nature due to frequent use of catch-up saccades and refixations (Figure 1.11B) (Dayton, Jones, Steele, et al., 1964; Dayton & Jones, 1964; Kremenitzer et al., 1979; Von Hofsten & Rosander, 1997). Kremenitzer et al. (1979) reported that newborn infants showed both SPEM and OKR, but that OKR was produced up to a higher stimulus velocity compared to SPEM, and optokinetic stimuli produced more rigorous pursuit than individual moving targets. They suggested that this result may reflect poor foveal function in newborn human infants. It has been suggested that the OKR observed in young infants may be LOKR rather than EOKR; however, human infants have been shown to exhibit EOKR from at least 22 days in age (Hainline et al., 1984). Taken together, this evidence indicates that a well-developed SPEM system may not be necessary to produce EOKR. Some researchers have suggested that SPEM may play a larger role in look OKR but not stare OKR. Harris, Kriss, et al. (1996) tested infants with delayed visual maturation (DVM), showing that during their early period of visual unresponsiveness, OKR but not SPEM could be induced. As these infants were otherwise visually unresponsive and unable to respond to individual stimulus features, it is likely that they exhibited a reflexive stare OKR and not look OKR. DVM infants and age-matched controls showed a similar OKR with a rapid build-up (EOKR), indicating that SPEM was not required for this OKR to occur. By extension, this suggests that the EOKR reported in visually normal newborns was not dependent on SPEM, providing further evidence that SPEM is not required for EOKR to occur.

The developmental timelines of SPEM and OKR can be examined to assess whether they may be related. Initially, human infants have asymmetrical OKR, with a more rigorous response in the TN direction (Garbutt & Harris, 1999). The emergence of OKR symmetry and SPEM have a similar developmental timeline. SPEM shows a rapid increase in gain within the first 3-4 months of life; by 5-6 months of age, SPEM has become much more adult-like, though it

has not reached full adult levels (Jacobs et al., 1997; Von Hofsten & Rosander, 1997). This is a similar timeline over which OKR symmetry develops (Harris et al., 1994), however, infant OKR appears more adult-like than infant SPEM (Figure 1.11). Early-onset strabismus is associated with OKR asymmetry (Valmaggia et al., 2003, 2005; Wright, 1996) as well as SPEM asymmetry (in monkeys: Lee et al., 2009; in humans: Tychsen & Lisberger, 1986), both favouring the TN direction of motion. However, correlations between the development of SPEM and OKR do not necessarily point to SPEM being directly involved in OKR. It may be that development of SPEM and OKR are simply both related to the development of binocular abilities, causing them to develop concurrently as the coordination between the two eyes improves (Garbutt & Harris, 1999). Evidence that the prevention of the development of normal binocularity impedes the development of symmetrical OKR and SPEM in monkeys and humans (Lee et al., 2009;

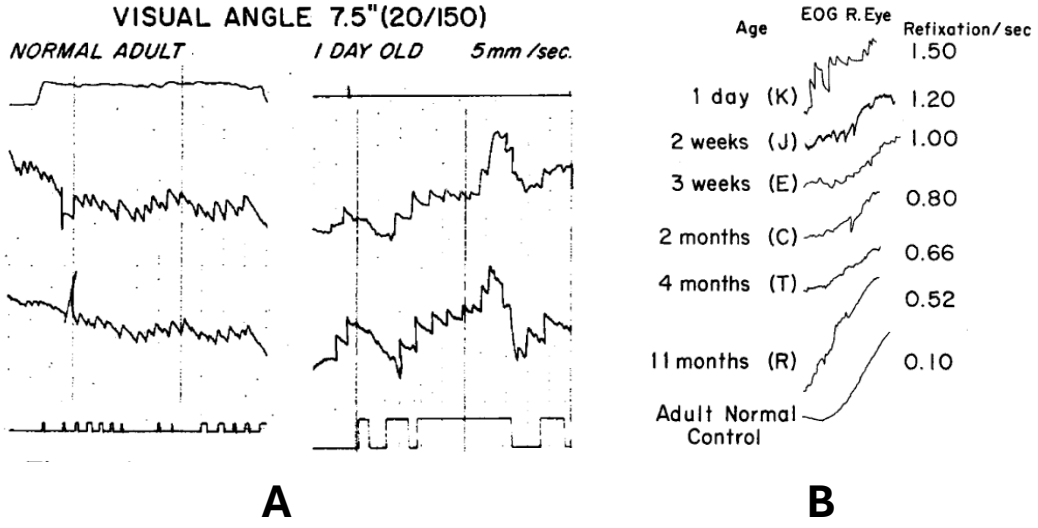

Figure 1.11: (A) From Dayton, Jones, Aiu, et al. (1964). Electro-oculography (EOG) trace showing OKR in a normal human adult (left) and in a one-day-old human infant (right). Note the similarity between the adult and infant OKR sawtooth waveform. (B) From Dayton, Jones, Steele, et al. (1964). EOG trace showing SPEM at various ages ranging from one day to adult, alongside the number of refixations made per second, which decreases as age increases. Note the dramatic difference in smoothness of the EOG trace between newborn infants and adults. Overall, the traces shown in A and B demonstrate that OKR in newborn infants appears to be better developed than SPEM.

Tychsen & Lisberger, 1986; Valmaggia et al., 2003, 2005; Wright, 1996) can be interpreted as supporting this outlook.

Finally, fMRI has been used to compare the OKR and SPEM systems. Konen et al. (2005) reported that in adult humans there were no oculomotor areas exclusively dedicated to either SPEM or OKR and that similar structures were activated during both eye movement types, including the SEF, FEF, posterior parietal cortex, regions within the ventrolateral premotor cortex, V1/V2, MT+ and the cerebellum. SPEM was associated with deactivation of the parieto-insular vestibular cortex, which has also been observed during OKR (Dieterich et al., 2003). Konen et al. (2005) argued that this evidence supports that OKR and SPEM are related. However, it should be noted that different stimuli were used to induce OKR and SPEM, and the recorded responses could thus be affected by this; OKR was induced using a drifting black and white stripe stimulus while SPEM involved pursuit of a single target against a black background. As some researchers have argued that it is look, not stare, OKR which is related to SPEM, it is also important to compare SPEM to each OKR type. Kashou et al. (2010) carried out such an experiment using drifting striped stimuli, reporting similarities in activation between SPEM, saccades and look OKR, but not stare OKR. From this, they argued that look OKR represents a series of alternating SPEM and saccades rather than being a 'true' OKR. However, as they did not employ eye tracking during scanning, the types of eye movements carried out by the participants cannot be confirmed.

1.9.2 Fast phases as saccades

The fast phases of OKR attract less research attention than the slow phases and as such the comparison between fast phases and saccades has not been given the same degree of attention as that of slow phases and SPEM. However, there is some evidence that the fast phases of OKR are not simply saccades. Saccades are known to be preceded by (and with their targets guided by) shifts in attention towards the endpoint of the saccade (Deubel & Schneider, 1996; Kustov & Robinson, 1996). In contrast, Hanning and Deubel (2019) reported that the fast phases of OKR are not preceded by shifts in attention, describing fast phases as instead being reflexive gaze-resetting eye movements controlled at a lower

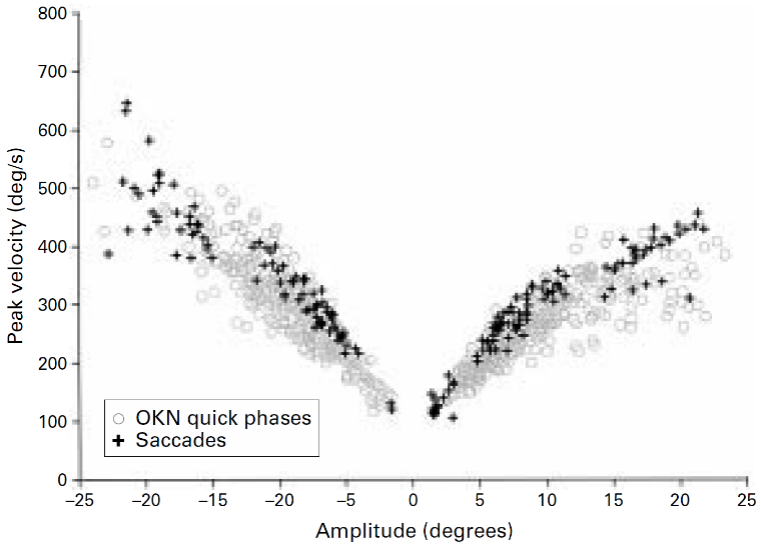

Figure 1.12: From Garbutt et al. (2001). Scatterplot of saccade and OKR fast phase peak velocity by amplitude in a typical adult human participant, based on data recorded using infrared limbal reflection. Note the higher average peak velocity of saccades (black crosses) compared to fast phases (grey circles).

level. Further, in an fMRI study of adult humans Kashou et al. (2010) reported that look OKR, compared to stare OKR, was more highly correlated with activation in areas associated with both SPEM and saccades, which indicates that these smooth pursuit and saccade areas are less involved in stare OKR. This could be interpreted as stare OKR being distinct from SPEM, saccades and look OKR. Comparing reflexive saccades and OKR fast phases in adult human observers, Garbutt et al. (2001) reported that while the main sequence for duration was the same for reflexive saccades and fast phases, OKR fast phases had a slightly lower peak velocity (Figure 1.12). Lower peak velocity of fast phases compared to saccades has also been reported by Henriksson et al. (1980). In sum, the evidence suggests that fast phases and saccades, though very similar, may not be identical.

1.10 Potential impact of OKR research

1.10.1 Diagnostic potential of the OKR

Suppressing the OKR in response to full-field motion is quite difficult in the absence of a fixation target, therefore a lack of a response to full-field motion may indicate that the stimulus has not been perceived. Similarly, if a stationary object is placed within the moving field without affecting the OKR, this may indicate that the stationary object has not been perceived. This means that the OKR may provide a useful objective tool for obtaining visual measures. OKR measures based on inducing OKR in response to full field motion are known as 'induction methods' whereas measures based on suppression of OKR using fixation targets are known as 'suppression methods' (Aleci et al., 2018; Shin et al., 2006). Such methods may be particularly valuable for testing individuals for whom traditional measures can pose complications, such as very young children. Research has highlighted the potential of OKR as a measure of various aspects of visual performance, including visual acuity (Aleci et al., 2018; Doustkouhi et al., 2020a; Gorman et al., 1957; Shin et al., 2006), contrast sensitivity (Dakin & Turnbull, 2016), colour vision deficit (Taore et al., 2022), visual field loss (Dakin et al., 2019; Doustkouhi et al., 2020b) and interocular suppression in amblyopia (Wen et al., 2018); a better understanding of the way in which stimulus area, retinal location of the stimulus, and attention impact OKR will increase its potential as an objective vision measure.

Gorman et al. (1957) were the first to attempt to assess vision in human infants using OKR, concluding that it may provide a useful measure of visual acuity. More recently, Shin et al. (2006) explored this possibility in adult patients with ocular disease. They reported that visual acuity was correlated with the width of stripes required to induce OKR (induction method) and the size of dots required to suppress OKR (suppression method). However, which method was more diagnostically useful was related to the visual acuity of the observer; they reported that the induction method was useful for patients with acuity of ≤20/60 while the suppression method was useful for patients with acuity ≥20/200. Similarly, as the acuity measurable by the stimulus is limited by its spatial and temporal frequencies, low stimulus velocities are reported to be more appropriate for measuring acuity in subjects with low visual acuity while higher velocities are

suitable for those with better visual acuity (Aleci et al., 2018; Han et al., 2011; Wester et al., 2007). For example, Han et al. (2011) noted that with a temporal resolution of 60Hz and a stimulus velocity of 10 deg/s, spatial resolution is limited to 6 cyc/deg; this corresponds to a Snellen acuity of 20/100. This means that a test under these parameters is only suitable for acuities up to 20/100. Aleci et al. (2018) also used OKR to measure visual acuity, finding that the best agreement between methods of acuity testing (OKR or Teller) was obtained in response to the minimum contrast level (20%), though the analysis of OKR was limited in this study due to the lack of eye tracking. Additionally, Doustkouhi et al. (2020a) reported that estimates of the mean spherical equivalent (MSE) derived from OKR correlated well with MSE estimates derived from autorefraction ($r = 0.88$). This evidence suggests that it is possible to use OKR to measure visual acuity, though different methods and stimuli are suitable for different levels of acuity. However, some studies have not been able to provide support for the clinical usefulness of OKR in acuity testing. Khan et al. (1976) utilised lenses and filters to progressively fog the vision of adults with normal vision and compared this to the results obtained from ocular disease patients. They reported that although there was a good correlation (correlation coefficients of +0.863 when vision is fogged with neutral-density filters, and +0.911 when vision is fogged with ophthalmic convex lenses) between OKR and acuity in individuals with good vision, this correlation was not significant in those with poor vision (correlation coefficient of +0.606), limiting its clinical usefulness. Further, Çetinkaya et al. (2008) reported no correlation between spatial frequency threshold for OKR induction and recognition visual acuity in children. Overall, the data regarding the usefulness of OKR as a measure of visual acuity are mixed, particularly with respect to individuals with poor vision.

Although visual acuity is the most commonly measured aspect of spatial vision quality, contrast sensitivity has been argued to provide a better predictor of functional vision (Owsley & Sloane, 1987). Unfortunately, deriving a contrast sensitivity function (CSF) is a relatively intensive and laborious process, relying on perceptual report (Dakin & Turnbull, 2016). This means that deriving a CSF in populations who struggle to provide accurate perceptual report can be challenging. Dakin and Turnbull (2016) obtained a CSF through perceptual report and through the use of OKR, reporting a high level of agreement between the

two methods (mean R = 0.95). They suggested that the OKR may provide a useful alternative method for measuring contrast sensitivity. In another OKR method utilising stimulus contrast, Wen et al. (2018) used dichoptic presentation of OKR stimuli with varying contrast ratios to assess interocular suppression in individuals with amblyopia. They showed that in normal observers the time spent pursuing the OKR stimulus was approximately equal across the two eyes. However, in observers with amblyopia, pursuit time in the dominant fellow eye was higher than that of the amblyopic eye. The effective contrast ratio required to produce a balanced response in such observers was correlated with the visual acuity in the amblyopic eye (Spearman's correlation coefficient = 0.97). They concluded that OKR in response to dichoptic gratings with different contrast ratios provides a reliable objective no-report measure of interocular suppression in amblyopia.

As OKR is affected both by stimulus area and visual field location, it is sensitive to visual field loss. Standard automated perimetry relies on perceptual report (Turalba & Grosskreutz, 2010), so like deriving a CSF, may prove challenging with regards to some child or patient populations. Dakin et al. (2019) reported that, in adults with asymmetric visual field loss, the difference in visual

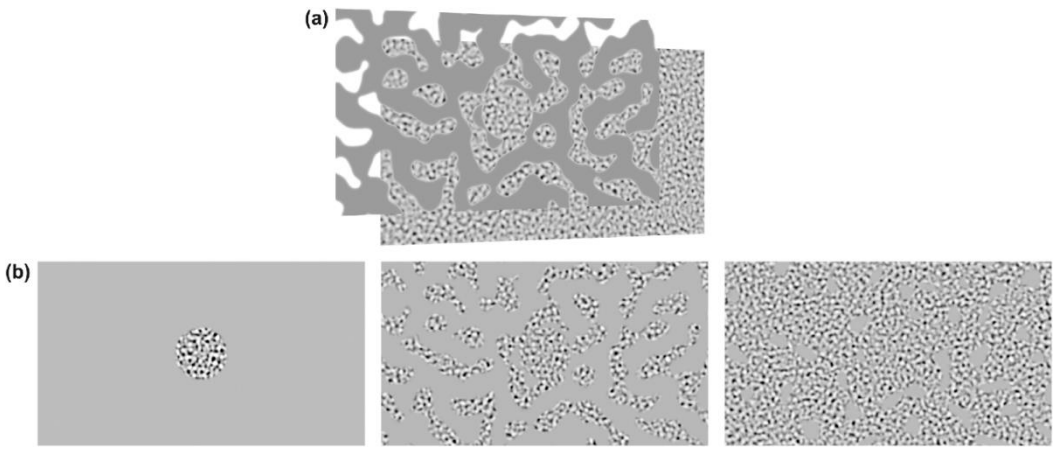

Figure 1.13: From Doustkouhi et al. (2020b). Stimuli used in a simulated visual field loss (SVFL) paradigm. (a) The stimulus is constructed in two layers, with a drifting isotropic noise carrier and a mask. (b) Examples of stimuli with varying levels of SVFL: from left to right, 3%, 39% and 88% of the noise carrier is visible through the mask.

field index (a metric to describe visual field function as a percentage that assigns more weight to central regions) across the eyes was correlated with OKR gain differences between the eyes (at 12.5% stimulus contrast, R = 0.61). This demonstrates that interocular gain differences can be used to assess differences in vision between the eyes. Doustkouhi et al. (2020b) explored the possibility of utilising OKR to measure extent of visual field loss using a simulated visual field loss (SFVL) paradigm (Figure 1.13). They reported that the gain of OKR was negatively correlated with the extent of SVFL (r = 0.88), though it did not provide topographical information, which could limit its usefulness. It may be the case that a better understanding of the way in which different visual field regions contribute to the OKR could open up the possibility of gaining topographical information about VFL using OKR.

When considering the use of OKR as an objective measure of vision, it is important to note that while Gorman et al. (1957) concluded that an OKR was indicative of the presence of vision, there is some evidence of OKR in individuals lacking conscious visual perception. Ter Braak et al. (1971) reported the case of an adult with acquired cortical blindness who said that he did not see motion, but in whom a passive OKR could be induced. A necropsy revealed partial cortical sparing which may have been responsible for the presence of the OKR. Similarly, Van Hof-Van Duin and Mohn (1983) reported OKR in children with cortical blindness. Such cases indicate that conscious perception is not necessary for OKR to occur. Additionally, factors other than an inability to see the stimulus could prevent an individual from producing an OKR. Bilateral lesions to the OKR pathways and gaze paresis (an inability to move the eyes together) can prevent OKR from occurring (Garbutt & Harris, 1999). Pathological nystagmus sometimes produces an OKR that appears reversed in direction (Hood & Leech, 1974), and in cases of gaze paretic nystagmus (nystagmus during eccentric gaze that is neurological in origin), OKR may be extremely disrupted or absent (Harris et al., 1993a; Harris et al., 1993b). Finally, absence of OKR can also be the result of an inability to produce saccades. For example, in individuals with ocular motor apraxia, who cannot produce fast phases, OKR stimuli will instead cause the eyes to drift to their mechanical limit (Harris, Shawkat et al., 1996). Given the variety of conditions that can affect the OKR, using OKR to test vision would require pathological influences on the OKR to be ruled out first.

The available evidence suggests that the OKR can be used to measure various aspects of visual performance, though it may have limitations. However, expanding the current knowledge of how various factors, such as stimulus area, observer attention and retinal location of the stimulus affect the resulting OKR can help quash some of these limitations. In this way, the full diagnostic potential of OKR may currently remain untapped.

1.10.2 OKR as a no-report measure in research

1.10.2.1 OKR as a measure of attention

Current tools for assessing the allocation of visual attention have limitations. For example, the useful field of view (UFOV) test is used to assess visual attention, but it involves identifying the location of peripheral static stimuli (Rubinstein & Abel, 2011), so it is limited in its range of stimulus types and locations, in addition to requiring participant report. Having tools for measuring attentional allocation that allow for both static and dynamic stimuli to be used and that remove the need for participant report is desirable for researchers.

Williams et al. (2006) assessed adult observers' ability to suppress OKR using a fixation point, as well as their ability to maintain this OKR suppression while attending to features of the OKR stimulus. They reported that during fixation there was near complete suppression of OKR. However, when observers were asked to pay covert attention to features of the moving stimulus, there was increased OKR breakthrough as their attention was divided between the stationary fixation point and the moving OKR stimulus. The amount of breakthrough was positively correlated with the age of the observer; while trying to suppress OKR (i.e. to achieve a gain of zero), the correlation between age and OKR gain was $r^2 = 0.81$. From these data, they suggested that OKR could be utilised to develop a measure of the ability to divide attention between stimuli. Williams et al. (2016) then compared multiple sclerosis (MS) patients and controls on this ability and tested cognitive abilities including attention and memory using the Audio Recorded Cognitive Screen (ARCS). They found that despite group-based differences in ARCS performance, MS patients were able to perform as well as controls on the OKR suppression task. They attributed this to the multi-faceted

nature of attention: differences in ARCS performance were not reflected in OKR suppression, likely due to the tasks involving different attentional demands. These studies indicate that OKR suppression and breakthrough can be used as a measure of divided visual attention, but this suppression task may not be sensitive to other forms of attention, such as those assessed by the ARCS.

Rubinstein and Abel (2011) expanded on the work of Williams et al. (2006), using a similar OKR suppression task to assess the allocation of visual attention. They presented both static and dynamic stimuli in central and peripheral visual field locations while participants were asked to maintain fixation on a central target. Optokinetic stimuli were made up of letters, for example blue Ts and red Cs, with an occasional red T. This stimulus was replicated from the stimulus used by Williams et al. (2006). An example of a dynamic task in this paradigm is identification of when a moving stimulus feature, such as the red T, passes a central or peripheral spot, whereas an example of a static task is the identification of the appearance or disappearance of a static stimulus such as a green star in the centre or periphery. They reported that dynamic stimuli elicited more OKR breakthrough than static stimuli, and that central stimuli elicited

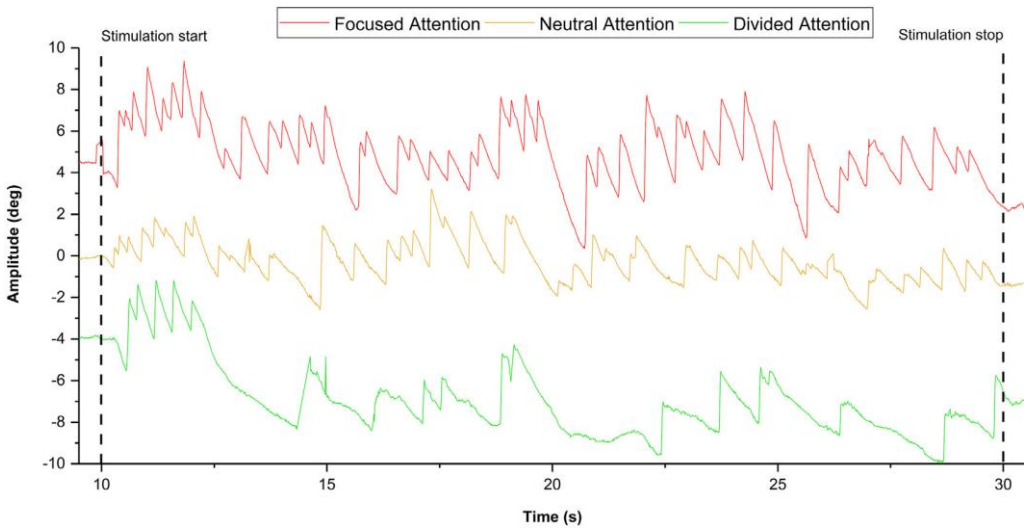

Figure 1.14: From Frattini and Wibble (2021). OKR eye movement traces showing displacement of gaze during focussed (red), neutral (yellow) and divided (green) attention conditions. Note the differences in frequency, smoothness and consistency of the waveform between conditions.

more breakthrough than peripheral stimuli. They concluded that OKR breakthrough is sensitive to the way in which visual attention is allocated, and thus may prove useful as a measure of visual attention.

More recently, Frattini and Wibble (2021) explored the use of OKR as a measure of attention while using pupil size to measure alertness. They used focussed attention, divided attention and neutral attention conditions. Focussed attention was achieved by asking participants to verbally report each rotation of a rotating optokinetic stimulus, whereas the neutral attention condition involved simply viewing the stimulus. During the divided attention condition, participants viewed the optokinetic stimulus while being presented with an auditory distractor task (the Paced Auditory Serial Addition Test), which required participants to add up a sequence of digits provided through a speaker and report the answer verbally. The number of nystagmus beats was highest during focussed attention and lowest when attention was divided, and the consistency of the OKR waveform was also higher during focussed attention, becoming more unstable during divided attention (see Figure 1.14). This indicates that OKR frequency is reflective of the observer's level of attention. Gain, however, appeared to be related to alertness, as the gain of the OKR was higher during focussed or divided attention conditions and lower during neutral attention. They also reported that there was more VSM activity during focussed attention, which they attributed to the higher OKR frequency seen during this condition. These results show that the OKR may provide a useful proxy measure for both attention and alertness.

Overall, these studies indicate that OKR provides a useful measure for the allocation of visual attention and is sensitive to both attention level and alertness. However, further research is required to understand the way in which attention to different visual field regions and stimuli impacts the OKR in order to fully utilise it as an attention measure.

1.10.2.2 Use of OKR in binocular rivalry research

Binocular rivalry studies typically rely on the observer to report perceptual reversals, such as by a button press (e.g. Logothetis et al., 1996). This can lead to individual differences in performance due to the subjective nature of perceptual judgments, as well as differences in time taken to react to perceptual

reversals. The latter is particularly problematic when perceptual reversals are very frequent (e.g. <200 ms) as it may not be possible for the observer to report every reversal (Aleshin et al., 2019). This therefore poses a threat to the precision

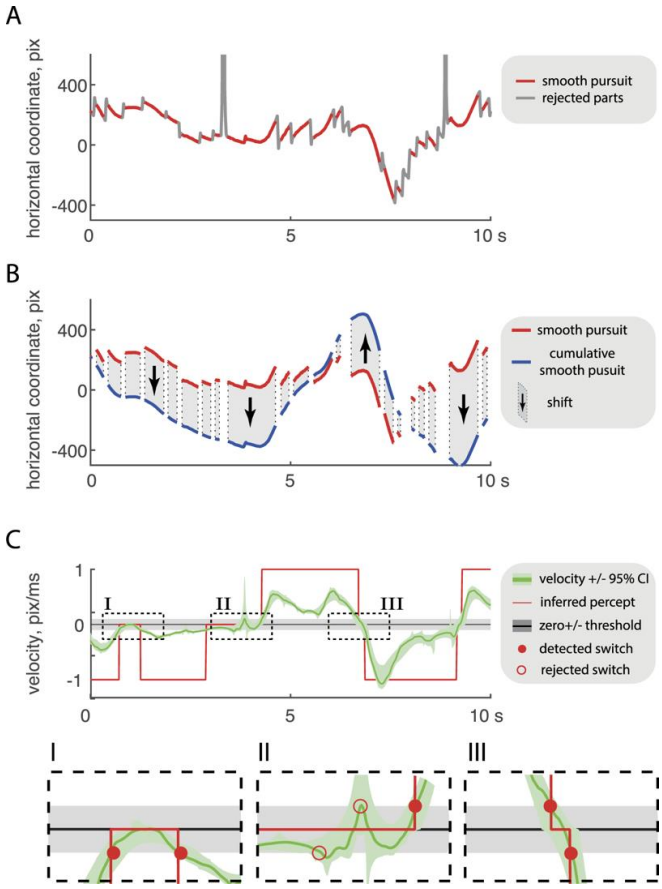

Figure 1.15: From Aleshin et al. (2019). (A) gaze displacement over time with OKR slow phases highlighted in red (here called 'smooth pursuit'). (B) These extracted segments were shifted into alignment (blue traces) as indicated by the arrows. These shifted segments were interpolated and jointed to form a continuous probability density (cumulative smooth pursuit/CSP). (C) Density of the CSP velocity is obtained via numerical differentiation; green trace and light green area indicates the 95% confidence interval (CI). Threshold crossings of the full CI were used to indicate perceptual state. (I) Return transition: CI crosses and re-crosses threshold. Red dots show the nearest mean velocity of the threshold crossing. (II) Red circles show rejected transitions of positive and negative thresholds; red circle shows the accepted transition of the positive threshold. (III) Forward transition: Crossing of the positive and negative threshold.

of the measurement of perceptual reversals. Additionally, the task of indicating the occurrence of a perceptual reversal may interfere with other aspects of some binocular rivalry studies. For example, some research has examined the effects of attention on binocular rivalry (Paffen et al., 2006; Paffen & Alais, 2011), but the task of pressing a button to indicate a reversal requires attention in itself, which may provide an unwanted distractor task during some experiments. OKR may provide a means to resolve this problem (Qian & Brascamp, 2019). Using OKR as a no-report measure for perceptual reversals would also allow for a wider range of observers to be tested, such as very young children and individuals with disabilities that may interfere with their ability to perform a traditional binocular rivalry task effectively.

Qian and Brascamp (2019) used OKR to create a no-report binocular rivalry study investigating the effects of attention on binocular rivalry. They noted discrepancies between studies into the effects of attention on binocular rivalry (e.g. Paffen et al., 2006) and computational models (e.g. Li et al., 2017), which they suggested may have been due to methodological issues arising from the need to report perceptual reversals. They dichoptically presented dot stimuli with different directions of motion while observers performed an auditory attention task. Unfortunately, as this work was presented in the form of an abstract, details of the auditory attention task and the way in which difficulty was manipulated were not provided. Their results showed that as the attention task became more challenging, the frequency of perceptual reversal decreased. This aligned with the results of previous research, leading them to suggest that these results were valid, and that computational models need to be revised to reflect this. Similarly, Aleshin et al. (2019) used OKR as a no-report measure for perceptual reversals in response to dichoptically presented grating stimuli of different colours, finding that compared to existing forms of measurement, their method was 55% less variable. They argued that their data were consistent with oculomotor transitions being reflective of perceptual reversals. They concluded that using 'cumulative smooth pursuit' obtained from OKR slow phases presented an improvement upon existing methods while also offering potentially superior temporal resolution (Figure 1.15).

OKR appears to provide a useful measure of perceptual reversal in binocular rivalry studies, with the potential to improve the temporal resolution of such

data and widen the participant pool. This will allow researchers to more precisely examine the temporal features of binocular rivalry, and to test observers who may otherwise be unable to participate.

1.11 Conclusion

The use of OKR as a measure for attention and perceptual reversals are just examples of its potential uses in research; a greater understanding of the OKR in terms of attention, task instruction, visual field location and stimulus features is needed, not only to better understand the fundamental mechanisms underlying mammalian vision, but because it is crucial if OKR is to be more widely implemented as an objective no-report proxy measure in research, adding a valuable tool to the researchers' arsenal. Beyond the world of research, the OKR may also provide a useful tool to measure a variety of visual parameters such as acuity, contrast sensitivity, stereopsis, colour sensitivity, and more, without the need for patient report. A greater understand of the way in which OKR is driven can therefore also improve the exploitation of OKR as a clinical tool. The creation of effective no-report measures for research and clinical settings will allow for the inclusion of a wider range of individuals in research and for greater accessibility to clinical testing of vision for individuals who may be unable to engage in traditional testing methods. The literature reviewed in this chapter represents decades of work carried out with the goal of understanding the OKR; however, unresolved issues remain. This project aims to address some of these issues. To this end, the following chapters will report three experiments conducted with the aim of better understanding the nature of the OKR and OKAN in normal adult human observers. These experiments will investigate the roles of stimulus size, speed and direction of motion, stimulus eccentricity, task instruction and attention in the human OKR.

Chapter 2

General Methods

2.1 Hardware

2.1.1 Eye tracker

Figure 2.1: Photographs of the experimental setup, showing the EyeLink 1000 (SR Research) in the tower mount setup. In front of the EyeLink is the BenQ TK700STi projector and projector screen used to display stimuli in experiments 2 and 3. In Experiment 1, an Iiyama Vision Master Pro 514 CRT monitor was used in place of the projector.

Eye movements were recorded monocularly using an EyeLink 1000 (SR Research) eye tracker in the tower mount setup with a 25mm lens (Figure 2.1). For all but one participant, the right eye was recorded; the left eye was recorded

from the remaining participant due to a long-standing ocular pathology that restricted visual function in the right eye. Participants requiring refractive correction were requested to use contact lenses. Gaze position and pupil size (using ellipse fitting model) were sampled at a rate of 500Hz; though the tracker was capable of a sample rate of up to 1000Hz, the initial data collected for the experiment was binocular, thus limited to a sample rate 500Hz. A decision was made to instead use monocular data due to a need to use the tower mount setup in place of the desktop emitter; however, to maintain consistency with the initial data, a sample rate of 500Hz continued to be used. The head was stabilised using an SR Research head and chin rest, onto which the eye tracker was mounted. Prior to each block of stimuli, the eye tracker was calibrated using a nine-point (3x3) calibration grid featuring a circular black calibration target against a grey background. Calibrations were validated to check for error, and only accepted when they achieved a rating of 'good' by the EyeLink system (worst point error <1.5°, average error <1.0°). Eye tracking was carried out in a dark room without windows.

2.1.2 Displays

Experiment 1 used an Iiyama Vision Master Pro 514 85Hz CRT monitor with a screen size of 40.5cm (width) by 30.5cm (height) and a resolution of 1024 (horizontal) by 768 (vertical) pixels. The display was viewed from a distance of 75cm, resulting in a subtended display size of 30.2 deg (width) by 22.9 deg (height).

All subsequent experiments displayed stimuli by front projecting them onto a white projection screen using a BenQ TK700STi projector set to a resolution of 1920 (horizontal) by 1080 (vertical) pixels and a frame rate of 240Hz. The average luminance of the display was 94.8lm (range: 0.38–310.5lm, gamma = 1.6). Stimuli were projected from a throw distance of 133.5cm, resulting in a projection size of 143cm (width) by 85cm (height). The display was viewed by participants from a distance of 170cm, resulting in a subtended display size of 45.6 deg (width) by 28.1 deg (height). An image of this setup is shown in Figure 2.1.

2.2 Software

Experiments were written and run using PsychToolbox-3 (http://psychtoolbox.org) (Brainard, 1997) in MATLAB (https://uk.mathworks.com/products/matlab.html) R2014b (Experiment 1) and MATLAB R2021a (all subsequent experiments). The eye tracking components of the experiment were written using the EyeLink Toolbox (Cornelissen et al., 2002) for PsychToolbox-3 in MATLAB. Data analysis was conducted using MATLAB R2020b, MATLAB R2023a and MATLAB R2024a. Circular statistics were conducted in MATLAB R2024a using the Circular Statistics Toolbox (Directional Statistics) (Berens, 2009).

2.3 Stimuli

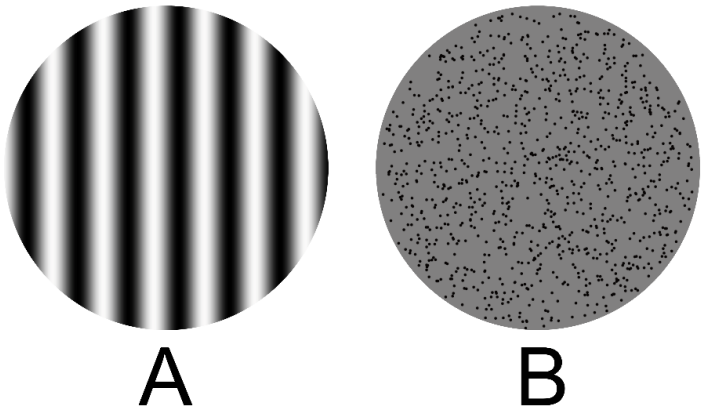

Figure 2.2: Examples of the main types of stimuli used in these experiments. (A) A sinusoidal luminance grating stimulus used in Experiment 1. The example shown, featuring vertical stripes, was used in trials with horizontal (left/right) motion; different orientations of gratings were used to display vertical and oblique motion. Gratings had an SF of 0.5 cyc/deg and drifted at 10, 20 and 40 deg/s. Grating stimuli were presented with a circular black aperture with a diameter of 21.52 deg. (B) A random-dot kinematogram, such as that used in Experiment 2 onwards. Random-dot kinematograms presented black dots against a grey background, drifting at 15 or 30 deg/s. Dot density, dot size and overall stimulus size varied across experiments.

Experiment 1 used black and white sinusoidal luminance grating stimuli (Figure 2.2, A), whereas all subsequent experiments used random-dot kinematograms (Figure 2.2, B). Across all experiments, all stimuli were displayed with circular apertures to allow for various directions of motion to be presented without the occurrence of edges perpendicular to the direction of motion. The stimulus parameters used in each experiment will be described in detail in the relevant chapters.

2.3.1 Grating stimuli

Sinusoidal grating stimuli were used to drive OKR and OKAN in Experiment 1 (Figure 2.2, A). These stimuli were black and white gratings with a spatial frequency of 0.5 cyc/deg. Grating stimuli were animated by updating the phase of the sinusoid on each frame. They were presented at speeds of 10 deg/s (5Hz), 20 deg/s (10Hz) and 40 deg/s (20Hz). Eight directions of motion were used across four orientations: horizontal (left/right) motion using vertical stripes; vertical (up/down) motion using horizontal stripes; oblique +45° (up-right/down-left) motion using -45° stripes; oblique -45° (up-left/down-right) motion using +45° stripes. Stimuli were each presented for 50 seconds and were displayed centrally.

2.3.2 Random-dot kinematogram (RDK) stimuli

Following Experiment 1, all subsequent stimuli used were circular random-dot kinematograms (RDKs) (Figure 2.2, B). Black dots (0.38lm) were presented against a grey (94.8lm) background. Dots drifted at a speed of 15 deg/s, with the exception of two conditions in Experiment 2 which were repeated at 30 deg/s to assess whether results remained consistent at a higher stimulus velocity. Dot size and density varied between experiments, in addition to the stimulated retinal location, stimulus area, and aperture type. RDK stimuli will thus be described in greater detail in the relevant chapters.

On initiation of the stimulus, each dot was assigned a random starting position; these starting positions were independent of each other, meaning that

dots sometimes overlapped and formed clusters. Dots drifted with 100% directional coherency in the majority of trials. During Experiment 2 trials using Brownian (random-walk) motion, global dot motion was not coherent, and dots were instead each assigned a random direction of motion on each frame. When dots reached the edge of the aperture, they were re-drawn on the opposite side. Each dot had a lifetime of 1000 frames (4.17 seconds). When the lifetime of a dot expired, it was re-drawn at a random location within the aperture. To prevent dot lifetimes from expiring simultaneously, the starting 'life' of each dot was randomly generated on the first frame of the stimulus.

2.4 Attention (counting) task

Experiments 2 onwards involved methods to increase the amount of visual attention being directed towards the stimulus, or towards particular regions

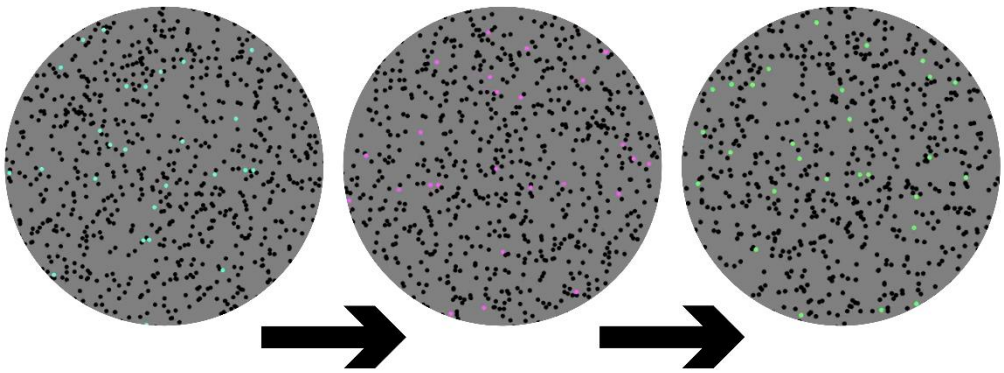

Figure 2.3: Example of the appearance of colour counting task dots in cyan, magenta and green. The density of coloured dots varied based on experiment and condition. Up to eight colours were presented: cyan, magenta, green, blue, purple, red, orange and yellow. Throughout the trial, this subset of dots cycled through the randomly pre-selected colours; participants were required to count the number of colours presented and report this number at the end of the trial.

of the stimulus, in order to assess the effects of attention on the OKR. A colour counting task was used to achieve this (Figure 2.3).

During trials using this task, a subset of dots was rendered in colour (cyan (x 0.5031, y 0.7794, z 0.6110), magenta (x 0.7041, y 0.6274, z 0.6364), green (x 0.4332, y 0.7515, z 0.2428), blue (x 0.2786, y 0.1904, z 0.9680), yellow (x 0.7930, y 0.9370, z 0.2597), orange (x 0.5673, y 0.5046, z 0.1254), red (x 0.4810, y 0.3130, z 0.1557) or purple (x 0.6385, y 0.3760, z 0.9848)) instead of black. At the start of each counting task trial, the number of colours to be used was randomly selected between two and eight. The colours to be presented in that trial were then randomly selected from the eight pre-defined colours. Throughout the trial, the subset of coloured task dots cycled through the selected colours in a random order, with each colour only being presented once within the trial, and not repeated. Participants were required to count the number of different colours presented throughout the trial and report this number at the end of the trial. The size, density and location of these coloured task dots varied according to condition and experiment, and as such, will be described in detail in the relevant chapters.

2.5 General procedure

Across all experiments, due to the large number of stimuli being presented, experiments were broken down into a series of blocks; at the end of each block of stimuli, participants were given the option of either continuing to the next block or terminating the session. The duration of each block of stimuli varied between 5-15 minutes, depending on the experiment and condition. Participants were encouraged to terminate the session if they felt fatigued or inattentive. As data were recorded, they were visualised on a display in real time to allow for monitoring of data quality and blink frequency. Prior to each block of stimuli, participants were encouraged to assume a comfortable position, with the aim of minimising head movement and thus eye tracker drift throughout the block. Participants were also instructed to use both the forehead and chin rest to minimise gradual rolling of the head throughout the trial. At the start of each block of stimuli, the eye tracker was calibrated using a nine-point calibration grid, and the calibration was then validated to assess for error. A limited number of blocks

were repeated due to low data quality, with the most frequent cause being signal loss caused by excessive blinking.

Procedures varied across experiments and as such will be provided in further detail in each experimental chapter.

2.6 Data analysis

2.6.1 Assessment of data quality

Prior to the analysis of each trial, raw gaze position and pupil size were plotted against time for visual inspection of the data. In some trials, low data quality resulting from excessive blinking or head movement prevented analysis of the data, therefore visual assessment of data quality was required. In cases of very low data quality that prevented analysis of the data, participants were asked to return to repeat the trial. During Experiment 1, the majority of participants were asked to return to re-record at least one trial. During Experiment 2, this need became less frequent, with fewer than half of participants asked to return to re-record trials. During Experiment 3, no repeating of trials was necessary. The data were inspected blind, prior to viewing trial parameters such as stimulus direction; this allowed a decision to be made about whether an OKR had occurred without that decision being biased by knowledge about the trial type. If the stimulus direction could not be discerned from the raw data due to the lack of clear slow and fast phases in any particular direction (see Figure 2.4), an absence of OKR was determined, and parameters such as gain were recorded as zero.

2.6.2 Segmentation of data based on velocity and direction

To determine when the fast phases started and ended, fast eye movements were detected based on their velocity. This was achieved using an existing code written for detection of microsaccades based on an algorithm developed by Engbert and Kliegl (Engbert & Kliegl, 2003; Engbert & Mergenthaler, 2006). However, as it was being used to detect the fast phases of OKR rather than saccades or microsaccades, the velocity threshold was adjusted to better suit this purpose.

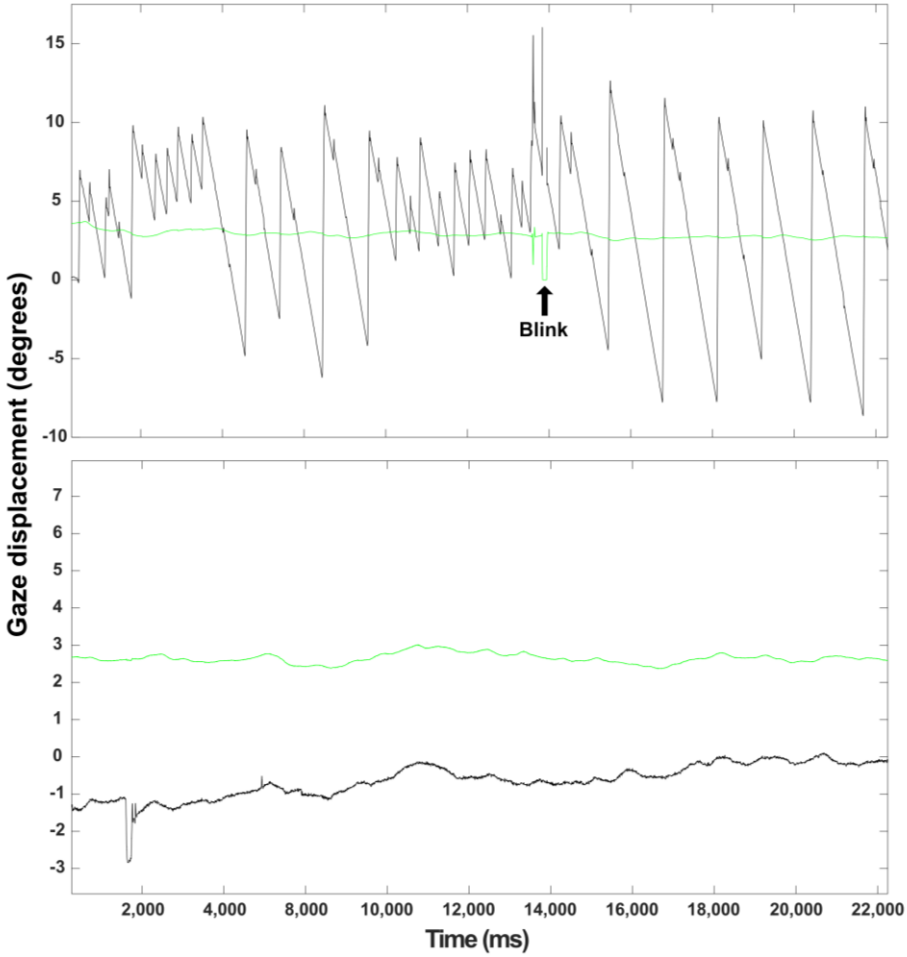

Figure 2.4: Plots comparing two trials, one with occurrence of OKR (upper) and one with a lack of OKR (lower). Gaze position is illustrated in black (deg. of visual angle), while pupil size is illustrated in green (arb. units). On the Y axis, zero indicates the midline of the display. UPPER: Plot showing horizontal gaze displacement over time in response to a leftward drifting stimulus. OKR is evident in the sawtooth waveform: fast phases move upwards and slow phases slope downwards, demonstrating an OKR with leftwards slow phases. LOWER: Plot showing vertical gaze position in response to a vertically drifting stimulus. There are no slow or fast phases, indicating that OKR did not occur during this trial.

This threshold was then continuously adjusted as required throughout the project, as there were large individual differences in fast phase velocity, as well as large differences between conditions. For example, during Experiment 2, which

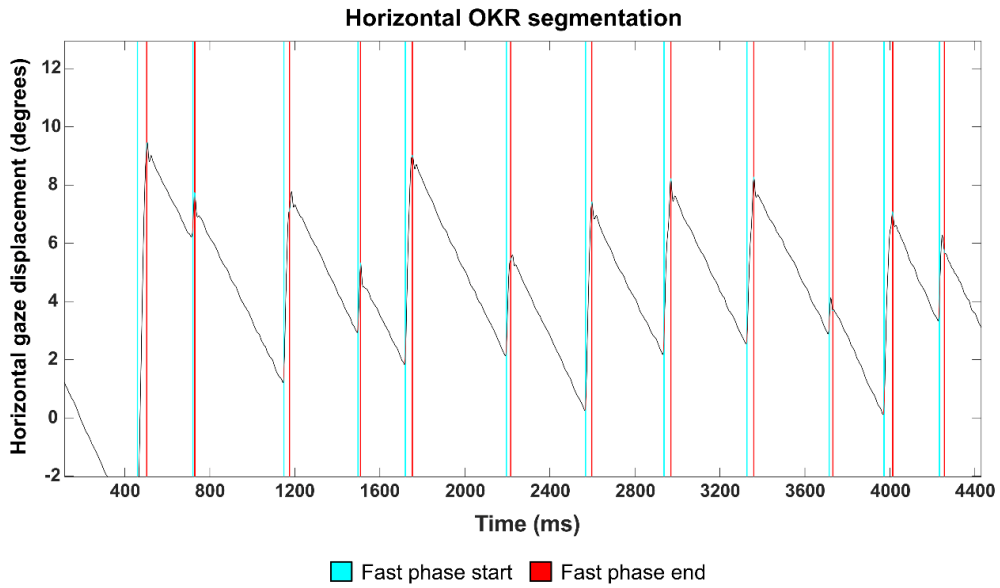

Figure 2.5: A visualisation of the segmentation of OKR data according to fast phase location, showing horizontal gaze displacement over time. Such plots are made following the analysis of each trial to assess how successful the analysis code has been in accurately segmenting the data. Shown here is an OKR in response to a stimulus drifting towards the left, evident due to slow phases sloping downwards. The Y axis shows the horizontal displacement of gaze in deg of visual angle; the X axis shows time in milliseconds. The identified location of the start of each fast phase is shown by vertical blue lines; the location of the end of each fast phase is shown by vertical red lines. By identifying the location of these fast phases through the use of the saccade detection algorithm, it was possible to segment the data into fast phases and slow phases.

used both central and peripheral stimuli, the observed median fast phase velocity per trial ranged from 21.39 deg/s to 488.98 deg/s.

Once the fast eye movements were detected, the data were segmented using this information (Figure 2.5), resulting in segments of data that either contained a fast eye movement or a slow eye movement. Some experimental conditions were associated with a direction-changing OKR, with these direction changes primarily occurring during the slow phases; these changes of slow phase direction were identified using the 'findpeaks' function in MATLAB, and this information was used to further segment the gaze position data (Figure 2.6). 'Minimum peak prominence' was specified as an input argument for the

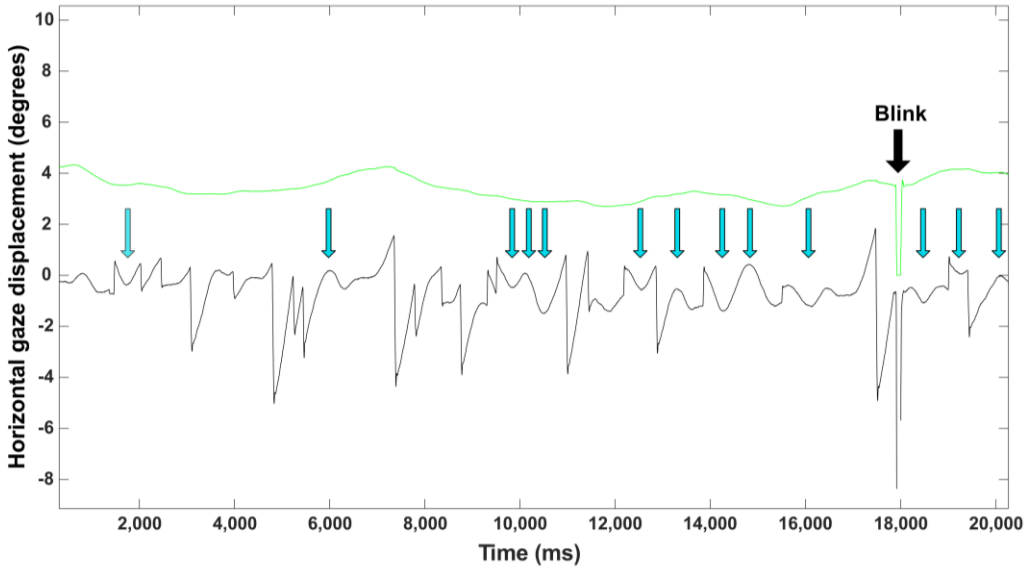

Figure 2.6: Horizontal gaze displacement in response to two simultaneously presented stimuli in a centre-surround configuration with opposing directions of horizontal motion in the centre and in the surround. Gaze position is illustrated in black (deg of visual angle) while pupil size (arb units) is illustrated in green. The black arrow highlights the location of a blink. The blue arrows indicate the locations of slow phase direction changes, forming smooth peaks and troughs in the eye movement trace. During trials containing a direction-changing OKR, the 'findpeaks' function in MATLAB is used to find the location of these peaks and troughs, allowing the direction-changing slow phases to be split. In this way, the portion of the slow phase in response to one direction of stimulus motion can be separated from the portion of the slow phase responding to the opposite direction of stimulus motion. This allows the gain in response to each of the two opposing stimuli to be calculated separately, as well as allowing for more accurate recording of the number of slow phases occurring in response to each stimulus.

'findpeaks' function; this value was set based on visual inspection of the data. Data were visualised as in Figure 2.6 and minimum peak prominence was set by visually assessing the prominence of the smallest peak.

2.6.3 Classification of slow and fast phases

With the data in the form of a series of segments containing slow and fast eye movements, it was possible to assess each segment and classify it as a slow phase, a fast phase, or as neither. This was achieved by first analysing the segment to extract information such as velocity, direction and duration. OKR has a sawtooth waveform, whereby the slow phases follow the approximate stimulus direction, and the fast phases follow a direction opposite to the slow phases. Stimulus direction was therefore taken into account when classifying each data segment, as a slow eye movement with a direction opposite to the stimulus was assumed to not be a slow phase, and a fast eye movement following the same direction as the stimulus was assumed to not be a fast phase. Importantly, this prevented catch-up saccades during slow phases from being classified as fast phases. The exception to this occurred during OKAN trials of Experiment 1, during which OKAN-II (reversed OKAN) was sometimes observed; during analysis of these trials, the data were visually inspected to assess the direction of OKAN, and this information was used in place of stimulus direction.

Velocity and duration thresholds were then used to identify whether each data segment was a fast phase or a slow phase. These thresholds were based on a combination of existing methods and trial-and-error with the present data sets, with the data being continuously plotted and visually assessed to monitor the success of the analysis. For example, the software 2D VOG Analysis Program Version 4.20 (John P. Kelly, https://faculty.washington.edu/jokelly/voganalysis/) can be used for analysis of video-oculography data and includes analysis of OKR. The parameters used by this software for analysis of OKR are the following: a minimum fast phase velocity of 50 deg/s; a maximum slow phase velocity of 150 deg/s; a slow phase duration between 50-1000 ms (reported in Costa, 2011). These were used as the initial parameters in the analysis.

The initial parameter of a maximum slow phase velocity of 150 deg/s was found to not be successful across the large stimulus velocity range used in Experiment 1: at 10 and 20 deg/s stimulus velocity, this threshold was found to be too high, with saccades such as catch-up saccades which follow the stimulus direction being misclassified as slow phases; however, at 40 deg/s stimulus velocity, this maximum peak velocity threshold was found to be too low, filtering some

slow phases out of the analysis. Additionally, there were substantial differences in slow phase velocity based on stimulus direction. As a result, different maximum slow phase velocities were used for different stimulus velocities and directions. The thresholds set for centrally-presented stimuli were as follows: up to 20 deg/s stimulus velocity, a maximum peak slow phase velocity threshold of 100 deg/s was applied for all directions of motion; for 30 deg/s stimulus velocities, and for vertical stimuli at 40 deg/s, a maximum slow phase velocity of 150 deg/s was applied; at 40 deg/s stimulus velocity with horizontal or oblique directions of motion, a maximum slow phase velocity threshold of 200 deg/s was applied. From Experiment 2 onwards, peripheral stimuli were presented; these stimuli were sometimes associated with a much lower slow phase amplitude and velocity, and there were substantial individual differences in peripheral responses. Further, peripheral responses tended to have a less consistent OKR, with a greater number of non-OKR eye movements. For this reason, velocity thresholds were frequently adjusted during analysis of such trials, with a maximum slow phase velocity as low as 15 deg/s being required in some cases.

In reference to fast phase velocity thresholds, the initial minimum velocity threshold of 50 deg/s was found to be too low in response to centrally presented stimuli, and during Experiment 1, fast phases were found to frequently exceed 300 deg/s. The minimum velocity threshold was thus increased to 100 deg/s. However, from Experiment 2 onwards, peripheral stimuli were presented; these stimuli were associated with a much lower fast phase amplitude and velocity. As a result, a lower minimum fast phase velocity threshold of 40 deg/s was implemented for such trials. However, as with the analysis of slow phases, this threshold for fast phase velocity was adjusted when necessary. Fast phases resemble saccades, and as such, peak velocity is positively related to amplitude and shows a large range (e.g. ~100-700 deg/s peak velocity observed across a range of amplitudes by (Garbutt et al., 2001)). For this reason, fast phase velocity varied considerably across conditions, as fast phase amplitude was very variable.

In addition to using direction and velocity to identify fast and slow phases of OKR, duration thresholds were also used in this process. In line with the threshold used by 2D VOG Analysis Program Version 4.20, an initial slow phase duration range of 50-1000 ms was used. This range proved unsuccessful in capturing the slow phases observed, particularly due to the difference in slow phase

duration between 'look' and 'stare' conditions in Experiment 1. Some observed slow phases fell around the minimum threshold, therefore this was decreased by a further 10 ms. During look OKR in response to 10 deg/s stimuli during Experiment 1, slow phase durations exceeding 3000 ms were observed, therefore the maximum slow phase duration was increased to 4000 ms. The final slow phase duration range used was therefore 40-4000 ms. Existing data regarding the duration of fast phases are more limited due to a focus on slow phases in the OKR literature, however, a starting threshold of a maximum of 400 ms was set. This threshold was found to be successful in extracting the observed fast phases.

Following the analysis of each trial, the results of the analysis were plotted and compared to the initial raw data to assess the success of the analysis. In some cases, it was clear that many slow phases had not been successfully extracted from the data, therefore thresholds were adjusted as required to maximise the success of the analysis.

2.6.4 Blink removal and data smoothing

Prior to data segmentation, blinks were identified based on a pupil size of zero (Figure 2.4, Figure 2.6). The 200 ms of data around each blink were also marked as part of the blink, to account for distortion of the data immediately preceding the blink and to allow time for recovery of the signal following each blink (as done by Kanari et al., 2017 and Kanari and Kaneko 2019). After segmentation of the data, any segment that was marked as part of a blink was removed. During trials in which participants were required to maintain gaze within a certain region of the display, gaze deviations away from this region were treated in the same manner as blinks to ensure that all data analysed were acquired while the participant viewed the correct region of the stimulus.

Velocities were smoothed using a Savitsky-Golay filter (as used by Doustkouhi et al., 2020b, and Ghasia and Shaikh, 2015) with a window size of 30 samples (60 ms) before being classified as slow phases or fast phases. Data smoothing occurred prior to any classification of eye movement types: velocities were smoothed prior to the initial detection of fast eye movements for data segmentation, and the raw, unsmoothed data were then segmented based on that information. The Savitsky-Golay filter was then applied to the segmented data

prior to slow and fast phase classification. The underlying reason for segmenting the unsmoothed data and then re-smoothing after segmentation was to prevent the sharp peaks and troughs in the nystagmus waveform from being dulled.

2.6.5 Calculating OKR measures

2.6.5.1 Velocity and gain

Velocity was calculated as the first derivative of position over time: displacement between adjacent gaze position samples was calculated for the X and Y gaze displacement separately (i.e. horizontal and vertical gaze displacement were first calculated separately). Displacement was then multiplied by the sample rate to obtain velocity across each X and Y gaze position vector, giving $X_{velocity}$ and $Y_{velocity}$. Resultant velocity was then calculated as:

$$\text{Resultant velocity} = \sqrt{X_{velocity}^{2} + Y_{velocity}^{2}}$$

Mean, median and peak velocities for each slow phase and fast phase were then obtained.

The 'gain' of the OKR is a ratio measure describing how closely the slow phase velocity matches the stimulus velocity, whereby a gain of 1.0 indicates identical slow phase and stimulus velocity. Gain was calculated as (e.g. Collewijn, 1985):

$$\text{Gain} = \frac{\text{Slow phase velocity}}{\text{Stimulus velocity}}$$

Mean and median gain were then obtained for each slow phase.

2.6.5.2 Amplitude

The amplitude represents the distance travelled in each phase, in deg of visual angle. Amplitude is thus the difference in gaze position between the start and end of the phase. To calculate this, the distance travelled was first calculated separately for the X and Y gaze displacement of each slow or fast phase (i.e. the horizontal and vertical amplitude were calculated separately). The overall amplitude of the phase was then calculated as:

$$\text{Amplitude} = \sqrt{X_{amplitude}^{\ 2} + Y_{amplitude}^{\ 2}}$$

2.6.5.3 Angle/Direction

Each slow or fast phase was also analysed to extract its average angle or direction. The X and Y amplitude of each phase was calculated separately as described above. These values were then used to trigonometrically calculate the overall angle of the eye movement, θ:

$$\theta = \tan^{-1}\left(Y_{amplitude} \Big/ X_{amplitude}\right)$$

2.6.5.4 Frequency

To calculate the frequency of the OKR, the number of slow phases that occurred during a given trial was divided by the duration of the trial in seconds, giving frequency in mean slow phases per second.

$$f = \frac{\text{Number of slow phases}}{\text{Trial duration}}$$

Chapter 3

Experiment 1: The effect of task instruction, stimulus speed and direction of motion

3.1 Introduction

The instructions given to an observer prior to viewing an optokinetic stimulus are known to impact the OKR produced in response to the stimulus. 'Look' OKR is produced when an observer is told to actively fixate and follow features of the moving stimulus, whereas 'stare' OKR is produced when an observer is told to passively gaze towards the stimulus (Garbutt & Harris, 1999). OKR therefore has both reflexive and voluntary components (Pola & Wyatt, 1985) which can be observed through manipulation of task instructions. In the following chapter, look and stare OKR will be investigated in response to a range of stimulus directions and velocities, and the resulting OKAN will be analysed.

Look and stare OKR have characteristic differences. Compared to stare OKR, look OKR is described as having lower frequency, higher amplitude slow phases (Knapp et al., 2008) and is often found to have higher gain (Valmaggia et al., 2005). The differences between look and stare OKR are reflected in the brain, with fMRI studies of humans showing higher levels of cortical activation during look OKR (Kashou et al., 2010; Konen et al., 2005) and greater similarity in activation sites between look OKR, smooth pursuit eye movements (SPEM) and saccades (Kashou et al., 2010). Some have referred to stare OKR as a 'passive' response and to look OKR as an 'active' response (Pola & Wyatt, 1985), while others have gone as far as to propose that look OKR is a combination of SPEM and saccades rather than being 'true' optokinesis like stare OKR (Kashou et al., 2010). Overall, look OKR is generally viewed as being a voluntary response whereas stare OKR is viewed as being involuntary and reflexive.

OKR also has short- and long-time-constant components: early OKR (EOKR) and late OKR (LOKR) (Garbutt & Harris, 1999), which are also referred to as the direct and indirect pathways, or as the fast and slow pathways, respectively. While EOKR is thought to be generated by a cortico-ponto-cerebellar pathway similar to that of SPEM, LOKR is thought to be mediated by a subcortical pathway (Fuchs & Mustari, 1993). Whereas LOKR slow phase velocity builds up gradually, EOKR is associated with a rapid build-up of slow phase velocity (~5 seconds, Abadi et al., 1994). LOKR is also associated with a gradual decay of slow phase velocity, manifesting as a post-exposure effect known as optokinetic after-nystagmus (OKAN) (Collewijn, 1985) which can be recorded when an observer is placed in complete darkness upon termination of the stimulus. OKAN can therefore be used as an indicator that LOKR has occurred (Lafortune et al., 1986b, 1986a).

One may be tempted to draw parallels between look OKR and EOKR, and between stare OKR and LOKR. Pola and Wyatt (1985) described look OKR as being a form of foveal tracking closely related to SPEM: voluntary and position-based. In contrast, they described stare OKR as being reflexive and velocity-based, stabilising the overall retinal image rather than foveating and stabilising individual stimulus features. The velocity-based nature of stare OKR implies that foveation of the stimulus is not necessary to produce it; perhaps relatedly, afoveate animals only produce LOKR (Collewijn, 1972, 1985) and LOKR dominates in humans with maldeveloped foveae (Baloh et al., 1980a). EOKR and LOKR are thought to be linked to cortical and subcortical pathways, respectively (Fuchs & Mustari, 1993; Leigh & Zee, 2015). Similarly, look OKR has been shown to involve higher levels of cortical activation compared to stare OKR (Kashou et al., 2010; Konen et al., 2005). Primates show both EOKR and LOKR (Cohen et al., 1977) though EOKR is known to dominate in humans under photopic conditions (Garbutt & Harris, 1999). Considering the above evidence, it may be the case that look OKR instructions encourage greater involvement of the cortical EOKR system while stare OKR instructions are associated with greater activity of the subcortical LOKR system or reduced activity of the EOKR system.

As previously stated, the occurrence of LOKR can be assessed by observing the occurrence of OKAN following termination of the stimulus (Lafortune et al., 1986b, 1986a). In this way, the following experiment will evaluate whether

look or stare instructions are more highly associated with activity of the LOKR component. Evidence from monkeys suggests that foveal tracking of optokinetic stimuli does not contribute significant charge to the velocity storage mechanism responsible for producing OKAN (Lisberger et al., 1981); this evidence has been used to suggest that OKAN, and thus LOKR, may be related to stare OKR (Knapp et al., 2013), though this has not been verified in humans. Past research in humans has shown that OKAN is associated with higher stimulus velocities. For example, Lafortune et al. (1986b) showed that OKAN was associated with a long-time-constant component which was maximally active in the 40-70 deg/s stimulus velocity range, whereas stimulus velocities in the range of 10-30 deg/s were more associated with a short-time-constant component that was attributed to SPEM. In the following experiment, stimuli are presented at velocities of 10 deg/s, 20 deg/s and 40 deg/s; it is expected that more OKAN will be observed following the presentation of stimuli moving at 40 deg/s. OKAN is thought to be the main evidence of LOKR activity in humans, with some studies reporting that the rapid build-up of OKR in humans resulting from EOKR activity prevents a gradual build-up of gain from being observed (Cohen et al., 1981). To verify this, build-up of gain will also be investigated in the following chapter.

The following experiment will also examine the effects of different directions of stimulus motion on both OKR and OKAN. The majority of past OKR research has involved measuring responses to horizontal stimulus motion, with a smaller number of studies investigating vertical motion. Human studies involving oblique stimulus motion are largely absent from the OKR literature. There have been inconsistencies regarding the up-down symmetry of the vertical OKR. Some studies have reported higher gain in response to upward drifting stimuli (Howard & Simpson, 1989; Murasugi & Howard, 1989b). While some have found that this asymmetry does not exist at low (~10-15 deg/s) stimulus velocities (Kanari et al., 2017; Murasugi & Howard, 1989b), others have reported asymmetry in response to 10 deg/s stimuli (Garbutt, Han, Kumar, Harwood, Harris, et al., 2003). To clarify this issue, the following experiment will investigate whether vertical OKR is asymmetrical, and if so, whether this is a velocity-based effect. Oblique OKR involves a combination of vertical and horizontal components; it is therefore expected that vertical OKR asymmetries will be reflected to a lesser extent in oblique OKR.

Oblique OKR in humans has not been well characterised. To rectify this, oblique OKR will be recorded in response to a range of stimulus speeds to assess whether characteristics, such as gain, fall precisely between those of vertical and horizontal OKR. This would indicate equal combination of vertical and horizontal components in producing oblique OKR. With the head upright, experiments involving monkeys have reported that oblique OKR shifts towards the horizontal axis at high stimulus velocities due to the breakdown of the vertical OKR component (Kröller & Behrens, 1995). Difficulty in producing vertical OKR at such high velocities results in a shift towards the horizontal axis to maintain gain. In humans, vertical OKR has been shown to lose gain at high stimulus velocities to a greater extent than horizontal OKR, particularly with reference to stare OKR (Valmaggia et al., 2005). It is therefore anticipated that at a high stimulus velocity (40 deg/s) a shift of oblique OKR direction towards the horizontal axis will too be observed, and stare OKR may be more severely affected. In monkeys, vertical OKAN asymmetry has been reported whereby upward OKAN is weak or absent (Raphan & Cohen, 1988; Matsuo & Cohen, 1984), with Kröller and Behrens (1995) reporting almost no vertical OKAN. The following experiment will confirm whether these effects reported in monkeys can be replicated in human observers.

Finally, the following experiment will also investigate OKAN reversal. Though reversal of OKAN (OKAN-II) with respect to the preceding stimulus has been widely reported in OKAN studies using humans, monkeys and cats (Brandt et al., 1974; Clément et al., 1981; Collewijn, 1985; Gygli et al., 2021; Raphan & Cohen, 1988; Ventre-Dominey & Luyat, 2009), the cause is not well understood. A velocity-based effect has been reported in which higher stimulus velocities are associated with OKAN reversal (Collewijn, 1985). Some authors (Brandt et al., 1974; Chen et al., 2014; Gygli et al., 2021; Ventre-Dominey & Luyat, 2009) have described OKAN reversal as partially resulting from a form of motion adaptation, due to finding reversed OKAN following fixation of a cross used to suppress OKR and following prolonged optokinetic stimulation. Brandt et al. (1974) suggested that if the remaining 'optokinetic charge' is outweighed by the 'habituative countercharge', OKAN direction will reverse. The suggestion is thus that greater retinal slip resulting from suppression of OKR during optokinetic stimulation results in motion habituation leading to OKAN reversal

(Ventre-Dominey & Luyat, 2009). It is suggested that OKAN-I and OKAN-II may thus be mediated by separate mechanisms (Gygli et al., 2021).

Building on this, one might expect that low gain OKR should also be associated with OKAN reversal due to higher levels of retinal slip. Similarly, an OKR that does not accurately follow the direction of stimulus motion might also result in OKAN reversal. While past research of OKAN reversal has primarily focussed on features of the optokinetic stimulus itself, an analysis that takes the preceding OKR into account may offer further information about the cause of reversal. In this way, the use of oblique optokinetic stimuli in the following experiment may offer insights into OKAN reversal; for example, if the findings of a shift of oblique OKR towards the horizontal axis can be replicated (Kröller & Behrens, 1995), one might expect to see an OKAN that is vertically reversed. This is because horizontally following an oblique stimulus would result in net vertical motion across the retina, potentially leading to adaptation to vertical, but not horizontal, motion. Further, an OKAN which is reversed in only its vertical or horizontal component would also imply that vertical and horizontal velocity storage is separate. In the following experiment, OKAN in response to multiple directions and velocities of stimulus motion will be recorded. OKAN will be analysed in a way which considers the preceding OKR in terms of its direction and gain in an attempt to better understand the cause of OKAN reversal.

In addition to addressing the outlined research questions, this initial experiment will play an important role in determining stimulus parameters for subsequent experiments. The use of a range of stimulus velocities and directions will allow for floor and ceiling effects in OKR capabilities to be assessed across a range of participants. This will provide a basis for selecting appropriate stimulus parameters moving forward.

The following experiment (Experiment 1) aims to measure OKR in terms of slow phase gain, amplitude, frequency and angular trajectory/direction in response to various directions and velocities of stimulus motion. Both look and stare OKR will be produced via the manipulation of task instructions. Issues identified during the course of this experiment leading to methodological changes for subsequent experiments will also be discussed.

3.2 Selection of stimulus parameters

The stimulus parameters used in this experiment were chosen based on the outcomes of past research. The following section will outline the basis of these decisions.

3.2.1 Velocity and spatial frequency

Past OKR and OKAN research has used a wide range of stimulus speeds and spatial frequencies (SFs). Table 3.1 displays examples of the stimulus velocity and SF used in past research of human OKR and OKAN and the reported outcomes in terms of gain. It should be noted that stimulus velocity and SF are not the only variables influencing these outcomes; OKR is also affected by factors such as stimulus size and direction of motion (Knapp et al., 2009).

As one of the aims of this experiment was to induce not only OKR, but also OKAN, stimulus parameters were chosen to effectively drive both. Lafortune et al. (1986b) tested OKR and OKAN at a range of stimulus velocities. They described OKAN magnitude as being low and constant at stimulus velocities 10-30 deg/s, and as being high and constant at stimulus velocities 40-70 deg/s, which they interpreted as reflecting the velocity ranges producing maximal activity of the EOKR and LOKR components, respectively. They reported that initial slow phase velocity of OKAN was dependent on stimulus velocity, whereas the decay time constant was not. Stimulus parameters were also chosen to avoid floor and ceiling effects; a range of OKR gain outcomes were desirable. As shown in Table 3.1, stimulus velocities of 10-20 deg/s are often reported to result in a high-gain (~0.80-1.0) OKR. The response to stimulus velocities of 30 deg/s and higher appear more mixed, likely a result of variation in other stimulus parameters such as direction of motion. For example, whereas Abadi et al. (2005) reported a gain of ~0.90 in response to a full-field 40 deg/s horizontally drifting grating stimulus, Murasugi and Howard (1989b) reported a gain of ~0.50-0.70 in response to a full-field 30 deg/s vertically drifting dot stimulus, with lower gain being obtained in response to downward-drifting stimuli compared to upward-drifting stimuli.

Table 3.1

Stimulus SF and velocity used in past OKR research

Author	Spatial Frequency	Velocity	Outcome
Howard and Gonzalez (1987) (experiment 1)	2.5° black stripes with 5° white stripes (square wave)	20 deg/s	OKR gain of ~0.70
Valmaggia et al. (2005)	0.25 cyc/deg black and white square wave grating	15, 30, 45 and 60 deg/s	OKR gain of ~0.90-1.00, ~0.65-0.90, ~0.50-0.80 and ~0.30-0.70, respectively (control group, all motion directions)
Murasugi and Howard (1989b)	2° dots with a density of 450 dots/m²	OKR: 10, 30, 50 and 70 deg/s OKAN: 30 deg/s	OKR gain of ~0.80-0.90, ~0.50-0.70, ~0.30-0.70 and ~0.25-0.35, respectively (full field) OKAN initial velocity of ~0.00-8.50 deg/s (full field)
Kanari and Kaneko (2019)	Dots with a density of 0.4 dots/deg²	31 deg/s	OKR gain of ~0.4 when vergence and attention are both at the centre
Abadi et al. (2005) (experiment 2)	0.25 cyc/deg black and white square wave grating	20, 40, 60 and 80 deg/s	Full field: OKR gain of ~0.90, ~0.90, ~0.80 and ~0.75, respectively 20° field: OKR gain of ~0.90, ~0.75, ~0.70 and 0.55, respectively
Doustkouhi et al. (2020b)	1.3 cyc/deg (SF filtered 2D random noise carrier)	10 deg/s	OKR gain of ~0.92

With consideration to past research, the selected stimulus velocities for this experiment are 10, 20 and 40 deg/s. Stimuli drifting at 10 deg/s are expected to produce high-gain OKR, whereas stimuli at 40 deg/s are expected to produce OKR with a lower gain. In light of Lafortune et al.'s (1986b) report, OKAN is

expected to be driven at these velocities, however, more OKAN is expected to result from the 40 deg/s stimulus. As shown in Table 3.1, the pattern and SF of OKR stimuli varies across studies, and selection of SF and velocity is limited by the frame rate of the display, as an insufficient frame rate for the chosen parameters will result in aliasing. It is also desirable to have multiple cycles available on-screen to increase the number of potential pursuit targets during look OKR. For these reasons, a black and white sinusoidal luminance grating with an SF of 0.5 cyc/deg was chosen, as this allowed for a grating to be presented at a range of stimulus velocities while avoiding aliasing of the 40 deg/s stimulus with an 85Hz display. These chosen stimulus velocities and SF produced gratings presented at 5Hz, 10Hz and 20Hz.

3.2.2 Duration of exposure

As the EOKR system is able to build up slow phase velocity to near stimulus velocity within five seconds (Abadi et al., 2005), it was expected that the EOKR system would be active even with a relatively short stimulus duration. The priority was therefore selecting a stimulus duration that would activate the LOKR system and produce OKAN. Examples of studies examining human OKAN with their stimulus durations and outcomes in terms of OKAN velocity and duration are reported in Table 3.2.

Though Bertolini et al. (2021) and Murasugi and Howard (1989b) used different stimulus durations (30 and 50 seconds, respectively) to produce OKAN, they both reported an OKAN with similar durations of 30 and 25 seconds, respectively. Despite Ventre-Dominey and Luyat (2009) using a stimulus duration almost double that of Murasugi and Howard (1989b), the reported initial OKAN velocity and duration was comparable. Lafortune et al. (1986a) tested a range of stimulus durations and reported their effects on different OKAN parameters such as cumulative displacement and slow phase duration. Though different OKAN parameters were found to have different time constants, they produced an estimate of the OKAN 'charging' time constant of 46.93±9.93 seconds based on an average of these parameters. In contrast, Cohen et al. (1981) produced a much lower estimate of the OKAN charging time constant based on slow phase

velocity to be ~20 seconds, highlighting the variation in estimates that can be produced when examining different outcome variables.

Lafortune et al.'s (1986a) study was used as the primary basis for the stimulus duration of 50 seconds selected for Experiment 1.

Table 3.2

Stimulus durations used in past OKAN research

Author	Stimulus duration	Outcome
Murasugi and Howard (1989b)	50 seconds	Initial OKAN velocity (gain): ~0.00-8.50 deg/s (~0.00-0.28) OKAN duration: 12-25 seconds
Bertolini et al. (2021)	30 seconds	OKAN produced with a velocity approaching 0 at ~30 seconds
Ventre-Dominey and Luyat (2009)	90 seconds	Initial OKAN velocity (gain): 7 deg/s (0.14) (OKAN-I) OKAN decay time constant: ~5 seconds (range 1.5-26 seconds) (OKAN-I)
Lafortune et al. (1986a)	5, 10, 20, 30, 40 and 60 seconds	Increasing exposure time up to 40 seconds significantly increased cumulative displacement and slow phase duration

3.2.3 Direction of motion

Past OKR research has focussed on horizontal and vertical motion, the result of which is that oblique OKR and OKAN is less well understood. In terms of OKAN reversal, use of oblique motion provides an opportunity to examine vertical and horizontal velocity storage together to examine the extent to which they are separate mechanisms, for example by testing whether OKAN can be reversed in one dimension but not the other. For these reasons, both cardinal and oblique directions of motion were used in Experiment 1. As there are inconsistencies in the literature regarding the symmetry of vertical OKR (Garbutt, Han, Kumar, Harwood, Harris, et al., 2003; Howard & Simpson, 1989; Kanari et al.,

2017; Murasugi & Howard, 1989b), both directions of motion were used for each orientation of motion (e.g. during horizontal motion, both leftward and rightward motion were used). Experiment 1 therefore used a total of eight directions of motion and four grating orientations: vertical (up/down) motion using horizontal gratings; horizontal (left/right) motion using vertical gratings; oblique +45° (up-right/down-left) motion using -45° gratings; -45° (up-left/down-right) motion using +45° gratings. Stimuli were presented within a circular aperture to avoid edge artefacts that would have a suppressive effect on the OKR (Murasugi et al., 1986). Importantly, this also avoided the aperture problem: presenting oblique motion within a square aperture results in the perception of vertical or horizontal motion.

3.2.4 Selection of look and stare OKR instructions

Past look and stare OKR research has used a variety of different instructions to produce look and stare OKR, which may result in variability between the resulting behaviours across studies. For example, Valmaggia et al. (2005) provided instructions that appeared to instruct participants towards a particular slow phase amplitude. During look conditions, participants were instructed to fixate a stripe as it entered the display and to continue fixating it until it left at the other side of the display, thus driving a slow phase amplitude with the approximate height or width of the display, depending on motion direction. It is therefore not surprising that horizontal amplitude is reported as being higher than vertical amplitude, as the horizontal extent of the display was 13° larger than the vertical extent. That their figures show a horizontal look OKR amplitude of 50° is also to be expected, as their display was 54° in width. In contrast, during stare OKR, participants were instructed to fixate stripes as they crossed the centre of the screen. It is thus possible that the resulting small amplitude OKR was a result of participants' attempts to maintain central gaze. These instructions are also unusual in that participants are told to fixate the stimulus features during stare conditions. The look and stare instructions provided by Valmaggia et al. (2005) appear to be based on the prior expectation that look OKR has a large amplitude whereas stare OKR has a small amplitude, potentially impacting the outcome.

Pola and Wyatt (1985) provided comparatively vague instructions to participants. During look conditions, participants were instructed to 'attempt to look at the round target' whereas during stare conditions they were instructed to 'gaze ahead, but avoid doing anything in particular'. While these instructions do not bias responses to a particular amplitude, as was the case for Valmaggia et al. (2005), they do leave open the possibility that participants may not converge on the stimulus during stare OKR conditions. Knapp et al. (2008) provided a different set of instructions to both Valmaggia et al. (2005) and Pola and Wyatt (1985). During look conditions, participants were told to 'actively fix and follow individual OKN target stripes' and during stare conditions were told to 'look towards the centre of the screen while keeping the stripes in focus'. These instructions encourage participants to pursue stimulus features during look conditions without defining a particular spatial extent of the pursuit movements, and they ensure that participants maintain vergence and ocular accommodation on the stimulus during stare OKR conditions without directly instructing them to fixate the stripes.

The instructions used in Experiment 1 aimed to avoid the prescriptive nature of Valmaggia et al.'s (2005) instructions and to instead allow the participants' eye movement behaviour to emerge more naturally. Ensuring that the participant's gaze was converged upon the stimulus during stare conditions was also desirable. For these reasons, the instructions of Knapp et al. (2008) were used as the basis for the instructions provided in Experiment 1, as they appeared to provide a comfortable mid-ground between being too specific or too vague. During stare conditions, participants were told to 'look towards the screen and keep the image on the screen in focus'; during look conditions, participants were told to 'fixate and follow individual stripes on the screen'.

In both conditions, participants were warned that the screen would turn black at the end of each stimulus. It is during this period of time that OKAN was recorded. The instructions thus also asked that participants continue to look towards the screen after it had turned black; this ensured that participants' gaze remained within an area that the eye tracker was able to record and prevented participants from closing their eyes.

3.3 Methods

3.3.1 Participants

Experiment 1 had an initial pool of 13 participants. However, two participants failed to complete all experimental conditions and the data of three participants who completed all experimental conditions was removed due to consistently low data quality. The remaining eight participants thus formed the final participant pool in this experiment.

Of the eight participants used in this experiment, six were postgraduate students and staff at the University of Nottingham. Three participants were female and the remaining five were male. The age range of participants was 22-53 years. All participants had normal or corrected-to-normal (with contact lenses) vision.

3.3.2 Stimuli

Stimuli were sinusoidal luminance gratings (Figure 3.1) presented at a viewing distance of 75 cm for a duration of 50 seconds. Stimuli had an SF of 0.5 cyc/deg (0.015 cyc/pix) and were presented at speeds of 10 deg/s (5Hz), 20

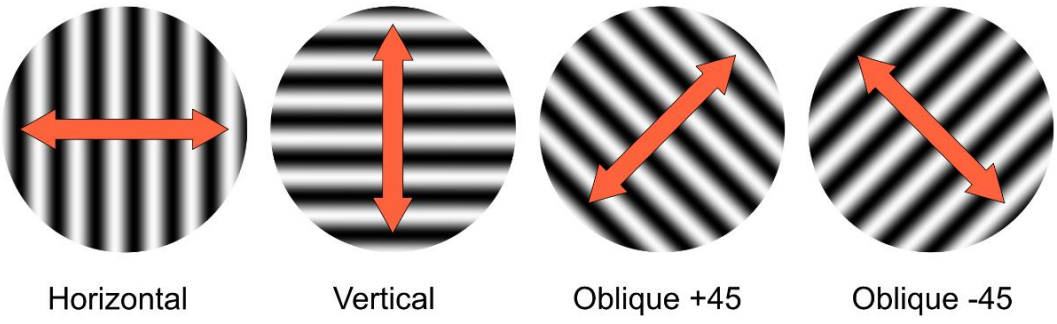

Figure 3.1: The four orientations of black and white sinusoidal luminance grating stimuli used in Experiment 1. The red arrows indicate the two directions of motion used for each grating orientation. Sinusoidal luminance gratings had an SF of 0.5 cyc/deg and were displayed drifting at velocities of 10 deg/s (5Hz), 20 deg/s (10Hz) and 40 deg/s (20Hz) for a duration of 50 seconds.

deg/s (10Hz) and 40 deg/s (20Hz). Stimuli had eight directions of motion across four grating orientations: vertical (up/down) motion using horizontal stripes; horizontal (left/right) motion using vertical stripes; oblique +45° (up-right/down-left) motion using -45° stripes; -45° (up-left/down-right) motion using +45° stripes. Stimuli were presented within a circular black aperture with a diameter of 21.52 deg of visual angle (area = 363.73 deg^2).

3.3.3 Experimental environment

To record OKAN, it is essential that the environment is completely dark. The experiment was thus completed in a dark room with all sources of light removed or covered. Participants were asked to cover any light-emitting devices such as mobile phones and watches to ensure that they were out of view. The eye tracker was used in the tower mount setup to keep the visible light from the IR emitter out of view.

3.3.4 Procedure

At the beginning of each block of stimuli, participants were provided with one of two sets of instructions (see section 3.2.4), depending on whether the block was a look OKR block or a stare OKR block.

The experiment was completed across six blocks, with each block presenting eight stimuli. Three blocks used stare OKR instructions whereas three blocks used look OKR instructions. Each block presented each of the eight directions of motion once and used a single stimulus velocity throughout. Of the three look and three stare OKR blocks, one block presented stimuli at 10 deg/s, one presented stimuli at 20 deg/s and one presented stimuli at 40 deg/s. The order of stimuli within each block and the order in which each participant completed the eight blocks was randomised. Participants were each shown a total of 48 stimuli across the experiment.

Prior to the presentation of instructions, the eye tracker was calibrated using a nine-point calibration grid and the calibration was then validated to assess for error. The instructions were presented to participants, who were given

an unlimited amount of time to read the instructions before initiating the block by pressing the Space key. There was a three-second countdown prior to the presentation of each stimulus in the form of black numbers against a grey background. The stimulus was then presented for 50 seconds. On termination of the stimulus, the screen turned black for 30 seconds to allow for OKAN to be recorded in scotopic conditions. At the end of this 30 seconds, the next stimulus was presented. After eight stimuli were presented and the block was complete, a message appeared on the screen informing the participant that the block had ended. At this point, participants were given the opportunity to continue to the next block or to terminate the session. Each block lasted for ~10.7 minutes, with the entire experiment taking ~64.2 minutes to complete. The lights were switched on between blocks to prevent participants from fully dark adapting throughout the experiment, as this may potentially reduce the amount of OKAN being produced.

Upon inspection of the data, some participants were asked to return to re-record certain trials due to low data quality. Most participants were required to re-record between one and eight trials.

3.4 Results: OKR

3.4.1 Gain

Slow phase gain is calculated by dividing the slow phase velocity by the stimulus velocity; a gain of 1.0 thus indicates that slow phase velocity matched stimulus velocity. The median gain of each slow phase was used due to a skewed velocity distribution within the phase. The mean slow phase gain across the whole trial was then taken. These means are plotted for each of the eight participants, with all directions of motions combined, in Figure 3.2.

Examining OKR data, a linear regression model was calculated to predict the gain of OKR using stimulus velocity (10, 20 and 40 deg/s), orientation of motion (horizontal, vertical and oblique) and instruction type (look and stare) as predictor variables. For orientation of motion, horizontal motion was used as a reference level while vertical and oblique motion were used as indicator variables.

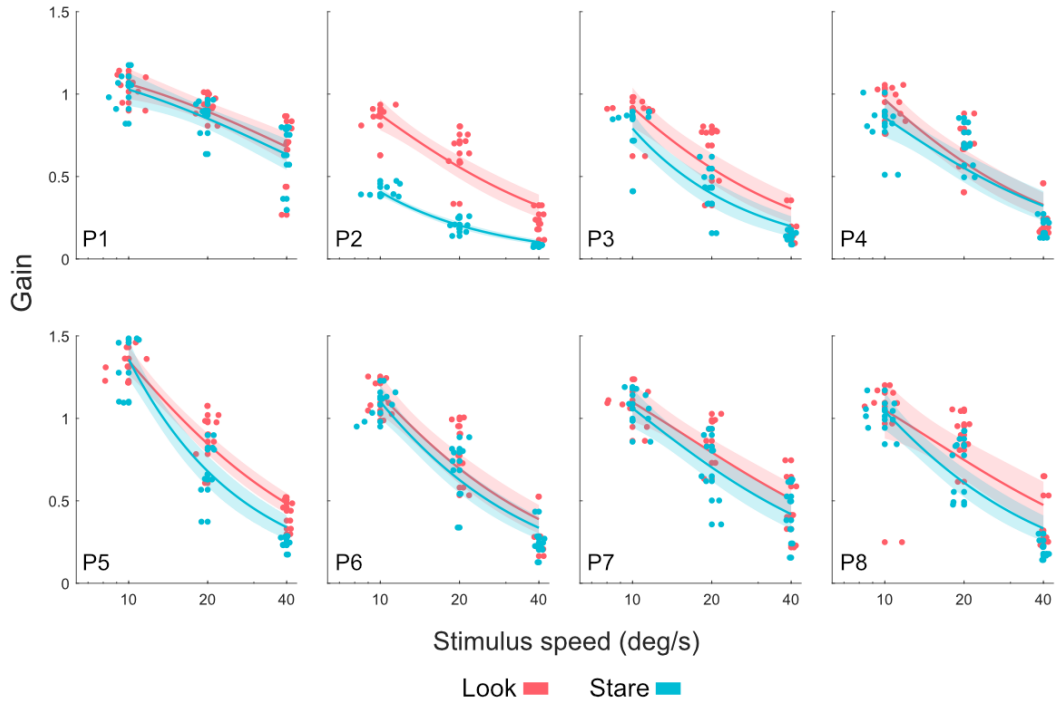

Figure 3.2: Gain in response to stimuli drifting at 10, 20 and 40 deg/s during look and stare OKR conditions in eight individual participants. Responses to look OKR are shown in red and responses to stare OKR are shown in blue. The shaded area indicates the 95% CI of the fitted function. A horizontal jitter of up to 4 deg/s has been applied to increase the visibility of the data points. Each data point represents the mean gain obtained by that participant in a single trial. Participant numbers are indicated in the lower left corner of each plot.

A significant regression equation was found ($F(4, 382) = 195.09$, $p < .001$) with an adjusted R^2 of .670. The results of this analysis are shown in Table 3.3. In this model, velocity ($F(1, 378) = 694.13$, $p < .001$), orientation of motion ($F(2, 378) = 30.662$, $p < .001$) and instruction type ($F(1, 378) = 28.689$, $p < .001$) were all found to significantly predict OKR gain. Using horizontal motion as a reference level, vertical motion was found to significantly reduce gain ($\beta = -0.218$, $p < .001$) whereas oblique motion was not ($\beta = -0.046$, $p = .077$). This effect is illustrated in Figure 3.3, which shows the gain obtained in response to each orientation of motion across stimulus velocity. Instruction type used look OKR as a reference; the negative coefficient obtained for this variable ($\beta = -0.113$, $p < .001$) therefore

indicates that gain was reduced by the use of stare instructions, as illustrated for each participant in Figure 3.2.

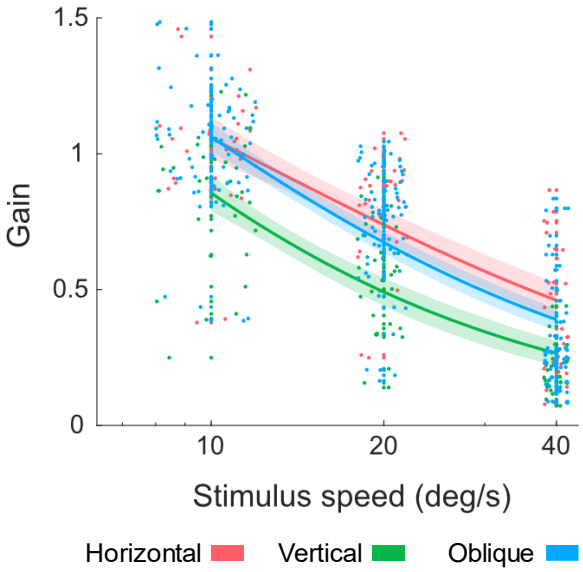

Figure 3.3: N = 8. Gain of OKR across stimulus velocity in response to different orientations of motion. The shaded area indicates the 95% CI of the fitted function, with data points showing the mean gain obtained by one participant in a single trial. A horizontal jitter of up to 4 deg/s has been applied. Responses to horizontal motion are shown in red; oblique motion in blue; vertical motion in green.

These regression models were then calculated at the individual participant level to assess the consistency of the observed effects. Significant regression equations were found for every participant (P1 ($F(4, 47) = 67.576$, $p < .001$, adjusted $R^2 = .850$), P2 ($F(4, 47) = 78.760$, $p < .001$, adjusted $R^2 = .869$), P3 ($F(4, 47) = 105.580$, $p < .001$, adjusted $R^2 = .899$), P4 ($F(4, 47) = 95.095$, $p < .001$, adjusted $R^2 = .889$), P5 ($F(4, 47) = 83.584$, $p < .001$, adjusted $R^2 = .875$), P6 ($F(4, 47) = 118.440$, $p < .001$, adjusted $R^2 = .909$), P7 ($F(4, 47) = 77.579$, $p < .001$, adjusted $R^2 = .867$), P8 ($F(4, 47) = 59.317$, $p < .001$, adjusted $R^2 = .832$)). Adjusted R^2 values ranged from .832 to .909, indicating that the models were able to account for 83.2-90.9% of the variance in OKR gain. The results of these models are presented in Table AB.1 (Appendix B). Increasing stimulus velocity significantly reduced gain in every participant. Vertical OKR gain was significantly lower than horizontal OKR gain in every participant, whereas oblique OKR gain did not differ from horizontal OKR gain in any participant. Stare OKR gain was lower than look OKR gain in five participants (P2, P3, P5, P7, P8) while the remaining three (P1, P4, P6) showed no significant effect of instruction type.

Table 3.3

Results of linear regression model to predict gain of OKR based on stimulus velocity, orientation of motion and instruction type

	β	SE	F	*p*
Intercept	1.326	0.031	42.961	< .001*
Velocity	-0.022	0.0008	-26.346	< .001*
Orientation (vertical)	-0.218	0.029	-7.256	< .001*
Orientation (oblique)	-0.046	0.026	-1.769	.077
Instruction type	-0.113	0.021	-5.356	< .001*

Note: horizontal motion is used as a reference level, with vertical and oblique motion as indicator variables.

Linear regression models were then calculated to investigate whether vertical OKR gain was symmetrical across stimulus velocity in look and stare OKR separately, and to assess for interactions between stimulus velocity and vertical symmetry. Significant regression equations were found in the prediction of look ($F(3, 47) = 43.050$, $p < .001$) and stare ($F(3, 47) = 26.900$, $p < .001$) vertical OKR gain, with adjusted R^2s of .729 and .623, respectively. The results of these analyses can be viewed in Table 3.4. In response to both look ($\beta = -0.0196$) and stare OKR ($\beta = -0.0188$), stimulus velocity significantly predicted vertical OKR gain ($p < .001$), indicating that increasing stimulus velocity reduced gain. Vertical motion direction was only a significant predictor of gain during look OKR conditions ($\beta = 0.2175$, $p = .041$), indicating that gain in response to upward motion (M = 0.641, SD = 0.323) was significantly higher than gain in response to downward motion (M = 0.511, SD = 0.319). Neither look nor stare OKR showed a significant interaction between stimulus velocity and direction of vertical motion. Mean gain in response to upward and downward motion at each stimulus velocity is shown for look and stare OKR in Figure 3.4.

T-tests were conducted at the individual participant level to assess the consistency of the effect of asymmetrical vertical look OKR; gain of individual slow phases was used rather than trial averages to increase statistical power. These tests found that OKR was significantly vertically asymmetrical in look conditions in five participants (P2 ($t(291) = 6.117$, $p < .001$), P3 ($t(270) = 1.988$, $p = .048$), P5 ($t(269) = 4.098$, $p < .001$), P7 ($t(345) = -3.820$, $p < .001$), P8 ($t(430)$

= 13.918, p < .001)), with all but one (P7) being associated with higher upward gain. Vertical asymmetry was seen in stare OKR in four participants (P1 (t(411) = 3.823, p < .001), P3 (t(323) = 8.182, p < .001), P4 (t(294) = 4.174, p < .001), P5 (t(482) = 3.172, p = .002), all of whom presented with higher upward gain. Participants exhibiting stare OKR asymmetry were compared to participants exhibiting look OKR asymmetry: t-tests showed that those exhibiting stare OKR asymmetry had significantly higher gain during vertical stare OKR compared to those that did not have asymmetrical vertical stare OKR ($t(2,220) = 10.050$, $p < .001$). Mean vertical stare OKR gain was 0.15 higher in those with asymmetrical vertical stare OKR. Similarly, this group also had significantly higher amplitude during vertical stare OKR than those without vertical stare asymmetry ($t(2,220) = 12.907$, $p < .001$). Mean slow phase amplitude during vertical stare OKR was 1.70 deg higher in those with vertical stare OKR asymmetry.

Table 3.4

Results of linear regression model to predict gain of vertical OKR based on stimulus velocity and direction of vertical motion

Look	β	SE	F	*p*
Intercept	0.9694	0.073	13.253	< .001*
Velocity	-0.0196	0.003	-7.106	< .001*
Direction	0.2175	0.103	2.103	.041*
Velocity*Direction	-0.0037	0.004	-0.955	.345
Stare	β	SE	F	*p*
Intercept	0.8705	0.085	10.289	< .001*
Velocity	-0.0188	0.003	-5.869	< .001*
Direction	0.1509	0.119	1.262	.214
Velocity*Direction	-0.0022	0.005	-0.497	.622

This analysis was then repeated to assess the vertical symmetry of oblique OKR gain across stimulus velocity. Regression models were calculated using stimulus velocity and direction of oblique motion (upward (up-left and up-

right 45°) or downward (down-left or down-right 45°) oblique) as predictors, with interaction terms included to assess for interaction between stimulus veloc-

Table 3.5

Results of linear regression model to predict gain of oblique OKR based on stimulus velocity and vertical direction of oblique motion

Look	β	SE	F	*p*
Intercept	1.3345	0.050	26.497	< .001*
Velocity	-0.0246	0.002	-12.915	< .001*
Direction	0.0025	0.071	0.0345	.973
Velocity*Direction	-0.0001	0.003	-0.039	.968
Stare	β	SE	F	*p*
Intercept	1.1994	0.077	15.487	< .001*
Velocity	-0.0236	0.003	-8.061	< .001*
Direction	-0.0343	0.109	-0.313	.755
Velocity*Direction	0.0009	0.004	0.228	.820

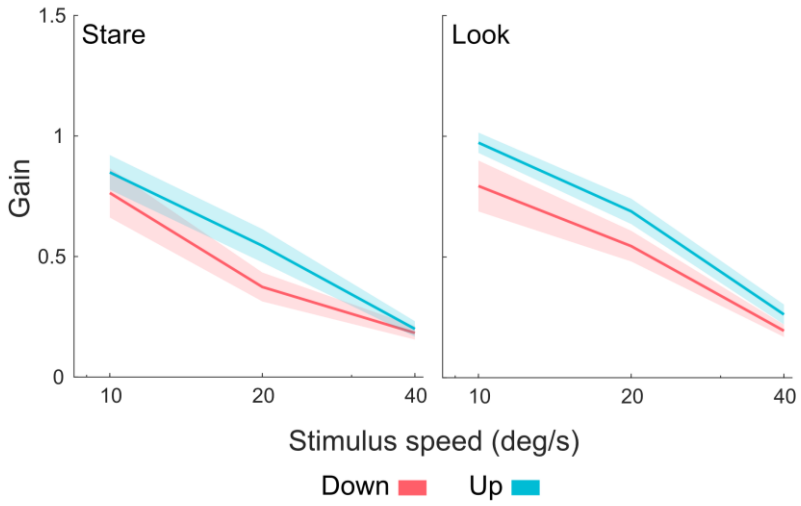

Figure 3.4: N = 8. Mean gain in response to upward (blue) and downward motion (red) drifting at 10, 20 and 40 deg/s during look (right) and stare (left) OKR conditions. Mean gain at each stimulus velocity is shown, with the shaded area indicating the standard error of the mean.

ity and vertical symmetry. Significant regression equations were found in the prediction of look ($F(3, 95) = 111.68$, $p < .001$) and stare ($F(3, 95) = 41.644$, $p < .001$) OKR, with adjusted R^2s of .778 and .562, respectively. In both models, stimulus velocity significantly predicted the gain of oblique OKR, indicating that gain was significantly lowered by increasing stimulus velocity. However, vertical direction of oblique stimulus motion was not a significant predictor of either look or stare OKR gain, and there were no significant interactions between stimulus velocity and direction of motion. The results of these analyses can be viewed in Table 3.5.

T-tests were again used at the individual participant level to assess the consistency of the lack of up-down symmetry during oblique OKR. Gain of individual slow phases throughout trials was used in place of overall trial averages. Results showed that there was no significant up-down asymmetry in the gain of oblique OKR in three participants during look and stare OKR (P3, P4 and P8). Three participants had a significant up-down gain asymmetry during oblique look OKR (P1 ($t(1036) = -5.152$, $p < .001$), P6 ($t(921) = -3.895$, $p < .001$), P7 ($t(1050) = -5.266$, $p < .001$)), with P1 and P6 producing higher downward gain and P7 producing higher upward gain. Four participants had significant asymmetries during oblique stare OKR (P2 ($t(772) = -3.307$, $p < .001$), P5 ($t(396) = 2.215$, $p = .027$), P6 ($t(1149) = 2.340$, $p = .019$), P7 ($t(881) = -12.573$, $p < .001$)), with P2 and P7 producing higher downward gain and P5 and P6 producing higher upward gain.

3.4.2 Frequency

In each trial, the number of slow phases was counted and divided by the duration of the trial (50 seconds) to obtain the OKR frequency expressed as slow phases per second. These data are illustrated for each participant during both look and stare conditions in Figure 3.5.

A linear regression model was calculated to predict the frequency of OKR using stimulus velocity, orientation of motion and instruction type. The results of this model are shown in Table 3.6. A significant regression equation was found ($F(4, 382) = 9.859$, $p < .001$) with an adjusted R^2 of .085. In this model, stimulus velocity ($F(1, 378) = 10.757$, $p = .001$), orientation of motion ($F(2, 378) = 12.033$,

$p < .001$) and instruction type ($F(1, 378) = 4.954$, $p = .027$) all significantly predicted OKR frequency. Increasing stimulus velocity reduced the OKR frequency ($\beta = -0.007$). In terms of orientation of motion, horizontal motion was used as a reference while vertical and oblique motion were used as indicators; the result shown in Table 3.6 thus indicates that, compared to horizontal motion, vertical motion significantly decreased frequency ($\beta = -0.263$, $p < .001$) whereas oblique motion did not ($p = .401$). In terms of instruction type, look OKR instructions formed the point of comparison, and the coefficient ($\beta = -0.119$) indicates that frequency of OKR was reduced by the use of stare OKR instructions. However, as shown in Figure 3.5, this was not a consistent pattern across all participants.

This analysis was repeated at the individual to assess the consistency of effects across participants. Regression models were calculated for each participant to predict OKR frequency using stimulus velocity, orientation of motion (horizontal/oblique/vertical) and instruction type (look/stare). Horizontal motion was used as a reference variable against which vertical and oblique motion were compared. Significant regression equations were found for six out of eight participants (P1 ($F(4, 47) = 4.961$, $p = .002$, adjusted $R^2 = .252$), P2 ($F(4, 47) = 9.853$, $p < .001$, adjusted $R^2 = .430$), P3 ($F(4, 47) = 3.762$, $p = .010$, adjusted $R^2 = .190$), P4 ($F(4, 47) = 3.567$, $p = .013$, adjusted $R^2 = .179$), P5 ($F(4, 47) = 13.903$, $p < .001$, adjusted $R2 = .523$), P8 ($F(4, 47) = 2.989$, $p = .029$, adjusted $R^2 = .145$)). Equations for two participants (P6 ($F(4, 47) = 2.025$, $p = .108$, adjusted $R^2 = .080$), P7 ($F(4, 47) = 0.885$, $p = .481$, adjusted $R^2 = -.010$)) were not statistically significant. The results of these models are shown in Table AB.2 (Appendix B). Increasing stimulus velocity significantly decreased OKR frequency in four participants (P1, P2, P3, P4) while having no significant effect on the remaining participants. Effects of orientation of motion observed at the group level appear to be primarily driven by P1 and P2, both of whom had significantly lower frequency in response to vertical stimuli compared to horizontal stimuli. Orientation of motion had no significant effect on the remaining participants, and the effect of oblique versus horizontal motion was not significant in any participant. Presenting stare OKR instructions significantly reduced frequency in P2, P5 and P8.

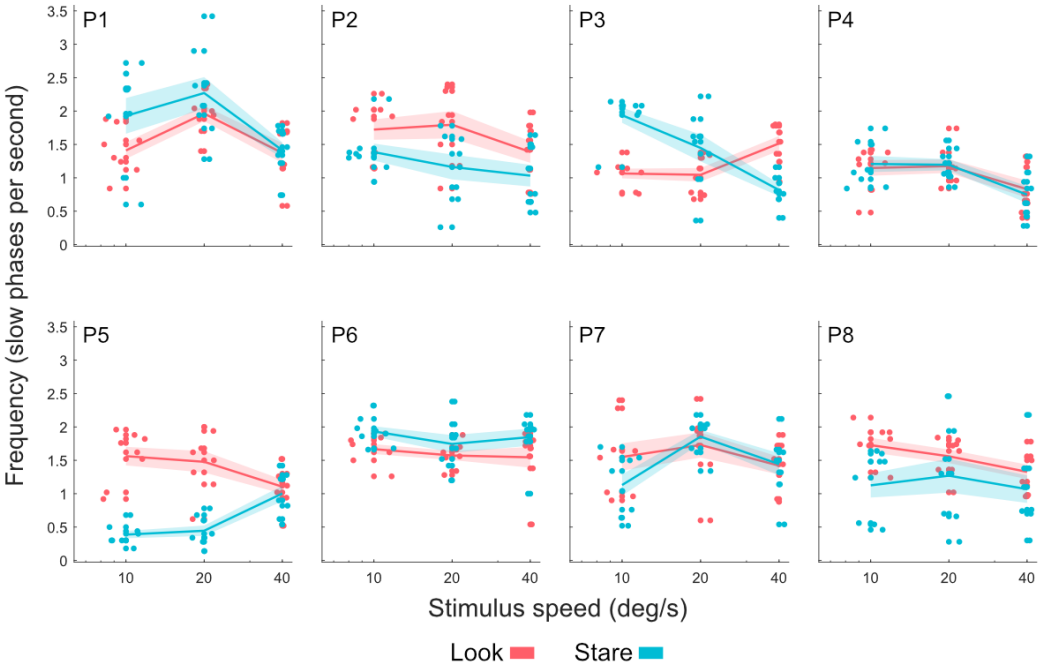

Figure 3.5: Mean frequency of OKR across stimulus velocity in look and stare conditions in eight individual participants. Responses to look OKR are shown in red whereas responses to stare OKR are shown in blue. Individual data points represent the mean frequency obtained by that participant in a single trial; a horizontal jitter of up to 4 deg/s has been applied to increase the visibility of the data points. The shaded area indicates the standard error of the mean. Participant numbers are indicated in the upper left of each plot.

Table 3.6

Results of linear regression model to predict frequency of OKR based on stimulus velocity, orientation of motion and instruction type

	β	SE	F	*p*
Intercept	1.647	0.078	21.098	< .001*
Velocity	-0.007	0.002	-3.279	.001*
Orientation (vertical)	-0.263	0.076	-3.468	< .001*
Orientation (oblique)	-0.055	0.065	0.840	.401
Instruction type	-0.119	0.053	-2.226	.027*

Note: horizontal motion is used as a reference level, with vertical and oblique motion as indicator variables.

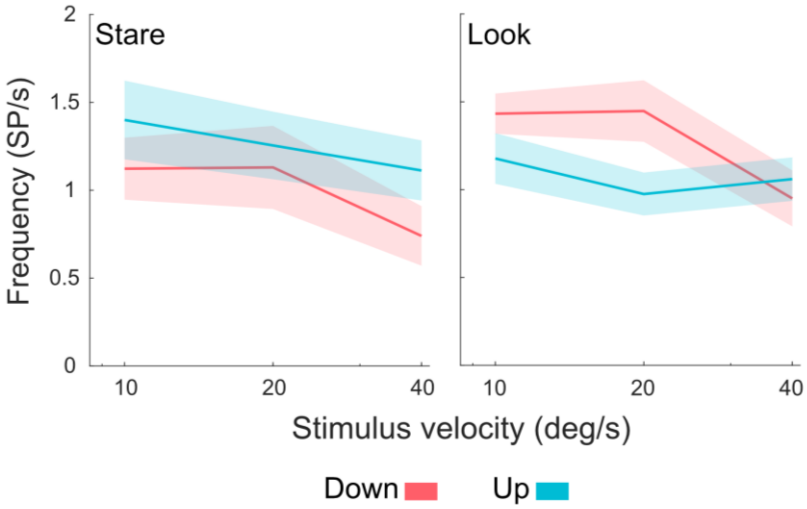

Figure 3.6: N = 8. Mean OKR frequency in response to upward (blue) and downward (red) motion at 10, 20 and 40 deg/s during look (right) and stare (left) OKR conditions. The shaded area indicates the standard error of the mean.

Analyses were then carried out to assess the vertical symmetry of look and stare OKR across stimulus velocity in terms of frequency (Figure 3.6). Linear models were calculated to predict the frequency of OKR using stimulus velocity and direction of vertical motion for look and stare OKR separately, with interaction terms included to assess for interaction between stimulus velocity and vertical symmetry. A significant regression equation was found in the prediction of vertical look OKR frequency ($F(3, 47) = 3.471$, $p = .023$) with an R^2 of .136; the model to predict the frequency of vertical stare OKR was not significant ($F(3, 47) = 2.042$, $p = .122$). The results of these analyses can be viewed in Table 3.7. During look OKR trials using vertical motion, frequency was significantly predicted by both velocity and direction of vertical motion, however, there was no interaction between the two predictors. The coefficients indicate that increasing stimulus velocity decreased vertical OKR frequency ($\beta = -0.0173$), and that frequency was higher in response to downward (M = 1.277, SD = 0.473) compared to upward (M = 1.071, SD = 0.362) stimulus motion ($\beta = -0.5462$).

Table 3.7

Results of linear regression model to predict frequency of vertical OKR based on stimulus velocity and vertical direction of oblique motion

Look	β	SE	F	*p*
Intercept	1.6812	0.173	9.728	< .001*
Velocity	-0.0173	0.006	-2.654	.011*
Direction	-0.5462	0.244	-2.235	.031*
Velocity*Direction	0.0146	0.009	1.579	.121
Stare (non-sig)	β	SE	F	*p*
Intercept	1.3175	0.236	5.581	< .001*
Velocity	-0.0137	0.009	-1.537	.131
Direction	0.1537	0.334	0.460	.647
Velocity*Direction	0.0045	0.013	0.355	.724

This analysis was repeated to assess whether oblique OKR is vertically symmetrical in terms of frequency. Linear regression models were calculated for look and stare OKR separately to predict frequency in response to oblique motion using stimulus velocity and vertical direction of motion as predictors. The resulting regression equations were not significant for look ($F(3, 95) = 2.181$, $p = .095$) or stare ($F(3, 95) = 0.581$, $p = .629$) OKR.

3.4.3 Amplitude

A linear regression model was calculated to predict the amplitude of the OKR using stimulus velocity, orientation of motion and instruction type. The results of this analysis are shown in Table 3.8. A significant regression equation was found ($F(4, 383) = 23.641$, $p < .001$) with an adjusted R^2 of .191. In this model, amplitude was significantly predicted by orientation of motion ($F(2, 379) = 9.567$, $p < .001$) and instruction type ($F(1, 379) = 75.042$, $p < .001$) but not by stimulus velocity ($F(1, 379) = 0.391$, $p = .532$). Horizontal motion was used as a reference variable; the coefficients therefore indicate that amplitude was reduced by presenting vertical ($\beta = -1.3756$) or oblique ($\beta = -0.8323$) motion, with

vertical motion having a larger effect. Presentation of stare instructions instead of look instructions also reduced OKR amplitude (β = -1.9475) (Figure 3.7).

Table 3.8

Results of linear regression model to predict amplitude of OKR based on stimulus velocity, orientation of motion and instruction type

	β	SE	F	*p*
Intercept	6.0556	0.328	18.478	< .001*
Velocity	0.0056	0.009	0.625	.532
Orientation (vertical)	-1.3756	0.318	-4.327	< .001*
Orientation (oblique)	-0.8323	0.275	-3.023	.002*
Instruction type	-1.9475	0.229	-8.663	< .001*

Note: horizontal motion is used as a reference level, with vertical and oblique motion as indicator variables.

These analyses were repeated on individual participants to assess the consistency of the observed effects across individuals. Regression models were calculated for each participant to predict OKR slow phase amplitude using velocity, orientation of motion direction and instruction type. Significant regression equations were found for all participants (P1 ($F(4, 47) = 34.944$, $p < .001$, adjusted $R^2 = .743$), P2 ($F(4, 47) = 27.881$, $p < .001$, adjusted $R^2 = .696$), P3 ($F(4, 47) = 15.781$, $p < .001$, adjusted $R^2 = .557$), P4 ($F(4, 47) = 4.700$, $p = .003$, adjusted $R^2 = .239$), P5 ($F(4, 47) = 7.863$, $p < .001$, adjusted $R^2 = .369$), P6 ($F(4, 47) = 2.958$, $p = .030$, adjusted $R^2 = .143$), P7 ($F(4, 47) = 9.058$, $p < .001$, adjusted $R^2 = .407$), P8 ($F(4, 47) = 4.627$, $p = .003$, adjusted $R^2 = .236$)). Though stimulus velocity did not have a significant effect at the group level, it was found to significantly affect amplitude in three participants, with P1 and P7 showing an increase in amplitude with velocity and P3 showing a decrease in amplitude with increasing velocity. The effect of vertical motion was found to be significant in four participants (P3, P4, P6, P7). Finally, the effect of instruction type was found to be significant in seven participants, with stare OKR instructions significantly reducing slow phase amplitude in all but P6. The results of these analyses can be seen in Table AB.3 (Appendix B).

Table 3.9

Results of linear regression model to predict amplitude of vertical OKR based on stimulus velocity and vertical direction of oblique motion

Look	β	SE	F	*p*
Intercept	4.4255	0.754	5.873	< .001*
Velocity	-0.0306	0.028	-1.076	.288
Direction	2.6093	1.066	2.448	.018*
Velocity*Direction	-0.0234	0.040	-0.581	.565
Stare (non-sig)	β	SE	F	*p*
Intercept	2.9781	0.778	3.829	< .001*
Velocity	-0.0067	0.029	-0.227	.821
Direction	0.2118	1.099	0.192	.848
Velocity*Direction	0.0004	0.041	0.011	.992

Look and stare OKR were then modelled separately to assess the up-down symmetry of amplitude in response to vertical motion (Figure 3.8). Linear models were calculated using stimulus velocity and direction of vertical motion as predictors, and the interaction between the two was assessed (Table 3.9). The resulting regression equations were significant for look ($F(3, 47) = 7.211$, $p < .001$, adjusted $R^2 = .284$) but not for stare ($F(3, 47) = 0.093$, $p = .963$) OKR. During look OKR in response to vertical motion, amplitude was significantly predicted by direction of vertical motion ($\beta = 2.6093$) but not by stimulus velocity. This indicates that amplitude was higher in response to upward (M = 5.774, SD = 2.204) compared to downward (M = 3.710, SD = 1.250) motion. There was no significant interaction between direction of vertical motion and stimulus velocity.

T-tests were conducted at the individual level to assess for up-down asymmetry of slow phase amplitude in look and stare OKR during vertically drifting stimuli. Results showed that vertical amplitude was significantly asymmetrical during look OKR in P1 ($t(371) = 6.404$, $p < .001$), P2 ($t(291) = 7.102$, $p < .001$), P3 ($t(270) = 3.492$, $p < .001$), P4 ($t(300) = 3.577$, $p < .001$), P5 ($t(269) = 4.732$, $p < .001$) and P6 ($t(525) = 5.090$, $p < .001$), all of whom had higher upward

amplitude. Stare OKR amplitude was vertically asymmetrical in P2 ($t(306) = 7.469$, $p < .001$), P3 ($t(323) = 4.434$, $p < .001$), P5 ($t(174) = 4.651$, $p < .001$) and P6 ($t(462) = 5.005$, $p < .001$), again all producing higher upward amplitude. Difference in amplitude between responses to upward and downward moving stimuli was calculated for each participant, and a t-test was used to assess whether there was a significant difference in the extent of up-down asymmetry between look and stare OKR at the group level. Results showed that look OKR amplitude was significantly more asymmetrical than that of stare OKR ($t(7) = 3.363$, $p = .010$). Upward look OKR amplitude was a mean of 1.861 deg (SD = 1.148) higher than downward look OKR amplitude, whereas upward stare OKR amplitude was 0.685 deg (SD = 0.598) higher than downward stare OKR amplitude.

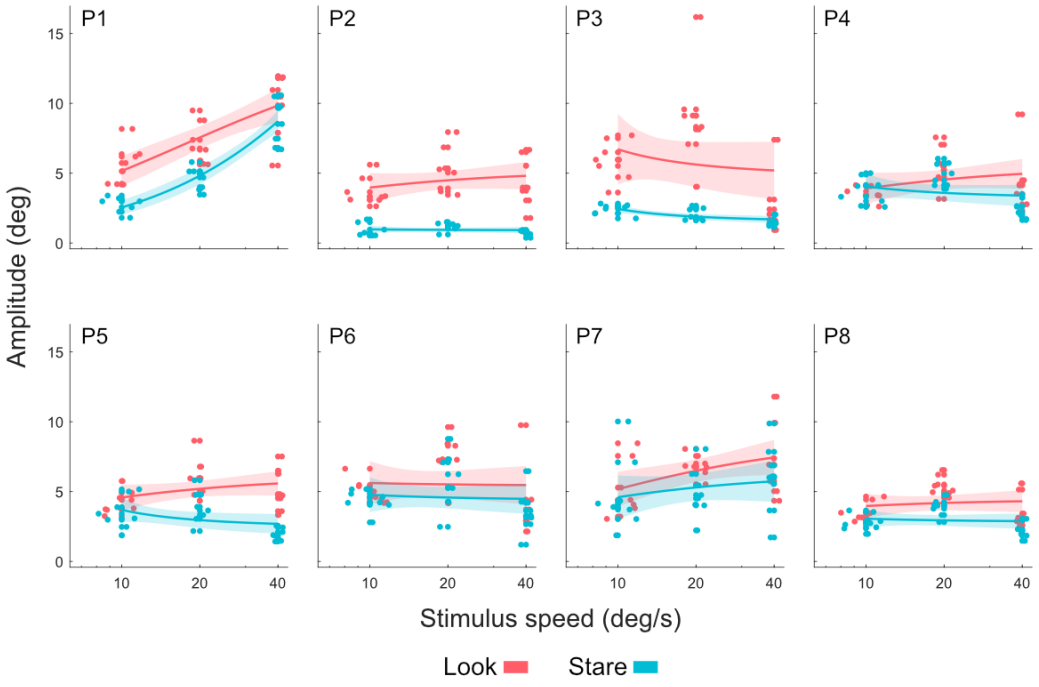

Figure 3.7: Amplitude of OKR slow phases in response to stimuli drifting at 10, 20 and 40 deg/s in eight individual participants. Responses to look OKR are shown in red and responses to stare OKR are shown in blue. The shaded area represents the 95% CI of the fitted function. A horizontal jitter of up to 4 deg/s has been applied to increase the visibility of the individual data points. Data points represent the mean slow phase amplitude obtained by that participant during one trial. Participant numbers are indicated in the upper left corner of each plot.

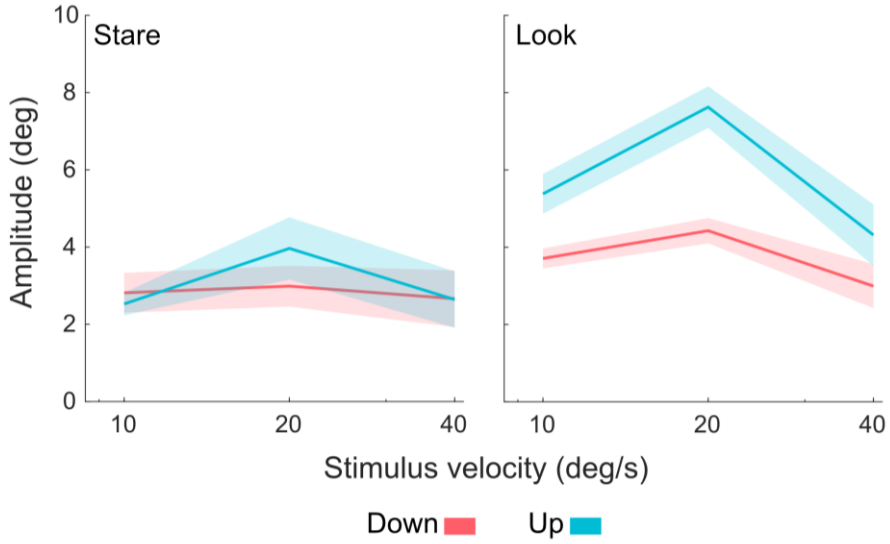

Figure 3.8: N = 8. Mean OKR amplitude in response to upward (blue) and downward (red) motion at 10, 20 and 40 deg/s during look (right) and stare (left) conditions. The shaded area indicates the standard error of the mean.

3.4.4 Slow phase angle/direction

The angle/direction of each slow phase was calculated whereby 0/360° indicates movement towards the right, 180° indicates movement towards the left, 90° indicates downward movement and 270° indicates upward movement. The mean slow phase angle obtained in each trial is displayed in Figure 3.9 for each direction of stimulus motion. Mean angles were calculated using the 'circ_mean' function from the Circular Statistics Toolbox (Directional Statistics) (Berens, 2009) for MATLAB.

Once mean slow phase angles had been calculated, the difference between slow phase direction and stimulus direction was calculated in deg for each trial. The mean deviation of the slow phase direction away from the stimulus direction is shown in deg for each direction of stimulus motion in Table 3.10. While deviation away from the stimulus direction was similar in response to both horizontal and vertical cardinal stimulus motion, deviation away from the stimulus direction during oblique stimulation was larger, particularly in response to oblique stimulation with downward motion: in response to upward obliques, mean deviation

was 10.8° (SD = 6.9°); in response to downward obliques, mean deviation was 20.0° (SD = 7.4°). During oblique stimulation, these deviations away from the stimulus direction shifted the direction of the slow phases towards the horizontal axis (Figure 3.9).

Table 3.10

Mean deviation of the slow phase direction away from the stimulus direction in response to each direction of stimulus motion. 'Overall' column shows the mean deviation for each orientation of stimulus motion.

Orientation	Direction	Mean (SD) deviation	Overall mean (SD)
Horizontal	Right (0/360°)	5.8° (4.1°)	5.9° (4.0°)
	Left (180°)	6.0° (3.9°)	
Vertical	Up (270°)	3.9° (2.5°)	6.5° (6.2°)
	Down (90°)	9.0° (7.8°)	
Oblique	Up-right (315°)	9.4° (6.1°)	15.4° (8.5°)
	Up-left (225°)	12.3° (7.4°)	
	Down-right (45°)	18.6° (8.0°)	
	Down-left (135°)	21.4° (6.6°)	

T-tests were carried out to assess whether the mean deviation of the slow phase direction away from the stimulus direction differed between directions of stimulus motion. First, a t-test was carried out to test for differences in deviation of slow phase direction between vertical and horizontal directions of stimulus motion; this showed no significant difference between the two orientations of stimulus motion ($t(189) = 0.735$, $p = .463$). Consequently, vertical and horizontal directions were combined and then compared to oblique directions of motion to assess whether the deviation of the slow phase direction away from the stimulus direction differed between oblique and cardinal directions of motion. The result showed a significant difference ($t(381) = -12.811$, $p < .001$) whereby the deviation of the slow phase direction away from the stimulus direction was significantly larger during oblique motion. Finally, a t-test was carried out comparing upward oblique motion (315°/225°) to downward oblique motion (45°/135°) in terms of

the mean deviation of the slow phase direction away from the stimulus direction. This showed a significant difference ($t(95) = -8.525$, $p < .001$) whereby the deviation of the slow phase direction was larger in response to downward oblique motion compared to upward oblique motion. Overall, the results of these tests indicate that slow phases in response to oblique motion show a significant shift of slow phase direction towards the horizontal axis, with responses to downward oblique motion being particularly affected. The direction of slow phases in response to cardinal directions of stimulus motion show significantly greater directional accuracy when compared to responses to oblique motion.

These analyses were repeated at the individual level to investigate the consistency of the effects. T-tests, as above, were conducted on individual participant data. The angle of individual slow phases was used rather than trial averages; the difference in angle between the stimulus direction and the direction of each slow phase was calculated and entered into the analysis. First, one-sample t-tests were used to assess whether the deviation of the slow phase direction away from the stimulus direction was significantly different from zero in response to any orientation of stimulus motion (vertical/horizontal/oblique). These t-tests found that deviations were significant for all participants during vertical motion (P1 ($t(785) = 27.733$, $p < .001$), P2 ($t(594) = 18.778$, $p < .001$), P3 ($t(566) = 20.016$, $p < .001$), P4 ($t(597) = 22.515$, $p < .001$), P5 ($t(457) = 18.383$, $p < .001$), P6 ($t(1010) = 35.229$, $p < .001$), P7 ($t(783) = 24.478$, $p < .001$), P8 ($t(721) = 22.960$, $p < .001$)), horizontal motion (P1 ($t(1060) = 41.258$, $p < .001$), P2 ($t(925) = 22.035$, $p < .001$), P3 ($t(793) = 19.265$, $p < .001$), P4 ($t(645) = 27.056$, $p < .001$), P5 ($t(639) = 21.230$, $p < .001$), P6 ($t(1038) = 28.757$, $p < .001$), P7 ($t(931) = 36.178$, $p < .001$), P8 ($t(793) = 35.244$, $p < .001$)) and oblique motion (P1 ($t(2294) = 79.602$, $p < .001$), P2 ($t(1872) = 39.965$, $p < .001$), P3 ($t(1728) = 67.850$, $p < .001$), P4 ($t(1276) = 35.993$, $p < .001$), P5 ($t(1293) = 31.569$, $p < .001$), P6 ($t(2073) = 61.884$, $p < .001$), P7 ($t(1934) = 67.124$, $p < .001$), P8 ($t(1714) = 51.275$, $p < .001$)).

T-tests were then used to determine whether the deviation of the slow phase direction away from the stimulus direction differed between responses to horizontal and vertical motion. This difference was found to be significant in six participants (P1 ($t(1845) = 7.181$, $p < .001$), P3 ($t(1359) = 13.716$, $p < .001$), P4 ($t(1242) = -5.557$, $p < .001$), P5 ($t(1096) = 3.460$, $p < .001$), P6 ($t(2048) = 18.725$,

$p < .001$), P7 ($t(1714) = 4.895$, $p < .001$)), with all but P4 deviating significantly more during vertical OKR. For these six participants, vertical and horizontal responses were thus kept separate and compared to oblique motion individually. These analyses found that deviation of the slow phase direction during oblique OKR was significantly larger than that during vertical (P1 ($t(3079) = -19.089$, $p < .001$), P3 ($t(2294) = -14.506$, $p < .001$), P4 ($t(1873) = -10.526$, $p < .001$), P5 ($t(1750) = -5.864$, $p < .001$), P6 ($t(3083) = -2.462$, $p = .014$), P7 ($t(2717) = -21.204$, $p < .001$)) and horizontal (P1 ($t(3354) = -30.997$, $p < .001$), P3 ($t(2521) = -35.226$, $p < .001$), P4 ($t(1921) = -5.886$, $p < .001$), P5 ($t(1932) = -9.999$, $p < .001$), P6 ($t(3111) = -25.121$, $p < .001$), P7($t(2865) = -28.929$, $p < .001$)) OKR for these six participants. For the remaining two participants (P2 and P8), who showed no significant difference in deviation between horizontal and vertical motion,

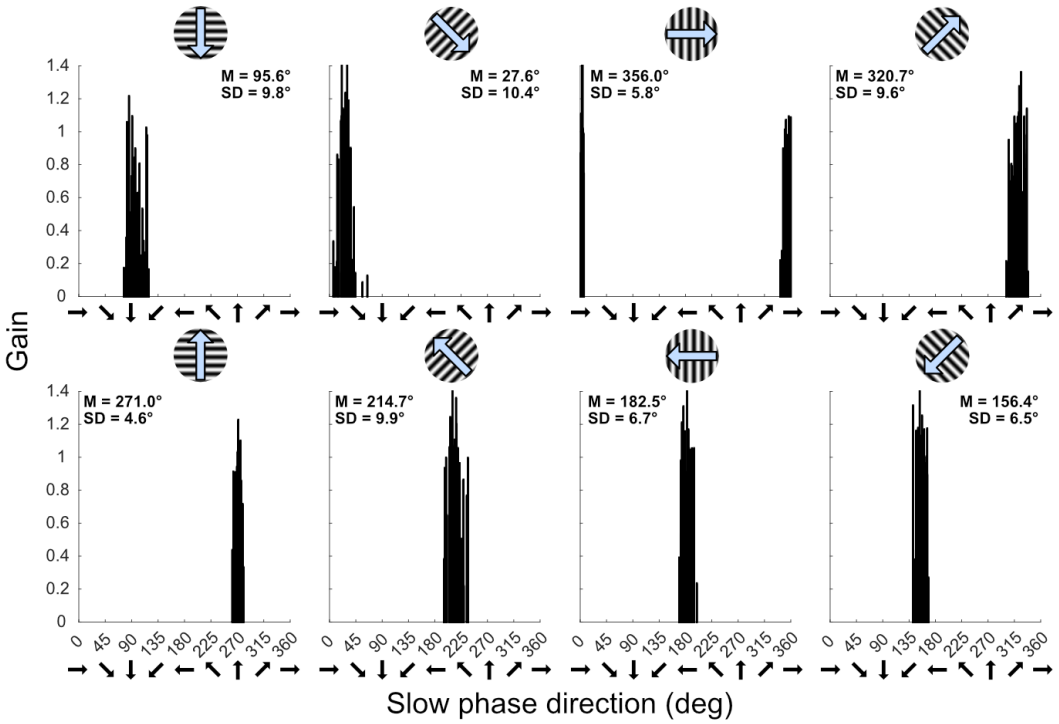

Figure 3.9: N = 8. Mean slow phase direction per trial in response to each direction of stimulus motion. Stimulus direction is indicated by the icon above each plot. Each bar on the plot represents the mean direction and gain of slow phases during one trial. Mean slow phase direction, and the standard deviation of the mean, are shown in the upper corner of each plot. Black arrows below the X axis indicate the direction associated with each angle.

deviations for vertical and horizontal motion were binned. Deviation during responses to cardinal and oblique motion were then compared, finding that deviation was again significantly larger during oblique stimulation (P2 ($t(3392) = -17.266$, $p < .001$), P8 ($t(3229) = -12.492$, $p < .001$)). Deviation of the slow phase direction away from the stimulus direction was then compared for upward versus downward obliques, finding that deviation during downward obliques was significantly larger for seven participants (P1 ($t(2293) = -32.402$, $p < .001$), P2 ($t(1871) = -15.584$, $p < .001$), P3 ($t(1727) = -10.794$, $p < .001$), P4 ($t(1275) = -13.882$, $p < .001$), P5 ($t(1292) = -4.687$, $p < .001$), P6 ($t(2072) = -20.116$, $p < .001$), P8 ($t(1713) = -31.324$, $p < .001$)), with only P7 producing larger deviations in response to upward-drifting oblique stimuli ($t(1933) = 10.830$, $p < .001$).

To assess whether deviation of the slow phase direction from the stimulus direction was related to instruction type, look and stare conditions were compared in response to each orientation of motion. Results showed that, during stimulation with horizontal motion, the deviation of the slow phase direction away from the stimulus direction was significantly larger in response to stare OKR conditions (M = 6.4°, SD = 4.4°) compared to look OKR conditions (M = 5.4°, SD = 3.5°) ($t(47) = -2.061$, $p = .045$). However, in response to vertical ($t(93) = 0.671$, $p = .504$) and oblique ($t(95) = -1.395$, $p = .166$) motion, no significant difference was found between look and stare conditions. A t-test also found no significant difference in slow phase angle deviation between 10 deg/s and 40 deg/s conditions ($t(253) = -0.863$, $p = .389$), indicating that deviation of the slow phase direction away from the stimulus direction did not change significantly with stimulus velocity.

T-tests were used to assess the impact of look and stare instructions on slow phase deviation away from the stimulus direction in each participant. Results showed that deviations were significantly larger during stare OKR in three participants (P1 ($t(4140) = -2.072$, $p = .038$), P5 ($t(2390) = -9.871$, $p < .001$), P8 ($t(3229) = -2{,}534$, $p = .011$)), and significantly larger during look OKR in one participant (P5 ($t(3088) = 2.067$, $p = .039$)). There was no difference in deviations between look and stare conditions in P2, P4, P6 and P7. T-tests were then used to investigate whether deviations varied with stimulus speed in each participant. Results showed that deviation of the slow phase direction away from the stimulus direction was generally largest during 40 deg/s conditions, with deviations

being larger during 40 deg/s conditions compared to 20 deg/s conditions in six participants (P2 ($t(2149) = 4.369$, $p < .001$), P3 ($t(1887) = 3.618$, $p < .001$), P4 ($t(1577) = 2.586$, $p = .010$), P5 ($t(1610) = 8.416$, $p < .001$), P6 ($t(2682) = 5.067$, $p < .001$), P8 ($t(2088) = 8.641$, $p < .001$)) and larger during 40 deg/s compared to 10 deg/s in the same six participants (P2 ($t(2209) = -4.572$, $p < .001$), P3 ($t(2091) = -7.421$, $p < .001$), P4 ($t(1571) = -2.926$, $p = .004$), P5 ($t(1621) = -7.632$, $p < .001$), P6 ($t(2795) = -4.154$, $p < .001$), P8 ($t(2097) = -8.317$, $p < .001$)). Regarding the difference in slow phase direction deviations between 10 deg/s and 20 deg/s stimuli, there was no difference between the two conditions in P1, P2, P4, P5, P6 and P8. Slow phase deviations were larger during 20 deg/s stimuli in P3 ($t(2196) = -4.232$, $p < .001$) and were larger during 10 deg/s stimuli in P7 ($t(2504) = 2.382$, $p = .017$)

3.4.5 Build-up of gain over time

To assess whether there was a significant increase in gain throughout the 50-second OKR trial, slow phases were binned into five-second epochs and were assessed via a one-way ANOVA to test for a significant main effect of time on gain. Data were also then assessed at the group and individual level by fitting two-piece linear functions. This analysis aimed to identify 'knot points' representing changes in the slope of the function of gain over time using a custom MATLAB script utilising the following equation, where m_1 and m_2 are the slopes of the two functions, k is the knot point, and c_1 is the y-intercept of the first function:

$$y(t) = \begin{cases} m_1 t + c_1 & t < k, \text{ where } k \text{ is the knot point} \\ m_2 t + k\,(m_1 - m_2) + c_1 & t \geq k \end{cases}$$

which was used to derive an anonymous function that was entered into 'lsqcurvefit' in MATLAB, which solves data-fitting problems using a least squares method. 95% confidence intervals (CIs) of the functions at either side of the knot point were calculated using 'regress' in MATLAB. It should be noted

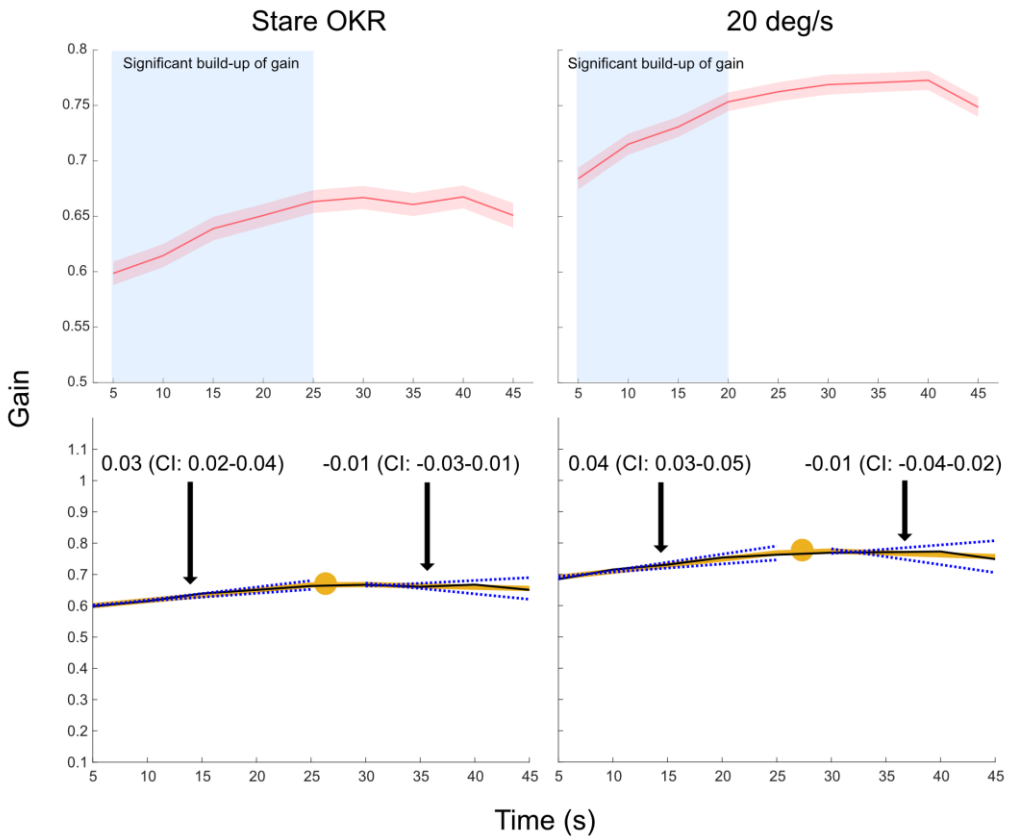

Figure 3.10: N = 8. Mean gain obtained during each five-second epoch during stare OKR conditions (left) and during conditions involving stimuli presented at a velocity of 20 deg/s (right). In the upper plots, the period during which a significant increase in gain was observed is highlighted by blue area. The red shaded area indicates the standard error of the mean. In the lower plots, mean gain is shown by the black line, with yellow lines indicated the two-piece linear function fit to the data. The yellow circle indicates the 'knot point' at which the slope of the function changes. The slope of the function (and 95% CI, shown in blue dash) is indicated in black text on the lower plots, with arrows pointing towards the corresponding function. It is expected that the gain obtained within the first five seconds of stimulation represents the activity of the EOKR system; further build-up beyond this time is expected to reflect activity of the LOKR system.

that the binning of data into five-second epochs was a necessary step due to issues with timestamp accuracy occurring during data collection; for this reason, the analysis is not sensitive to increases in gain occurring within the first five seconds of stimulation. As EOKR-related gain increases are likely to occur during these initial five seconds, identified knot points are unlikely to reflect a transition

from EOKR to LOKR; rather, they likely reflect transitions from slow LOKR-related build up into steady-state OKR. As the effect of interest is the build-up of gain over time, data showing a decline in gain over time (thus an initial function with a negative slope) were disregarded. 95% CIs of the slopes of functions on each side of the knot point were used to assess the significance of the knot point; overlapping CIs indicate that the function at either side of the knot point cannot be considered to have a significantly different slope, therefore the knot point itself is not considered to be significant as a transition point in the slope.

With all stimulus velocities combined, during look OKR trials there was no significant main effect of time on gain ($F(8, 12582) = 1.340$, $p = .218$). During stare OKR trials, there was a significant main effect of time on gain ($F(8, 11331) = 5.420$, $p < .001$). To investigate this main effect, pairwise t-tests were carried out to assess the difference in gain between adjacent five-second bins. These t-tests showed that gain continued to build up throughout the first 25 seconds of the trial. Gain increased significantly between the first and second five-second bins ($t(1259) = -3.176$, $p = .001$), between the second and third five-second bins ($t(1259) = -4.555$, $p < .001$), between the third and fourth five-second bins ($t(1259) = -2.177$, $p = .029$), and between the fourth and fifth five-second bins ($t(1259) = -2.279$, $p = .023$), with gain increasing from 0.598 (SD = 0.371) within the first five seconds to 0.663 (SD = 0.367) by the fifth five-second bin. Subsequent time bins did not differ significantly (Figure 3.10, upper left). A two-piece linear function was fit to the data to further examine the build-up of gain over time (Figure 3.10, lower left), showing an initial ramp with a slope of 0.03 (CI: 0.02, 0.04), and a knot point at 25 seconds, likely indicating a transition into steady-state OKR as the function after the knot point had a slope (-0.01) that, based on its 95% CI, could not be considered significantly different from zero (slope: -0.01; CI: -0.03, 0.01).

These analyses were also carried out to assess whether there was a significant build-up of slow phase gain throughout trials at different stimulus velocities. During trials presenting stimuli at a velocity of 10 deg/s, there was a significant main effect of time on gain ($F(8, 8244) = 3.050$, $p = .002$). Pairwise t-tests were again used to assess the change in gain between five-second bins, finding significant increases in gain only between the second and third five-second bins ($t(916) = -2.842$, $p = .005$) and between the fifth and sixth five-second bins

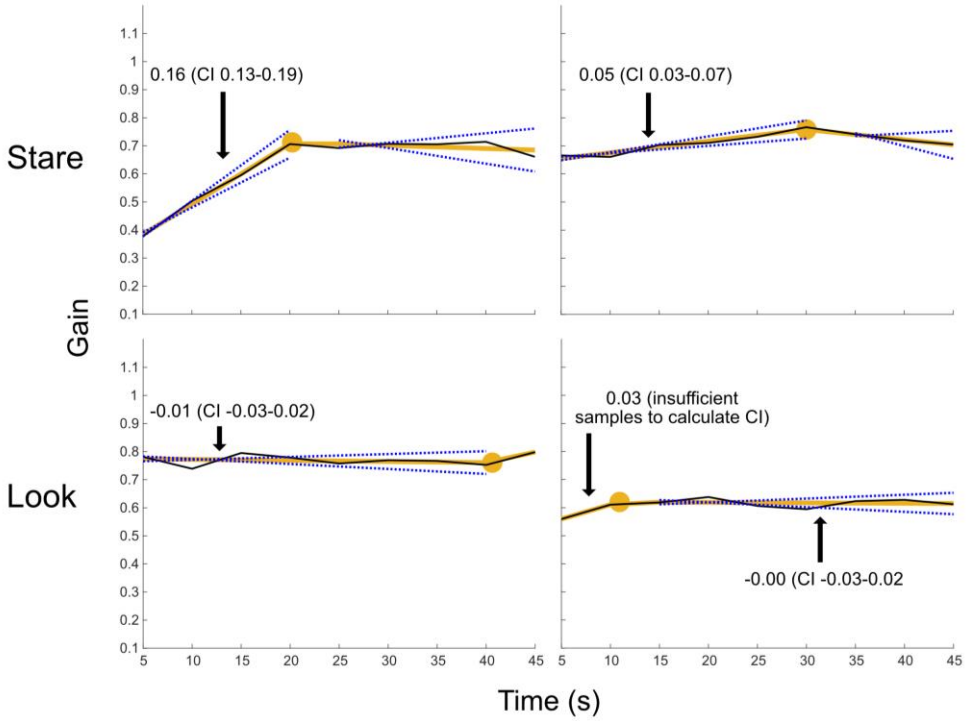

Figure 3.11: Four examples of typical build-up of gain over time during look (lower) and stare (upper) OKR trials. Gain over time is illustrated in black, with yellow lines indicating the two-piece linear function that has been fit to the data. Yellow circles indicate the identified knot point (point at which the gradient changes/intercept of the two linear functions). Dashed blue lines indicate the upper and lower 95% CI of the identified linear functions. Text with arrows indicates the slope, and calculated upper and lower CI, of the functions. The absence of upper and lower CIs on a function indicates that insufficient samples occurred during that time to allow for CIs to be calculated.

($t(916) = -2.224$, $p = .026$). Fitting of a two-piece linear function to the data revealed a flat function with a slope not distinguishable from zero (0.02; CI: 0.00, 0.04) and no significant knot points. During trials presenting stimuli at a velocity of 20 deg/s, there was again a significant main effect of time on gain ($F(8, 8523) = 11.380$, $p < .001$). Pairwise t-tests showed that gain increased significantly throughout the first 20 seconds of the trial. Gain increased significantly between the first and second five-second bins ($t(947) = -4.348$, $p < .001$), between the second and third five-second bins ($t(947) = -2.146$, $p = .032$) and between the third and fourth five-second bins ($t(947) = -3.192$, $p < .001$), with gain increasing from 0.684 (SD = 0.302) in the first five seconds to 0.753 (SD = 0.259) in the fourth

five-second bin. Subsequent time bins did not differ significantly (Figure 3.10, right). 20 deg/s data were further assessed through the fitting of a two-piece linear function (Figure 3.10, lower right). This analysis identified an initial positive slope of 0.04 (CI: 0.03, 0.05) before reaching a knot point (change in slope) at approximately 25 seconds. Beyond this, the slope of the function was not considered to be significantly different from zero, likely reflecting steady-state OKR. During trials presenting stimuli at 40 deg/s, there was no significant main effect of time on gain ($F(8, 7137) = 0.590$, $p = .789$), and a function fit to the data corroborated this finding, as its slope (0.01) was not distinguishable from zero (CI: 0.00, 0.01), and no significant knot points were identified.

Data were also analysed at the individual level by fitting two-piece linear functions to individual participant data for look and stare conditions. During look OKR conditions, an initial positive gradient was only identified in 25.0% of trials. In 62.5% of cases, the initial slope was not significantly different from zero, indicating that steady-state OKR had likely been reached within the first few seconds of the trial (a time period that this analysis was not sensitive to). However, even in trials showing an increase in gain over time, the identified knot points were not considered to be significant, as the CIs of the first and second half of the functions overlapped, with the second functions being generally flat. These findings thus agree with the ANOVA, indicating no significant effect of time on gain during look OKR conditions. Examples of typical look OKR timeseries, with fitted two-piece linear functions, can be seen in Figure 3.11 (lower).

This analysis was repeated to assess stare OKR data. In contrast to look OKR, stare OKR trials produced a notable increase in gain over time, with positive initial ramps in gain identified in 62.5% of cases (Figure 3.11, upper). Many identified knot points could not be considered to be significant due to overlapping CIs for the slopes of the functions fitted before and after the knot point. Only two participants produced stare OKR data showing both a significant increase in gain throughout the start of the trial as well as significant knot points likely showing a transition to steady-state OKR: P4 and P7. These significant knot points fell between 20-30 seconds into the trial, indicating that gain continued to increase until this time. In P4, initial ramps in gain had an average slope of 0.16 (95% CI: 0.13, 0.19). After the knot point, the slope of the function was not significantly different from zero, likely indicating steady-state OKR. In P7, the initial ramps

in gain had an average slope of 0.05 (95% CI: 0.03, 0.07). After the knot point, the slope of the function was again not significantly different from zero, likely indicating steady-state OKR. It should be noted that the absence of significant knot points in other participants does not necessarily indicate that an LOKR-related build-up in gain did not occur, as positive ramps in gain were still observed; in five participants (P2, P3, P5, P6, P8), the absence of a knot point was generally due to gain continuing to increase across the duration of the trial. However, in one participant (P1) a decline in gain over time was reliably observed under both look and stare conditions, possibly signifying an effect such as a decline in attention across the trial, obscuring the effects of EOKR/LOKR-related gain build-up.

3.5 Results: OKAN

Table 3.11

Results of logistic binomial linear regression analysis to predict the occurrence of OKAN based on five predictor variables.

(non-sig)	β	SE	F	*p*
Intercept	-0.3681	0.735	-0.501	.617
Velocity	0.0012	0.014	0.086	.931
Orientation (vertical)	0.4835	0.312	1.549	.121
Orientation (up oblique)	0.3548	0.303	1.169	.242
Orientation (down oblique)	-0.0401	0.374	-0.108	.913
Instruction type	0.0040	0.214	0.019	.985
Angular SP deviation	0.0204	0.017	1.226	.220
Gain	-0.1609	0.501	-0.321	.748

Note: Analysis of orientation uses horizontal motion as a reference variable

Out of 383 trials in which OKR was produced, 189 (49.35%) were followed by OKAN. These trials were all accounted for by six of the eight participants; two participants (P3 and P5) did not produce any OKAN. Of the 189 trials that resulted in OKAN, 94 (49.74%) were look OKR trials and 95 (50.26%) were

stare OKR trials, indicating that both look and stare instructions were equally associated with OKAN. Of the 189 trials which resulted in OKAN, 50 (26.45%) presented stimuli at 10 deg/s, 80 (42.32%) presented stimuli at 20 deg/s, and the remaining 59 (31.22%) presented stimuli at 40 deg/s. Of the 189 trials leading to OKAN, 40 (21.16%) involved horizontal stimulus motion, 52 (27.51%) involved vertical stimulus motion, 51 (26.98%) involved upward oblique motion and 46 (24.33%) involved downward oblique stimulus motion. The mean OKAN slow phase direction obtained in each trial is shown in Figure 3.16.

To assess whether the orientation of motion (horizontal, vertical, downwards oblique or upwards oblique), velocity of motion, instruction type, slow phase gain or angular deviation of the slow phase direction away from the stimulus direction predicted whether or not OKAN occurred, a logistic binomial generalised linear regression model was calculated. The resulting model was not significant ($F(375) = 6.090$, $p = .529$) and is shown in Table 3.11. This indicates that occurrence of OKAN was not explained by any of the predictor variables. Similarly, a model was calculated to predict occurrence of OKAN with the same predictor variables as the above model, with the exception of OKR gain, which was replaced with frequency. The resulting model was significant ($F(375) = 14.900$, $p = .037$, adjusted $R^2 = .020$) and can be viewed in Table AB.5 (Appendix B). In this model, OKAN was significantly predicted by the frequency of the preceding OKR, with higher OKR frequency being associated with increased OKAN occurrence.

Regression models were then calculated to predict OKAN occurrence in individuals. Only participants who produced OKAN were thus included in this analysis. Generalised linear regression models were calculated for six participants to predict occurrence of OKAN using stimulus velocity, orientation of motion, instruction type, angular slow phase deviation and OKR gain. Significant regression equations were found for just two participants (P1 ($F(40) = 25.900$, $p < .001$, adjusted $R^2 = .433$), P7 ($F(40) = 15.000$, $p = .036$, adjusted $R^2 = .150$)) whereas models for the remaining four participants were not significant. The results of these analyses can be viewed in Table AB.4 (Appendix B). In the two participants with significant regression models, increasing stimulus velocity significantly decreased probability of OKAN occurring. In P1, upward oblique stimuli were associated with significantly more OKAN; in P7, vertical stimuli were

associated with significantly less OKAN. There was a significant effect of instruction type in P1, with look OKR instructions leading to more OKAN occurrences. Finally, gain of the preceding OKR was a significant predictor of OKAN in both P1 and P7, with higher gain OKR being associated with fewer OKAN occurrences.

T-tests were used to compare OKR in participants who did produce OKAN (P1, P2, P4, P6, P7, P8) and those who did not (P3 and P5). Results showed no significant difference in OKR gain between the two groups ($t(381) = -0.152$, $p = .879$). However, OKR frequency was significantly higher in participants that produced OKAN ($t(381) = 4.905$, $p < .001$), as was slow phase amplitude ($t(381) = 1.968$, $p = .049$).

3.5.1 OKAN reversal

Table 3.12

Results of logistic binomial linear regression analysis to predict the reversal of OKAN based on five predictor variables: velocity, orientation of motion, instruction type, angular SP deviation and gain.

	β	SE	F	*p*
Intercept	6.9914	1.715	4.077	< .001*
Velocity	-0.1208	0.031	-3.983	< .001*
Orientation (vertical)	-0.6172	0.552	-1.117	.264
Orientation (up oblique)	-1.7326	0.585	-2.962	.003*
Orientation (down oblique)	0.4648	0.638	0.728	.466
Instruction type	-0.3706	0.392	-0.945	.345
Angular SP deviation	0.0757	0.030	2.536	.011*
Gain	-6.6973	1.279	-5.236	< .001*

Note: horizontal motion was used as a reference variable for analysis of orientation

The mean OKAN slow phase direction in each trial was classed as reversed (1) or not reversed (0), depending on whether slow phases drifted towards the direction of the preceding OKR stimulus or in a direction opposite to that of

the preceding OKR stimulus. A logistic binomial linear regression model was then calculated to predict reversal of OKAN based on the velocity of motion, orientation of motion, instruction type and angular deviation of the slow phase direction away from the stimulus direction and slow phase gain during the preceding OKR. The resulting model was significant ($F(181) = 77.00$, $p < .001$) and had an adjusted R^2 of .336, indicating that the reversal of OKAN was significantly predicted by the stimulus velocity ($\beta = -0.1208$, $p < .001$), presentation of upwards oblique (315°/225°) motion ($\beta = -1.7326$, $p = .003$), the angular deviation of the OKR slow phase direction away from the stimulus direction ($\beta = 0.0757$, $p = .011$) and the gain ($\beta = -6.6973$, $p < .001$) of the preceding OKR. The results of this analysis are shown in Table 3.12. The significant effect of velocity indicates that, as stimulus velocity increases, the proportion of trials in which OKAN is reversed increases: at 10 deg/s, 40.00% of OKAN reversed; at 20 deg/s, 44.30% of OKAN reversed; at 40 deg/s, 58.33% of OKAN reversed. In terms of orientation of motion, horizontal motion was used as a reference; the significant effect of presentation of upward oblique motion indicates that, compared to presentation of horizontal motion, upward oblique motion was less associated with OKAN reversal. Following presentation of horizontal motion, 42.50% of OKAN was reversed; following presentation of upward oblique motion, 21.57% of OKAN was reversed. The significant effect of angular deviation of the slow phase direction away from the stimulus direction indicates that OKAN reversal was associated with increased angular slow phase deviation away from the stimulus direction. Of trials that preceded a reversed OKAN, the mean angular deviation was 13.4° (SD = 9.0°); of trials that preceded a non-reversed OKAN, the mean angular deviation was 9.3° (SD = 7.6°). The significant effect of gain of the preceding OKR on the reversal of OKAN indicates that reversed OKAN was associated with a preceding OKR with lower gain. Mean gain obtained in trials preceding reversed OKAN was 0.523 (SD = 0.336) whereas mean gain obtained in trials preceding non-reversed OKAN was 0.769 (SD = 0.276). This formed the largest predictor of OKAN reversal.

Table 3.13

Results of logistic binomial linear regression analysis to predict the reversal of OKAN following 20 deg/s stimuli, based on four predictor variables: orientation of motion, instruction type, angular SP deviation and gain.

	β	SE	F	*p*
Intercept	5.7274	2.224	2.575	.010*
Orientation (vertical)	-0.3101	1.014	-0.306	.760
Orientation (up oblique)	-2.1122	1.173	-1.800	.072
Orientation (down oblique)	-0.1169	1.165	-0.100	.920
Instruction type	-0.6677	0.699	-0.956	.339
Angular SP deviation	0.1892	0.067	2.805	.005*
Gain	-9.8157	2.653	-3.700	< .001*

Note: horizontal motion was used as a reference variable for analysis of orientation

This analysis was repeated using only data obtained in response to trials using stimuli drifting at 20 deg/s in order to address a collinearity issue between gain and velocity: gain decreases as stimulus velocity increases, therefore it is unclear which variable is contributing to reversal as the two are intrinsically linked. 20 deg/s trials were selected for this analysis due to having the highest number of trials resulting in OKAN. A logistic binomial linear regression analysis was carried out to predict the reversal of OKAN following 20 deg/s motion using orientation of motion, instruction type, angular deviation of the slow phase direction away from the stimulus direction, and OKR gain. The results of this analysis are shown in Table 3.13. A significant regression equation was found ($F(72) = 47.60$, $p < .001$) with an adjusted R^2 of .450. In this model, the reversal of OKAN was significantly predicted by the angular deviation of the slow phase direction away from the stimulus direction during the preceding OKR ($\beta = 0.1892$, $p = .005$) and by the gain of the preceding OKR ($\beta = -9.8157$, $p < .001$), indicating that, with velocity controlled for, slow phase gain still predicts OKAN reversal. The significant effect of gain of the preceding OKR indicates that OKAN reversal is associated with lower OKR gain: OKR preceding non-reversed OKAN had a mean gain of 0.816 (SD = 0.145) whereas mean gain preceding reversed OKAN was 0.581 (SD = 0.264). OKAN reversal was also associated

with greater deviation of the slow phase direction away from the stimulus direction during the preceding OKR: mean deviation in trials with non-reversed OKAN was 8.8° (SD = 6.5°) whereas mean angular slow phase deviation preceding reversed OKAN was 13.5° (SD = 8.9°).

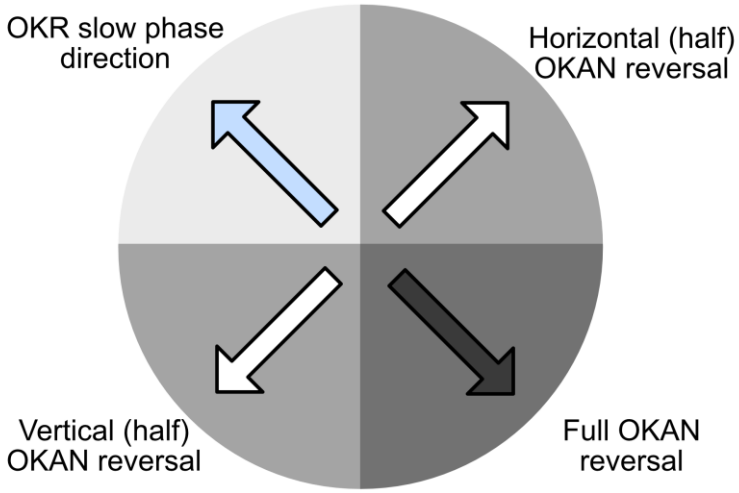

Figure 3.12: Example of the way in which OKAN reversal was classified based on the quadrant in which the OKAN slow phase direction fell. The blue arrow shows the direction of the OKR slow phases (i.e. stimulus direction). White arrows show half reversals; the black arrow shows full reversal.

This analysis was also conducted on individual participants to assess the consistency of the effects. Regression models were calculated for the six participants who produced OKAN to predict OKAN reversal using stimulus velocity, instruction type, angular slow phase deviation and OKR gain. Significant regression equations were found for five out of six participants (P1 ($F(33) = 34.00$, $p < .001$, adjusted $R^2 = .717$), P2 ($F(24) = 19.70$, $p < .001$, adjusted $R^2 = .572$), P4 ($F(34) = 24.90$, $p < .001$, adjusted $R^2 = .446$), P6 ($F(28) = 12.100$, $p = .017$, adjusted $R^2 = .248$), P8 ($F(20) = 13.300$, $p = .010$, adjusted $R^2 = .420$)). The results

of these models can be found in Table AB.6 (Appendix B). Higher angular deviation of the slow phase direction away from the stimulus direction predicted increased occurrence of reversed OKAN in three participants (P1, P4 and P8). OKAN reversal was predicted by a preceding OKR with lower gain in three participants (P1, P4 and P6).

During some trials, OKR direction was reversed only in the horizontal or vertical dimension. The result is that three patterns of OKAN direction are seen: no reversal; full reversal; half reversal. Traces illustrating examples of no reversal (OKAN-I), half reversal and full reversal (OKAN-II) are shown in figures 3.13, 3.14 and 3.15, respectively. Though it was possible for cardinal OKR to show half reversal, as illustrated in Figure 3.14, oblique OKAN was the focus of the analysis of half-reversal due to having consistently larger OKR magnitude in both (vertical and horizontal) dimensions. Among trials involving oblique stimulus motion, OKAN was classed as fully reversed (OKAN slow phase direction falls in a quadrant opposite to that of the preceding OKR slow phase direction) or half-reversed (OKAN slow phase direction falls in a quadrant adjacent to the quadrant of the preceding OKR slow phase direction) (Figure 3.12).

Table 3.14

Results of logistic binomial linear regression analysis to predict the half-reversal of OKAN based on five predictor variables: velocity, direction of motion, instruction type, angular SP deviation and gain.

	β	SE	F	*p*
Intercept	-9.4103	3.465	-2.716	.007*
Velocity	0.2162	0.075	2.889	.004*
Direction (down oblique)	-0.1862	0.715	-0.260	.795
Instruction type	0.3040	0.642	0.474	.636
Angular SP deviation	-0.0498	0.041	-1.224	.221
Gain	8.5988	2.686	3.201	.001*

Note: upward oblique motion was used as a reference variable for analysis of direction

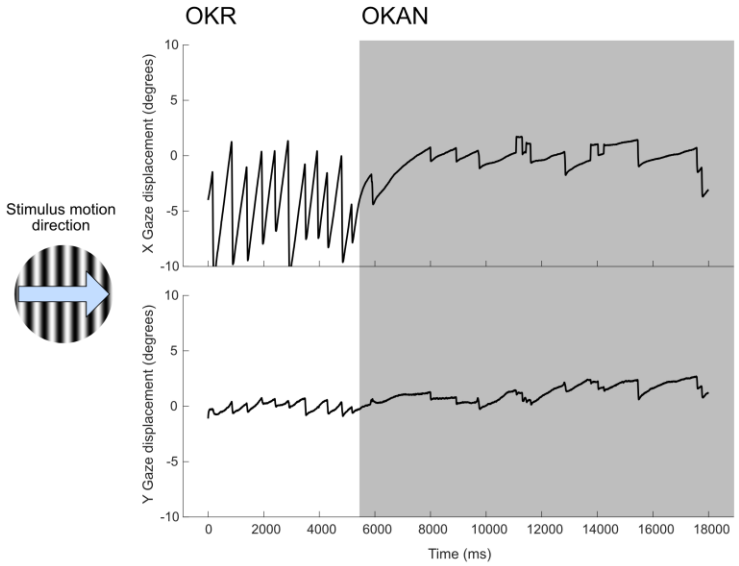

Figure 3.13: Example of OKAN-I: OKAN which follows the direction of the preceding OKR. The upper trace shows horizontal gaze displacement while the lower trace shows vertical displacement. The final few seconds of an OKR trial are shown (white) in addition to the OKAN that followed (grey). Response shown is to rightward motion (20 deg/s) with stare OKR instructions.

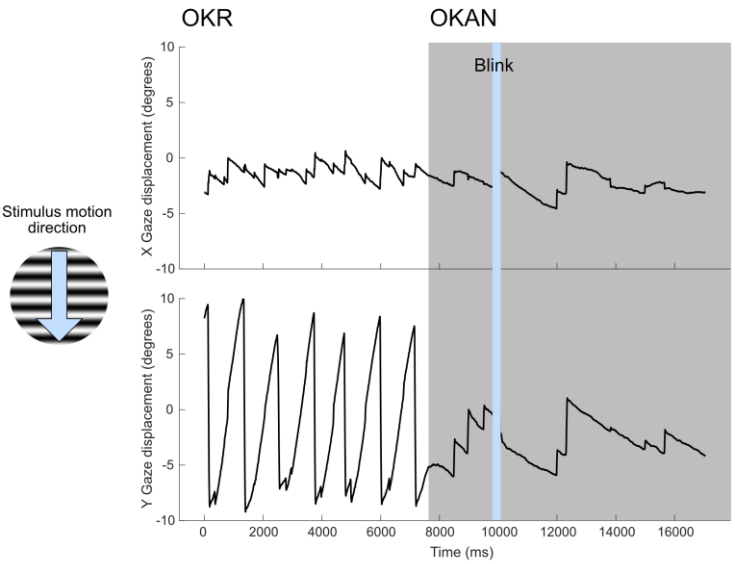

Figure 3.14: Example of half-reversed OKAN. The final few seconds of OKR are shown (white) and the OKAN that follows (grey). While the horizontal gaze (upper) trace shows an OKAN following the direction of the preceding OKR slow phases, the vertical gaze (lower) trace shows an OKAN with a direction opposite to that of the preceding OKR slow phases. Response shown is to downward motion (20 deg/s) with look OKR instructions.

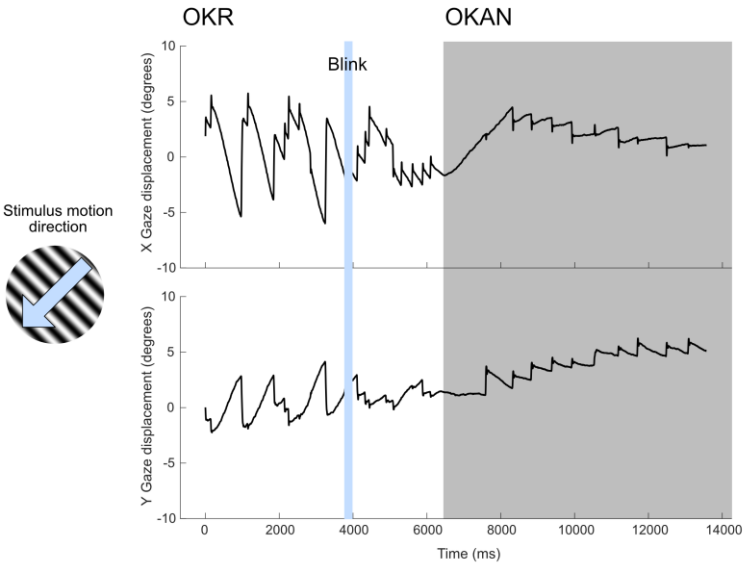

Figure 3.15: Example of OKAN-II without preceding OKAN-I: full reversal of slow phase direction. The final few seconds of OKR are shown (white) and the OKAN that followed (grey). While the horizontal (upper) trace shows an OKR with leftward slow phases, the OKAN slow phases drift to the right; while the vertical (lower) trace shows downward OKR (white), the OKAN slow phases drift upward. Response shown is to oblique down-left motion (40 deg/s) with look OKR instructions.

Looking at OKAN that followed oblique stimulus motion, reversed OKAN were categorised as fully reversed or half reversed. A logistic binomial linear regression analysis was then carried out to predict the half-reversal of OKAN, as opposed to the full reversal, using stimulus velocity, direction of motion (upwards oblique or downwards oblique), instruction type (look or stare), mean angular deviation of the preceding OKR slow phase direction away from the stimulus direction, and the gain of the preceding OKR as predictor variables. A significant regression equation was found ($F(60) = 23.500$, $p < .001$) with an adjusted R^2 of .242. The results of this analysis are shown in Table 3.14.

In this model, the half reversal of OKAN (as compared to the full reversal of OKAN) following stimulation with oblique stimulus motion was predicted by the stimulus velocity ($\beta = 0.2162$, $p = .004$) and the gain of the preceding OKR

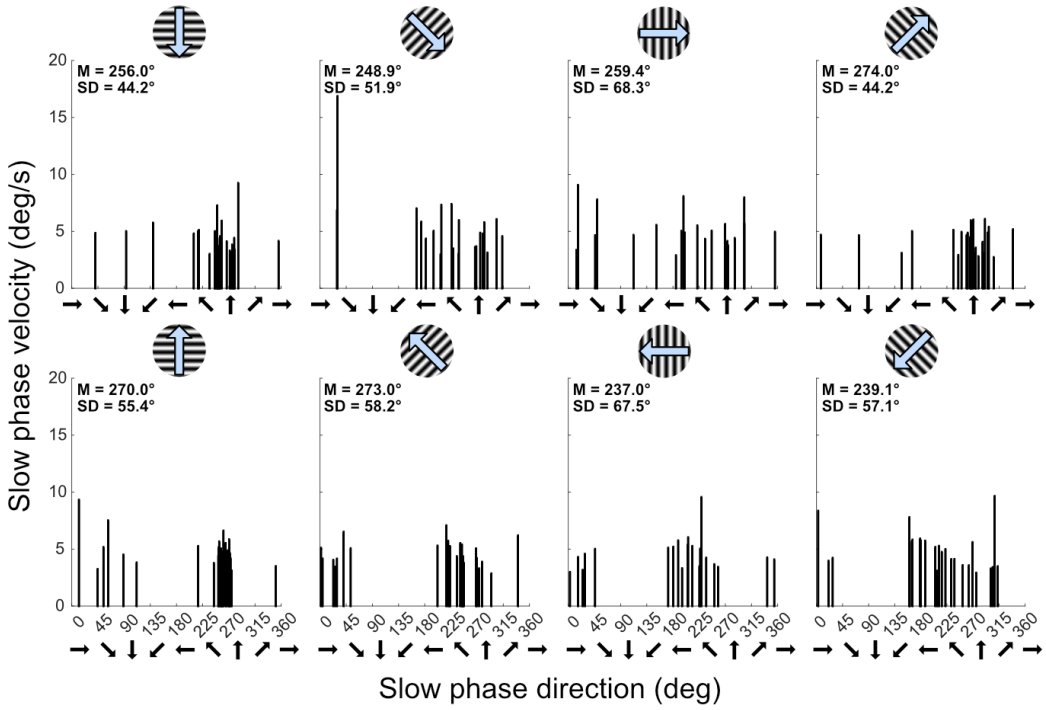

Figure 3.16: Mean direction and velocity of OKAN slow phases in each trial. The stimulus direction during stimulation preceding the OKAN is shown by an icon above each plot. Arrows below the X axis indicate the direction associated with each angle. Mean OKAN slow phase direction following each stimulus direction, and standard deviation of the mean, is show in the upper left corner of each plot.

(β = 8.5988, p = .001). The significant effect of velocity indicates a general upward trend whereby increasing stimulus velocity is associated with increased instance of half-reversed OKR rather than fully reversed OKR. The significant effect of the gain of the preceding OKR indicates that the half-reversal of OKAN, as opposed to full reversal of OKAN, is associated with a preceding OKR with a higher gain: mean gain of oblique OKR preceding fully reversed OKAN was 0.509 (SD = 0.350) whereas that preceding half-reversed OKAN was 0.714 (SD = 0.315).

To address a potential collinearity issue between stimulus velocity and the gain of the preceding OKR, this analysis was repeated using only OKAN following trials that presented oblique motion at 20 deg/s. The results of this analysis are shown in Table 3.15. A significant regression equation was found ($F(21) = 20.50$, $p < .001$) with an adjusted R^2 of .582. This model confirmed that slow phase deviation away from the stimulus direction (β = -0.3247, p = .045) and the gain of the preceding OKR (β = 17.6920, p = .016) significantly predicted whether reversed OKAN was fully or partially reversed, with full reversal of OKAN associated with lower OKR gain than half reversal (Table 3.15).

As there was a significant shift of oblique OKR towards the horizontal axis, t-tests were used to assess whether this shift towards the horizontal axis, leading to greater vertical traversing of the stimulus across the retina, was associated more greatly with vertical reversal of OKAN. Comparing vertically- and horizontally-reversed OKAN, a t-test found a significant difference in the mean angular deviation of the slow phase direction away from the stimulus direction during the preceding OKR ($t(39) = -7.394$, $p < .001$) . This indicates that vertically reversed OKAN following oblique stimulation was associated with significantly greater deviation of the slow phase direction towards the horizontal axis (M = 23.5°, SD = 6.4°) compared to horizontally reversed OKAN following oblique stimulation (M = 9.5°, SD = 5.6°). These t-tests were repeated on individual participant data to examine whether this effect could be consistently observed in the six participants who produced OKAN. Mean angular slow phase deviation towards the horizontal axis was compared in OKRs preceding vertical OKAN reversal and horizontal OKAN reversal, finding that this angular deviation was significantly larger during OKR preceding vertical reversal in five out of six participants (P1 ($t(10) = 3.520$, p = .006), P2 ($t(2) = 21.232$, p = .001), P4

($t(3) = 3.694$, $p = .034$), P6 ($t(6) = 3.629$, $p = .011$), P8 ($t(5) = 4.547$, $p = .006$)), indicating that this was a highly consistent pattern. Mean angular slow phase deviation towards the horizontal axis was calculated for each participant. Mean angular slow phase deviation preceding a horizontal reversal ranged from 0.5° to 15.5° across the six participants, whereas mean angular slow phase deviation preceding vertical OKAN reversal ranged from 16.9° to 33.1°.

Table 3.15

Results of logistic binomial linear regression analysis to predict the half-reversal of OKAN following stimulation at 20 deg/s based on four predictor variables: direction, instructions, angular SP deviation and gain.

	β	SE	F	*p*
Intercept	-7.3281	4.053	-1.808	.071
Direction (down oblique)	-1.1973	1.465	-0.817	.414
Instruction type	2.3667	1.789	1.323	.186
Angular SP deviation	-0.3247	0.162	-1.999	.045*
Gain	17.6920	7.370	2.4005	.016*

Note: upward oblique motion was used as a reference variable for analysis of direction

3.6 Discussion

Regression modelling of OKR showed that 67.0% of the variation in gain, 8.5% of the variation in frequency and 19.1% of the variation in amplitude can be explained by stimulus velocity, direction of motion and instruction type. The lower predictive power of these variables towards the frequency of OKR may reflect the dramatic individual differences seen in OKR frequency; the pattern by which stimulus velocity and instruction condition affect frequency was inconsistent across observers (Figure 3.5). Gain in response to stimuli drifting at 40 deg/s was approximately three times lower than that in response to 10 deg/s stimuli, with one participant producing no downward OKR in response to 40 deg/s stimuli during stare conditions. Vertical motion was associated with lower gain compared to horizontal motion, though gain in response to oblique motion did not differ from that of horizontal motion. As shown in Figure 3.3, the gain-

stimulus velocity response function of oblique motion resembles that of horizontal motion rather than falling halfway between horizontal and vertical motion. This may be due to the angular deviation of the slow phase direction away from the stimulus direction during stimulation with oblique motion; analyses showed that oblique motion, particularly downwards oblique motion, was associated with a significant shift of OKR slow phase direction towards the horizontal axis. This indicates that the horizontal and vertical components did not contribute equally to OKR in response to 45° stimuli; rather, the horizontal component was larger. For example, during stimulation with oblique motion in a downward direction, a mean shift of the slow phase direction of 20.0° was observed; this means that rather than tracking the stimulus along its true 45° direction, observers tracked the stimulus at 25.0°. Kröller and Behrens (1995) and Raphan and Cohen (1988) both showed a tendency for oblique slow phases to shift towards the horizontal axis in monkeys; the result of the present study indicates that this also occurs in human OKR.

Due to inconsistencies in previous research regarding the up-down symmetry of vertical OKR, both vertical and oblique OKR were assessed for up-down symmetry. Murasugi and Howard (1989b), Howard and Simpson (1989) and Garbutt, Han, Kumar, Harwood, Harris, et al. (2003) reported up-down asymmetry in vertical OKR, with higher gain in response to upward-drifting stimuli. Murasugi and Howard (1989b) found this to be a velocity-based effect; there is evidence that at stimulus velocities of ~10-15 deg/s, OKR is vertically symmetrical (Kanari et al., 2017; Murasugi & Howard, 1989b). In the present study, direction of vertical motion was found to significantly predict gain during look OKR conditions, but no effect was seen during stare conditions at the group level. There was no interaction between direction of vertical motion and velocity, indicating that the effect was not velocity dependent within the tested velocity range. Similar effects were seen in frequency and amplitude, with no asymmetry in response to stare OKR conditions. Upward motion elicited higher slow phase amplitude and lower OKR frequency during look, but not stare, OKR. This evidence indicates that, rather than being an effect of velocity, vertical OKR asymmetry is related to whether the response is active (look OKR) or passive (stare OKR). During look OKR, downward OKR was associated with a smaller amplitude, higher frequency, lower gain OKR. Oblique OKR was also assessed for up-

down asymmetry, but no effect was found in either look or stare OKR; this may again be related to the significant shift of oblique OKR slow phase direction towards the horizontal axis, reducing the role of the vertical component. It is noted that some participants did exhibit a vertical stare OKR asymmetry, producing higher gain in response to upward-drifting stimuli. However, further analysis found that these participants had significantly higher vertical stare OKR gain and slow phase amplitude compared to those without vertical stare OKR asymmetry. This may point towards these individuals producing a more look-OKR-like nystagmus during stare OKR conditions; despite careful presentation of instructions to differentiate look and stare OKR conditions, it cannot be guaranteed that participants did not attempt to pursue targets during stare conditions. The vertical asymmetry found in these participants during stare OKR conditions may thus reflect a failure to adequately follow the provided instructions. Additionally, regression models at the individual level showed that participants who presented with significant look OKR asymmetry were those who also had a significant effect of instruction type on gain, indicating that these participants more effectively followed the provided look and stare OKR instructions.

Oblique OKR showed a significant shift of slow phase direction towards the horizontal axis, therefore OKR in response to cardinal motion showed significantly greater directional accuracy. Kröller and Behrens (1995) suggested that the shift towards the horizontal axis may reflect a breakdown of the vertical component, due to the EOKR system struggling to maintain vertical gain at high stimulus velocities. Due to the finding of lower gain in response to stare OKR, it was expected that stare OKR should be more greatly affected in this case. Analysis was therefore carried out to assess whether the mean angular deviation of slow phase direction away from the stimulus direction was related to stimulus velocity or instruction type. Results showed that there was no effect of stimulus velocity on angular slow phase deviation, and that the only difference between look and stare OKR in terms of angular slow phase deviation occurred in response to horizontal stimulus motion. These findings do not support the assertion that angular slow phase deviation towards the horizontal axis during oblique stimulation occurs as a result of lower vertical gain and the breakdown of the vertical component at high velocity, as increasing stimulus velocity was

not associated with greater angular slow phase deviation, and both look and stare OKR were equally affected despite stare OKR having lower gain.

To investigate the possibility that stare OKR is more associated with the activity of the LOKR system than look OKR, the build-up of gain throughout the trial was tested. Past evidence suggested that the build-up of gain is not visible in humans due to EOKR activity (Cohen et al., 1981). The present analysis showed that during look OKR conditions there was no significant effect of time on gain; gain reached asymptote within the first five seconds of stimulation, indicating that the response was generated by the EOKR system (Abadi et al., 1994). As EOKR is thought to be mediated by a cortical pathway (Fuchs & Mustari, 1993), this finding is in keeping with reports of greater cortical activity during look, compared to stare, OKR (Kashou et al., 2010; Konen et al., 2005). However, surprisingly, during stare OKR gain continued to increase significantly for ~25 seconds, indicating a role of the LOKR system in stare OKR. The possibility of a velocity dependent effect of involvement of the LOKR system was also assessed; there is previous evidence that the LOKR component is maximally active in the 40-70 deg/s range (Lafortune et al., 1986b), therefore it was expected that higher stimulus velocity would be associated with greater build-up of gain throughout the trial. However, no effect of time on gain was observed at 40 deg/s, though a significant effect was seen in response to motion at 20 deg/s, whereby gain continued to increase significantly for the first ~20 seconds of stimulation. Additionally, while OKAN is thought to be related to the activity of the LOKR component, stimulus velocity did not significantly predict the occurrence of OKAN. Taken together, these findings do not offer support for LOKR being maximally active at a higher stimulus velocity. It should be noted, however, that stimulus velocities beyond 40 deg/s were not tested in the present study; it is possible that further increasing stimulus velocity may show an effect, as the stimulus velocity used here was at the low end the 40-70 deg/s range suggested by Lafortune et al. (1986b). Additionally, an absence of build-up of OKR gain does not indicate an absence of LOKR activity; rather, it indicates dominance of EOKR activity (Cohen et al., 1981) such that activity of the LOKR system is obscured.

OKAN was produced by six of the eight tested observers, highlighting the presence of individual differences in OKAN occurrence. The occurrence of

OKAN was not explained by any of the predictor variables (stimulus velocity, direction of motion, angular deviation of the preceding OKR, gain of the preceding OKR). Despite stare OKR showing a greater build-up of gain throughout the trial, indicating a role of the LOKR system, stare OKR was not associated with significantly more OKAN occurrences than look OKR. It may therefore be the case that rather than being associated with increased activity of the LOKR system compared to look OKR, stare OKR may be associated with decreased activity of the EOKR system compared to look OKR. Again, this assertion is in keeping with evidence of lower cortical activity during stare, compared to look, OKR (Kashou et al., 2010; Konen et al., 2005).

Past literature has offered many potential explanations of the reversal of OKAN (OKAN-II). It has been suggested that lower stimulus velocities may be associated with OKAN-I, while higher stimulus velocities are associated with OKAN-II (Collewijn, 1985). The findings of the present study showed that OKAN reversal was predicted by stimulus velocity, whereby higher stimulus velocities were associated with higher rates of OKAN reversal. This lends support to suggestions of a relationship with stimulus velocity, however, issues of collinearity between stimulus velocity and OKR gain leave a question mark over the true contribution of stimulus velocity. Motion habituation has also been suggested to play a role in OKAN reversal (Brandt et al., 1974; Chen et al., 2014; Gygli et al., 2021; Ventre-Dominey & Luyat, 2009), therefore the role of gain and angular slow phase deviation during the preceding OKR was investigated. If OKAN reversal is related to motion habituation, it would be expected that conditions during which there is greater retinal slip, such as would occur during OKR with lower directional and gain accuracy, should result in higher instances of OKAN reversal. The data supported a link between motion habituation and OKAN reversal: lower OKR gain and greater angular deviation of the OKR slow phase direction were associated with higher rates of OKAN reversal. As the gain of the OKR and stimulus velocity are strongly related, the analysis was re-run at a single stimulus velocity (20 deg/s) to verify that the significant effect of OKR gain on OKAN reversal was in fact a consequence of lower gain and not of increased stimulus velocity. The results showed that gain remained a significant predictor of OKAN reversal. Due to the large variation in gain in response to different stimulus velocities, controlling for gain to assess the role of velocity

was not possible. Therefore, while the gain of the preceding OKR has been confirmed as a predictor of OKAN reversal, the role of stimulus velocity remains unclear due to its collinearity with gain.

Many OKAN were neither in the direction of the preceding OKR nor fully reversed; these OKAN were reversed in only the vertical or horizontal component. The occurrence of OKAN that is reversed in only one component provides strong evidence for separate velocity storage for horizontal and vertical motion. The occurrence of half-reversed OKAN, as opposed to fully reversed OKAN, was modelled. While the analysis of the occurrence of OKAN reversal indicated that reversed OKAN was associated with lower OKR gain compared to OKAN-I, analysis of half reversal indicated that full reversal is associated with lower OKR gain than half reversal. This suggests that the lower the gain of the preceding OKR, the more complete the reversal of the following OKAN. This was again repeated using only OKAN following a single stimulus velocity (20 deg/s) to verify that this was not an effect of stimulus velocity, confirming that the extent of reversal was predicted by the preceding OKR gain. These findings provide further evidence that reversal of OKAN may be related to the extent of residual retinal slip during optokinetic stimulation, with greater retinal slip leading to OKAN reversal in a way that is related to habituation to this motion. This was further substantiated by the finding that, following oblique stimulation, vertically reversed OKAN was associated with a significantly greater shift of the OKR slow phase towards the horizontal axis. This suggests that, when OKR slow phases shift towards the horizontal axis, the greater vertical retinal slip that results from the angular shift of the slow phase causes the following OKAN to be reversed in only the vertical dimension.

While the results of Ventre-Dominey and Luyat (2009) showed occurrence of OKAN with a vertical component, monkey studies have reported weak or no vertical OKAN (Kröller & Behrens, 1995) or a lack of upward OKAN (Raphan & Cohen, 1988; Matsuo & Cohen, 1984). In contrast, the present study showed that vertical OKAN does occur, with upward OKAN observed more frequently than downward OKAN (Figure 3.16). Both upward and downward stimulation were associated with an upward OKAN; it is possible that this was related to the lower gain in response to stimulation with downward motion compared to upward motion. The discrepancy between these results and those of studies

involving monkeys (Kröller & Behrens, 1995; Raphan & Cohen, 1988; Matsuo & Cohen, 1984) may indicate differences in vertical velocity storage between primate species.

Experiment 1: Summary of key findings

- Increasing stimulus velocity and use of stare instructions significantly decreased OKR gain
- Oblique OKR was more similar to horizontal OKR; this may be due to oblique OKR slow phases shifting towards the horizontal axis, resulting in a greater contribution from the horizontal component during oblique OKR
- Vertical OKR was asymmetric in terms of gain, amplitude and frequency, with stronger responses to upward motion, most evident during look OKR conditions; this effect was not reflected in the oblique OKR and was not dependent on velocity
- Stare OKR showed a significant build-up of slow phase velocity throughout the trial, whereas look OKR did not; however, both OKR types were similarly associated with OKAN, indicating equal LOKR activity. Taken together, this indicates that rather than being associated with increased LOKR activity, stare OKR may be associated with decreased EOKR activity
- Reversal of OKAN was predicted by the gain and angular slow phase deviation of the preceding OKR, with oblique slow phase shifts towards the horizontal axis being associated with vertical OKAN reversal; this indicates that reversal of OKAN may be related to increased retinal slip during the preceding OKR, possibly as a result of motion habituation
- Half reversal of OKAN points to separate velocity storage for vertical and horizontal components

3.6.1 New stimulus for future experiments

Due to observers reporting feelings of discomfort caused by the grating stimulus, finding the stimulus visually unpleasant due to strobing, and one participant reporting severe motion sickness induced by the stimulus, a different

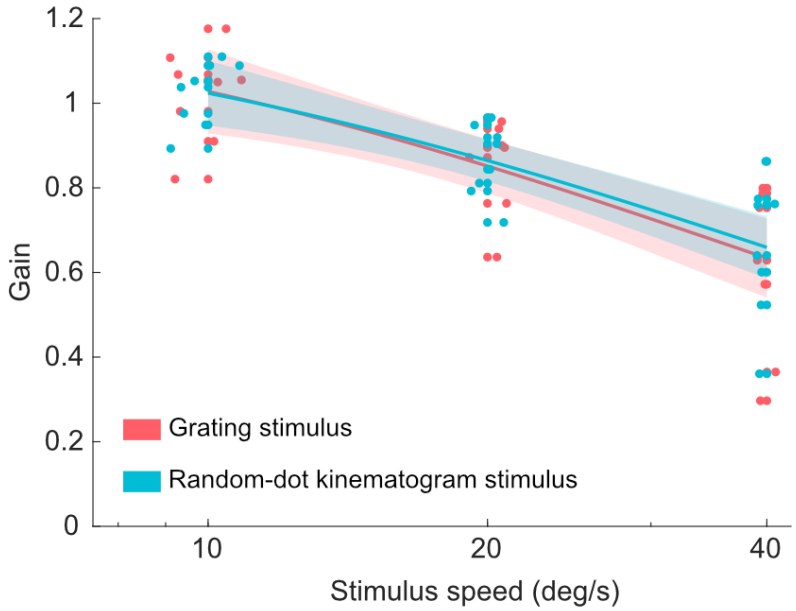

Figure 3.17: N = 1. Gain in response to stimulus motion at 10 deg/s, 20 deg/s and 40 deg/s during stimulation with a sinusoidal luminance grating stimulus (red) and a RDK stimulus (blue). Individual data points show the mean gain obtained in a single trial; the shaded area indicates the 95% CI of the fitted function. A horizontal jitter of up to 4 deg/s has been applied to improve the visibility of data points.

stimulus was developed for use in subsequent experiments. The new pilot stimulus presented dots with an approximate density of 0.63 dots/deg^2, drifting with 100% coherency. Random-dot kinematogram (RDK) stimuli have been used widely in OKR research and are effective at driving an OKR (e.g. Kanari et al., 2017; Murasugi & Howard, 1989b, 1989a; Ventre-Dominey & Luyat, 2009). To confirm suitability, the new RDK stimulus gain was plotted against that obtained by the same observer in response to the grating stimulus (Figure 3.17). Stimuli were presented at 10 deg/s, 20 deg/s and 40 deg/s to enable comparison between responses to RDK and grating stimuli. Excellent agreement in gain was obtained at each stimulus velocity. It was therefore assumed that the RDK stimulus provides a suitable alternative stimulus to be used in future experiments.

Chapter 4

Experiment 2: The effect of stimulus area, retinal location, attention and different directions of stimulus motion

4.1 Introduction

In the previous chapter, OKR was investigated in terms of its variation based on task instruction, stimulus velocity and direction of stimulus motion. In the following chapter, OKR will be investigated in terms of the role of visual attention, stimulus size, visual field region, and the effect of the presence of two different directions of stimulus motion. The effect of stimulus area in both central and peripheral visual field regions will be tested to assess whether the impact of stimulus area on the OKR is similar across the visual field, and to assess whether the impact of attention varies across stimulus area or visual field region. Stimuli with a centre-surround configuration will be presented with different directions of motion in each region, while visual attention is directed to either the centre or the surround. Such stimuli will be used to investigate whether a peripheral OKR can be induced in the presence of opposing central motion, and whether the presence of incongruent (opposing or Brownian) motion has an impact on the response to each visual field region.

The effect of stimulus area upon the gain of the OKR has been studied repeatedly, with past research agreeing that increasing stimulus area is associated with an increase in gain (Abadi et al., 2005; Cheng & Outerbridge, 1975). As stimulus area increases, so does the upper velocity limit of the OKR. This is thought to be the result of the peripheral contribution to the OKR (Dichgans, 1977; Hood, 1967, 1975). However, the vast majority of research regarding the impact of stimulus area on the OKR has involved stimulating the central visual

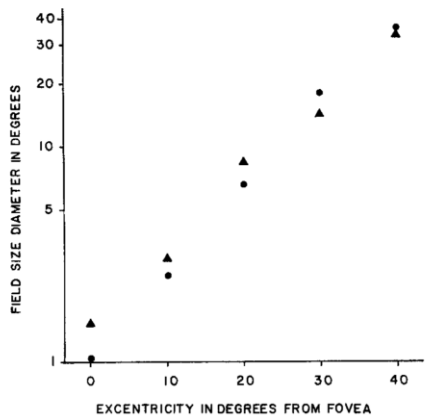

Figure 4.1: From Koerner and Schiller (1972). Minimum stimulus diameter required to elicit an OKR in two monkeys (circles or triangles) under open-loop conditions, across stimulus eccentricity.

field; less is known about the impact of stimulus area in peripheral visual field regions. In a study using monkeys, Koerner and Schiller (1972) reported that the size of a stimulus required to produce OKR was an exponential function of eccentricity, with more eccentric regions requiring larger stimuli to drive the response (Figure 4.1).

Though most OKR research has involved central stimuli, some studies have investigated the peripheral response. Evidence from humans and monkeys has shown that an OKR can be produced even when the central visual field is occluded, though the gain is lower (Abadi et al., 1999, 2005; Abadi & Pascal, 1991; Cheng & Outerbridge, 1975; Dichgans, 1977; Dubois & Collewijn, 1979; Howard & Ohmi, 1984; Koerner & Schiller, 1972; van Die & Collewijn, 1986; van Die and Collewijn, 1982). In monkeys, Koerner and Schiller (1972) found that as the size of a central occlusion was increased, the gain of the OKR decreased; however, even with a central occlusion of 40 deg, OKR was still produced. Abadi et al. (2005) also showed that peripheral stimulation can produce an OKR with lower gain, however, the rate of build-up of the OKR was similar in response to both central and peripheral stimulation. Based on this information, they argued that the central and peripheral visual fields have common access to mechanisms driving early/fast OKR (EOKR).

It has been suggested that differences in response to retinal slip between central and peripheral regions may be related to the characteristics of motion-sensitive visual feedback mechanisms in the two regions (Abadi et al., 2005); the smaller receptive fields in the centre allow for greater sensitivity to low-velocity

motion, such as would be experienced during high-gain OKR, allowing responses to the centre to be more finely tuned to stimulus velocity (Barnes, 1993; Smith & Snowden, 1994). However, the nature of the response during simultaneous stimulation with differing central and peripheral stimuli is unclear. Abadi and Pascal (1991) reported that, though stimulation of the periphery alone produced a peripheral OKR, in the presence of central and peripheral stimuli with different motion directions the response was driven by the central stimulus. This indicates motion in the centre may be more highly weighted in driving the OKR. Central superiority and higher weighting have been described in many domains: perceptual integration studies using motion stimuli suggest that top-down feedback aiding feature binding is stronger in central compared to peripheral vision (Bi et al., 2022), and perceptual decision-making studies indicate that humans place more weight on foveal than peripheral information (Gloriani & Schütz, 2019).

Attention is known to affect the OKR. It can be used to manipulate the driving stimulus. Maruyama et al. (2003) superimposed two stimuli with different directions of motion onto the same plane, reporting that though OKR initially followed the vector average of the two orthogonally drifting stimuli, attentional selection quickly caused the OKR to follow just the attended stimulus. Attention can also affect OKR measures obtained in response to a stimulus. Frattini and Wibble (2021) showed that increasing attention towards a stimulus increased the frequency of the OKR, whereas alertness (measured using pupil size) was related to gain. OKR is facilitated by unity between the locus of attention and of gaze, with higher gain being reported when the two are at the same location (Kanari et al., 2017). This evidence suggests that the OKR is impacted by the attention of the observer, with increased attention towards a stimulus having a facilitative effect.

The intersection of the roles of attention, stimulus area and visual field location in OKR is under studied. Additionally, imprecise manipulation of attention in past research may contribute to a lack of clarity regarding the effect of the presence of multiple directions of stimulus motion. While Abadi and Pascal (1991) showed that the centre dominates the response while attention is uncontrolled, other research has sought to investigate the role of attention in such effects. Howard and Ohmi (1984) showed that, in the absence of central stimulation, attention to the peripheral stimulus was not required to drive a peripheral

OKR. In a subsequent study (Howard & Gonzalez, 1987), different directions of motion were presented to the centre and to the periphery; in this case, instructing observers to attend to the periphery was insufficient in generating a peripheral OKR. Taken together, this evidence indicates that while attention to the periphery is not required to drive a peripheral OKR, central motion, when present, will be prioritised in driving the response. Kanari et al. (2017) disputed this conclusion, arguing that there is an attentional bias in favour of the central visual field, and attention had not been precisely manipulated in past research; observers were simply instructed to 'attend to' the peripheral stimulus. Presenting opposing directions of random-dot kinematogram stimulus motion to different visual field regions, including in a centre-surround configuration (Chapter 1 (General Introduction), Figure 1.9), they manipulated attention towards each region by using a counting task. Their study showed that directing attention towards the visual periphery was sufficient to produce a response to the periphery even in the presence of incongruent central motion. Further, they reported that the peripheral response was nearly the same regardless of whether motion was presented to the centre, noting that during attention to the periphery, very few slow phases were made in response to the centre.

Eccentricity effects in vision are often attributed to anatomical differences between central and peripheral visual field regions at multiple levels of processing, such as higher cone cell density in the central retina leading to greater central acuity (Anstis, 1998; Curcio et al., 1990; Curcio & Allen, 1990). However, accounting for these differences using methods such as M-scaling does not always completely remove eccentricity effects (Bao et al., 2013; Staugaard et al., 2016; Valsecchi et al., 2013; Wolfe et al., 1998), leaving open the possibility that there is another factor contributing to such effects. Attention is often suggested as being an additional source of eccentricity effects in vision. Increasing attention towards the visual periphery has been shown to alleviate some eccentricity effects in vision (Kirsch et al., 2020; Staugaard et al., 2016; Kanari et al., 2017), indicating a role of attention in these eccentricity effects. As OKR has been shown to be affected by both eccentricity and attention, it is possible that attention contributes to eccentricity effects in the OKR. If attention can raise the peripheral performance to the level of central performance, this is an indicator that the eccentricity effect is caused by attentional differences across the visual field.

The following chapter presents Experiment 2, which is divided into three parts. In Part 1, central and peripheral stimuli will be presented separately while stimulus area and visual attention are manipulated. In Part 2, stimuli with a centre-surround configuration will be presented with opposite directions of motion shown in each region, while stimulus area and attention are manipulated. In Part 3, centre-surround stimuli will again be presented, however, motion in one region will be coherent while motion in the other region will be Brownian. This will aid in assessing the extent to which results obtained in Part 2 are a consequence of the presence of two opposing optokinetic stimuli or a consequence of the presence of incongruent motion more generally.

4.2 Methods

4.2.1 Participants

Participants were postgraduate students and staff at the University of Nottingham who were naïve to the purposes of the experiment. The experiment was divided into three parts: Part 1 and Part 2 used the same nine participants. One participant (P2) was no longer available for Part 3, resulting in a replacement participant (P10) being used. One participant (P5) had an ocular pathology in the right eye therefore the left eye was recorded from this participant, though the right eye was recorded from every other participant. Each part of the experiment used five male and four female participants. The overall age range of participants was 22-60 years (M = 32.9 years).

4.2.2 Stimuli

Stimuli were random-dot kinematograms (RDKs) with an approximate density of 7.64 dots/deg^2 (Figure 4.2). RDKs presented black dots (0.38lm) against a grey (94.8lm) background. Each dot was seven pixels in size (diameter: 3 pixels, ~0.075 deg). Dot motion was either horizontal with 100% coherency or Brownian (0% coherency, random-walk). Coherent dots drifted towards the right in 50% of trials and towards the left in 50% of trials. Two stimulus velocities were used: 15 deg/s and 30 deg/s. A drift velocity of 15 deg/s was used across

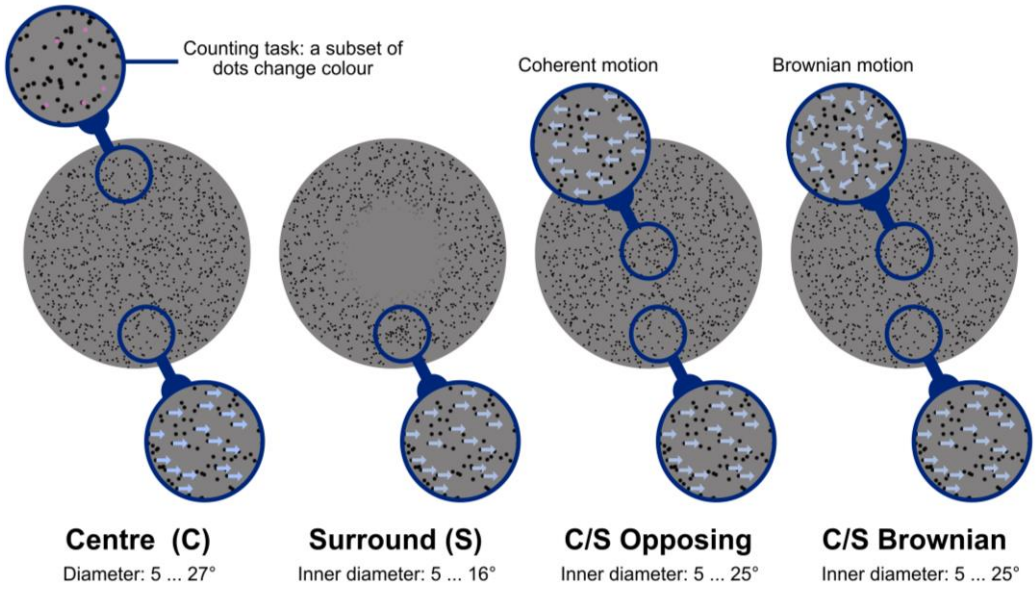

Figure 4.2: The four stimulus configurations used: Centre (C), Surround (S), Centre-Surround with opposing motion (C/S Opposing) and Centre-Surround with Brownian motion (C/S Brownian). Arrows in magnified bubbles indicate dot coherency with example dot direction; dots drifted with 100% coherency, with the exception of Brownian stimuli, in which dots within one region had 0% coherency (random-walk). Coherent dot motion was horizontal, drifting either towards the left or towards the right. The appearance of the counting task is indicated in the upper left bubble: a subset of dots (shown here as magenta) changed colour throughout each trial. For Centre (C) stimuli, 'diameter' refers to outer diameter of the stimulus; for all other stimuli, the outer diameter was 27 deg, with 'inner diameter' referring to the diameter of the central region of the C/S stimulus, or the central occluding mask diameter of the Surround (S) stimulus.

all conditions, whereas conditions involving presentation of Centre (C) and Surround (S) stimuli were repeated in a subset of four participants at a velocity of 30 deg/s. Dot behaviour was as described in General Methods (Chapter 2, section 2.3.2). Dots in Brownian stimuli had the same behaviours as coherent dots with the exception of dot direction; Brownian motion dots were each assigned a random direction of motion on every frame of the stimulus (random-walk). Each stimulus was shown for a duration of 20 seconds.

Stimuli had four configurations (Figure 4.2): Centre (C), Surround (S), Centre-Surround Opposing (C/S Opposing) and Centre-Surround Brownian (C/S Brownian).

4.2.2.1 Centre (C) stimuli

Centre stimuli (Figure 4.2, Centre (C)) had a range of diameters: 5, 7, 10, 13, 16, 19, 22, 25 and 27 deg of visual angle. The overall stimulated area therefore ranged from 19.63-572.56 deg^2. Centre stimuli used coherent horizontal dot motion.

4.2.2.2 Surround (S) stimuli

Surround stimuli (Figure 4.2, Surround (S)) had an outer diameter of 27 deg of visual angle. A grey mask matching the background colour with a Gaussian blurred edge was used to occlude the central region of the stimulus. A range of inner diameters (diameter of the mask) was used: 5, 7, 10, 13 and 16 deg. The stimulated area therefore ranged from ~371.57-552.93 deg^2. Surround stimuli used coherent horizontal dot motion.

4.2.2.3 Centre-surround opposing stimuli (C/S Opposing)

C/S Opposing stimuli (Figure 4.2, C/S Opposing) had an outer diameter of 27 deg of visual angle. These stimuli presented one direction of dot motion to a central region while the opposite direction of motion was presented in the surround. These stimuli used coherent horizontal dot motion. In 50% of trials, the centre contained leftward drifting motion while the surround contained rightward drifting motion; in the other 50% of trials, these motion directions were reversed. The range of inner diameters (diameter of the central region) used was 5, 7, 10, 13, 16, 19, 22 and 25 deg. The overall stimulated area therefore remained constant at 572.56 deg^2, with the ratio of centre to surround area varying. The area of the central region ranged from 19.63-490.87 deg^2. As the inner diameter was increased, the surround region became smaller and more eccentric; the area of the surround ranged from 81.69-552.93 deg^2.

4.2.2.4 Centre-surround Brownian stimuli (C/S Brownian)

C/S Brownian stimuli (Figure 4.2, C/S Brownian) were the same as the C/S Opposing stimuli in terms of the outer diameter and the range of inner

diameters used. However, instead of presenting opposite directions of coherent dot motion in each region, C/S Brownian stimuli presented coherent horizontal dot motion in one region (centre or surround) while presenting Brownian motion in the other region. In 50% of trials, motion in the centre was coherent while motion in the surround was Brownian; in the other 50% of trials, motion in the surround was coherent while motion in the centre was Brownian. Coherent motion drifted in a leftward direction in half of trials and in a rightward direction in the other half of trials.

4.2.3 Attention (counting) task

A counting task, such as described in General Methods (Chapter 2, section 2.4), was presented during some trials to increase the attention directed to the stimulus, or to particular regions of the stimulus (Figure 2.3 (General Methods, section 2.4), Figure 4.2).

Coloured task dots had an approximate density of 0.175 dots/deg^2 when presented in a Centre (C)/centre region of C/S stimulus, or in a Surround (S) stimulus/surround region of a C/S stimulus with an inner diameter up to 13 deg of visual angle. Surround (S) and surround regions of C/S stimuli which involved an inner diameter of over 13 deg used a higher proportion of coloured task dots to increase the visibility of these coloured dots, as peripheral vision has reduced colour sensitivity (e.g. Hansen et al., 2009) and the small area of some surround regions would otherwise result in very few coloured dots being shown on a given frame. At an inner diameter of 16 deg, the proportion of coloured task dots in the surround was increased by 50% to a density of ~0.262 dots/deg^2; at an inner diameter of 19 deg, the proportion of coloured task in the surround dots was increased by 70% relative to that of central presentation, to a density of ~0.297 dots/deg^2; at an inner diameter of 22 deg and above, the proportion of coloured task dots in the surround was increased by 100% relative to that of central presentation, to a density of ~0.349 dots/deg^2. Overall dot density was consistent across all stimuli; as the number of coloured dots increased, the number of black dots decreased in order to maintain a consistent overall dot density of ~7.640 dots/deg^2.

With the exception of their colour and density, coloured task dots followed the same behaviour as the task-irrelevant black dots. They followed the same speed and direction as the task-irrelevant black dots of the region in which they were presented. During Centre (C) and Surround (S) stimuli, coloured task dots were presented across the entire stimulated area. During C/S stimuli, coloured task dots were presented either in the centre or in the surround in order to manipulate which region the participant attended to. During C/S Brownian stimuli, the location of the coloured task dots was always the region using coherent motion; coloured dots were not presented to regions using Brownian motion.

4.3 Part 1: Centre (C) and Surround (S) stimuli

4.3.1 Methods

4.3.1.1 Participants

During Part 1, nine participants (five male, four female) took part in all trials involving stimuli drifting at 15 deg/s. The age range of these participants was 23-60 years (M = 32.9 years). These trials were later repeated at 30 deg/s using just four of the participants (two male, two female) with the aim of confirming whether the observed effects can be generalised to other stimulus velocities. The age range of these participants was 23-39 years (M = 30.8 years).

4.3.1.2 Stimuli

Part 1 used the previously described Centre (C) and Surround (S) stimuli (Figure 4.2). Stimuli were presented to all participants with a dot speed of 15 deg/s; in four participants, these stimuli were also presented at 30 deg/s. The counting task was presented during 50% of trials.

4.3.1.3 Design

During Part 1, participants were each presented with a total of 56 stimuli: 36 Centre (C) stimuli and 20 Surround (S) stimuli. Stimuli varied in size, with each size of stimulus being shown four times: using leftward motion, once with

the counting task and once without; using rightward motion, once with the counting task and once without. Stimuli were shown across multiple blocks, and the order of blocks was randomised for each participant.

Gaze monitoring

Gaze location was monitored throughout the experiment to ensure that participants were viewing the correct region of the stimulus. During presentation of Centre (C) stimuli, this prevented participants from gazing towards the edges of the stimulus, as stationary edges have a suppressive effect on OKR gain (Murasugi et al., 1986). Additionally, maintaining central gaze ensures that the extent of optokinetic stimulation is approximately equal on either side of the fovea. During Surround (S) stimuli, gaze position monitoring was used to ensure that only peripheral regions would be stimulated while gaze was maintained within the central mask. During smaller Centre stimuli (<16 deg diameter) and Surround stimuli, participants were prevented from gazing within 1 deg of the edge of the stimulus or mask. At 16 deg diameter and above, this restriction was increased to within 1.5 deg of the edge. With a stimulus or central mask size of 5 or 7 deg diameter, the limitation of not looking within 1 deg of the edge was found to be too restrictive, as the OKR being produced had an amplitude which exceeded the allowed area; for this reason, during these conditions, the restriction was reduced whereby participants were not able to gaze within 0.5 deg of the edge.

When a participant viewed a disallowed region of the stimulus for 700ms, a warning reading '*LOOK AT THE MIDDLE*!' was displayed in red text at the centre of the screen for 1000ms, and an extra 1000ms was added to the overall stimulus duration to account for the interruption. Such gaze deviations were marked in the data file so that data gathered while the participant viewed disallowed areas of the stimulus could be removed.

Centre (C) stimulus block design

To limit the duration of each block, the nine sizes of Centre stimuli were split in two: one block contained the 5 to 16 deg diameter stimulus range, and

another block contained the 19 to 27 deg stimulus range. As both directions of horizontal motion were used, this resulted in blocks containing ten and eight stimuli, respectively. Counting task and non-task conditions were shown in separate blocks. Centre stimuli were therefore shown across a total of four blocks: the smaller (5-16 deg) stimuli, one block with and one block without the counting task; the larger stimuli (19-27 deg), one block with and one block without the counting task. The order of stimuli within each block was randomised.

Surround (S) stimulus block design

Surround stimuli had a smaller range of sizes (5-16 deg mask diameters), so all sizes were shown within a single block. Both directions of horizontal motion were used, resulting in 10 stimuli being presented in a block. Surround stimuli were therefore shown across two blocks: one with the counting task and one without. The order of stimuli within each block was randomised.

4.3.1.4 Procedure

Participants were provided with verbal instructions and shown example trials to allow them to familiarise with the stimuli and task. Written instructions were also provided on-screen prior to the presentation of each stimulus. At the start of each block, the eye tracker was calibrated using a nine-point calibration grid.

Non-counting task condition

During the trials that did not use the counting task, prior to the presentation of each stimulus, instructions reading '*Please look towards the centre of the screen. Press SPACE to continue.*' were presented in black text at the centre of the display. Each trial began with a three-second on-screen countdown to prepare the participant for the onset of the stimulus. The stimulus was then presented for 20 seconds, during which time the participant's eye movements were recorded. An on-screen message informed participants when the block had come to

an end, at which point they were given the opportunity to continue to the next block or to terminate the session.

Counting task condition

During trials that used the counting task, prior to the presentation of each stimulus, instructions written in black text were displayed at the centre of the screen. During Centre (C) stimulus blocks, the instructions read '*Please look towards the centre of the screen while counting the number of colours presented at the CENTRE of the screen. Press SPACE to continue.*' During Surround (S) stimulus blocks, the instructions read '*Please look towards the centre of the screen while counting the number of colours presented in the SURROUND of the screen. Press SPACE to continue.*' Each trial began with a three-second on-screen countdown. The stimulus was then shown for 20 seconds while the participant's eye movements were recorded. At the end of each trial, black on-screen text read '*How many different colours did you see? Using the keyboard, provide a response between 1 and 9.*' Once a response was provided, the next trial began. An on-screen message informed participants when the block had come to an end, at which point they were given the opportunity to continue to the next block or to terminate the session.

4.3.2 Results

4.3.2.1 Centre (C) stimulus: Gain

A linear regression model was calculated to predict OKR gain obtained during Centre stimulus conditions based on stimulus area, counting task condition (with task or without task) and stimulus velocity (15 or 30 deg/s) and to examine whether there was an interaction between stimulus area and counting task condition. A significant regression equation was found ($F(4, 467) = 182.24$, $p < .001$) with an adjusted R^2 of .608. There was no significant interaction between stimulus area and task condition ($p = .079$). The coefficients indicate that increasing stimulus area increased gain ($\beta = 0.0008$), that increasing stimulus velocity decreased gain ($\beta = -0.0151$) and that presentation of the counting task increased gain ($\beta = 0.1560$). The results of this analysis are shown in Table 4.1.

OKR gain obtained during centre stimulus conditions in response to each stimulus velocity is shown in Figure 4.4.

Analyses were carried out to assess whether effects of use of the counting task on gain differed between 15 deg/s and 30 deg/s stimuli (figures 4.3 and 4.4), finding no significant difference ($t(115) = 1.690$, $p = .090$) in the impact of the counting task on gain between the two conditions.

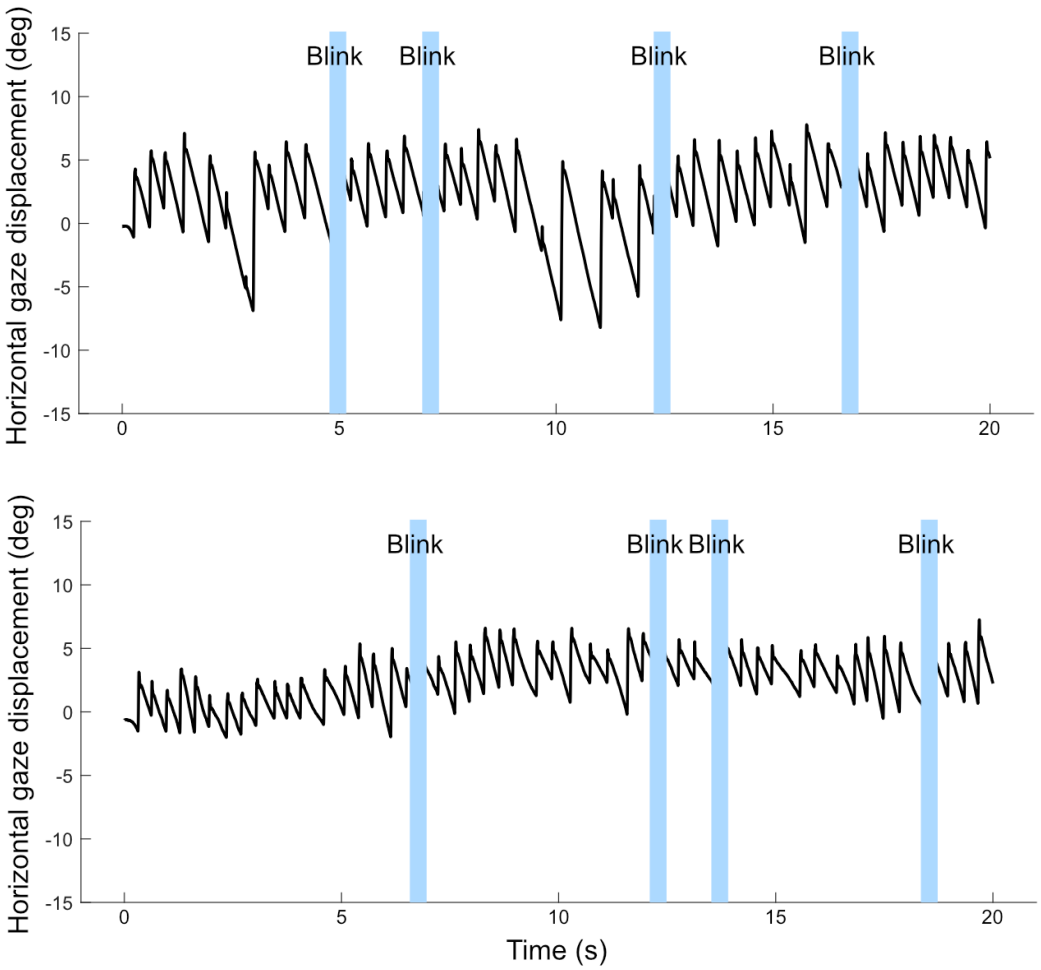

Figure 4.3: Horizontal eye movement traces obtained during two trials with the same participant. Responses shown are to a leftward drifting Centre stimulus with a diameter of 16 deg, with dots drifting at 15 (upper) and 30 (lower) deg/s. On the Y axis, zero indicates the midline of the display: positive numbers indicate the right and negative numbers indicate the left. Blinks are indicated with vertical blue bars.

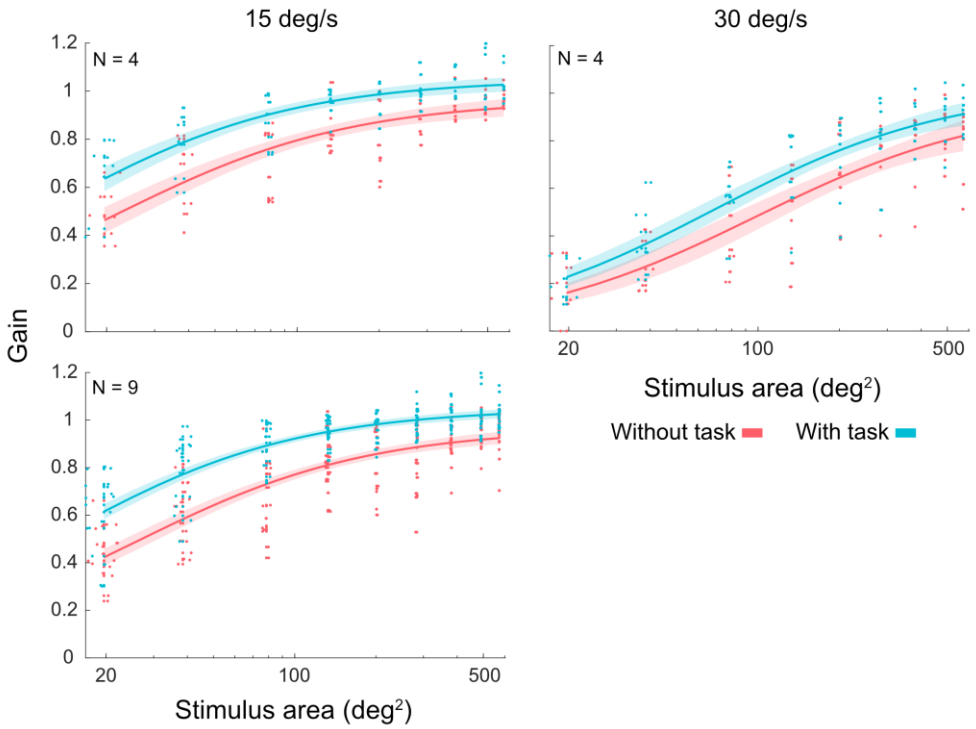

Figure 4.4: Gain in response to Centre (C) stimuli drifting at 15 deg/s (upper left, N = 4, lower left, N = 9) and 30 deg/s (right, N = 4) across stimulus area. Upper plots (N = 4) reflect responses at each stimulus speed using the same subset of four participants. Gain in response to trials using the counting task is shown in blue, with response to trials without the counting task shown in red. A horizontal jitter of up to 6 deg has been applied to increase visibility of data points, which each represent the mean gain obtained in a single trial. The shaded area indicates the 95% CI of the fitted function.

Table 4.1

Results of linear regression model to predict gain in response to a Centre (C) stimulus based on three predictor variables (stimulus area, stimulus velocity and task condition)

	β	SE	F	*p*
Intercept	0.8118	0.025	31.479	<.001*
Area	0.0008	0.0001	15.867	<.001*
Velocity	-0.0151	0.001	-14.855	<.001*
Task	0.1560	0.023	6.793	<.001*
Area*Task	-0.0001	0.0001	-1.761	.079

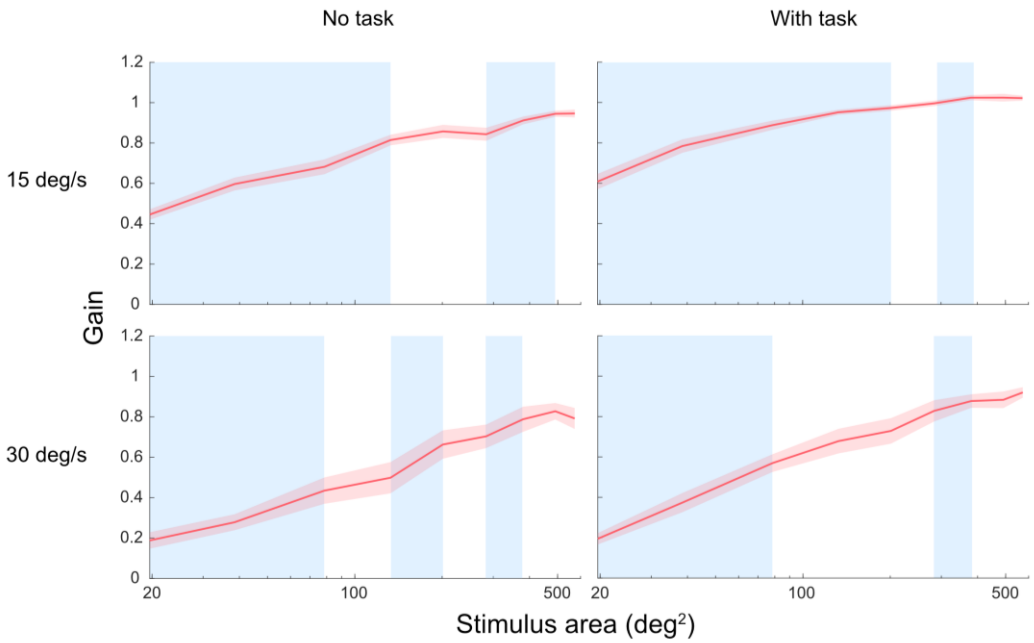

Figure 4.5: Mean gain across Centre (C) stimulus area in response to 15 deg/s (upper, N = 9) and 30 deg/s (lower, N = 4) stimulus velocity, in conditions that did not use the counting task (left) and that did use the counting task (right). The red shaded area indicates the standard error of the mean. The blue shaded area indicates significant increase in gain between each stimulus area increment.

Investigating the significant effect of stimulus area on gain, pairwise t-tests were used to evaluate adjacent pairs of stimulus sizes for significant increases in gain in response to both stimulus velocities and both counting task conditions. The means obtained in each condition are shown in Figure 4.5, with blue shaded areas indicating regions of significant gain increase.

As shown in Figure 4.5 (upper left), during non-counting task Centre (C) stimulus conditions presenting stimuli at 15 deg/s, gain increased significantly for the first three increments in stimulus area (19.63–132.73 deg², $p < .020$) and from 283.53 deg² to 490.87 deg² ($p < .035$). Under similar conditions that did present the counting task (Figure 4.5, upper right), gain increased significantly between the first four increments in stimulus area, from 19.63 deg² to 201.06 deg² ($p < .045$) and between 283.53 deg² and 380.13 deg² ($t(8) = -2.843$, $p = .022$).

During conditions using Centre (C) stimuli with 30 deg/s motion and no counting task (Figure 4.5, lower left), gain increased significantly across the first two increments in stimulus area (19.63-78.54 deg^2, $p < .030$), with further gain increases observed between 132.73 deg^2 and 201.06 deg^2 ($t(3) = -4.879$, $p = .016$) and between 283.53 deg^2 and 380.13 deg^2 ($t(3) = -5.287$, $p = .013$). During similar conditions that did use the counting task (Figure 4.5, lower right), gain again

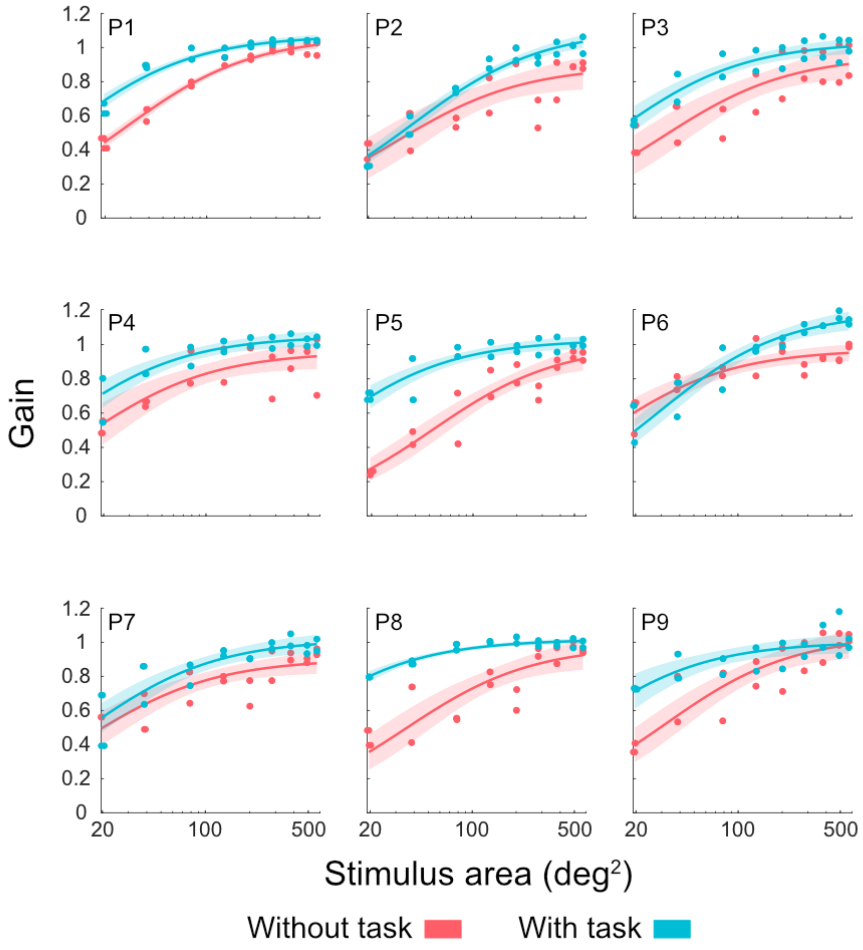

Figure 4.6: Gain across stimulus area in response to a Centre (C) stimulus with dots drifting at 15 deg/s in nine individual participants. The data points represent the mean gain obtained in a single trial; there are two points of the same colour per stimulus size as two directions of motion (left/right) were used. Data obtained while using the counting task are shown in blue, whereas data obtained without the counting task are shown in red. The shaded area indicates the 95% CI of the fitted function. The participant number is indicated at the upper left corner of each plot.

increased significantly across the first two increments in stimulus area (19.63-78.54 deg², $p < .020$). The only other stimulus size increment associated with significant gain increase was from an area of 283.53 deg² to 380.13 deg² ($t(3) = -3.359$, $p = .044$).

As subsequent parts of the experiment present only stimuli at 15 deg/s velocity, attention then turned to analysing just gain in response to Centre stimuli at 15 deg/s. The gain obtained during these conditions is shown for each participant in Figure 4.6.

Table 4.2

Results of linear regression model to predict gain in response to a Centre (C) stimulus at 15 deg/s based on two predictor variables (stimulus area and task condition)

	β	SE	F	*p*
Intercept	0.6033	0.017	35.343	< .001*
Area	0.0007	0.0001	13.303	< .001*
Task	0.1846	0.024	7.646	< .001*
Area*Task	-0.0002	0.0001	-2.529	.012*

A regression model was calculated to assess the contribution of stimulus area and counting task condition, and the interaction between the two, on the gain of the OKR in response to 15 deg/s stimuli. A significant regression equation was found ($F(3, 323) = 118.81$, $p < .001$) with an adjusted R^2 of .523. The results of this analysis are shown in Table 4.2. Again, both stimulus area and counting task condition were found to significantly predict OKR gain: increasing area and using the counting task increased gain. This model showed a significant interaction between stimulus area and task condition. To probe this interaction, the difference in gain between task a non-task conditions was calculated for each stimulus area and correlated across stimulus area. The results showed a significant negative correlation between the difference in gain caused by task condition across stimulus area ($R = -.862$, $p = .003$) whereby as stimulus area increased,

the effect of the use of the counting task on gain decreased. A scatterplot illustrating this relationship is shown in Figure 4.7.

Figure 4.7: N = 9. Scatterplot showing the mean difference in gain between task and non-task conditions across stimulus area during Centre (C) stimulus conditions presenting stimuli at a velocity of 15 deg/s. Difference in gain was obtained by subtracting the means of the 'no task' condition from the means of the 'with task' condition.

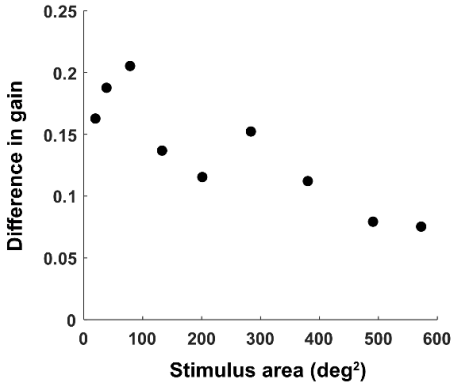

4.3.2.2 Centre (C) stimulus: Frequency

Table 4.3

Results of linear regression model to predict OKR frequency in response to a Centre (C) stimulus based on three predictor variables (stimulus area, stimulus velocity and task condition)

	β	SE	F	*p*
Intercept	1.9514	0.087	22.223	< .001*
Area	0.0002	0.0001	1.339	.181
Velocity	0.0035	0.004	0.939	.348
Task	0.4959	0.051	9.655	< .001*

A regression model was calculated to predict OKR frequency obtained during Centre stimulus conditions (Figure 4.8) based on stimulus area, counting task condition (with task or without task) and stimulus velocity (15 or 30 deg/s). A significant regression equation was found ($F(3, 467) = 31.963$, $p < .001$) with an adjusted R^2 of .166. In this model, the only significant predictor of OKR

frequency was found to be counting task condition ($p < .001$), with the presentation of the counting task increasing the frequency of OKR ($\beta = 0.4959$). The results of this analysis are shown in Table 4.3. A t-test showed that the impact of counting task on the frequency of OKR was similar for 15 and 30 deg/s conditions ($t(232) = 0.315$, $p = .753$).

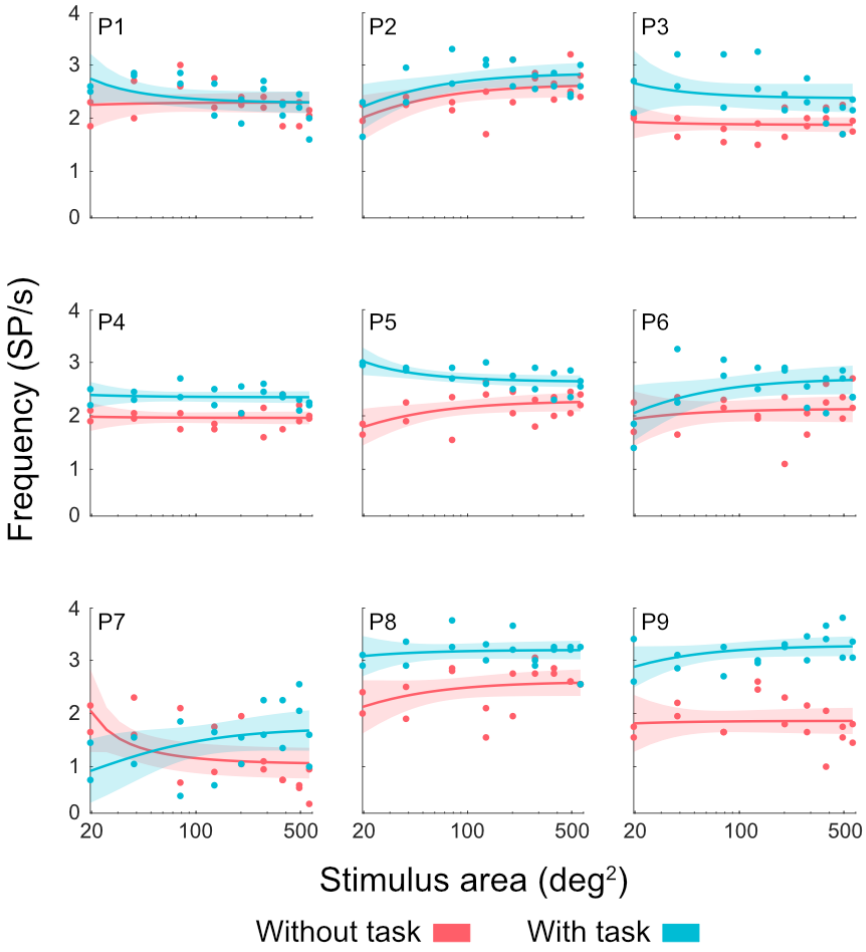

Figure 4.8: Frequency across stimulus area in response to Centre (C) stimuli with dots drifting at 15 deg/s in nine individual participants. Individual data points represent the mean frequency (slow phases per second) obtained in a single trial. Data obtained during trials using the counting task are shown in blue whereas those obtained without the counting task are shown in red. The shaded area indicates the 95% CI of the fitted function. Participant numbers are indicated in the upper left corner of each plot.

4.3.2.3 Centre (C) stimulus: Amplitude

Finally, a regression model was calculated to predict the amplitude of the OKR slow phases in response to a Centre (C) stimulus (Figure 4.9) using stimulus area, stimulus velocity and task condition as predictors. A significant regression equation was found ($F(3, 467) = 103.16$, $p < .001$) with an adjusted R^2 of .396. In this model, stimulus area ($p < .001$) and stimulus velocity ($p < .001$) were

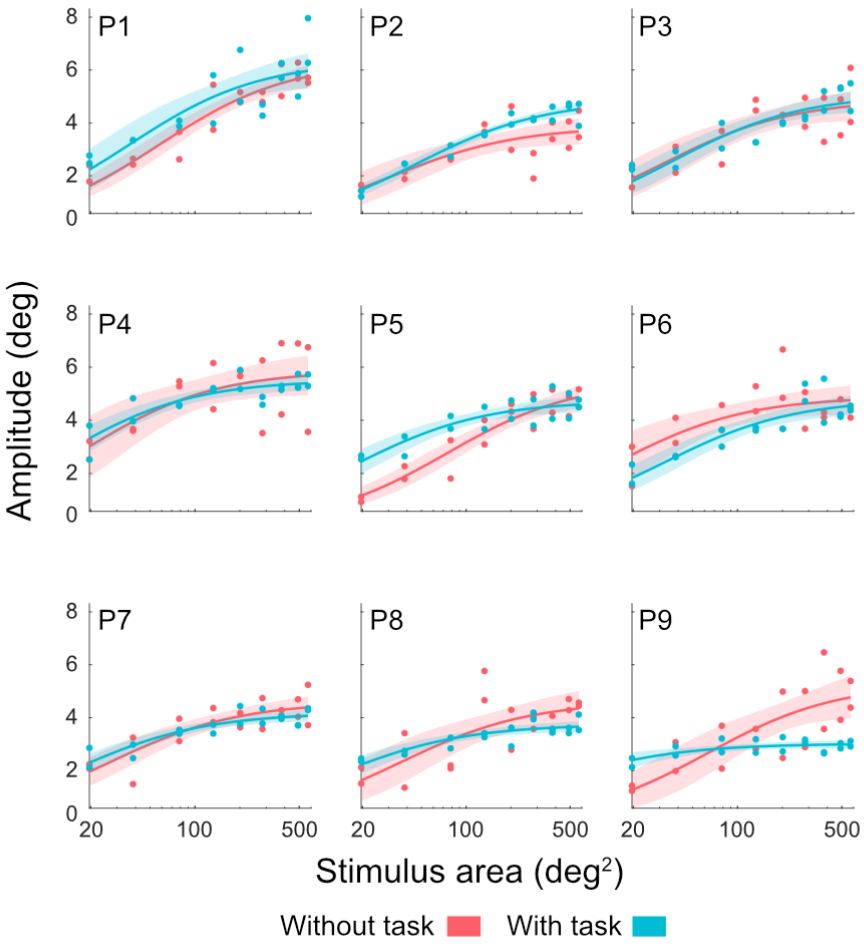

Figure 4.9: Mean slow phase amplitude obtained in response to Centre (C) stimuli with dots drifting at 15 deg/s in nine individual participants. Each data point indicates the mean amplitude obtained in a single trial; the shaded area indicates the 95% confidence interval of the fitted function. Data obtained during trials using the counting task are shown in blue; those obtained without the counting task are shown in red. Participant numbers are indicated in the upper left corner of each plot.

found to significantly predict amplitude, whereas counting task condition was not (p = .751). Increasing stimulus area (β = 0.0056) and velocity (β = 0.0710) resulted in higher slow phase amplitude. The results of this analysis are shown in Table 4.4. A t-test found no difference between 15 deg/s and 30 deg/s conditions in terms of the difference between the amplitude obtained in task and non-task conditions ($t(232)$ = 0.502, p = .616).

Table 4.4

Results of linear regression model to predict OKR amplitude in response to a Centre (C) stimulus based on three predictor variables (stimulus area, stimulus velocity and task condition)

	β	SE	F	p
Intercept	1.4359	0.229	6.275	< .001*
Area	0.0056	0.0003	15.982	< .001*
Velocity	0.0710	0.009	7.346	< .001*
Task	-0.0425	0.134	-0.318	.751

4.3.2.4 Surround (S) stimulus: Gain

Table 4.5

Results of linear regression model to predict gain in response to a Surround (S) stimulus based on three predictor variables (stimulus area, stimulus velocity and task condition)

	β	SE	F	p
Intercept	0.683	0.079	8.562	<.001*
Area	-0.0004	0.0002	-2.877	.004*
Velocity	-0.014	0.001	-12.657	<.001*
Task	0.301	0.109	2.762	.006*
Area*Task	-0.0002	0.0002	-1.022	.308

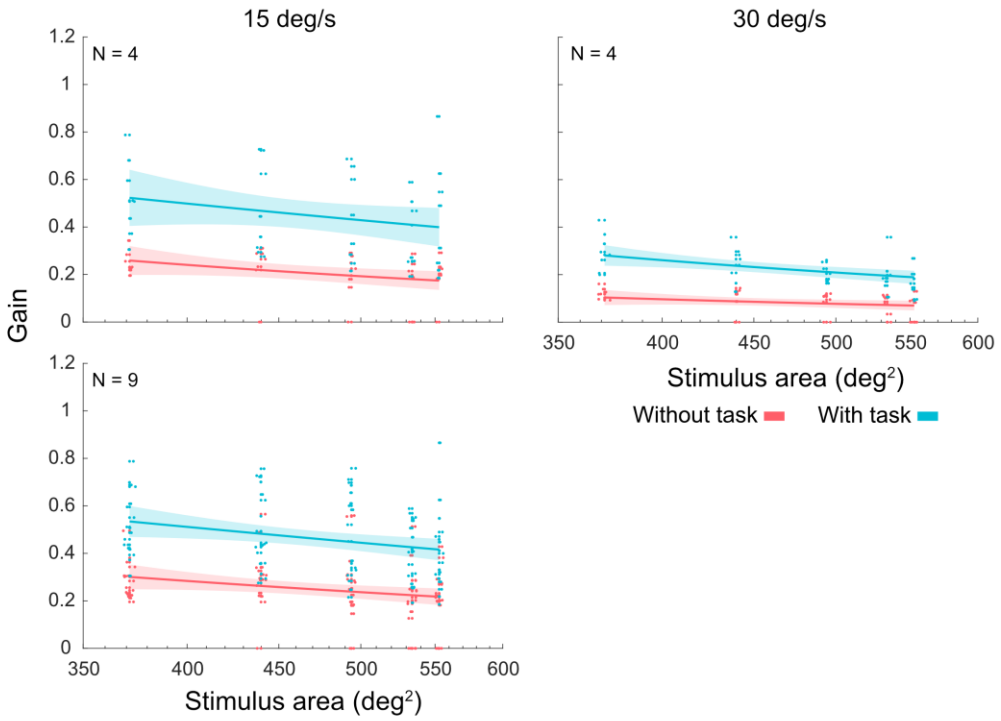

Figure 4.10: Gain obtained in response to Surround (S) stimuli drifting at 15 (upper left, N = 4, lower left, N = 9) and 30 (right, N = 4) deg/s across stimulus area. Upper plots (N = 4) reflect data obtained from the same subset of four participants. Gain during trials that used the counting task is shown in blue, whereas gain during trials that did not use the counting task is shown in red. The shaded area indicates the 95% CI of the fitted function.

A linear regression model was calculated to predict gain in response to Surround (S) stimuli, using stimulus area, counting task condition (with task or without task, Figure 4.11) and stimulus velocity (15 or 30 deg/s, Figure 4.10) as predictor variables. The interaction between stimulus area and task was also assessed. The results of this analysis are shown in Table 4.5. A significant regression equation was found ($F(4, 259) = 87.717$, $p < .001$) with an adjusted R^2 of .573. There was no significant interaction between stimulus area and counting task condition ($p = .308$).

A two-sample t-test was used to assess whether the effect of the counting task on gain in Surround (S) stimulus conditions differed between 15 and 30 deg/s stimulus velocities. The result showed a significant difference in gain between the two velocities ($t(63) = -2.36$, $p = .02$), indicating that the difference in

gain between counting task and non-task trials was larger in response to 15 deg/s stimuli (M = 0.21, SD = 0.13) compared to 30 deg/s stimuli (M = 0.14, SD = 0.05) (Figure 4.10).

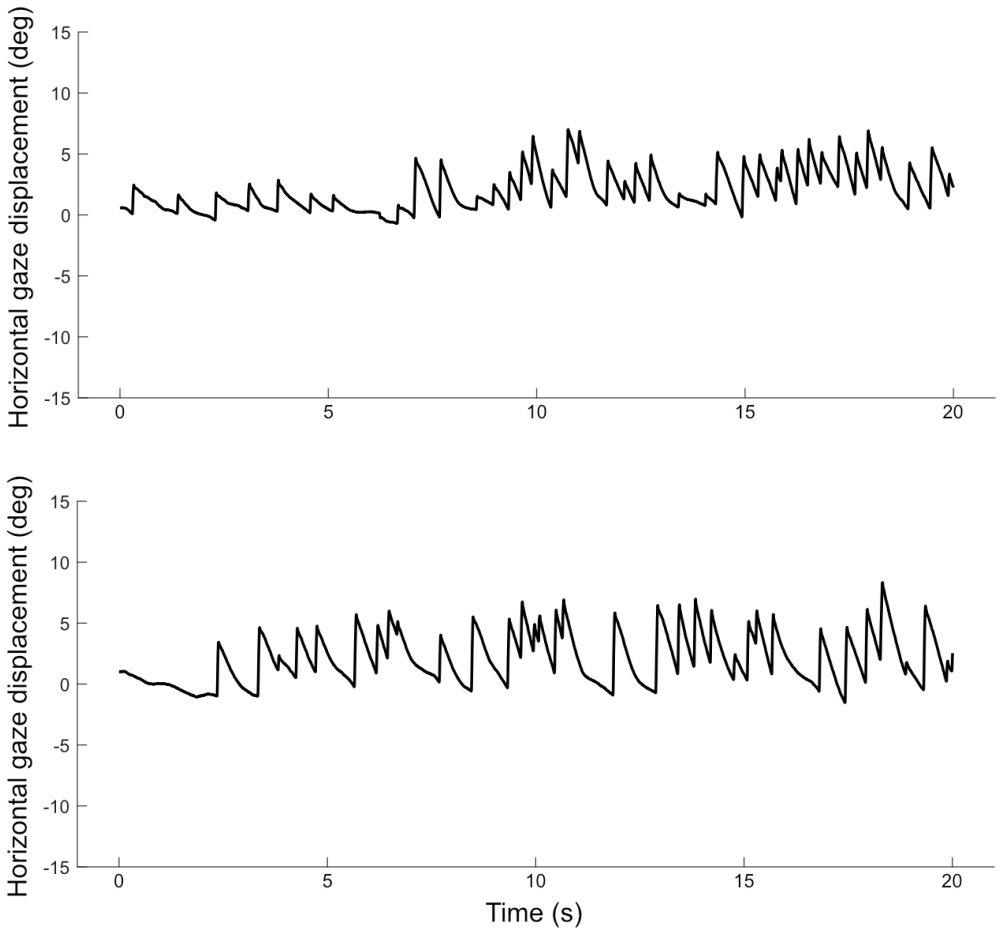

Figure 4.11: Horizontal eye movement traces obtained from the same participant and the same Surround (S) stimulus (15 deg/s), without the counting task (upper) and with the counting task (lower). On the Y axis, zero indicates the midline of the display, with positive numbers indicating the right of the midline and negative numbers indicating the left of the midline.

Focus then turned to the trials which were of primary interest: those involving stimuli with dots drifting at 15 deg/s (Figure 4.12). A linear regression model was calculated using stimulus area and task condition to predict gain. The

results of this analysis are shown in Table 4.6. A significant regression equation was found ($F(3, 179) = 40.522$, $p < .001$) with an adjusted R^2 of .398. The model did not show a significant interaction between stimulus area and task condition ($p = .554$). Increasing area significantly reduced gain ($\beta = -0.0005$, $p = .023$) and use of the counting task significantly increased gain ($\beta = 0.3012$, $p = .047$).

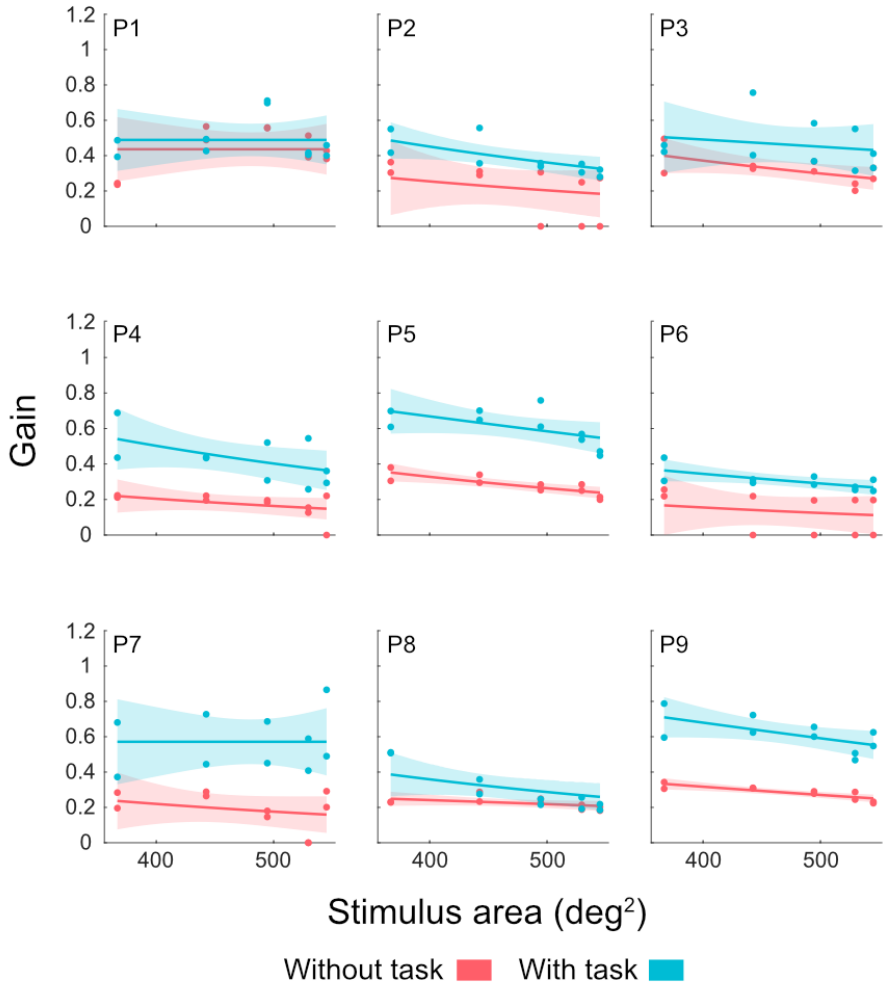

Figure 4.12: Gain across stimulus area in response to a Surround (S) stimulus with dots drifting at 15 deg/s in nine individual participants. Data points represent the mean slow phase gain obtained in a single trial. Data obtained during trials using the counting task are shown in blue; those obtained without the counting task are shown in red. The shaded area indicated the 95% CI of the fitted function. Participant numbers are indicated at the upper left corner of each plot.

Table 4.6

Results of linear regression model to predict gain in response to a Surround (S) stimulus at 15 deg/s based on two predictor variables (stimulus area and task condition)

	β	SE	F	*p*
Intercept	0.4897	0.106	4.599	< .001*
Area	-0.0005	0.0002	-2.285	.023*
Task	0.3012	0.151	1.999	.047*
Area*Task	-0.0002	0.0003	-0.593	.554

4.3.2.5 Surround (S) stimulus: Frequency

Table 4.7

Results of linear regression model to predict OKR frequency in response to a Surround (S) stimulus based on three predictor variables (stimulus area, stimulus velocity and task condition)

	β	SE	F	*p*
Intercept	1.7305	0.345	5.008	< .001*
Area	-0.0011	0.001	-1.721	.086
Velocity	-0.0087	0.006	-1.376	.170
Task	0.6046	0.087	6.917	< .001*

A linear regression model was calculated to predict OKR frequency in response to Surround stimuli, using stimulus area, counting task condition and stimulus velocity as predictors. A significant regression equation was found ($F(3, 259) = 17.566$, $p < .001$) with an adjusted R^2 of .161. In this model, counting task condition was the only significant predictor of OKR frequency ($\beta = 0.6046$ $p < .001$), increasing the frequency of OKR. The results of this analysis are shown in Table 4.7. Individual frequency plots in response to 15 deg/s stimuli are shown in Figure 4.14, highlighting the individual differences present in this measure.

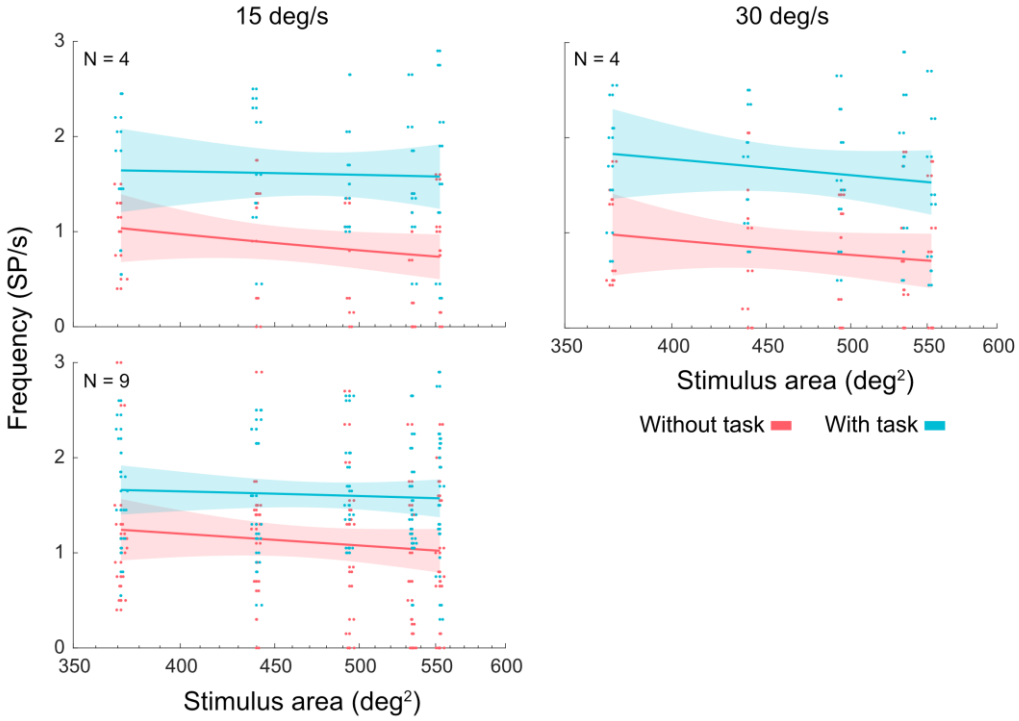

Figure 4.13: OKR frequency, in slow phases per second, across stimulus area during 15 deg/s (upper left N = 4, lower left N = 9) and 30 deg/s (right, N = 4) stimulus velocity conditions in response to Surround (S) stimuli. Upper plots (N = 4) reflect data obtained from the same subset of four participants. Responses to trials using the counting task are shown in blue and responses to trials without the counting task are shown in red. Data points represent mean frequency in a single trial, with a horizontal jitter of 6 deg applied. The shaded area indicates the 95% CI of the fitted function.

T-tests were carried out to assess whether the increase in frequency caused by the use of the counting task differed between 15 deg/s and 30 deg/s Surround (S) stimuli (Figure 4.13). A two-sample t-test showed a significant difference between the two conditions ($t(128) = -3.277$, $p = .001$), indicating that the difference in frequency between task and non-task conditions in response to 30 deg/s stimuli (M = 0.84, SD = 0.46) was significantly larger than that in response to 15 deg/s stimuli (M = 0.50, SD = 0.57).

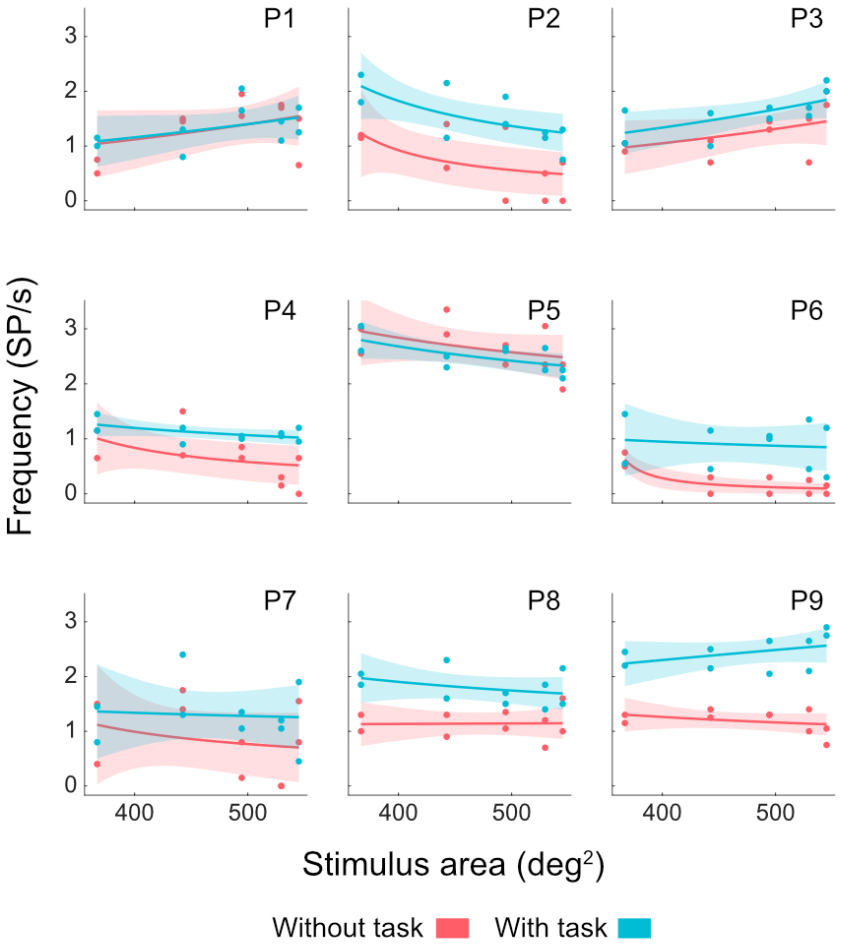

Figure 4.14: Frequency across stimulus area in response to a Surround (S) stimulus with dots drifting at 15 deg/s in nine individual participants. Data points represent the frequency, in slow phases per second, obtained during that trial. Data obtained during trials using the counting task are shown in blue; those obtained without the use of the counting task are shown in red. The shaded area indicates the 95% CI of the fitted function. Participant numbers are indicated in the upper right corner of each plot.

4.3.2.6 Surround (S) stimulus: Amplitude

Finally, a linear regression model was calculated to predict OKR slow phase amplitude in response to Surround (S) stimuli using stimulus velocity, stimulus area and counting task condition as predictors. A significant regression equation was found ($F(3, 259) = 69.548$, $p < .001$), with an adjusted R^2 of .443. The results of this analysis are shown in Table 4.8. In this model, stimulus area,

Table 4.8

Results of linear regression model to predict OKR slow phase amplitude in response to a Surround (S) stimulus based on three predictor variables (stimulus area, stimulus velocity and task condition)

	β	SE	F	*p*
Intercept	3.6259	0.381	9.518	< .001*
Area	-0.0040	0.001	-5.486	< .001*
Velocity	-0.0418	0.007	-6.0004	< .001*
Task	1.1506	0.096	11.939	< .001*

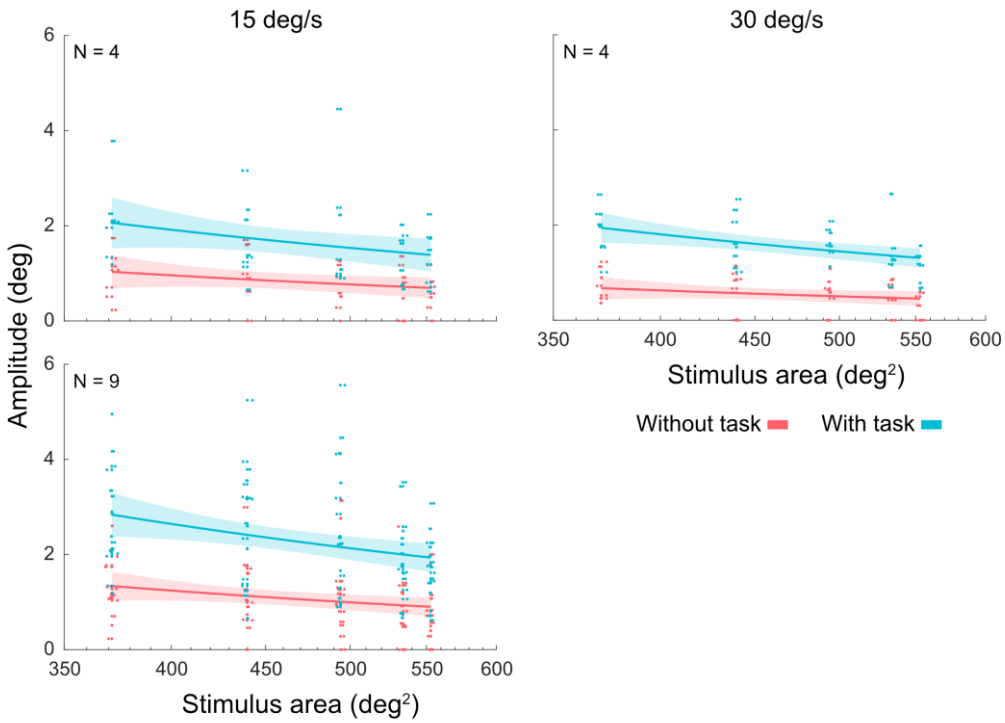

Figure 4.15: Slow phase amplitude in response to Surround (S) stimuli with dots drifting at 15 deg/s (upper left N = 4, lower left N = 9) and at 30 deg/s (right, N = 4) during trials using the counting task (blue) and trials that did not use the counting task (red). Upper plots (N = 4) reflect data obtained from the same subset of four participants. Data points indicate mean amplitude in a single trial, with a horizontal jitter of up to 6 deg applied. The shaded area indicates the 95% CI of the fitted function.

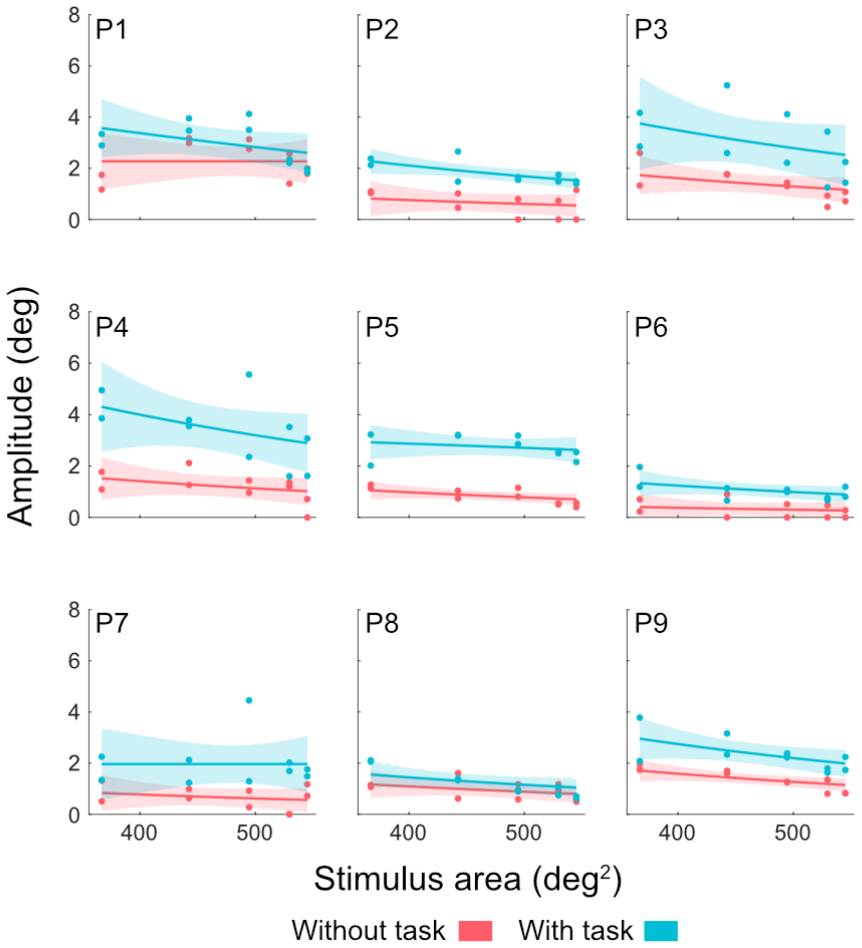

Figure 4.16: Mean slow phase amplitude obtained in response to Surround (S) stimuli with dots drifting at 15 deg/s in nine individual participants. Each data point represents the mean amplitude obtained in a single trial; the shaded area indicates the 95% CI of the fitted function. Data obtained in response to trials using the counting task are shown in blue; those obtained without the counting task are shown in red. Participant numbers are indicated in the upper left corner of each plot.

stimulus velocity and counting task condition were all found to significantly predict OKR slow phase amplitude. Increasing stimulus area (β = -0.0040, $p < .001$) and velocity (β = -0.0418, $p < .001$) were both found to decrease slow phase amplitude, whereas use of the counting task (β = 1.1506, $p < .001$) was found to increase slow phase amplitude.

A t-test showed no significant difference between 15 deg/s and 30 deg/s stimulus velocity conditions (Figure 4.15) in terms of the impact of the counting

task on the amplitude of OKR ($t(128) = 1.269$, $p = .207$). Individual slow phase amplitude during 15 deg/s stimulus velocity conditions is shown in Figure 4.16.

4.3.2.7 Modelling and comparing Centre and Surround responses

Table 4.9

Results of linear regression models to predict OKR gain, frequency and amplitude based on four predictor variables (stimulus area, stimulus velocity, stimulus type and task condition)

Gain	β	SE	F	*p*
Intercept	0.1766	0.026	6.828	< .001*
Area	0.0007	0.00003	19.113	< .001*
Velocity	-0.0146	0.0008	-17.952	< .001*
Stimulus type	0.6493	0.014	44.966	< .001*
Task	0.1479	0.011	13.144	< .001*
Frequency	β	SE	F	*p*
Intercept	1.0203	0.104	9.732	< .001*
Area	0.0001	0.0001	0.675	.499
Velocity	-0.0009	0.003	-0.261	.794
Stimulus type	1.0174	0.058	17.381	< .001*
Task	0.5347	0.046	11.721	< .001*
Amplitude	β	SE	F	*p*
Intercept	-0.3147	0.294	-1.0667	.286
Area	0.0050	0.0003	15.981	< .001*
Velocity	-0.0418	0.012	-3.494	< .001*
Stimulus type	1.6864	0.319	5.289	< .001*
Task	0.3836	0.099	3.878	< .001*
Stim type*Velocity	0.1128	0.015	7.565	< .001*

To investigate differences between the two stimulus types (Centre (C) or Surround (S)), linear regression models were calculated to predict the gain, frequency and amplitude of the OKR based on stimulus area, velocity, type, and counting task condition. In the analysis of amplitude, an interaction term was included to test for interaction between stimulus type and velocity. The results of these analyses are shown in Table 4.9. Significant regression equations were found in the prediction of the gain ($F(4, 723) = 648$, $p < .001$, adjusted $R^2 = .781$), frequency ($F(4, 727) = 143.53$, $p < .001$, adjusted $R^2 = .440$) and amplitude ($F(5,$

727) = 208.01, $p < .001$, adjusted $R^2 = .587$) of the OKR. The gain of the OKR was increased by increasing stimulus area and by using the counting task, and was reduced by increasing stimulus velocity. Centre (C) stimuli were associated with higher gain than Surround (S) stimuli. The frequency of the OKR was increased by presenting a Centre (C) stimulus or using the counting task; stimulus area and velocity did not significantly predict frequency. Amplitude was increased by increasing stimulus area, presenting a Centre (C) stimulus and using the counting task. Increasing stimulus velocity lowered the amplitude, but this variable interacted with stimulus type. Table 4.4 shows that, in response to a Centre stimulus, increasing velocity is associated with an increase in amplitude ($\beta = 0.0710$) whereas Table 4.8 shows that in response to a Surround stimulus, increasing velocity is associated with a decrease in amplitude ($\beta = -0.0418$), explaining the source of this interaction.

T-tests were used to investigate whether the impact of the counting task on the gain, frequency and amplitude of the OKR differed significantly between Centre (C) and Surround (S) stimuli. The impact of the counting task on gain was significantly larger in response to Surround (S) stimuli (M = 0.21, SD = 0.13) compared to Centre (C) stimuli (M = 0.14, SD = 0.12) ($t(124) = 3.35$, $p = .001$). This pattern was also reflected in the amplitude, with a significantly larger effect in response to Surround stimuli ($t(362) = -9.698$, $p < .001$). The impact of the counting task on frequency did not differ significantly between stimulus types ($t(362) = 1.67$, $p = .094$).

Part 1: Summary of key findings

- OKR measures (gain, frequency and amplitude) are significantly higher in response to Centre (C) stimuli
- Increasing Surround (S) stimulus area does not increase gain
- Increasing attention towards the stimulus by using a counting task significantly increases OKR measures to both stimulus regions
- Smaller stimuli see a significantly greater impact of the counting task on OKR measures
- The impact of the counting task on the gain and amplitude of the OKR is significantly higher in response to Surround (S) stimuli

4.4 Part 2: Centre-surround with opposing motion

Part 1 has demonstrated the characteristics of the OKR in response to central and peripheral stimulation separately. In Part 2, the centre and the surround will be stimulated simultaneously with opposite directions of coherent motion. Centre-surround stimuli will be used to test whether a peripheral OKR can be induced in the presence of opposing central motion, as well as whether the presence of opposing motion impacts OKR measures obtained in response to the centre or the surround.

4.4.1 Methods

4.4.1.1 Participants

Part 2 used the same nine participants that were used for 15 deg/s conditions in Part 1.

4.4.1.2 Stimuli

Part 2 used the previously described C/S Opposing stimuli (Figure 4.2), which presented opposite directions of coherent horizontal dot motion to centre and surround regions simultaneously while varying the diameter of the central region. All stimuli were presented with a dot speed of 15 deg/s.

4.4.1.3 Design

During Part 2, every trial used the colour counting task. Coloured task dots were either presented in the central region or in the surround region of the C/S stimulus; this allowed attention to be directed towards the centre or towards the surround, depending on condition.

Participants each viewed a total of 32 stimuli. Eight inner diameters were used for these stimuli, and these were split across blocks: inner diameters of 5-13 deg were presented in one block and inner diameters of 16-25 deg were presented in another. As both directions of horizontal motion were used, each block

contained 16 stimuli. In total, there were two blocks of 16 stimuli: one block presenting stimuli with inner diameters 5-13 deg, with half of trials presenting the counting task to the centre and half to the surround; one block presenting inner diameters 16-15 deg, with half of trials presenting the counting task to the centre and half to the surround. The order of blocks, and of trials within each block, was randomised.

Like in Part 1, gaze monitoring was used to ensure that participants were viewing the correct region of the stimulus, so that the surround stimulus region remained in the periphery. The restrictions used mirrored those of Part 1.

4.4.1.4 Procedure

The procedure followed that of counting task trials of Part 1, though slightly different instructions were presented. During trials that involved presenting the counting task to the centre, the on-screen instructions shown before each trial read '*Please look towards the centre of the screen while counting the number of colours presented at the CENTRE of the screen. Press SPACE to continue.*' During trials that involved presenting the counting task to the surround, the instructions read '*Please look towards the centre of the screen while counting the number of colours presented in the SURROUND of the screen. Press SPACE to continue.*'

4.4.2 Results

4.4.2.1 Response to centre region of C/S Opposing stimulus: Gain

One purpose of using C/S Opposing stimuli was to assess whether the OKR is affected by the presence of opposing motion (Figure 4.17). Linear regression models were used to investigate this: Part 2 trials involving presentation of the counting task to the centre of the C/S stimulus were used, along with Part 1 trials which involved presenting the counting task during a Centre (C) stimulus. As all Part 2 trials used the counting task, Part 1 trials that did not use the counting task were excluded. As Part 1 used a larger centre stimulus range extending to 27 deg diameter whereas Part 2 used a range extending only up to 25 deg, Part 1 trials using 27 deg stimuli were excluded from the analysis. As Part

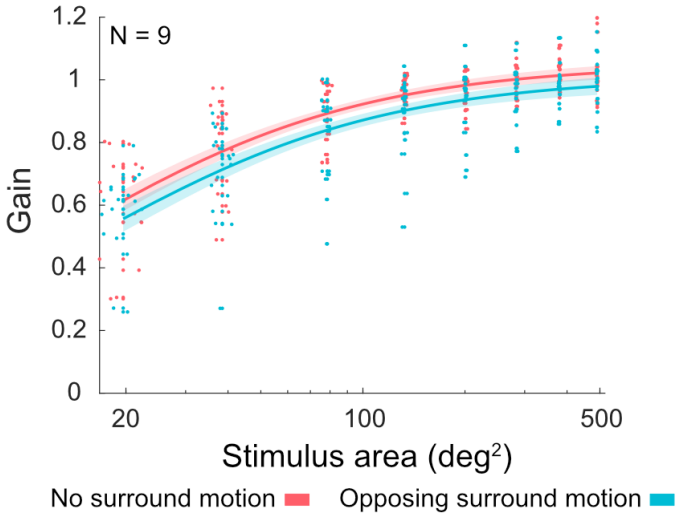

Figure 4.17: N = 9. Gain in response to a central stimulus region across stimulus area, in the presence or absence of opposing motion in the surround. No surround motion (red) draws data from Part 1 Centre (C) stimulus conditions using the counting task; Opposing surround motion (blue) draws data from Part 2 C/S Opposing conditions using the counting task in the centre. Data points indicate mean gain in a single trial, with a horizontal jitter of up to 6 deg applied. Part 1 trials involving stimulus areas and velocities not used in Part 2 were excluded. The shaded area indicates the 95% CI of the fitted function.

2 trials only used dot motion at 15 deg/s, Part 1 trials using 30 deg/s motion were also excluded from the analysis. In this way, the only difference between the two datasets was the absence or presence of opposing motion in the surround region.

Table 4.10

Results of linear regression model to predict OKR gain based on three predictor variables (stimulus area, stimulus type and motion direction)

	β	SE	F	*p*
Intercept	0.7502	0.019	38.710	< .001*
Area	0.0007	0.0001	9.754	< .001*
Direction	0.0389	0.015	2.513	.012*
Stimulus type	-0.0621	0.025	-2.472	.014*
Area*Stimulus type	0.0001	0.0001	0.659	.509

A linear regression model was calculated to predict OKR gain using stimulus area, stimulus type (Centre or C/S Opposing) and motion direction (TN or NT) as predictor variables. Motion direction was included due to noting a tendency for higher gain in response to temporonasal (TN) motion during data processing. The possibility of an interaction between stimulus area and stimulus type was also assessed. A significant regression equation was found ($F(4, 287) = 56.427$, $p < .001$) with an adjusted R^2 of .436. Stimulus area ($\beta = 0.0007$, $p < .001$), stimulus type ($\beta = -0.0621$, $p = .014$) and direction of motion ($\beta = 0.0389$, $p =$

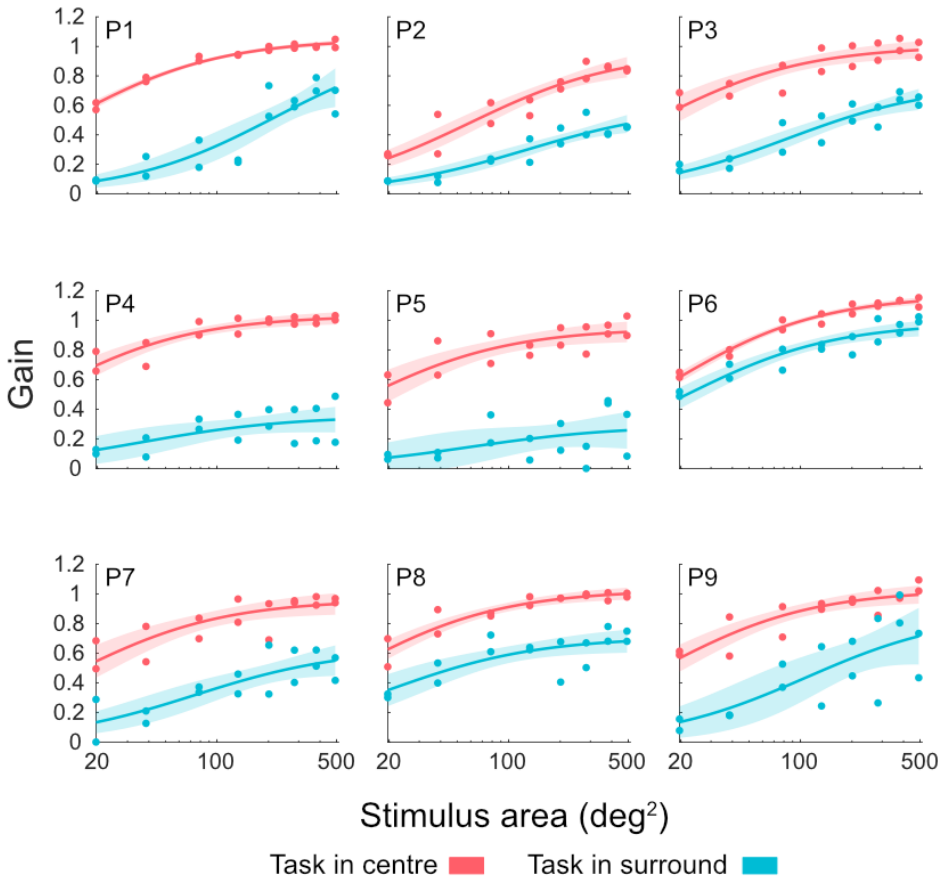

Figure 4.18: Gain of OKR in response to the centre region of a C/S Opposing stimulus with the counting task presented to the centre region (red) and to the surround region (blue) in nine individual participants. Individual data points represent the mean gain obtained during a single trial; the shaded area indicates the 95% CI of the fitted function. Participant numbers are displayed in the upper left corner of each plot.

.012) were all found to significantly predict gain, with stimulus type forming the largest contribution (β = -0.0621). There was no significant interaction between stimulus area and stimulus type (p = .509). The results of this analysis are shown in Table 4.10. Increasing stimulus area was found to increase gain (β = 0.0007). The significance of stimulus direction indicates that gain in response to TN motion (M = 0.901, SD = 0.168) was higher than gain in response to NT motion (M = 0.862, SD = 0.179), as the use of TN motion increased gain (β = 0.0388). The significance of stimulus type indicates that the presence of opposing motion in the surround reduced gain (Figure 4.17), with a mean gain of 0.857 (SD = 0.182) during C/S Opposing stimuli with the counting task presented to the centre, compared to a mean gain of 0.906 (SD = 0.165) during comparable Centre stimulus (Part 1) conditions.

Table 4.11

Results of linear regression model to predict OKR gain in response to the centre based on two predictor variables (stimulus area, counting task location)

	β	SE	F	p
Intercept	0.7013	0.021	34.013	< .001*
Area	0.0008	0.0001	11.270	< .001*
Task location	-0.4272	0.022	-19.753	< .001*

During C/S Opposing stimuli that presented the counting task to the surround, slow phases in response to the centre region often occurred (Figure 4.24). Analysis was carried out to assess gain in response to the centre region of the C/S Opposing stimulus when the counting task was presented to the centre and when the counting task was presented to the surround (Figure 4.18). A linear regression model was calculated to predict OKR gain in response to the centre region of a C/S Opposing stimulus, using stimulus area and counting task location (centre or surround) as predictors. A significant regression equation was found ($F(2, 287) = 258.590$, $p < .001$) with an adjusted R^2 of .642. The results of this analysis are shown in Table 4.11. In this model, both stimulus area and

counting task location were found to significantly predict the gain of OKR ($p <$ .001), with counting task location forming the largest contribution ($\beta = -0.4272$). These coefficients indicate that increasing stimulus area increased gain, and that presenting the counting task to the surround region of the stimulus reduced gain compared to when the counting task was presented to the central region.

4.4.2.2 Response to centre region of C/S Opposing stimulus: Frequency

These analyses were repeated using frequency instead of gain. A linear regression model was calculated to predict the frequency of OKR in response to the centre using stimulus area, motion direction (NT or TN) and stimulus type (C/S Opposing or Centre) as predictors, again examining a potential interaction between stimulus area and type. The resulting regression model was not significant ($F(3, 287) = 1.292$, $p = .277$, adjusted $R^2 = .003$). The results of this analysis are shown in Table 4.12, with the corresponding group data fits shown in Figure 4.19.

Table 4.12

Results of linear regression model to predict OKR frequency in response to the centre based on three predictor variables (stimulus area, stimulus type and motion direction)

(non-sig)	β	SE	F	*p*
Intercept	2.4941	0.091	27.336	< .001*
Area	0.0001	0.0003	0.203	.839
Direction	0.1233	0.118	1.232	.219
Stimulus type	0.1457	0.073	1.691	.092
Area*Stimulus type	-0.0005	0.0004	-1.031	.303

A regression model was calculated to predict OKR frequency in response to the centre of a C/S stimulus using stimulus area and counting task location (task in centre or task in surround) as predictor variables, with an interaction term included to assess potential interaction between the two predictors. A significant regression equation was found ($F(3, 287) = 104.630$, $p < .001$) with an

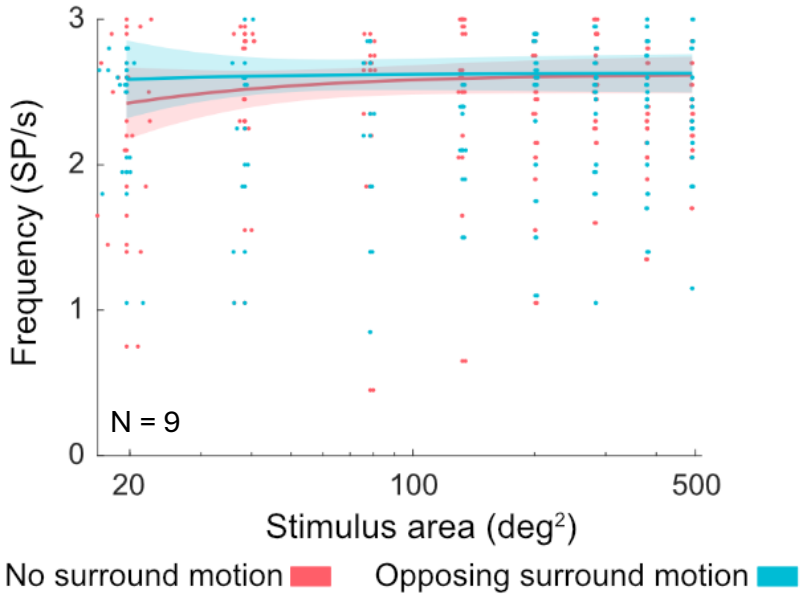

Figure 4.19: N = 9. Frequency of OKR in the absence or presence of surround motion. No surround motion (red) data are drawn from Part 1 trials using a centre stimulus with the counting task. Opposing surround motion data are drawn from Part 2 trials with the counting task presented to the centre. Data points show mean frequency obtained in a single trial, with a horizontal jitter of 6 deg applied. The shaded area indicates the 95% CI of the fitted function.

adjusted R^2 of .520. The results of this analysis are displayed in Table 4.13. In this model, stimulus area was not a significant predictor of frequency ($p = .252$) whereas task location was ($p < .001$), indicating that the frequency of OKR in response to the centre is significantly lowered ($\beta = -0.0004$) by presenting the counting task in the surround compared to in the centre. A significant interaction between stimulus area and counting task location was also identified. Assessing this interaction, the difference in frequency between centre and surround counting task presentation was calculated for the smallest and largest stimulus area tested and compared via paired samples t-test. The result showed a significant difference ($t(17) = 2.311$, $p = .034$) whereby the difference in frequency between the two task locations was significantly larger in response to a smaller stimulus. Individual plots showing frequency across stimulus area with the counting task presented in the centre and in the surround are shown in Figure 4.20.

Table 4.13

Results of linear regression model to predict OKR frequency in response to the centre based on two predictor variables (stimulus area, counting task location)

	β	SE	F	*p*
Intercept	2.7014	0.091	29.523	< .001*
Area	-0.0004	0.0003	-1.147	.252
Task location	-1.6057	0.129	-12.409	< .001*
Area*Task location	0.0009	0.0005	1.9875	.047*

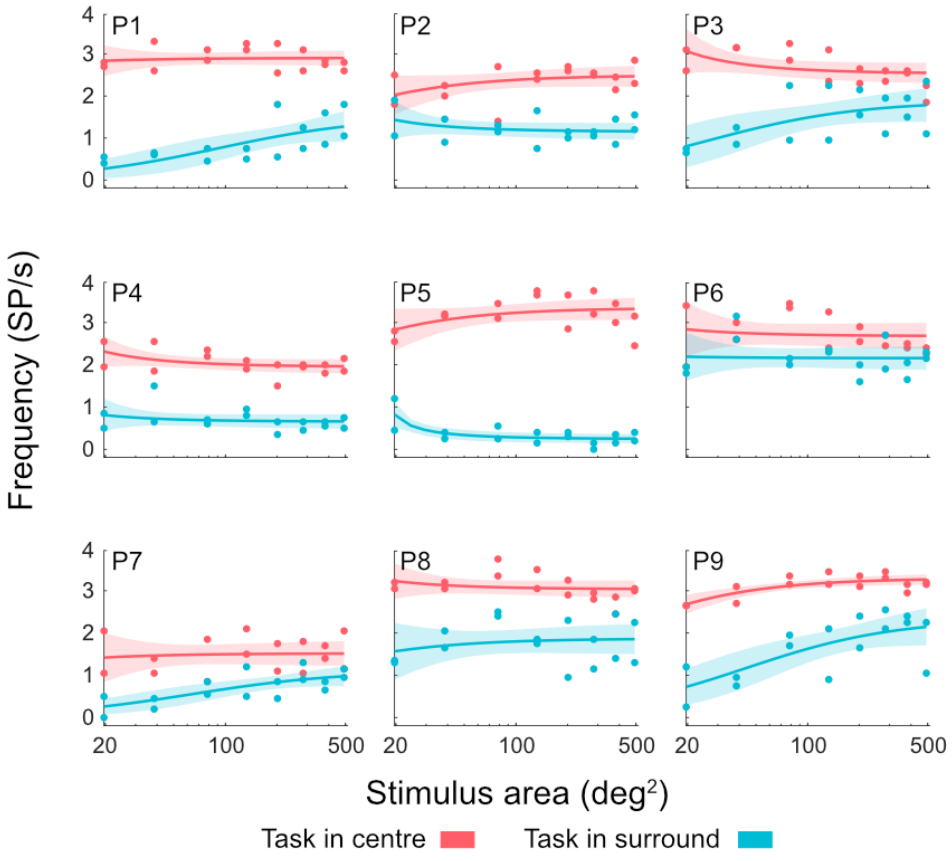

Figure 4.20: Frequency of OKR in response to the centre region of a C/S Opposing stimulus when the counting task is presented in the centre (red) and in the surround (blue) in nine individual participants. Individual data points represent the frequency obtained in a single trial; the shaded area indicates the 95% CI of the fitted function. Participant numbers are indicated in the upper left corner of each plot.

4.4.2.3 Response to centre region of C/S Opposing stimulus: Amplitude

These analyses were again repeated using amplitude data. A linear regression model was calculated to predict the amplitude of the OKR in response to centrally presented stimuli, using stimulus area, stimulus type (Centre or C/S Opposing) and motion direction as predictors. The results of this analysis are shown in Table 4.14. A significant regression equation was found ($F(3, 287) = 53.815$, $p < .001$) with an adjusted R^2 of .356. In this model, stimulus area and stimulus type were both significant predictors of OKR amplitude ($p < .001$), whereas direction of motion was not ($p = .496$). Increasing stimulus area increased slow phase amplitude ($\beta = 0.0037$) and the presence of opposing surround motion (i.e. use of a C/S Opposing stimulus) reduced amplitude ($\beta = -0.3691$). The corresponding group data fits are displayed in Figure 4.21.

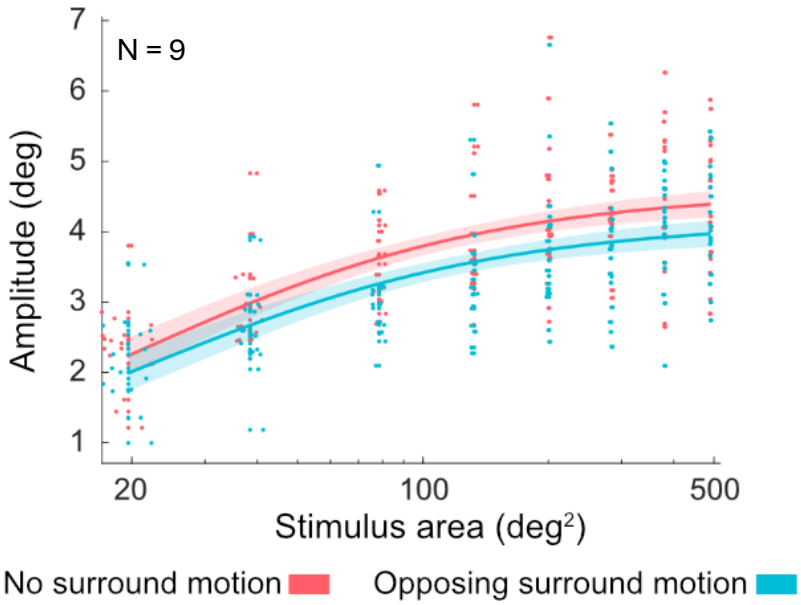

Figure 4.21: N = 9. Slow phase amplitude across stimulus area in the presence (blue) and absence (red) of opposing surround motion. Data without surround motion is drawn from Part 1 trials in which the counting task was presented during a Centre (C) stimulus. Data with surround motion is drawn from Part 2 trials using a C/S Opposing stimulus with the counting task presented to the centre. Data points indicate mean amplitude in a single trial, with up to 6 deg horizontal jitter applied. The shaded area indicates the 95% CI of the fitted function.

Table 4.14

Results of linear regression model to predict OKR amplitude in response to the centre based on three predictor variables (stimulus area, stimulus type and motion direction)

	β	SE	F	*p*
Intercept	2.9513	0.105	27.885	< .001*
Area	0.0037	0.0003	12.120	< .001*
Direction	0.0670	0.098	0.682	.496
Stimulus type	-0.3691	0.098	-3.754	< .001*

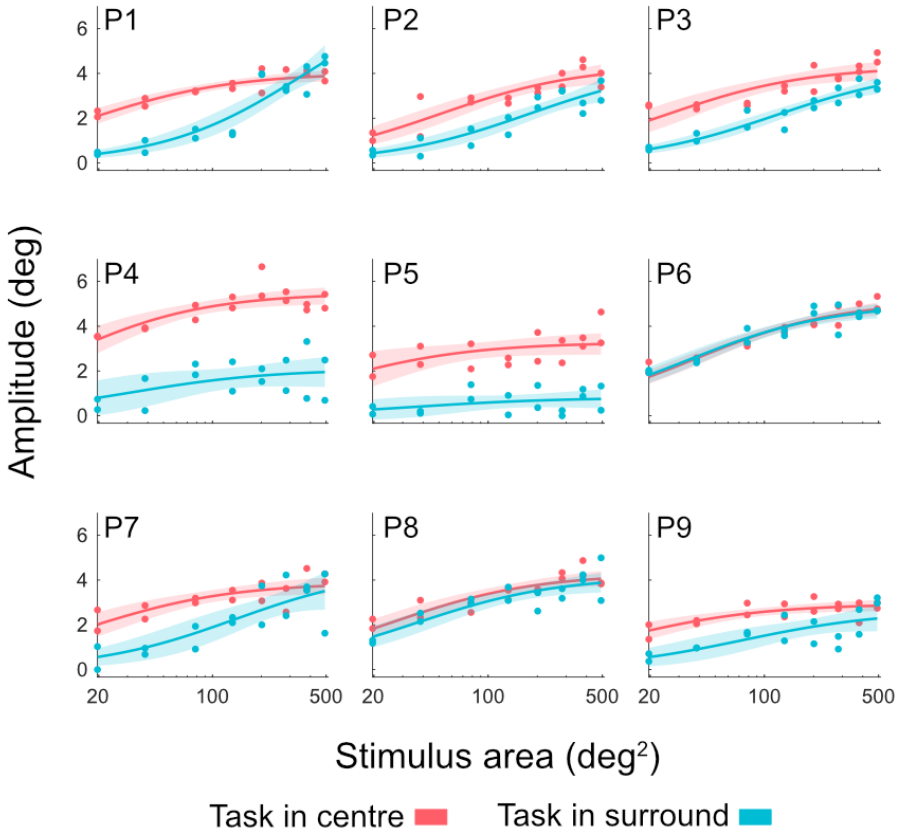

Figure 4.22: OKR slow phase amplitude across stimulus area in response to the centre region of a C/S Opposing stimulus when the counting task is presented to the centre (red) or to the surround (blue) in nine individual participants. Individual data points represent the mean amplitude obtained in a single trial. The shaded area indicates the 95% CI of the fitted function. Participant numbers are displayed in the upper left corner of each plot.

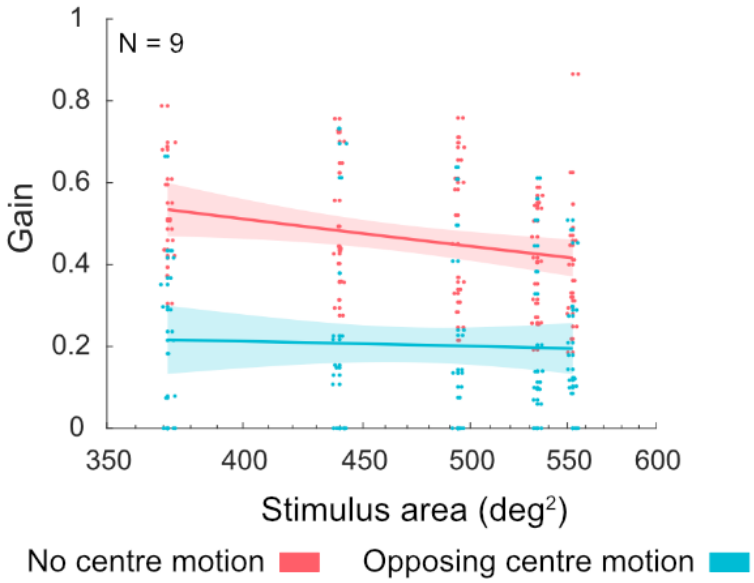

Figure 4.23: Group (N = 9) gain in response to the surround in the absence of motion in the centre (red) and in the presence of opposing motion in the centre (blue). Data with no motion in the centre were obtained from Part 1 Surround (S) stimulus trials using the counting task and presenting motion at 15 deg/s. Data with opposing motion in the centre were obtained from Part 2 C/S Opposing stimulus trials in which the counting task was presented to the surround. The shaded area indicates the 95% CI of the fitted function. A horizontal jitter of up to 6 deg has been applied to data points.

Looking just at C/S Opposing stimuli, another regression model was calculated to predict slow phase amplitude in response to the centre using stimulus area and counting task location (task presented to centre or surround) as predictor variables. A significant regression equation was found ($F(2, 287) = 119.590$, $p < .001$) with an adjusted R^2 of .452. The results of this analysis are displayed in Table 4.15. In this model, both stimulus area and counting task location significantly predicted OKR slow phase amplitude ($p < .001$), with task location forming the largest contribution ($\beta = -1.2158$). These coefficients indicate that increasing stimulus area increased amplitude and that presenting the counting task to the surround rather than to the centre reduced amplitude. The corresponding individual data are shown in Figure 4.22.

Table 4.15

Results of linear regression model to predict OKR amplitude in response to the centre based on two predictor variables (stimulus area, counting task location)

	β	SE	F	*p*
Intercept	2.5252	0.111	22.704	< .001*
Area	0.0042	0.0004	11.427	< .001*
Task location	-1.2158	0.117	-10.421	< .001*

4.4.2.4 Response to surround region of C/S Opposing stimulus: Gain

Table 4.16

Results of linear regression model to predict OKR gain in response to the surround based on three predictor variables (stimulus area, stimulus type and motion direction)

	β	SE	F	*p*
Intercept	0.7759	0.139	5.564	< .001*
Area	-0.0007	0.0003	-2.397	.017*
Direction	0.0299	0.027	1.117	.265
Stimulus type	-0.5352	0.196	-2.726	.007*
Area*Stimulus type	0.0006	0.0004	1.427	.155

Mean gain obtained in each trial in response to surround regions of C/S Opposing stimuli in each of the nine participants is shown in Figure 4.25, with responses to Surround (S) stimuli (15 deg/s, with counting task) from Part 1 included for comparison. A linear regression model was calculated to predict the gain of OKR in response to the surround in the presence or absence of opposing motion in the centre, i.e. in response to a C/S Opposing stimulus or in response to a Surround stimulus, respectively. As C/S Opposing stimuli used a larger range of stimulus sizes due to employing central patches with diameters larger than 16 deg, only the shared stimulus area range (371.57-552.93 deg^2) was used in this model. C/S Opposing stimuli with surround areas of under 371.57 deg^2

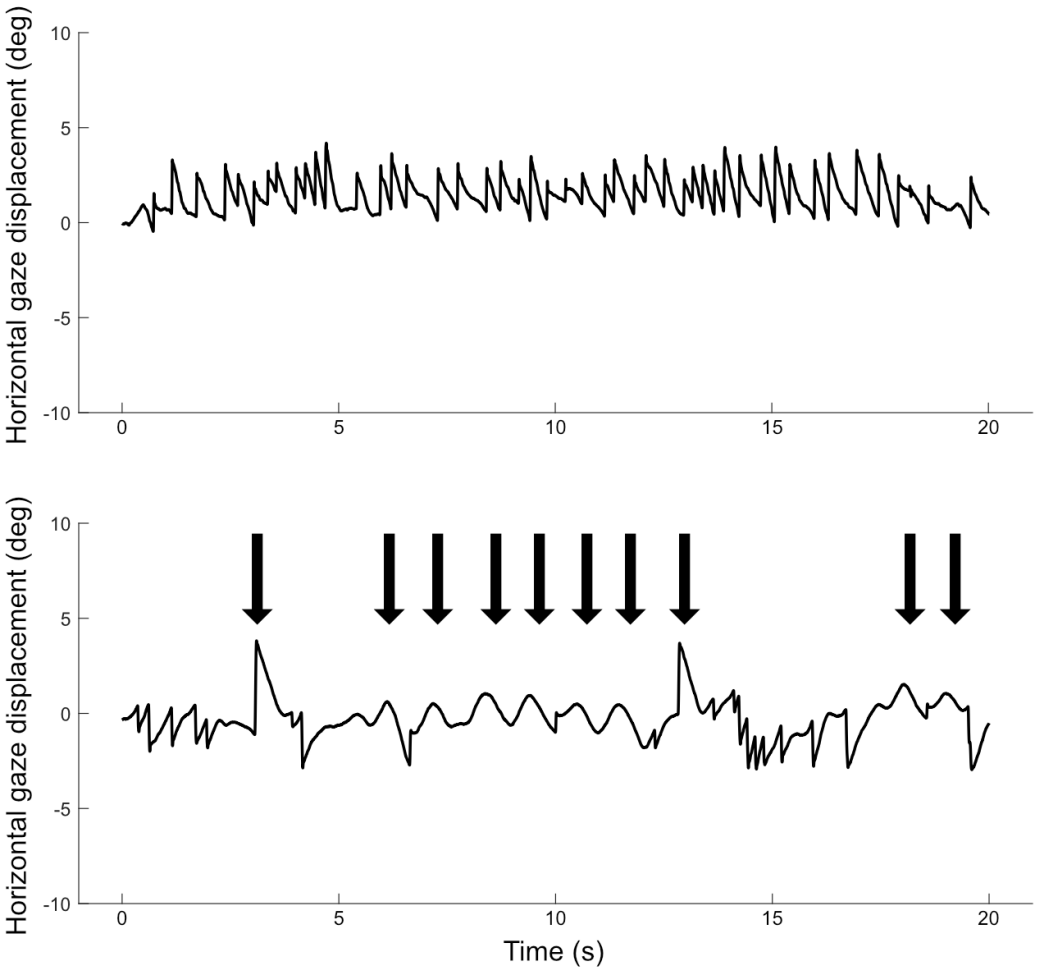

Figure 4.24: Eye movement traces from two different participants in response to a C/S Opposing stimulus in which the surround motion drifts towards the left, with the counting task presented to the surround. The upper trace shows an OKR that consistently follows the direction of the surround; the lower trace shows an OKR which alternates between following centre and surround, with black arrows highlighting the locations of slow phases consistent with the direction of the surround motion.

were excluded. As C/S Opposing stimuli only used a stimulus velocity of 15 deg/s, Surround stimuli using 30 deg/s dot motion were also excluded. Finally, as C/S Opposing stimuli used the counting task in all trials, only Surround stimuli using the counting task were included in the analysis. The stimuli used to calculate the model therefore only differed in terms of whether there was opposing motion present in the centre (C/S Opposing) or whether there was simply a central occluding mask (Surround).

A linear regression model was calculated to predict the gain of the OKR in response to the surround, using stimulus area, motion direction (NT or TN motion) and stimulus type (C/S Opposing or Surround) as predictors, with an interaction term included to assess for interaction between stimulus area and stimulus type. A significant regression equation was found ($F(4, 179) = 24.841$, $p < .001$) with an adjusted R^2 of .348. The results of this analysis are shown in Table 4.16. In this model, area was found to significantly predict OKR gain in response to the surround ($p = .017$) whereby increasing the area of the surround

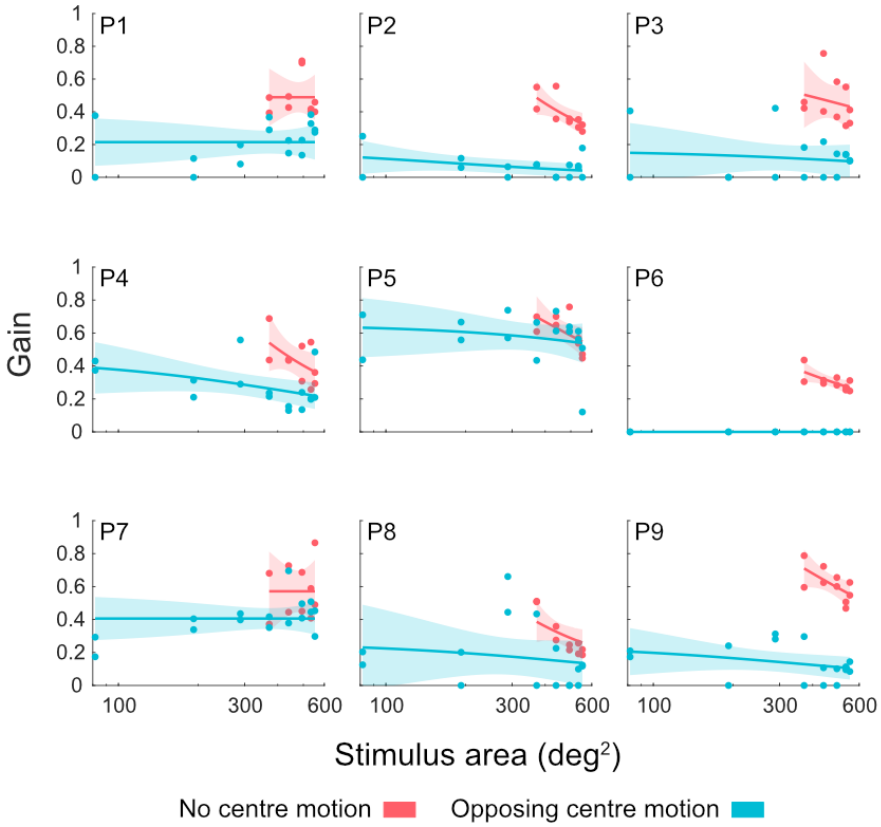

Figure 4.25: Gain in response to the surround region of a C/S Opposing stimulus with the counting task presented to the surround (blue) and in response to a Surround (S) stimulus using the counting task and dots drifting at 15 deg/s (red) in nine individual participants, across stimulus area. Individual data points represent the mean gain obtained in a single trial. Participant numbers are indicated in the upper left corner of each plot. The shaded area indicates the 95% CI of the fitted function. Note that a larger range of stimulus sizes was used for surround regions of C/S Opposing (Part 2) stimuli compared to Surround (S) (Part 1) stimuli.

resulted in a decrease in gain (β = -0.0007). Stimulus type was also found to significantly predict gain (p = .007): presenting stimuli with opposing motion in the centre reduced gain relative to stimuli with no motion in the centre (β = -0.5352). Motion direction (p = .265) did not significantly predict gain, and there was no interaction between stimulus area and type (p = .155). The group fits corresponding to the data used in this model are shown in Figure 4.23.

4.4.2.5 Response to surround region of C/S Opposing stimulus: Frequency

Individual frequency across stimulus area in response to surround regions of C/S Opposing stimuli are shown in Figure 4.27, with responses to Surround (Part 1) stimuli included for comparison.

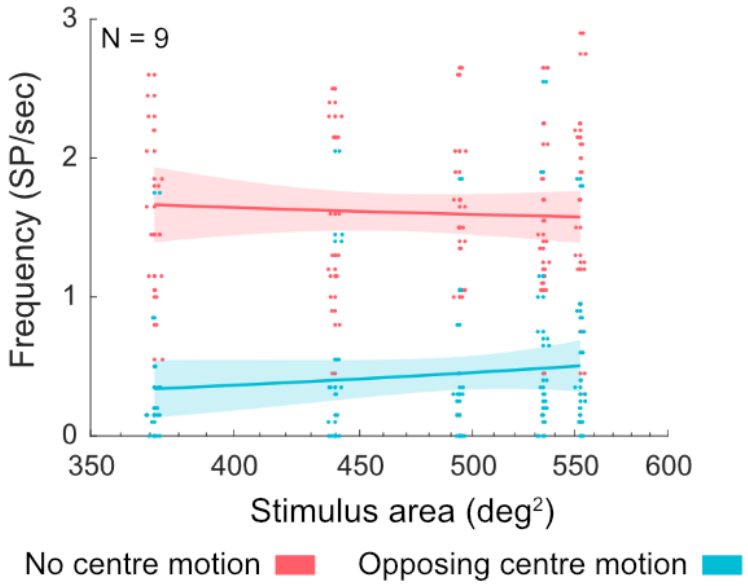

Figure 4.26: Group (N = 9) frequency (slow phases per second) across stimulus area in response to the surround region of a C/S Opposing stimulus with the counting task presented to the surround (blue) and in response to a Surround (S) stimulus at 15 deg/s while using the counting task (red). Data points indicate mean gain in a single trial, with a horizontal jitter of up to 6 deg applied. The shaded area indicates the 95% CI of the fitted function. Only the shared stimulus area range has been included.

The above analysis was repeated to investigate frequency data rather than gain. The same exclusion criteria were used as in the above analysis so that the only difference between the two stimuli used in the analysis was the presence or absence of motion in the centre; stimulus size range, velocity and use of the counting task remained the same. A linear regression model was calculated to predict the frequency of OKR using stimulus area, motion direction (NT or TN) and stimulus type (C/S Opposing or Surround) as predictors, with an interaction term included to assess for interactions between stimulus area and type. A

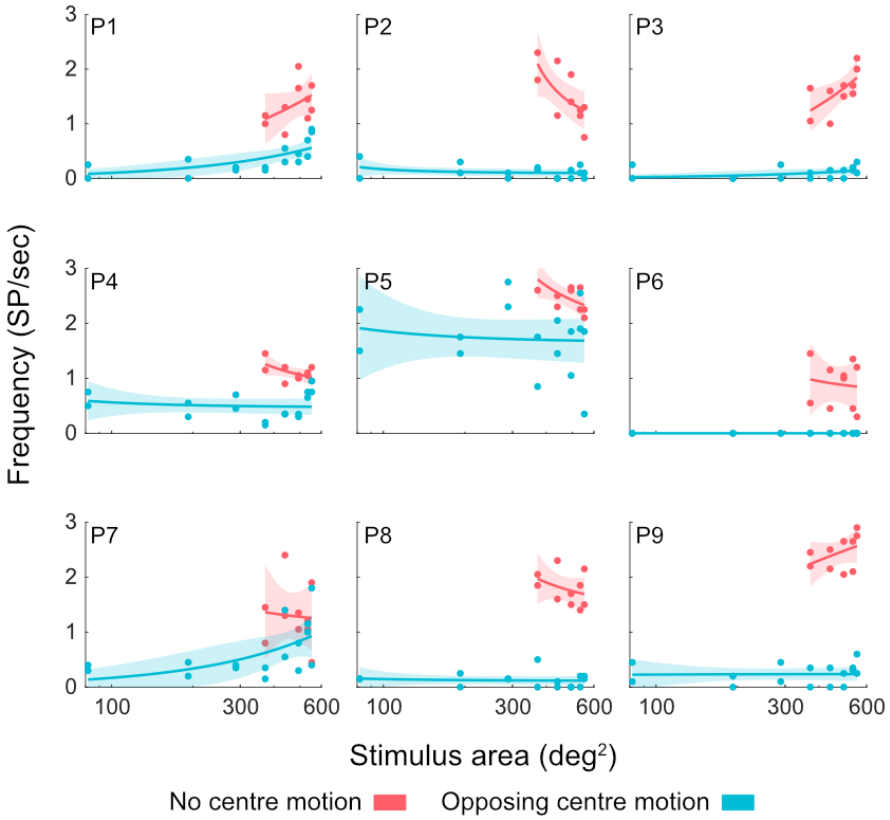

Figure 4.27: Frequency in response to the surround across stimulus area in nine individual participants. Frequency obtained from trials using C/S Opposing stimuli with the counting task presented to the surround is shown in blue. Frequency obtained from trials using a Surround (S) (Part 1) stimulus at 15 deg/s with the counting task is shown in red. Individual data points represent the frequency obtained in that trial. The shaded area indicates the 95% CI of the fitted function. Participant numbers are displayed in the upper left corner of each plot. Note that a larger range of stimulus sizes was used for C/S Opposing stimuli compared to Surround (S) stimuli.

significant regression equation was found ($F(4, 179) = 43.900$, $p < .001$) with an adjusted R^2 of .489. The results of this analysis are shown in Table 4.17. In this model, the only significant predictor of OKR frequency in response to the surround was stimulus type ($\beta = -2.0861$, $p = .002$), whereby frequency was reduced by the presence of opposing motion in the centre. The group fits corresponding to the data used in this model are displayed in Figure 4.26.

Table 4.17

Results of linear regression model to predict OKR frequency in response to the surround based on three predictor variables (stimulus area, stimulus type and motion direction)

	β	SE	F	*p*
Intercept	1.8585	0.465	3.999	< .001*
Area	-0.0005	0.001	-0.505	.614
Direction	-0.0378	0.089	-0.422	.673
Stimulus type	-2.0861	0.654	-3.189	.002*
Area*Stimulus type	0.0019	0.001	1.403	.162

4.4.2.6 Response to surround region of C/S Opposing stimulus: Amplitude

Finally, a linear regression model was calculated to predict the amplitude of OKR using stimulus area, direction of motion (NT or TN) and stimulus type (C/S Opposing or Surround) as predictor variables, as well as to examine a potential interaction between stimulus area and type. The same exclusion criteria were followed as in the gain and frequency analyses. A significant regression equation was found ($F(4, 179) = 24.865$, $p < .001$) with an adjusted R^2 of .348. The results of this analysis are displayed in Table 4.18. In this model, stimulus area ($p < .001$) and stimulus type ($p = .002$) were both found to be significant predictors of OKR amplitude in response to the surround, with stimulus type forming the largest contribution ($\beta = -3.3825$). This indicates that increasing stimulus area reduced amplitude ($\beta = -0.0056$), and that the presence of opposing motion in the centre also reduced amplitude. There was no significant interaction between stimulus area and stimulus type ($p = .064$). Group fits corresponding to data used in this model are shown in Figure 4.28.

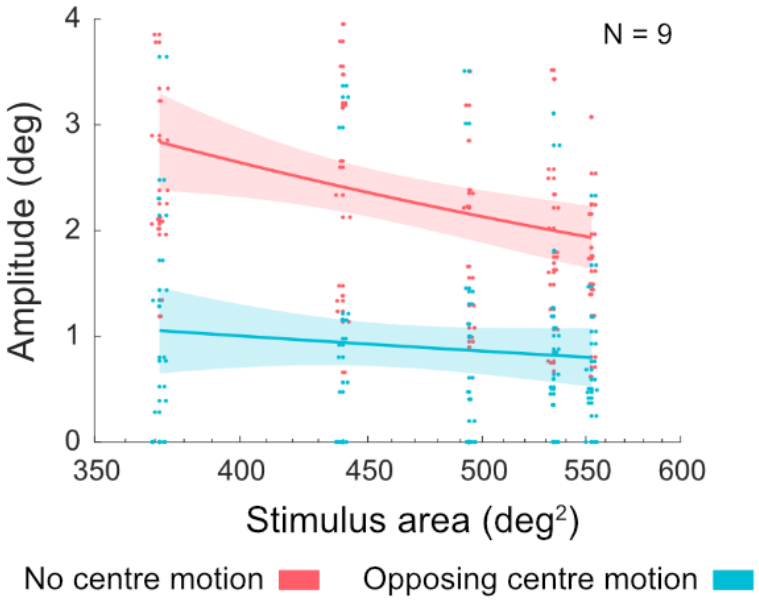

Figure 4.28: N = 9. Amplitude in response to the surround, obtained during trials involving a C/S Opposing stimulus with the counting task presented to the surround (blue) or Part 1 Surround (S) stimulus trials at 15 deg/s using the counting task. Data points indicate mean amplitude in a single trial, with a horizontal jitter of up to 6 deg applied. The shaded area indicates the 95% CI of the fitted function.

Mean amplitude per trial in each of the nine participants during C/S opposing stimuli is shown in Figure 4.29, with amplitude in response to Surround (Part 1) stimuli at 15 deg/s in trials using the counting task included for comparison.

Table 4.18

Results of linear regression model to predict OKR amplitude in response to the surround based on three predictor variables (stimulus area, stimulus type and motion direction)

	β	SE	F	*p*
Intercept	4.8288	0.775	6.232	< .001*
Area	-0.0056	0.001	-3.500	< .001*
Direction	0.2217	0.149	1.486	.139
Stimulus type	-3.3825	1.091	-3.101	.002*
Area*Stimulus type	0.0042	0.002	1.864	.064

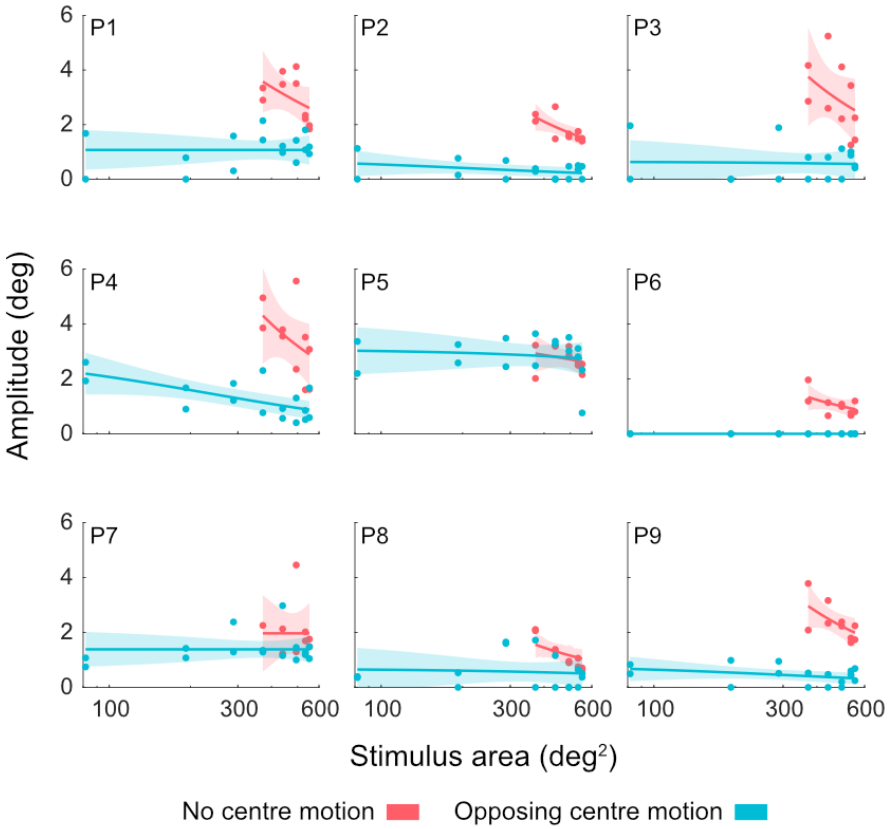

Figure 4.29: Amplitude in response to the surround across stimulus area during trials using C/S Opposing stimuli with the task presented to the surround (blue) and Part 1 Surround (S) stimuli at 15 deg/s with the counting task presented to the surround (red). Individual data points represent the mean gain obtained in that trial. The shaded area indicates the 95% CI of the fitted function. Participant numbers are indicated in the upper left corner of each plot.

Part 2: Summary of key findings

- Responses to the centre and to the surround are suppressed by opposing motion in the complementary region, with responses to the surround being particularly affected
- Increasing stimulus area does not increase gain in response to the surround
- Presenting the counting task to the surround dramatically reduces OKR measures in response to the centre
- A peripheral OKR can be generated in the presence of a competing central optokinetic stimulus

4.5 Part 3: Centre-surround with Brownian motion

Part 2 found that the presence of opposing motion impacted the OKR in response to the centre and the surround, such as by reducing the gain and amplitude of the OKR. Part 3 used C/S stimuli with Brownian motion presented to either the centre or the surround region in order to assess whether the effect seen in Part 2 was unique to the presence of a competing optokinetic stimulus or whether it was caused by the presence of incongruent motion, regardless of whether that motion was in the form of an optokinetic stimulus. Unlike Part 2, Part 3 involved the use of non-counting task conditions; this allowed for investigation of whether the counting task was required to produce an OKR in response to the surround in the presence of incongruent central motion. The block design was altered following Part 2 to reduce the duration of each block.

4.5.1 Methods

4.5.1.1 Participants

Of the nine participants used in Part 1 and Part 2, one (P2) was unavailable to participate in Part 3, therefore a replacement participant (P10) was used (female, age = 22 years). The remaining eight participants were the same as those used in Part 1 and Part 2.

4.5.1.2 Stimuli

Part 3 used the previously described C/S Brownian stimuli (Figure 4.2), which used circular random-dot kinematograms with a centre-surround configuration. Coherent horizontal dot motion was presented to one region (centre or surround) while random-walk (Brownian) motion was presented to the other. The size of the central region was varied. All stimuli were presented with a dot speed of 15 deg/s. During trials using the counting task, coloured task dots were presented within the region of the stimulus displaying coherent motion.

4.5.1.3 Design

During Part 3, half of trials used the counting task and half did not. Half of trials presented Brownian motion in the centre and coherent motion in the surround while the other half presented Brownian motion in the surround and coherent motion in the centre. The same range of stimulus sizes was used as in Part 2 and both directions of horizontal motion were presented. This resulted in a total of 64 trials per participant.

Counting task and non-task trials were presented in separate blocks. Throughout each block, coherent motion was presented either in the centre for the full block or in the surround for the full block. The eight central diameter sizes were split across blocks: central diameters of 5, 10, 16 and 22 deg were presented with both directions of motion in one block of eight stimuli, whereas central diameters of 7, 13, 19 and 25 deg were presented in another block of eight stimuli. Consequently, stimuli were presented across eight blocks, each containing eight trials. The order of blocks, and of trials within each block, was randomised.

Gaze monitoring was used to ensure that participants viewed the central region of the stimulus; this followed the same restrictions used within Part 1 and Part 2.

4.5.1.4 Procedure

The procedure followed that of Part 1 and the same set of instructions were used.

4.5.2 Results

4.5.2.1 Response to centre region of C/S Brownian stimulus: Gain

Analyses mirrored those of Part 2: trials in which coherent motion was presented to the centre region of a C/S Brownian stimulus, and Centre stimulus (Part 1) trials using 15 deg/sec dot motion, using only the shared stimulus area range, were used to calculate a regression model. The included trials therefore

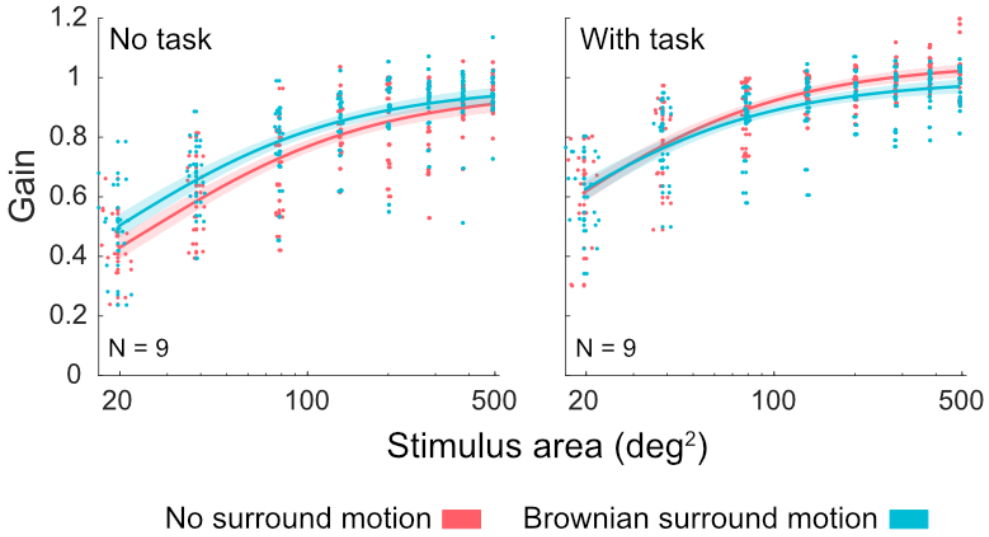

Figure 4.30: N = 9. Mean gain in response to the centre during trials without (left) and with (right) the counting task, during Centre (C) (Part 1) trials with 15 deg/s stimuli (red) and C/S Brownian (Part 3) trials presenting coherent motion to the centre (blue). Data points indicate mean gain in a single trial, with a horizontal jitter of 6 deg applied. The shaded area indicates the 95% CI of the fitted function. Note that 'no surround motion' data include P2, who is replaced by P10 in the 'Brownian surround motion' data.

only differed in terms of whether Brownian motion was present in the surround. A linear regression model was calculated to predict the gain of OKR in response to the centre using stimulus area, direction of motion (NT or TN), stimulus type (Centre (Part 1) or C/S Brownian (Part 3)) and counting task condition (with task or without task) as predictor variables. An interaction term was included to assess for interaction between stimulus type and task condition. The results of this analysis are shown in Table 4.19. A significant regression equation was found ($F(5, 575) = 101.530$, $p < .001$) with an adjusted R^2 of .466. In this model, every predictor was found to significantly predict gain, with counting task condition ($\beta = 0.1439$) forming the largest contribution. The coefficients indicate that increasing stimulus area increased gain ($\beta = 0.0007$), presenting TN motion rather than NT motion increased gain ($\beta = 0.0350$), presenting central motion without surrounding Brownian motion increased gain ($\beta = 0.0461$) and presenting the counting task increased gain ($\beta = 0.1439$). However, t-tests examining the interaction between stimulus type and task condition showed that, during

non-task conditions, gain was significantly higher in response to C/S Brownian stimuli (M = 0.808, SD = 0.187) compared to Centre (C) (Part 1) stimuli (M = 0.762, SD = 0.199) ($t(143) = -3.593$, $p = .004$); however, during conditions that did use the counting task, gain was significantly higher in response to Centre stimuli (M = 0.906, SD = 0.165) compared to C/S Brownian stimuli (M = 0.874, SD = 0.154) ($t(143) = 2.637$, $p = .009$). This interaction effect can be seen in fits presented in Figure 4.30.

Table 4.19

Results of linear regression model to predict OKR gain in response to the centre based on four predictor variables (stimulus area, stimulus type, motion direction and task condition)

	β	SE	F	*p*
Intercept	0.6007	0.015	41.302	< .001*
Area	0.0007	0.00003	19.988	< .001*
Direction	0.0350	0.011	3.102	.002*
Stimulus type	0.0461	0.016	2.886	.004*
Task condition	0.1439	0.016	9.018	< .001*
Stimulus type*Task	-0.0784	0.023	-3.475	< .001*

T-tests were carried out to assess whether the difference in gain caused by the use of the counting task differed significantly between Centre (Part 1) stimuli and C/S Brownian (Part 3) stimuli. This showed that the counting task caused a significantly larger increase in gain in response to Centre stimuli (M = 0.144, SD = 0.135) compared to in response to the coherent centre of C/S Brownian stimuli (M = 0.065, SD = 0.115) ($t(143) = 6.119$, $p < .001$).

As the use of the C/S Brownian stimulus was intended to assess whether the presence of incongruent motion in general impacted the OKR, a regression model was calculated to examine this. Part 2 trials all involved the counting task, therefore only Part 3 trials that used the counting task were included in the model. A linear regression model was calculated to predict the gain of OKR in response to the centre of a C/S stimulus presenting the counting task to the

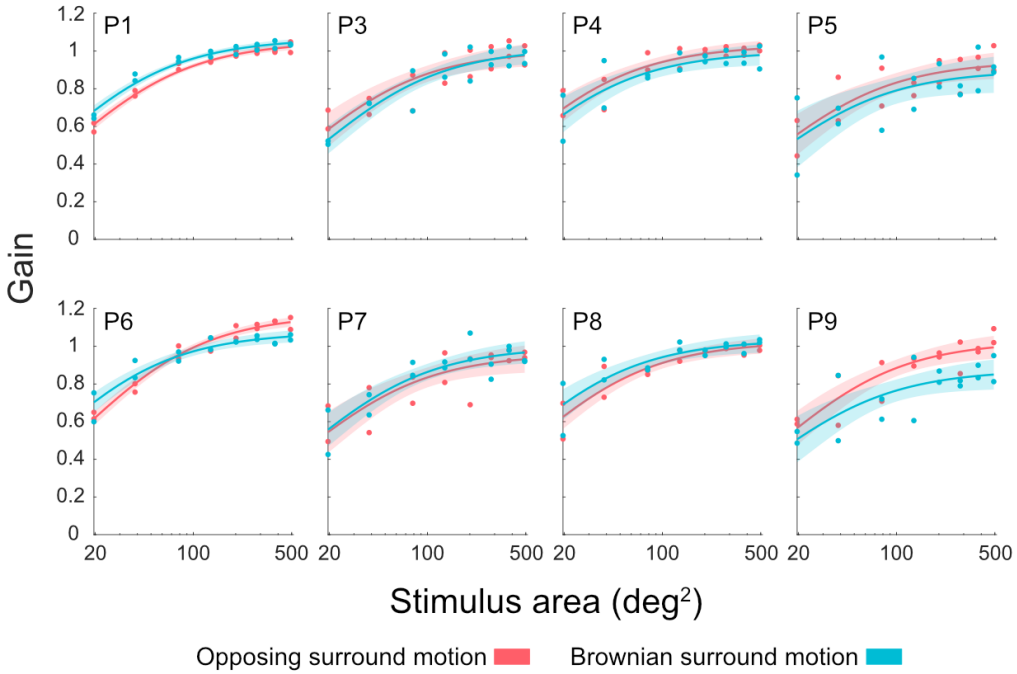

Figure 4.31: Mean gain obtained during C/S trials with the counting task presented to the centre with opposing surround motion (Part 2) (red) and Brownian surround motion (Part 3) (blue). Individual data points represent the mean gain obtained in a single trial. The shaded area indicates the 95% CI of the fitted function. Participant numbers are shown in the upper left corner of each plot. Not shown are participants 2 and 10, as they did not participate in the C/S Brownian and C/S Opposing trials, respectively, though their data did contribute towards the regression model.

centre, using stimulus area, direction of motion (NT or TN) and stimulus type (C/S Opposing or C/S Brownian) as predictors. A significant regression equation was found ($F(3, 287) = 59.832$, $p < .001$) with an adjusted R^2 of .381. The results of this analysis are displayed in Table 4.20. In this model, stimulus area ($p < .001$) and direction of motion ($p = .021$) both significantly predicted gain, but stimulus type did not ($p = .286$). Increasing area increased gain ($\beta = 0.0006$), and presenting TN motion (M = 0.883, SD = 0.162) rather than NT motion (M = 0.847, SD = 0.172) increased gain ($\beta = 0.0359$). Plots showing individual responses to C/S Brownian and C/S Opposing stimuli are displayed in Figure 4.31.

Table 4.20

Results of linear regression model to predict OKR gain in response to the centre based on three predictor variables (stimulus area, stimulus type and motion direction)

	β	SE	F	*p*
Intercept	0.7080	0.017	42.185	< .001*
Area	0.0006	0.00004	13.154	< .001*
Direction	0.0359	0.016	2.305	.021*
Stimulus type	0.0167	0.016	1.068	.286

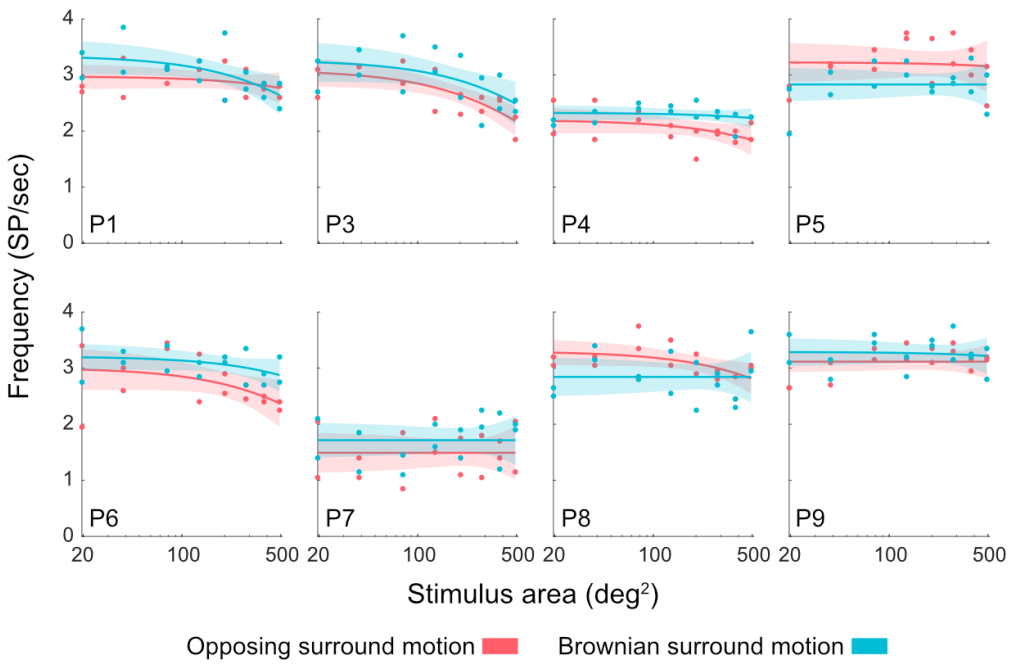

Figure 4.32: Frequency in response to the centre of a C/S Brownian stimulus (blue) and a C/S Opposing stimulus (red) in nine participants. Individual data points represent the frequency obtained in a single trial. The shaded area indicates the 95% CI of the fitted function. Participant numbers are displayed in the lower left corner of each plot. Note that two participants, P2 and P10, are not shown as they did not participate in C/S Brownian and C/S Opposing trials, respectively, though their data did contribute towards the model.

4.5.2.2 Response to centre region of C/S Brownian stimulus: Frequency

Frequency in response to C/S Brownian and C/S Opposing stimuli was modelled. A linear regression model was calculated to predict the frequency of the OKR, using stimulus area, direction of motion (NT or TN) and stimulus type (C/S Opposing or C/S Brownian) as predictors. For C/S Brownian data, only responses to trials using the counting task were included. The resulting regression equation was not significant ($F(3, 287) = 1.673$, $p = .173$). The results of this analysis are shown in Table 4.21, with the corresponding individual data shown in Figure 4.32.

Table 4.21

Results of linear regression model to predict OKR frequency in response to the centre (C/S Brownian or C/S Opposing stimulus) based on three predictor variables (stimulus area, stimulus type and motion direction)

(non-sig)	β	SE	F	*p*
Intercept	2.7208	0.079	34.036	< .001*
Area	-0.0005	0.0002	-2.189	.029*
Direction	0.0038	0.074	0.051	.959
Stimulus type	0.0351	0.074	0.472	.637

4.5.2.3 Response to centre region of C/S Brownian stimulus: Amplitude

Using amplitude in response to a Centre (C) (Part 1) stimulus and the coherent centre of a C/S Brownian (Part 3) stimulus, a linear regression model was calculated to predict the amplitude of the OKR using stimulus area, direction of motion (NT or TN), stimulus type (Centre or C/S Brownian) and task condition (with counting task or without counting task) as predictors. A significant regression equation was found ($F(4, 575) = 81.378$, $p < .001$) with an adjusted R^2 of .359. This model confirmed that presenting a Centre stimulus with no surround motion (M = 3.751, SD = 1.206) rather than a C/S stimulus with Brownian motion in the surround (M = 3.536, SD = 1.077) increased amplitude (β = -0.2151). The results of this analysis are shown in Table 4.22, with group fits corresponding to the data shown in Figure 4.33.

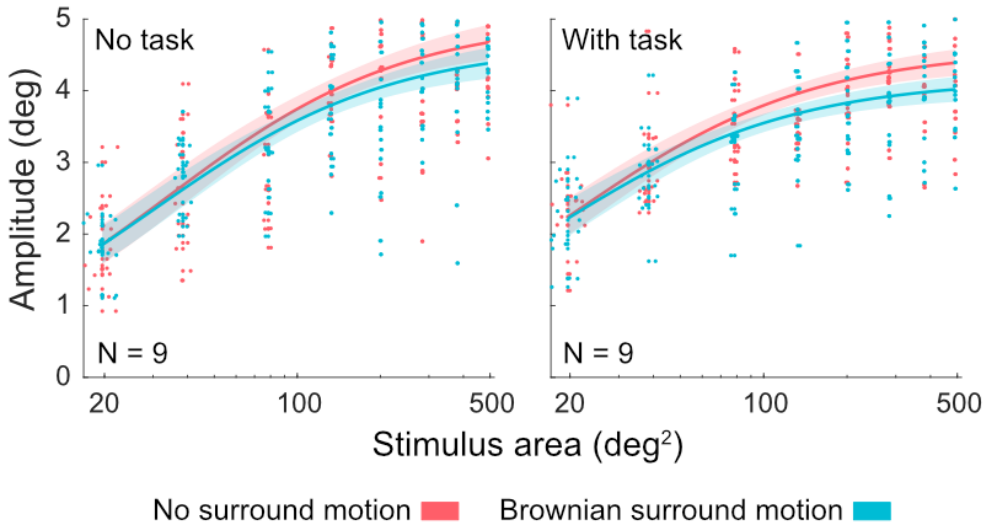

Figure 4.33: N = 9. Amplitude in response to a Centre (Part 1) stimulus or the coherent centre of a C/S Brownian (Part 3) stimulus during trials without the counting task (left) and with the counting task (right). Data points indicate the mean amplitude obtained in a single trial, with a horizontal jitter of up to 6 deg applied. The shaded area indicates the 95% CI of the fitted function. Note that 'no surround motion' data includes P2, who was replaced by P10 in 'Brownian surround motion' trials.

Table 4.22

Results of linear regression model to predict OKR amplitude in response to the centre (Centre or C/S Brownian stimulus) based on four predictor variables (stimulus area, stimulus type, motion direction and task condition)

	β	SE	F	*p*
Intercept	2.7820	0.091	30.606	< .001*
Area	0.0042	0.0002	17.447	< .001*
Direction	0.2746	0.077	3.586	< .001*
Stimulus type	-0.2151	0.077	-2.809	.005*
Task condition	-0.0455	0.077	-0.594	.553

Analyses were then carried out to assess amplitude in response to the centre of a C/S stimulus using a counting task with Brownian motion or opposing motion in the surround. A linear regression model was calculated to predict

the amplitude of the OKR in response to the centre of a C/S stimulus using stimulus area, direction of motion (NT or TN) and stimulus type (C/S Brownian or C/S Opposing) as predictors. A significant regression equation was found ($F(3, 287) = 50.613$, $p < .001$) with an adjusted R^2 of .341. In this model, increasing stimulus area increased amplitude ($\beta = 0.0036$, $p < .001$), but direction of motion and stimulus type were not significant predictors of amplitude. The results of this analysis are shown in Table 4.23.

Table 4.23

Results of linear regression model to predict OKR amplitude in response to the centre (C/S Brownian or C/S Opposing stimulus) based on three predictor variables (stimulus area, stimulus type and motion direction)

	β	SE	F	*p*
Intercept	2.5809	0.100	25.792	< .001*
Area	0.0036	0.0003	12.153	< .001*
Direction	0.1487	0.093	1.255	.111
Stimulus type	0.1167	0.093	1.599	.210

4.5.2.4 Response to surround region of C/S Brownian stimulus: Gain

Similar analyses were carried out to assess responses to the surround (Figure 4.34). A regression model was calculated to predict the gain of OKR using data obtained in response to the Surround (S) stimulus (Part 1) and in response to the coherent surround of a C/S Brownian (Part 3) stimulus. As C/S stimuli used a wider range of surround region areas compared to surround (Part 1) stimuli, only the shared stimulus area range was included in this model. Only Part 1 trials using a stimulus velocity of 15 deg/s were included.

A linear regression model was calculated to predict gain in response to the surround, using stimulus area, direction of motion, stimulus type (Figure 4.35) and counting task condition (Figure 4.35) as predictors. Interactions between stimulus type and stimulus area and between stimulus type and counting task condition were also assessed. The results of this analysis are shown in Table

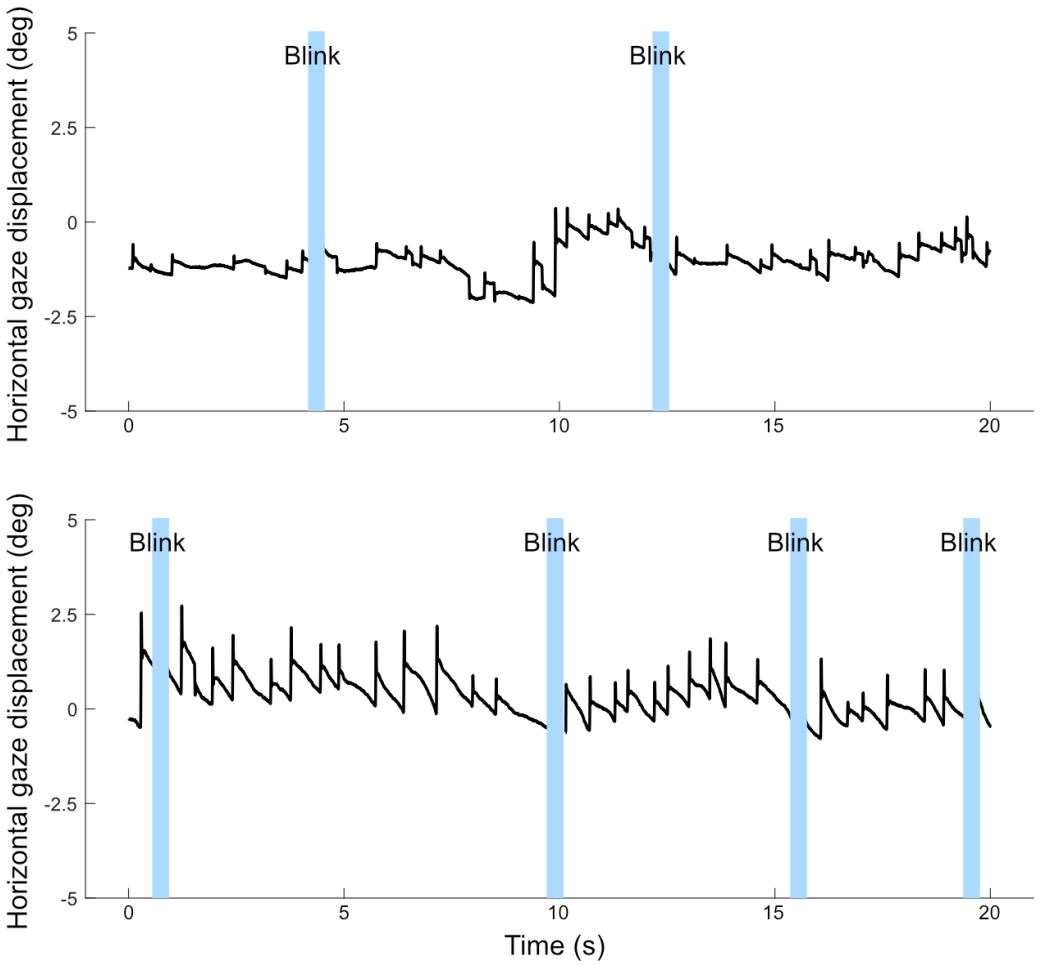

Figure 4.34: Horizontal eye movement traces obtained from the same stimulus size and direction from the same participant during C/S Brownian trials presenting coherent dot motion to the surround. Traces show a response to motion drifting towards the left. The upper trace shows a trial that did not use the counting task while the lower trace shows a trial that did use the counting task. Blink locations are indicated by vertical blue bars.

4.24. A significant regression equation was found ($F(6, 359) = 82.17$, $p < .001$) with an adjusted R^2 of .576. In this model, all predictors with the exception of direction of motion were found to significantly predict gain, with stimulus type forming the largest contribution ($\beta = -0.5376$). The model confirmed that Brownian motion in the centre reduced gain. T-tests were carried out to assess the interactions. The impact of the counting task on gain was found to be larger during Surround (S) stimuli ($t(89) = 2.447$, $p = .016$). The analysis of Part 1 showed that the Surround (S) stimulus at a speed of 15 deg/s was associated with

a significant decrease in gain as the area of the stimulus was increased; this analysis was repeated on C/S Brownian data, using only the shared stimulus area range, finding that stimulus area did not significantly predict gain ($\beta = 0.0001$, $p = .213$) ($F(3, 179) = 32.155$, $p < .001$, adjusted $R^2 = .343$).

Data from the two C/S conditions (C/S Opposing and C/S Brownian) were then modelled to assess whether the type of motion in the centre impacted the OKR. The full stimulus area range was used. As C/S Opposing stimuli used the counting task during every trial, only C/S Brownian trials including the counting task were used. A linear regression model was calculated to predict the gain of OKR, using stimulus area, direction of motion (TN or NT) and stimulus type (C/S Opposing or C/S Brownian) as predictors. The resulting regression equation was not significant ($F(3, 287) = 1.069$, $p = .362$). Individual data corresponding to that used in this analysis are shown in Figure 4.36.

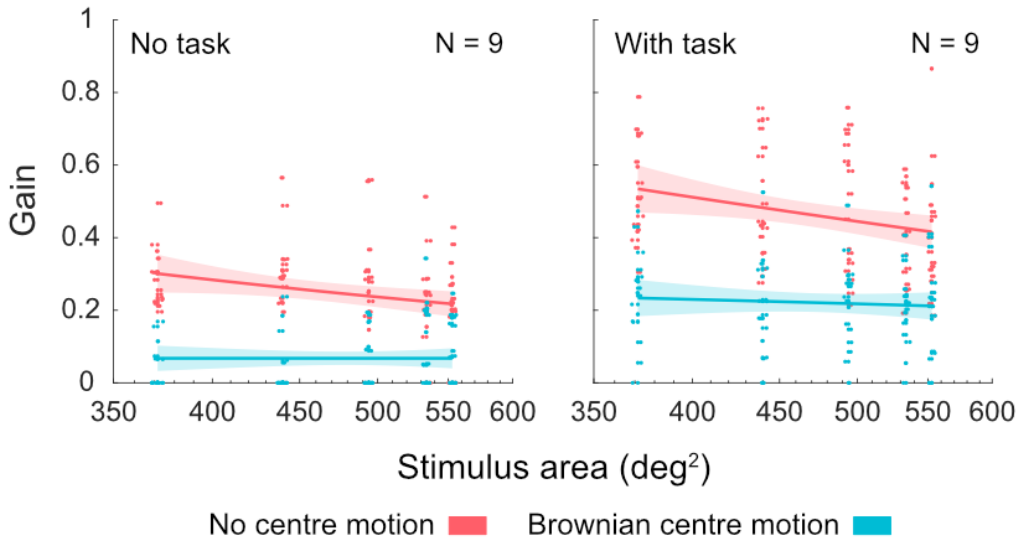

Figure 4.35: N = 9. Gain obtained in response to a Surround (Part 1) stimulus (red) or the coherent surround of a C/S Brownian (Part 3) stimulus in trials using the counting task (right) and trials without the counting task (left). Individual data points represent the mean gain obtained in a single trial, with a horizontal jitter of up to 6 deg applied. The shaded area indicates the 95% CI of the fitted function. 'No centre motion' data includes P2, who was replaced by P10 in the 'Brownian centre motion' data.

Table 4.24

Results of linear regression model to predict OKR gain in response to the surround (Surround or C/S Brownian stimulus) based on four predictor variables (stimulus area, stimulus type, motion direction and task condition)

	β	SE	F	*p*
Intercept	0.5255	0.068	7.755	< .001*
Area	-0.0001	0.0001	-4.310	< .001*
Direction	0.0169	0.013	1.312	.190
Stimulus type	-0.5376	0.095	-5.636	< .001*
Task condition	0.2126	0.018	11.632	< .001*
Stimulus Type*Area	0.0007	0.0002	3.808	< .001*
Stimulus Type*Task	-0.0597	0.026	-2.309	.021*

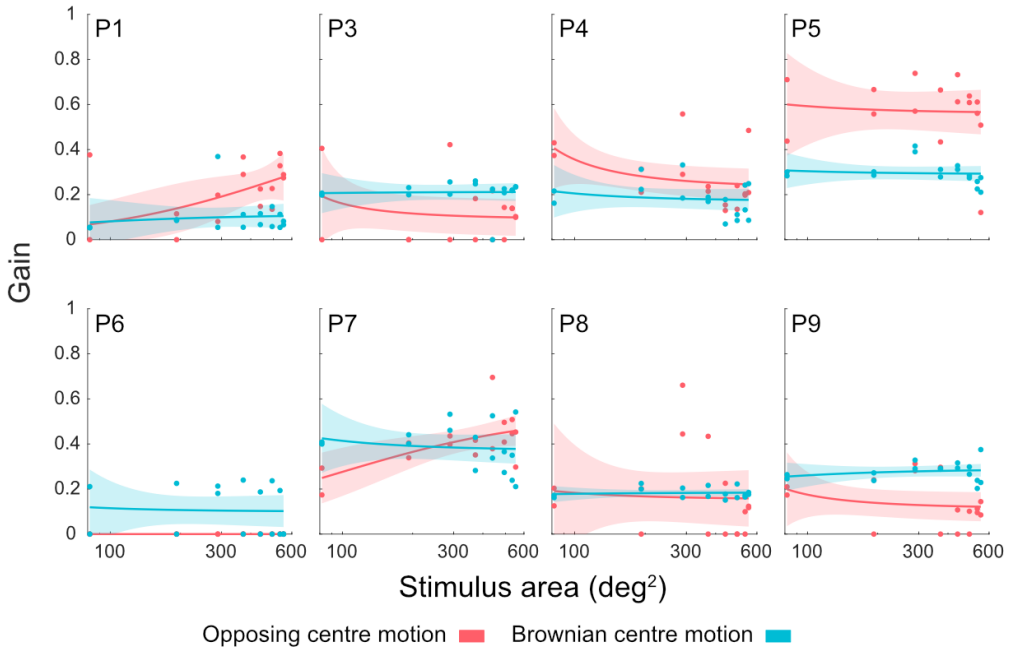

Figure 4.36: Mean gain obtained in response to the surround region of a C/S stimulus with opposing motion in the centre (red) and with Brownian motion in the centre (blue) during trials presenting the counting task to the surround. Each individual data point represents the mean gain obtained during a single trial; the shaded area indicates the 95% CI of the fitted function. Not shown are P2 and P10, as they did not participate in C/S Brownian and C/S Opposing trials, respectively.

4.5.2.5 Response to surround region of C/S Brownian stimulus: Frequency

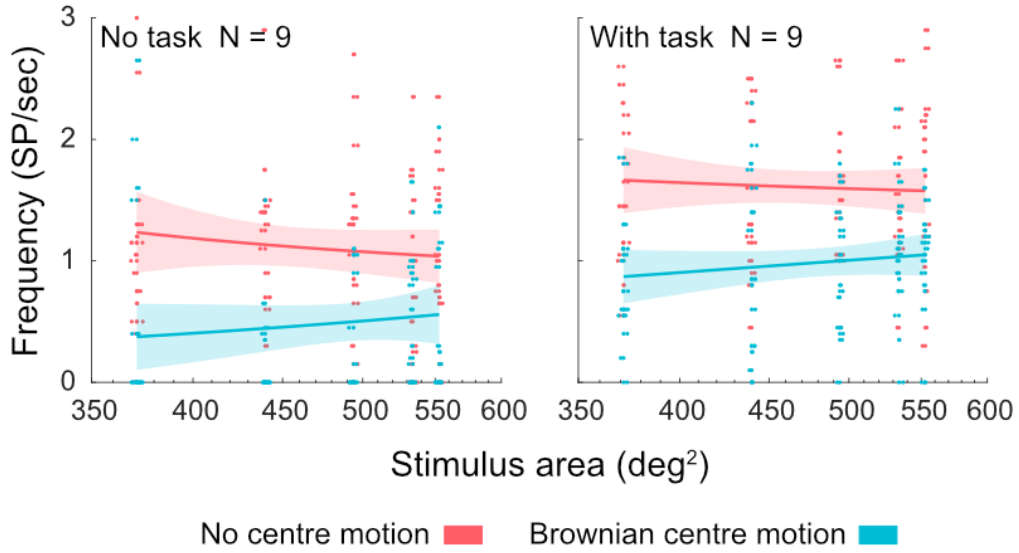

Figure 4.37: N = 9. Frequency in response to a surround stimulus with no motion in the centre (Surround (S), Part 1) (red) and with Brownian motion in the centre (Part 3) (blue) during trials that did use the counting task (right) and trials that did not use the counting task (left). Data points indicate the mean frequency obtained in a single trial, with a horizontal jitter of up to 6 deg applied. The shaded area indicates the 95% CI of the fitted function. 'No centre motion' data included P2, who was replaced by P10 during 'Brownian centre motion' trials.

These analyses were then repeated to investigate the contribution of different parameters towards the frequency of the OKR. A linear model was calculated to predict the frequency of OKR in response to the surround region of a stimulus with no motion in the centre (Surround (S) stimulus, Part 1) and with Brownian motion in the centre (C/S Brownian, Part 3) (Figure 4.37) using stimulus area, direction of motion (NT or TN), stimulus type (Surround or C/S Brownian) and counting task condition (with or without task) as predictors (Table 4.25). Interactions between stimulus type and stimulus area and between stimulus type and counting task condition were also assessed. Again, only the range of stimulus areas shared by both stimuli were included in the analysis. A

significant regression equation was found ($F(6, 359) = 21.967$, $p < .001$) with an adjusted R^2 of .259.

Table 4.25

Results of linear regression model to predict OKR frequency in response to the surround (Surround or C/S Brownian stimulus) based on four predictor variables (stimulus area, stimulus type, motion direction and task condition)

	β	SE	F	*p*
Intercept	1.5556	0.374	4.163	< .001*
Area	-0.0009	0.001	-1.194	.233
Direction	-0.0250	0.071	-0.351	.726
Stimulus type	-1.6834	0.526	-3.200	.001*
Task condition	0.5011	0.101	4.971	< .001*
Stimulus Type*Area	0.0022	0.001	2.041	.041*
Stimulus Type*Task	0.0011	0.142	0.008	.994

Table 4.26

Results of linear regression model to predict OKR frequency in response to the surround (C/S Brownian or C/S Opposing stimulus) based on three predictor variables (stimulus area, stimulus type and motion direction)

	β	SE	F	*p*
Intercept	0.3635	0.099	3.659	< .001*
Area	0.0002	0.0002	1.071	.285
Direction	-0.0545	0.068	-0.796	.427
Stimulus type	0.5496	0.068	8.022	< .001*

In this model, stimulus type and counting task condition both significantly predicted frequency, and there was a significant interaction between stimulus type and stimulus area. Frequency was significantly increased by the use of the counting task ($\beta = 0.5011$, $p < .001$). T-tests were used to assess the interaction between stimulus type and area, finding that the effect of stimulus area on

frequency was only significant during C/S Brownian stimuli ($t(35) = 2.669$, $p = .011$).

Analyses then turned to assessing whether the type of motion in the centre region of a C/S stimulus significantly predicted frequency of OKR. A linear regression model was calculated to predict the frequency of the OKR using stimulus area, stimulus type (C/S Opposing or C/S Brownian) and direction of motion (NT or TN) as predictors. The model used the full stimulus area range, and only included trials that used the counting task. The results of this analysis are shown in Table 4.26. A significant regression equation was found ($F(3, 287) = 22.042$, $p < .001$) with an adjusted R^2 of .180. In this model, only stimulus type significantly predicted OKR frequency ($\beta = 0.5496$), indicating that frequency

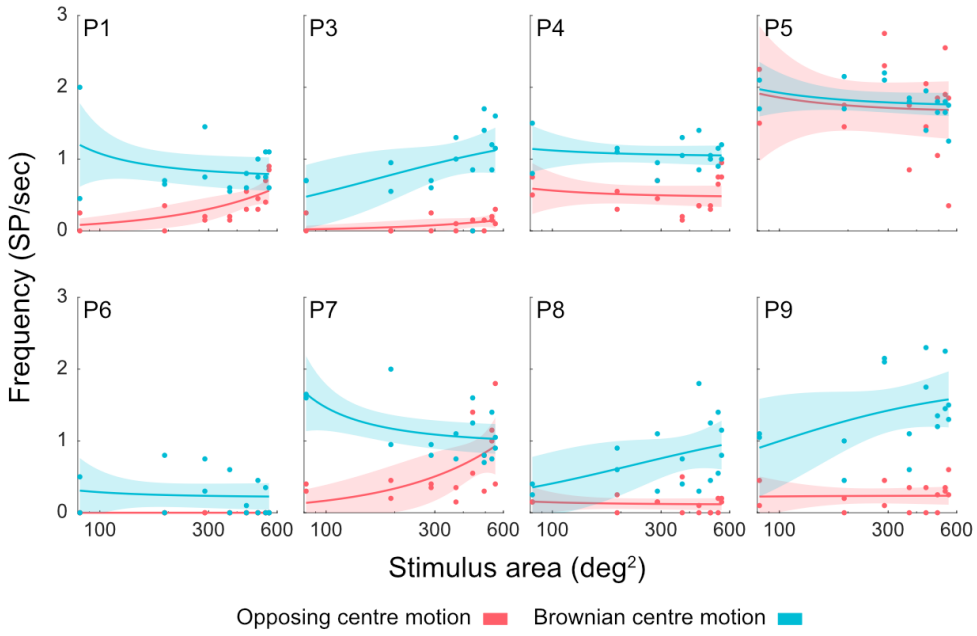

Figure 4.38: Frequency obtained in response to the surround region of C/S stimuli with the counting task presented to the surround and opposing motion in the centre (C/S Opposing, Part 2) (red) or Brownian motion in the centre (C/S Brownian, Part 3) (blue) in eight participants. Individual data points represent the frequency obtained in that trial; the shaded area indicates the 95% CI of the fitted function. Participant numbers are displayed in the upper left corner of each plot. Not shown are P2 and P10 as they did not participate in C/S Brownian and C/S Opposing trials, respectively.

was higher when motion in the centre was Brownian (M = 0.971, SD = 0.581) rather than opposing (M = 0.421, SD = 0.582). Individual data showing frequency in response to C/S stimuli are displayed in Figure 4.38.

4.5.2.6 Response to surround region of C/S Brownian stimulus: Amplitude

Finally, slow phase amplitude in response to the surround region of the stimulus was investigated (Figure 4.39). Using amplitude in response to the Surround (S) (Part 1) stimulus and amplitude in response to the coherent surround of a C/S Brownian (Part 3) stimulus, a linear regression model ($F(6, 340) = 76.407$, $p < .001$) with an adjusted R^2 of .571 confirmed that amplitude was decreased by the presence of Brownian motion in the surround ($\beta = -2.9208$, $p < .001$) (Table 4.27). There was an interaction between stimulus type and area. In the Part 1 results section, a regression model of the response to the surround found that during presentation of Surround (S) stimuli, increasing area was associated with a decrease in amplitude (Table 4.8). However, when examining just C/S Brownian stimuli, stimulus area did not significantly predict the amplitude of the OKR in response to the surround ($\beta = -0.0001$, $p = .800$) ($F(3, 179) = 34.370$, $p < .001$, adjusted $R^2 = .359$). An interaction between stimulus type and task was also examined, finding a significantly larger effect of the task in response to the Surround stimulus ($t(89) = 6.437$, $p < .001$).

Table 4.27

Results of linear regression model to predict OKR amplitude in response to the surround (Surround or C/S Brownian stimulus) based on four predictor variables (stimulus area, stimulus type, motion direction and task condition)

	β	SE	F	*p*
Intercept	3.0988	0.374	8.274	< .001*
Area	-0.0044	0.001	-5.802	< .001*
Direction	0.1567	0.071	2.194	.029*
Stimulus type	-2.9208	0.527	-5.540	< .001*
Task condition	1.2111	0.101	11.988	< .001*
Stimulus Type*Area	0.0043	0.001	4.005	< .001*
Stimulus Type*Task	-0.6541	0.143	-4.579	< .001*

Investigating the effect of motion type, data from both C/S (Brownian and Opposing) stimuli were used in a linear regression model to predict the amplitude of OKR using stimulus area, direction of motion and stimulus type as predictors. The resulting model was not significant ($F(3, 287) = 1.485$, $p = .219$).

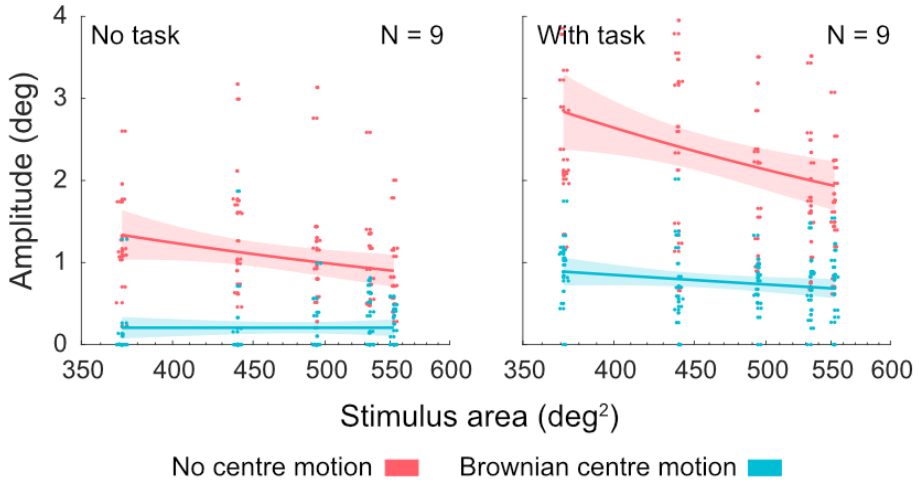

Figure 4.39: N = 9. Amplitude obtained in response to a Surround (Part 1) stimulus (red) or a C/S Brownian stimulus (Part 3) (blue). Data points indicate mean amplitude in a single trial, with a horizontal jitter of 6 deg applied. The shaded area indicates the 95% CI of the fitted function. Note that Part 1 (red) data includes P2, who is replaced by P10 in Part 3 (blue).

Part 3: Summary of key findings

- Again, increasing surround stimulus area did not increase gain in response to the periphery
- The impact of Brownian motion on OKR measures was comparable to that of opposing motion
- Attention to the surround was not required to generate a peripheral OKR in the presence of incongruent central motion
- OKR measures were again enhanced by attending to the stimulus

4.6 Individual analyses

To address concerns of individual differences in performance across conditions, further analysis was conducted at the individual level. Regression analyses were repeated on individual participants to assess the consistency of the observed effects across individuals. Such analyses only included participants who completed all three parts of the experiment (i.e. participants P2 and P10 were not included).

4.6.1 Gain in response to centre and surround stimulus regions

First, responses to centre and surround regions of stimuli were modelled separately to investigate the extent to which stimulus area and counting task condition impacted each participant in response to central or peripheral stimuli. As gain forms the most objective variable by providing a measure of tracking 'quality' and is the variable of primary interest in these experiments, only gain was considered in this analysis.

Linear regression models were calculated for participants P1, P3, P4, P5, P6, P7, P8 and P9 using stimulus area, motion direction and counting task condition as predictors of OKR gain in response to a centre stimulus (Centre (C) or central region of C/S stimulus). Significant regression equations were found in the prediction of gain in response to the centre for all participants (P1: ($F(3, 83) = 30.051$, $p < .001$, adjusted $R^2 = .512$); P3: ($F(3, 83) = 57.011$, $p < .001$, adjusted $R^2 = .669$); P4: ($F(3, 83) = 27.461$, $p < .001$, adjusted $R^2 = .489$); P5: ($F(3, 83) = 44.468$, $p < .001$, adjusted $R^2 = .611$); P6: ($F(3, 83) = 27.398$, $p < .001$, adjusted $R^2 = .400$); P7: ($F(3, 83) = 37.873$, $p < .001$, adjusted $R^2 = .482$); P8: ($F(3, 83) = 33.681$, $p < .001$, adjusted $R^2 = .452$); P9: ($F(3, 83) = 23.913$, $p < .001$, adjusted $R^2 = .366$)). The results of these analyses are summarised in Table 4.28. Results showed that increasing the area of a central stimulus and using the counting task significantly increased OKR gain in every participant. Motion direction significantly predicted gain in five participants, all of whom showed a preference for motion in the temporonasal direction (leftward motion, right eye recorded: P3, P4, P7, P9; rightward motion, left eye recorded: P5).

Table 4.28

Results of linear regression models to predict OKR gain in response to central (Centre (C) or central region of C/S) stimuli in eight individual participants using stimulus area, motion direction and task condition as predictor variables.

P1 Gain	β	SE	F	*p*
Intercept	0.7267	0.026	28.194	< .001*
Area	0.0006	0.0006	8.964	< .001*
Direction	0.0142	0.023	0.626	.533
Task	0.0751	0.023	3.245	.002*
P3 Gain	β	SE	F	*p*
Intercept	0.5546	0.025	21.969	< .001*
Area	0.0007	0.0001	11.179	< .001*
Direction	0.1185	0.022	5.324	< .001*
Task	0.1004	0.023	4.428	< .001*
P4 Gain	β	SE	F	*p*
Intercept	0.6481	0.029	22.530	< .001*
Area	0.0005	0.0001	7.104	< .001*
Direction	0.0835	0.025	3.292	.001*
Task	0.1222	0.026	4.729	< .001*
P5 Gain	β	SE	F	*p*
Intercept	0.5223	0.032	16.079	< .001*
Area	0.0007	0.0001	8.845	< .001*
Direction	-0.0806	0.029	-2.814	.006*
Task	0.2056	0.029	7.046	< .001*
P6 Gain	β	SE	F	*p*
Intercept	0.6827	0.034	19.837	< .001*
Area	0.0007	0.0001	8.461	< .001*
Direction	-0.0584	0.031	-1.895	.061
Task	0.0873	0.031	2.805	.006*
P7 Gain	β	SE	F	*p*
Intercept	0.5329	0.029	18.177	< .001*
Area	0.0007	0.0001	9.713	< .001*
Direction	0.0993	0.026	3.778	< .001*
Task	0.0641	0.026	2.416	.017*
P8 Gain	β	SE	F	*p*
Intercept	0.5153	0.036	14.166	< .001*
Area	0.0008	0.0001	8.896	< .001*
Direction	0.0332	0.033	1.019	.310
Task	0.1557	0.033	4.732	< .001*
P9 Gain	β	SE	F	*p*
Intercept	0.4185	0.042	10.066	< .001*
Area	0.0007	0.0001	7.190	< .001*
Direction	0.1162	0.037	3.120	.002*
Task	0.1257	0.038	3.343	.001*

Table 4.29

Results of linear regression models to predict OKR gain in response to surround (Surround (S) or surround region of C/S) stimuli in eight individual participants using stimulus area, motion direction and task condition as predictor variables.

P1 Gain	β	SE	F	*p*
Intercept	-0.0257	0.078	-0.330	.743
Area	0.0005	0.0002	3.247	.002*
Direction	-0.0328	0.046	-0.713	.479
Task	0.0761	0.047	1.603	.113
P3 Gain	β	SE	F	*p*
Intercept	0.0296	0.067	0.438	.663
Area	0.0003	0.0001	1.886	.064
Direction	0.0235	0.040	0.589	.557
Task	0.0912	0.041	2.224	.030*
P4 Gain	β	SE	F	*p*
Intercept	0.0449	0.053	0.854	.396
Area	-0.000001	0.0001	-0.007	.995
Direction	0.0441	0.031	1.420	.160
Task	0.2097	0.032	6.559	< .001*
P5 Gain	β	SE	F	*p*
Intercept	0.1479	0.066	2.250	.028*
Area	0.00004	0.0001	0.368	.714
Direction	-0.0378	0.039	-0.974	.334
Task	0.3269	0.040	8.176	< .001*
P6 Gain	β	SE	F	*p*
Intercept	0.0777	0.045	1.744	.085
Area	0.0001	0.0001	0.778	.439
Direction	-0.0654	0.024	-2.686	.009*
Task	0.0571	0.025	2.298	.024*
P7 Gain	β	SE	F	*p*
Intercept	0.0160	0.051	0.314	.755
Area	0.0001	0.0001	1.438	.154
Direction	0.0478	0.028	1.709	.091
Task	0.3052	0.029	10.706	< .001*
P8 Gain	β	SE	F	*p*
Intercept	0.1624	0.045	3.633	< .001*
Area	-0.00003	0.0001	-0.397	.692
Direction	-0.0329	0.024	-1.348	.181
Task	0.0610	0.025	2.450	.016*
P9 Gain	β	SE	F	*p*
Intercept	0.1005	0.061	1.647	.103
Area	0.0001	0.0001	0.941	.350
Direction	0.0370	0.033	1.108	.271
Task	0.1287	0.034	3.783	< .001*

This analysis was then repeated to examine gain in response to surround (Surround (S) or surround region of C/S) stimuli. Linear regression models were calculated for participants P1, P3, P4, P5, P6, P7, P8 and P9 using stimulus area, motion direction and counting task condition as predictors of OKR gain. Significant regression equations were found for all participants (P1: ($F(3, 67) = 4.367$, $p = .007$, adjusted $R^2 = .131$); P3: ($F(3, 67) = 2.810$, $p = .046$, adjusted $R^2 = .075$); P4: ($F(3, 67) = 15.056$, $p < .001$, adjusted $R^2 = .386$); P5: ($F(3, 67) = 22.599$, $p < .001$, adjusted $R^2 = .492$); P6: ($F(3, 67) = 4.296$, $p = .007$, adjusted $R^2 = .102$); P7: ($F(3, 67) = 39.353$, $p < .001$, adjusted $R^2 = .569$); P8: ($F(3, 67) = 2.713$, $p = .050$, adjusted $R^2 = .056$); P9: ($F(3, 67) = 5.338$, $p = .002$, adjusted $R^2 = .130$)). The results of these analyses are summarised in Table 4.29. In line with group analyses presented in this chapter, stimulus area was not found to significantly predict OKR gain in response to a surround stimulus in the majority of participants: only one participant (P1) showed a significant effect of stimulus area on gain, with increasing stimulus area causing an increase in gain. The counting task was found to significantly increase gain in response to a surround stimulus in all but one (P1) participant. Stimulus motion direction did not significantly predict OKR in response to a surround stimulus.

4.6.2 Overall models for individuals

Regression models were calculated for each participant to predict the gain, frequency and amplitude of the OKR. Data from all three parts of the experiment were entered into these models. Only participants that completed all three parts of the experiment were thus included (i.e. participants P2 and P10 were not included). Stimulus area, stimulus region driving the response (centre or surround), motion direction (leftward or rightward) and counting task condition were used as predictors. For participants who repeated some conditions at 30 deg/s (Part 1: P6, P7, P8 and P9), stimulus velocity was also included as a predictor.

Significant regression equations were found in the prediction of OKR gain ($F(4, 167) = 154.530$, $p < .001$, adjusted $R^2 = .786$), frequency ($F(4, 167) = 70.011$, $p < .001$, adjusted $R^2 = .623$) and amplitude ($F(4, 167) = 95.640$, $p < .001$, adjusted $R^2 = .694$) for P1 (Table 4.30). These models show that increasing the

area of the stimulus significantly increased the gain and amplitude of the OKR, whereas responses to central stimuli compared to surround stimuli were significantly higher for all three OKR measures. In this participant, only the gain of the OKR was significantly impacted by the counting task, with the task increasing gain.

Table 4.30

Results of linear regression models to predict OKR gain, frequency and amplitude in P1 using stimulus area, region, motion direction and counting task condition as predictors

P1 Gain	β	SE	F	*p*
Intercept	-0.0516	0.047	-1.089	.278
Area	0.0006	0.0001	7.499	< .001*
Stim region	0.7775	0.033	23.866	< .001*
Direction	-0.0092	0.027	-0.336	.738
Task	0.0738	0.028	2.649	.009*
P1 Frequency	β	SE	F	*p*
Intercept	0.7215	0.192	3.752	< .001*
Area	0.0003	0.0003	0.791	.473
Stim region	1.8977	0.132	14.344	< .001*
Direction	-0.1066	0.111	-0.960	.338
Task	0.1540	0.113	1.361	.175
P1 Amplitude	β	SE	F	*p*
Intercept	-0.7669	0.271	-2.827	.005*
Area	0.0044	0.0005	8.847	< .001*
Stim region	3.6227	0.187	19.406	< .001*
Direction	0.0957	0.157	0.612	.542
Task	0.2489	0.160	1.560	.121

Significant regression equations were also found for P3 in the prediction of OKR gain ($F(4, 167) = 140.970$, $p < .001$, adjusted $R^2 = .770$), frequency ($F(4, 167) = 52.647$, $p < .001$, adjusted $R^2 = .553$) and amplitude ($F(4, 167) = 93.559$, $p < .001$, adjusted $R^2 = .689$) (Table 4.31). Again, increasing stimulus area was found to significantly increase both the gain and amplitude of the OKR whereas all three measures were significantly increased by responding to a central rather than surround stimulus region. This participant showed a preference for leftward (TN) motion, with gain and amplitude both significantly increased by motion in

this direction. Finally, only the gain was significantly increased by using the counting task.

Table 4.31

Results of linear regression models to predict OKR gain, frequency and amplitude in P3 using stimulus area, region, motion direction and counting task condition as predictors

P3 Gain	β	SE	F	*p*
Intercept	-0.1012	0.045	-2.252	.026*
Area	0.0006	0.0001	7.923	< .001*
Stim region	0.7045	0.031	22.783	< .001*
Direction	0.0827	0.026	3.190	.002*
Task	0.0739	0.026	2.796	.006*
P3 Frequency	β	SE	F	*p*
Intercept	0.6101	0.191	3.187	.002*
Area	0.0002	0.0003	0.708	.480
Stim region	1.6288	0.132	12.367	< .001*
Direction	0.2018	0.110	1.827	.070
Task	0.1848	0.113	1.641	.103
P3 Amplitude	β	SE	F	*p*
Intercept	-0.6624	0.238	-2.782	.006*
Area	0.0037	0.0004	8.461	< .001*
Stim region	3.1169	0.164	19.027	< .001*
Direction	0.3153	0.137	2.295	.023*
Task	0.2407	0.140	1.718	.088

Significant regression equations were also found in the prediction of gain ($F(4, 167) = 174.260$, $p < .001$, adjusted $R^2 = .806$), frequency ($F(4, 167) = 120.560$, $p < .001$, adjusted $R^2 = .741$) and amplitude ($F(4, 167) = 98.045$, $p < .001$, adjusted $R^2 = .699$) in P4 (Table 4.32). Again, increasing stimulus area significantly increased both the gain and the amplitude whereas responding to a centre region as opposed to a surround region was associated with increases in all three OKR measures. This participant showed significantly higher gain and amplitude in response to leftward (TN) motion. Use of the counting task significantly increased all three OKR measures.

Table 4.32

Results of linear regression models to predict OKR gain, frequency and amplitude in P4 using stimulus area, region, motion direction and counting task condition as predictors

P4 Gain	β	SE	F	*p*
Intercept	-0.0524	0.043	-1.208	.229
Area	0.0004	0.0001	5.388	< .001*
Stim region	0.7164	0.030	24.011	< .001*
Direction	0.0674	0.030	2.693	.008*
Task	0.1436	0.025	5.629	< .001*
P4 Frequency	β	SE	F	*p*
Intercept	0.4030	0.115	3.500	< .001*
Area	0.0003	0.0002	1.462	.146
Stim region	1.4899	0.079	18.805	< .001*
Direction	0.0708	0.066	1.066	.288
Task	0.2897	0.068	4.277	< .001*
P4 Amplitude	β	SE	F	*p*
Intercept	-0.2098	0.297	-0.705	.482
Area	0.0027	0.0005	4.950	< .001*
Stim region	3.7758	0.205	18.457	< .001*
Direction	0.3863	0.172	2.252	.026*
Task	0.5741	0.175	3.282	.001*

Table 4.33

Results of linear regression models to predict OKR gain, frequency and amplitude in P5 using stimulus area, region, motion direction and counting task condition as predictors

P5 Gain	β	SE	F	*p*
Intercept	0.0161	0.043	0.377	.707
Area	0.0005	0.0001	6.396	< .001*
Stim region	0.5029	0.029	17.102	< .001*
Direction	-0.0594	0.025	-2.409	.017*
Task	0.2791	0.025	11.099	< .001*
P5 Frequency	β	SE	F	*p*
Intercept	1.3635	0.168	8.116	< .001*
Area	0.0003	0.0003	1.020	.309
Stim region	0.9297	0.116	8.043	< .001*
Direction	-0.0464	0.097	-0.479	.633
Task	0.5568	0.099	5.633	< .001*
P5 Amplitude	β	SE	F	*p*
Intercept	-0.0906	0.252	-0.360	.719
Area	0.0028	0.0005	6.218	< .001*
Stim region	2.2952	0.173	13.250	< .001*
Direction	-0.2990	0.145	-2.059	.041*
Task	1.0199	0.148	6.886	< .001*

Table 4.33 presents the results of significant regression models assessing the prediction of gain ($F(4, 167) = 106.860$, $p < .001$, adjusted $R^2 = .717$), frequency ($F(4, 167) = 28.065$, $p < .001$, adjusted $R^2 = .393$) and amplitude ($F(4, 167) = 56.224$, $p < .001$, adjusted $R^2 = .569$) in P5. As in previous participants, increasing stimulus area significantly increased the gain and amplitude of the OKR whereas responding to a centre region instead of a surround region was associated with significant increases in all three OKR measures. This participant showed significant higher gain and amplitude in response to rightward (TN) motion, and the counting task caused a significant increase in all three OKR measures.

Table 4.34

Results of linear regression models to predict OKR gain, frequency and amplitude in P6 using stimulus area, region, motion direction, counting task condition and motion velocity as predictors

P6 Gain	β	SE	F	*p*
Intercept	0.0373	0.042	0.883	.378
Area	0.0005	0.0001	9.501	< .001*
Stim region	0.8841	0.023	38.097	< .001*
Direction	-0.0614	0.012	-3.125	.002*
Task	0.0658	0.020	3.293	.001*
Velocity	-0.0098	0.002	-6.535	< .001*
P6 Frequency	β	SE	F	*p*
Intercept	0.3564	0.133	2.678	.008*
Area	-0.0001	0.0002	-0.368	.713
Stim region	2.1789	0.073	29.814	< .001*
Direction	-0.2053	0.062	-3.318	.001*
Task	0.3648	0.063	5.797	< .001*
Velocity	-0.0070	0.005	-1.485	.139
P6 Amplitude	β	SE	F	*p*
Intercept	-2.9003	0.372	-7.802	< .001*
Area	0.0041	0.0005	7.597	< .001*
Stim region	4.8409	0.204	23.707	< .001*
Direction	-0.2691	0.173	-1.557	.121
Task	-0.1981	0.176	-1.127	.261
Velocity	0.1011	0.013	7.673	< .001*

The remaining participants (P6, P7, P8 and P9) also completed Part 1 trials at a higher (30 deg/s) stimulus velocity, therefore velocity has been included as a predictor in the following models.

Significant regression equations were found for P6 in the prediction of gain ($F(5, 207) = 321.610$, $p < .001$, adjusted $R^2 = .886$), frequency ($F(5, 207) = 251.340$, $p < .001$, adjusted $R^2 = .858$) and amplitude ($F(5, 207) = 141.790$, $p < .001$, adjusted $R^2 = .773$) of OKR (Table 4.34). In line with previous participants, increasing the stimulus area led to a significant increase in both gain and amplitude whereas responding to a centre rather than surround stimulus region increased all three OKR measures. This participant showed significantly higher gain and frequency in response to a rightward-drifting (NT) stimulus. The counting task significantly increased both the gain and frequency of the OKR. Increasing the stimulus velocity was associated with a significant decrease in OKR gain and an increase in slow phase amplitude.

Table 4.35

Results of linear regression models to predict OKR gain, frequency and amplitude in P7 using stimulus area, region, motion direction, counting task condition and motion velocity as predictors

P7 Gain	β	SE	F	*p*
Intercept	0.0918	0.043	2.157	.032
Area	0.0006	0.0001	9.537	< .001*
Stim region	0.6258	0.023	26.783	< .001*
Direction	0.0775	0.020	3.917	< .001*
Task	0.1555	0.020	7.730	< .001*
Velocity	-0.0101	0.002	-6.680	< .001*
P7 Frequency	β	SE	F	*p*
Intercept	-0.2466	0.157	-1.567	.119
Area	0.0002	0.0002	1.079	.282
Stim region	0.8673	0.086	10.035	< .001*
Direction	0.2904	0.073	3.968	< .001*
Task	0.3219	0.074	4.325	< .001*
Velocity	0.0365	0.006	6.535	< .001*
P7 Amplitude	β	SE	F	*p*
Intercept	-2.2482	0.306	-7.337	< .001*
Area	0.0037	0.0004	8.449	< .001*
Stim region	3.6461	0.168	21.664	< .001*
Direction	0.3164	0.142	2.221	.027*
Task	0.3900	0.145	2.691	.007*
Velocity	0.0709	0.011	6.529	< .001*

Significant regression equations were found in the prediction of the gain ($F(5, 207) = 164.860$, $p < .001$, adjusted $R^2 = .798$), frequency ($F(5, 207) = 41.607$, $p < .001$, adjusted $R^2 = .495$) and amplitude ($F(5, 207) = 113.920$, $p < .001$, adjusted $R^2 = .732$) of OKR in P7 (Table 4.35). Increasing stimulus area significantly increased the gain and amplitude of the OKR, whereas responding to a centre rather than surround region significantly increased all three OKR measures. This participant showed a significant preference for leftward (TN) motion, with significantly higher gain, frequency and amplitude in this direction. Increasing the velocity of the stimulus significantly decreased the gain and increased the frequency and amplitude. Finally, the counting task significantly increased all three OKR measures.

Table 4.36

Results of linear regression models to predict OKR gain, frequency and amplitude in P8 using stimulus area, region, motion direction, counting task condition and motion velocity as predictors

P8 Gain	β	SE	F	*p*
Intercept	0.0737	0.044	1.682	.094
Area	0.0006	0.0001	9.799	< .001*
Stim region	0.7721	0.024	32.088	< .001*
Direction	0.0052	0.020	0.257	.798
Task	0.1047	0.021	5.056	< .001*
Velocity	-0.0125	0.002	-8.060	< .001*
P8 Frequency	β	SE	F	*p*
Intercept	0.3398	0.153	2.224	.027*
Area	0.0008	0.0002	3.780	< .001*
Stim region	2.0179	0.084	24.042	< .001*
Direction	-0.3649	0.071	-5.135	< .001*
Task	0.4643	0.072	6.424	< .001*
Velocity	0.0041	0.005	0.764	.446
P8 Amplitude	β	SE	F	*p*
Intercept	-1.9816	0.353	-5.616	< .001*
Area	0.0042	0.001	8.238	< .001*
Stim region	3.9517	0.194	20.388	< .001*
Direction	0.3303	0.164	2.013	.045*
Task	-0.0602	0.167	-0.361	.719
Velocity	0.0511	0.013	4.083	< .001*

Table 4.36 presents the results of significant regression models predicting the gain ($F(5, 207) = 226.200$, $p < .001$, adjusted $R^2 = .845$), frequency ($F(5, 207) = 148.860$, $p < .001$, adjusted $R^2 = .781$) and amplitude ($F(5, 207) = 94.352$, $p < .001$, adjusted $R^2 = .693$) of OKR for P8. In this participant, increasing the stimulus area significantly increased the gain, frequency and amplitude of the OKR. Responding the centre rather than to the surround also significantly increased all three measures. The counting task significantly increased the gain and the frequency. Increasing the stimulus velocity reduced the gain but increased the amplitude and frequency of the OKR. This participant did not show a preference for either motion direction in terms of gain, however, leftward (TN) motion produced an OKR with a lower beat frequency and a higher slow phase amplitude.

Table 4.37

Results of linear regression models to predict OKR gain, frequency and amplitude in P9 using stimulus area, region, motion direction, counting task condition and motion velocity as predictors

P9 Gain	β	SE	F	*p*
Intercept	0.2027	0.044	4.568	< .001*
Area	0.0006	0.0001	10.083	< .001*
Stim region	0.6208	0.024	25.478	< .001*
Direction	0.0827	0.021	4.008	< .001*
Task	0.1080	0.021	5.147	< .001*
Velocity	-0.0182	0.002	-11.564	< .001*
P9 Frequency	β	SE	F	*p*
Intercept	0.2214	0.207	1.070	.286
Area	0.0010	0.0003	3.250	.001*
Stim region	1.4642	0.114	12.883	< .001*
Direction	0.1543	0.096	1.604	.110
Task	0.7009	0.098	7.161	< .001*
Velocity	0.0135	0.007	1.841	.067
P9 Amplitude	β	SE	F	*p*
Intercept	-0.9769	0.286	-3.416	< .001*
Area	0.0037	0.0004	8.930	< .001*
Stim region	2.6796	0.157	17.058	< .001*
Direction	0.4239	0.133	3.187	.002*
Task	0.1583	0.135	1.171	.243
Velocity	0.0048	0.010	0.475	.635

Finally, significant regression equations were found for P9 in the prediction of OKR gain ($F(5, 207) = 155.920$, $p < .001$, adjusted $R^2 = .789$), frequency ($F(5, 207) = 47.529$, $p < .001$, adjusted $R^2 = .529$) and amplitude ($F(5, 207) = 61.723$, $p < .001$, adjusted $R^2 = .595$) (Table 4.37). Increasing stimulus area once again increased the gain and amplitude of the OKR, in addition to the frequency, whereas responding to a central stimulus instead of a surround stimulus significantly increased all three OKR measures. This participant showed a significant effect of motion direction, with higher gain and amplitude in response to leftward (TN) motion. Increasing stimulus velocity decreased the gain, but not the amplitude or frequency, whereas the counting task significantly increased the gain and frequency, but not the amplitude.

4.6.3 Impact of incongruent motion

To investigate the impact of incongruent (opposing or Brownian) motion at the individual level, further regression models were calculated to test whether the presence of incongruent motion in the surround impacted responses to the centre, and whether the presence of incongruent centre motion impacted responses to the surround, in each participant that completed all three parts of the experiment. This involved calculating models for the response to the centre, which assessed whether stimulus type (Centre (C), C/S Opposing and C/S Brownian) impacted the gain of the OKR. Similar models were then calculated to assess effects of central motion in response to the surround.

Regression modelling carried out separately on the central OKR gain of P1 ($F(3, 47) = 16.003$, $p < .001$, adjusted $R^2 = .489$), P3 ($F(3, 47) = 15.964$, $p < .001$, adjusted $R^2 = .489$), P4 ($F(3, 47) = 10.204$, $p < .001$, adjusted $R^2 = .370$), P5 ($F(3, 47) = 14.154$, $p < .001$, adjusted $R^2 = .456$), P6 ($F(3, 47) = 20.931$, $p < .001$, adjusted $R^2 = .560$), P7 ($F(3, 47) = 12.790$, $p < .001$, adjusted $R^2 = .429$), P8 ($F(3, 47) = 11.206$, $p < .001$, adjusted $R^2 = .394$) and P9 ($F(3, 47) = 23.994$, $p < .001$, adjusted $R^2 = .595$) revealed that the presence of opposing motion in the surround significantly reduced the gain in response to the centre only in P5 ($\beta = -0.105$, $p = .015$), whereas the presence of Brownian motion in the surround significantly reduced gain in response to the centre in P5 ($\beta = -0.146$, $p = .001$) and P9 ($\beta = -0.160$, $p < .001$).

Regression modelling carried out separately on the gain of OKR in response to the surround in P1 ($F(3, 29) = 35.197$, $p < .001$, adjusted $R^2 = .780$), P3 ($F(3, 29) = 21.847$, $p < .001$, adjusted $R^2 = .683$), P4 ($F(3, 29) = 13.051$, $p < .001$, adjusted $R^2 = .555$), P5 ($F(3, 29) = 19.894$, $p < .001$, adjusted $R^2 = .662$), P6 ($F(3, 29) = 35.076$, $p < .001$, adjusted $R^2 = .779$), P7 ($F(3, 29) = 4.413$, $p = .012$, adjusted $R^2 = .261$), P8 ($F(3, 29) = 10.395$, $p < .001$, adjusted $R^2 = .493$) and P9 ($F(3, 29) = 79.309$, $p < .001$, adjusted $R^2 = .890$) revealed that the presence of opposing motion in the centre significantly reduced gain in response to the surround in P1 ($\beta = -0.222$ $p < .001$), P3 ($\beta = -0.358$ $p < .001$), P4 ($\beta = -0.208$ $p < .001$), P6 ($\beta = -0.305$ $p < .001$), P7 ($\beta = -0.126$ $p = .044$), P8 ($\beta = -0.197$ $p < .001$) and P9 ($\beta = -0.519$ $p < .001$), whereas the presence of Brownian motion in the centre significantly reduced surround gain in P1 ($\beta = -0.402$ $p < .001$), P3 ($\beta = -0.253$ $p < .001$), P4 ($\beta = -0.277$ $p < .001$), P5 ($\beta = -0.329$ $p < .001$), P6 ($\beta = -0.219$ $p < .001$), P7 ($\beta = -0.216$ $p = .001$), P8 ($\beta = -0.117$ $p = .010$) and P9 ($\beta = -0.333$ $p < .001$).

4.6.4 Summary of consistent effects across individuals

The above models showcase the consistency of certain effects across participants. As shown in Table 4.28, responses to central stimuli were characterised by a consistent effect of stimulus area on gain. An increase in stimulus area yielded an increase in gain in every participant, with β-coefficients ranging from 0.0005 to 0.0008. Increasing attention to the stimulus by using the counting task also significantly increased gain in every participant, with β-coefficients ranging from 0.0641 to 0.2056. Adjusted R^2 values showed moderate strength of the models, with values ranging from .366 to .669, suggesting that the models were able to account for 36.6-66.9% of the variability in OKR gain in response to central stimuli, depending on participant. This highlights that, while there are individual differences in performance, the observed patterns show high consistency across individuals.

Models examining gain in response to surround stimuli (Table 4.29) were weaker and showed more variability when compared with models for central stimuli, with adjusted R^2 values ranging from .056 to .569, indicating that these

models accounted for 5.6-56.9% of the variability in gain in response to a surround stimulus, depending on participant. This highlights greater individual differences in performance when compared to OKR in response to central stimuli. Despite this, the observed patterns remain consistent: increasing stimulus area does not significantly increase gain in response to a surround stimulus, whereas using the counting task does increase gain. Only one participant (P1) was an outlier in these effects.

When examining the gain, frequency and amplitude across the whole experiment for each participant, consistencies in patterns once again emerged. Models were moderate to strong, with adjusted R^2 values ranging from .393 to .886, indicating that the models are able to account for 39.3-88.6% of the variability in gain, frequency or amplitude of the OKR. Models predicting gain produced the highest adjusted R^2 values, with a mean of .800 (range: .717 to .886); this was followed by models predicting amplitude, with a mean adjusted R^2 of .701 (range: .569 to .736); models predicting OKR frequency produced the lowest adjusted R^2 values, with a mean of .663 (range: .393 to .858) Every participant showed a pattern whereby increasing stimulus area increased the gain and amplitude, but not the frequency, of the OKR. Stimulus region (centre vs surround) was shown to significantly affect all three measures, with central stimuli producing significantly higher gain, frequency and amplitude. The counting task increased gain in all participants, whereas its effects on frequency and amplitude were more varied. All but two participants showed a significant increase in frequency as a result of the counting task, whereas the counting task increased OKR slow phase amplitude in three participants. In the four participants who completed Part 1 conditions at a higher (30 deg/s) velocity, this higher stimulus velocity was associated with reduced OKR gain in all four participants and increased slow phase amplitude in three (P6, P7, P8) participants, whereas frequency was only affected by stimulus velocity in P7, with higher velocity causing higher OKR beat frequency. Stimulus motion direction produced variable effects, with P1 showing no effect, P6 showing higher gain in the nasotemporal direction, and P3, P4, P5, P7 and P9 showing higher gain in the temporonasal direction. P6 and P8 had higher NT frequency whereas P7 had higher TN frequency. P3, P4, P5, P7, P8 and P9 all exhibited higher TN slow phase amplitude.

The impact of incongruent motion in the complementary region of the C/S stimulus on OKR gain was also assessed via individual regression models. This showed that, in response to the centre, the majority of participants' gain was unaffected by the presence of incongruent motion in the surround, with only P5 and P9 presenting exceptions. The impact of incongruent central motion in response to the surround was found to be much more consistent, with gain being significantly reduced in all participants during C/S stimuli compared to Surround (S) stimuli.

4.7 General results

4.7.1 Eccentricity effects in OKR: The role of attention

One purpose of these experiments was to assess whether directing attention to the visual periphery is sufficient to raise the gain of the OKR to the level of the centre; this would indicate that eccentricity effects seen in OKR may be a consequence of attention. The results of Part 1 showed that the effect of the counting task on gain was significantly larger in response to Surround (S) stimuli than Centre (C) stimuli. However, this increase was not sufficient to raise gain in response to the surround to the level of gain in response to the centre during any of the presented stimulus configurations. Looking at trials in which a counting task was used, gain in response to the centre ($M = 0.855$, $SD = 0.198$) remains significantly higher than gain in response to the surround ($M = 0.275$, $SD = 0.188$) ($t(938) = 45.614$, $p < .001$).

4.7.2 Accuracy in the counting task

Analysis was carried out to assess whether the proportion of trials in which a correct response was provided to the counting task differed between centre and surround presentation of the task, and whether gain, frequency and amplitude of the OKR were affected by accuracy. Many participants reported difficulty in discriminating between certain pairs of colours during the counting task, namely yellow and orange. For this reason, responses to the task were

considered 'correct' when they were within one of the true answer (i.e. with five colours presented, answers ranging from 4-6 were marked as correct).

Of the 522 trials that involved presentation of the counting task to a Centre (C) stimulus or to the centre region of a C/S Opposing or C/S Brownian stimulus, an incorrect response was provided in just seven (1.34%) trials across a range of participants and stimulus configurations. Considering the low number of trials in which an incorrect response was provided, it is not possible to accurately assess whether this was associated with lower gain, frequency or amplitude compared to trials in which a correct response was provided.

Of the 418 trials that involved presentation of the counting task to a Surround (S) stimulus or to the surround region of a C/S Opposing or C/S Brownian stimulus, an incorrect response was provided in 33 (7.89%) trials. Of these trials, only two involved presentation of a C/S Opposing stimulus, nine involved presentation of a Surround (S) stimulus, and the remaining 22 involved presentation of a C/S Brownian stimulus. Despite an incorrect response to the counting task, OKR in response to the surround still occurred in 31 (93.94%) of the 33 trials. To assess whether correct responses were associated with differences in gain, frequency or amplitude, t-tests were carried out. Only C/S Brownian stimuli presenting coherent motion to the surround were used, as these trials presented the highest rate of incorrect responses. No significant difference was found in the gain ($t(142) = -0.815$, $p = .417$), frequency ($t(142) = -1.741$, $p = .083$) or amplitude ($t(142) = -1.787$, $p = .076$) of correct and incorrect C/S Brownian trials.

4.8 Discussion

4.8.1 Effect of stimulus area in the centre and periphery

Previous work has consistently reported that increasing the area of a stimulus is associated with higher OKR gain. Across all stimuli, this effect was confirmed in response to central motion. However, this relationship between area and gain was not reflected in the response to peripheral stimulation. In fact, Surround (S) stimuli (Part 1) were associated with a decrease in gain as the area of the stimulus increased. It seems likely that this effect results from the proximity

of the edge of the central mask to the fovea; larger surround stimuli were created by using a smaller central mask diameter, meaning that larger stimuli were less eccentric. The mask may have created a stationary luminance edge which suppressed gain (Howard & Gonzalez, 1987), despite the edge being blurred. C/S stimuli lacked this edge by having a consistent density of moving dots across the entire stimulus. In response to C/S Brownian stimuli, there was no relationship between stimulated area and gain in response to the surround.

While van Die and Collewijn (1982) reported that progressively masking the periphery does not impact gain as long as the centre remains stimulated, analyses in Part 1 (Figure 4.5) showed that significant increases in gain occur beyond a stimulus area of 283.53 deg^2 (radius = 9.5 deg) indicating that gain is not at maximum until peripheral stimulation is included, particularly in response to higher stimulus velocity. At a dot speed of 30 deg/s, gain obtained in response to the largest stimulus tested (radius = 13.5 deg) with the counting task was 0.919 (SD = 0.074) and without the counting task was 0.792 (SD = 0.147), demonstrating that slow phase velocity did not reach stimulus velocity even in response to a 572.56 deg^2 stimulus. The stimulated area required to produce a gain of ~1.0 may therefore depend on both the velocity of the stimulus and the attentional state of the observer. It appears that stimulation of the periphery plays an important role in determining the overall gain of the response, though area becomes less important when central stimulation is removed.

In response to central stimulation, increases in area were associated with higher slow phase amplitude. However, the reverse was seen in the response to the surround, with larger stimuli being associated with smaller slow phase amplitude. This is likely related to the stimulus configuration; larger surround regions were associated with smaller central regions within which participants were required to maintain gaze. Larger surround stimuli were therefore more restrictive in terms of the region in which participants could move their eyes, which may have limited slow phase amplitude. The relationship between peripheral stimulus area and OKR amplitude should thus be investigated using a different stimulus configuration. For example, rather than using a peripheral stimulus with an annular shape, one could present a stimulus above or below the central visual field (see 'experiment 1' of Kanari and Kaneko (2017)) while varying stimulus area.

It should be noted that the area of Surround (S) stimuli and surround regions of C/S stimuli were linked to their eccentricity, with larger stimuli being less eccentric. This was due to the way stimuli were configured: stimulated peripheral area was reduced by increasing the diameter of the centre/mask, thus increasing the eccentricity of the inner edge of the annular surround region. It is therefore possible that results regarding the effect of area in response to surround stimuli have been affected by this variation in eccentricity. To further explore this, stimuli could be developed that vary the area of the stimulus while maintaining a consistent eccentricity, and stimuli of the same area could be tested across a range of eccentricities. The latter will be the focus of Experiment 3: the effect of stimulus eccentricity on the OKR will be more precisely investigated while stimulus area is held constant.

4.8.2 Effect of occluding the centre

Occlusion of the central visual field reduces OKR gain (Cheng & Outerbridge, 1975; Howard & Ohmi, 1984; Valmaggia et al., 2001; van Die and Collewijn, 1982, 1986). The results of the present study are in agreement with this, showing reduced gain as a result of central masking. However, while some studies (Howard & Ohmi, 1984; Valmaggia et al., 2001) have reported that the detrimental effects of occlusion of the centre only occur in response to stimulus velocities exceeding 30 deg/s, the present study (Part 1) demonstrated that this is the case for slower (15 deg/s) stimuli. This effect occurred even with very small occlusions; while Valmaggia et al. (2001) reported that only patients with scotomas larger than 20 deg were affected, the present study found that a central mask just 5 deg in diameter was sufficient to disrupt the OKR and reduce gain. It may be the case, however, that OKR is affected differently by simulated occlusions and pathological scotoma, with simulated occlusions causing a more dramatic effect on gain due to patients' ability to 'fill in', resulting in a milder effect (Valmaggia & Gottlob, 2002). The present data are in agreement with those of van Die and Collewijn (1982) who reported that removing a central patch 5 deg across markedly lowered gain across a broad range of stimulus velocities (6-180 deg/s). Combined with the effects of stimulus area in the centre and the periphery, these findings indicate that while increasing the stimulated area from the

centre outwards is associated with a steady increase in gain until the image is stabilised on the retina (i.e. until a gain of ~1.0), removing stimulation from the centre results in a fixed drop in gain that is largely invariant to the size of the occlusion. This suggests that even a small loss of sensitivity in the central visual field can have a dramatic effect on the ability to stabilise the retinal image, which in turn may reduce visual clarity of patients with central vision loss in the presence of large field visual motion, such as that induced while moving through an environment, by increasing motion smear. However, studies such as that of Valmaggia and Gottlob (2002) suggest that in patients, these effects may be less severe than predicted by simulated occlusion.

4.8.3 Effect of attention in the centre and periphery

Across all stimuli tested, increasing attention towards the stimulus increased gain. After retinal location (centre or surround stimulation), this was found to be the largest determinant of gain, frequency and amplitude. That the counting task was able to increase the response to the centre suggests that attention to the central stimulus was not fully saturated during passive viewing. Directing attention towards the periphery facilitated OKR to be produced in response to peripheral stimulation, even in the presence of incongruent central motion. This finding agrees with that of Kanari et al. (2017), corroborating the claim that results of previous studies (e.g. Abadi & Pascal, 1991; Howard & Gonzalez, 1987), showing that OKR in response to the periphery is prevented by motion in the centre, may have been a consequence of insufficient attention being directed towards the visual periphery. However, the attended stimulus did not solely drive OKR in some cases. For example, a direction-changing OKR that alternated between responding to the centre and to the periphery was sometimes observed during C/S Opposing conditions involving attention directed to the surround (Figure 4.24, lower). This could reflect fluctuations in observers' attention throughout the trial. Alternatively, it may indicate a state in which the weighting of each region in its contribution to the OKR is approximately equal, resulting in an alternating response as each region competes for access to oculomotor control, demonstrating a form of OKR rivalry between the centre and periphery. Under normal viewing conditions, the centre appears to be more highly weighted

in the response; however, attention is able to reweight the contribution of each region to the OKR. If attention is directed towards the visual periphery, the reweighting can be sufficient to cause the periphery to be prioritised in driving the response. By using a Brownian stimulus surrounded by coherent motion, the results of Part 3 confirm that directing attention towards the periphery is not a requirement to produce a peripheral OKR in the presence of incoherent central motion.

A key interest in this experiment was to assess whether attentional modulation was able to raise peripheral OKR measures to the level of the centre; such an outcome would indicate that eccentricity effects in OKR (Abadi & Pascal, 1991; Cheng & Outerbridge, 1975; Howard & Ohmi, 1984; Murasugi et al., 1986; van Die & Collewijn, 1982) are a result of attentional differences across the visual field rather than being a consequence of structural differences. While the counting task had a significantly larger impact on gain and amplitude in response to the periphery compared to the centre, this was not sufficient to bring these parameters to the level of the central response; the gain, frequency and amplitude of the OKR remained higher in response to central stimulation. The greater impact of attention on the peripheral response indicates that part of the eccentricity effect in OKR may be due to less attention being naturally deployed to the periphery; however, the large residual difference in gain between the centre and periphery indicates that the eccentricity effect seen is largely due to anatomy. It should be noted that the error rate exhibited during the counting task was higher when presented in the surround compared to the centre, indicating greater difficulty in completing the task peripherally. This may be due to the use of colour in the task, as there is reduced colour sensitivity in more eccentric regions of the visual field (Hansen et al., 2009; Mullen, 1991; Newton & Eskew, 2003). Alternatively, this effect may reflect a difficulty in directing visual attention towards peripheral visual field regions.

While directing attention towards a region of the stimulus increased the response to that region, taking attention away from a region of the stimulus had the opposite effect. During C/S Opposing stimuli with the counting task presented to the surround, a response to the centre still occurred in many cases (Figure 4.24, lower); this either represented a non-attention or divided attention condition, depending on the observer's ability to disengage attention from the

centre. Analysis showed that the largest determinant of gain, frequency and amplitude in response to the centre was the counting task location; removing attention from the centre significantly lowered all three OKR parameters. This indicates that the gain, frequency and amplitude of the central OKR are all affected by the level of endogenous attention of the observer and are therefore at least partially mediated by top-down processes. This result is in contrast with that of Frattini and Wibble (2021), who found that divided attention conditions resulted in an increase in gain; they asserted that this was indicative of gain being related to the alertness of the observer. The present study instead found that gain was higher when attention was focussed on the centre rather than divided between the centre and the surround.

Regardless of task location, increasing the area of the stimulus significantly increased both the gain and amplitude of the central OKR, indicating a role of bottom-up processes in driving these parameters, as this pattern was seen regardless of the direction of attention. The frequency of the OKR, on the other hand, was found to be related only to the task use or location, suggesting that this parameter may be more strongly linked to the level of endogenous attention of the observer, and therefore may be driven by top-down processes. This link between OKR frequency and attention level is in agreement with Frattini and Wibble's (2021) findings. It should be noted that there were individual differences in the extent to which the OKR followed the centre or the surround during C/S Opposing conditions with the counting task in the surround. Figure 4.24 shows the response from two participants: in the upper plot, the response consistently follows the surround; in the lower plot, the response alternates between following the centre and the surround. Further, figures 4.25, 4.27 and 4.29 show that one participant (P6) exhibited no OKR in response to the surround during C/S Opposing conditions, despite showing a response during Surround and C/S Brownian conditions. Such individual differences between participants may be a consequence of differences in the ability to direct covert visual attention to peripheral regions in the presence of a central optokinetic stimulus. However, that P6 correctly responded to the counting task on every C/S Opposing trial indicates that they were able to direct sufficient attention to the surround to carry out the task, despite their OKR consistently following the direction of the centre. It may be the case that the task was simply too easy for this participant, causing

them to perform at ceiling despite following the centre. It should be noted that participant P6 does exhibit an ocular pathology in the right eye, therefore it cannot be ruled out that this pathology has contributed to this outcome, though their performance was comparable to other participants in all other domains.

The possibility that the use of the counting task caused a shift from 'stare' OKR to 'look' OKR was considered, as look OKR is associated with higher OKR gain and amplitude. The counting task may have shifted the OKR type being exhibited by observers, and this shift may account for the observed difference in gain, frequency and amplitude. However, while look OKR is described as involving a foveal tracking system based on position of individual stimulus features, stare OKR is described as being based on stimulus velocity rather than position (Pola & Wyatt, 1985). By this account, look OKR necessitates foveation of the stimulus features, and a peripheral stimulus should therefore not elicit look OKR. In the present study, the counting task did increase the amplitude of the slow phase, but this occurred in response to both central and peripheral stimuli. It is therefore unlikely that the increase in amplitude seen in response to a peripheral stimulus can be attributed to a shift to look OKR. In response to the centre, mean amplitude during trials that did not use the counting task was 3.76 deg, increasing to 3.97 deg when the counting task was used. This small increase is less than would be expected from a shift from stare to look OKR; the amplitude of look OKR is often reported as being at least double that of stare OKR (Knapp et al., 2008, 2009; Valmaggia et al., 2005). Taken together, this indicates that it is unlikely that the effects seen here were a result of the counting task causing a shift towards look OKR.

The possibility that the effect of attention on gain was a consequence of an attention-based increase in perceived velocity was also explored. Turatto et al. (2007) showed that the perceived speed of a motion stimulus was increased by attending to the stimulus. However, they found a modest perceived speed increase of 0.50 deg/s, whereas the increase in slow phase velocity generated by the counting task was substantially higher in the present study. For example, during Part 1, the mean increase in slow phase velocity by the counting task in response to the Surround (S) stimulus was 3.15 deg/s. It is therefore unlikely that the increase in gain resulting from the counting task can be solely attributed to an increase perceived speed of the motion stimulus.

4.8.4 Effect of incongruent motion

Both the response to the centre and to the surround were impacted by the presence of incongruent motion in the complementary region, with responses to the surround being particularly affected by central motion. This finding is in contrast with that of Kanari et al. (2017), who reported no suppressive effect of incongruent motion. Looking at stimuli presented at a velocity of 15 deg/s, and excluding the largest stimulus size which was unique to the Centre (C) stimulus, mean gain in response to the centre during trials using the counting task was 0.906 (SD = 0.165) in the absence of surround motion, 0.874 (SD = 0.154) in the presence of Brownian surround motion, and 0.807 (SD = 0.206) in the presence of opposing surround motion. This indicates that the presence of incongruent motion in the surround impacts the OKR in response to the centre, even when the incongruent motion is not a competing optokinetic stimulus. However, it should be noted that this effect appears to have been largely driven by a subset of two participants (P5 and P9), as individual regression analyses indicated that the majority of participants showed no significant effect of incongruent motion on gain in response to the centre (though these analyses excluded P2 and P10).

The impact of incongruent central motion on the response to the surround was more than double that of the effect on the centre, and individual analyses showed that this effect was present in every participant. Looking at stimuli presented with a velocity of 15 deg/s, and only including the shared area range across surround regions, mean gain in response to the surround region during trials using the counting task was 0.387 (SD = 0.178) with no motion in the centre, 0.232 (SD = 0.121) in the presence of central Brownian motion, and 0.213 (SD = 0.203) in the presence of opposing motion in the centre. This supports the assertion that central motion is more heavily weighted in the OKR. One possibility is that central motion falls within the integration zone for visual motion estimation while viewing a central stimulus (Watamaniuk & Sekuler, 1992), whereas motion in surround regions may sometimes fall beyond this zone. Watamaniuk and Sekuler (1992) estimated the spatial integration limit for random-dot kinematograms to be at least 63 deg^2 (diameter: 9 deg); only two central stimuli smaller than this size were used. As a result, motion in central areas of the visual field may contribute more towards estimates of retinal slip that are used to calculate slow phase velocity. However, in this case we would expect to

see a larger impact of opposing motion compared to Brownian motion due to Brownian motion containing no net directional information, thus not contributing a directional global motion signal to estimations of visual motion; the results of Part 3 showed that this was not the case, as Brownian and opposing motion did not differ significantly in their impacts on the OKR. Possible explanations of this suppressive effect of incongruent motion will be explored in detail the General Discussion (Chapter 6).

The results of Experiment 2 indicate that despite the reflexive nature of the OKR, top-down factors such as endogenous visual feature and spatial attention have a powerful ability to modulate the response. Such factors should thus be carefully considered when using OKR as a means of objective testing. The implications of these findings for the use of OKR as a no-report measure in clinical and research settings will be considered in the General Discussion (Chapter 6).

Chapter 5

Experiment 3: The effect of eccentricity and attention on HOKR and VOKR

5.1 Introduction

Experiment 1 presented evidence of vertical OKR asymmetry whereby upward gain was higher than downward gain. This effect was present in look OKR in response to all tested stimulus velocities (10-40 deg/s). Superior response to upward motion is thought to result from a greater number of cells in regions such as the terminal nuclei of the AOS being tuned for upward motion compared to downward motion (in monkeys: Mustari et al., 1988) and upward-selective cells in these regions being tuned to higher velocities than downward-selective cells (in cats: Grasse et al., 1984). In humans, Murasugi and Howard (1989b) showed that this vertical asymmetry in the OKR may be limited to peripheral stimulation. A central strip (10x6 deg in size) produced an OKR with no vertical asymmetry, whereas peripheral stimulation resulted in reduced downward gain. From this, they concluded that asymmetrical vertical OKR is limited to the peripheral response, which they argued provided evidence that the asymmetry resides within the LOKR system. In the following chapter, this assertion will be investigated; various visual field regions will be selectively stimulated with upward and downward motion in order to assess the role of eccentricity in vertical OKR asymmetry, and the impact of stimulus eccentricity on the OKR more generally.

Asymmetry in visual performance is also reported between the upper and lower visual hemifields with superior thresholds in response to stimuli presented to the lower visual hemifield. Cone and ganglion cell density are higher in the upper hemiretina (Curcio et al., 1990; Curcio & Allen, 1990) and this asymmetry extends into extrastriate areas, including the dorsal pathway (Rossit et al., 2013). The lower visual field is associated with shorter reaction times (Payne, 1967),

higher visual acuity (Millodot & Lamont, 1974), higher temporal resolution (Tyler, 1987), superior colour sensitivity (Levine & McAnany, 2005) and superior motion processing (Lakha & Humphreys, 2005). In the upper hemifield, a greater impact of attention on visual performance has been reported by Kristjánsson and Sigurdardottir (2008), who suggested that visual field regions of lower performance benefit more from increased visual attention. Upper and lower visual hemifield asymmetry has also been reported in OKR. Murasugi and Howard (1989a) reported that all five of their observers produced higher gain OKR in response to stimuli presented in the lower visual field. In the following chapter, upper-lower visual hemifield asymmetry in OKR gain, frequency and amplitude will be assessed, in addition to the way in which the upper and lower hemifields are impacted by attention as manipulated by use of a counting task.

Visual performance is often reported to be better along the horizontal meridian than the vertical meridian, an effect known as horizontal-vertical anisotropy (Barbot et al., 2021). The bias towards the horizontal meridian is already apparent in the retina, where the corresponding region contains a particularly high density of photoreceptors (Curcio et al., 1990). Asymmetries in performance across the visual field are known as 'performance fields' (Altpeter et al., 2000; Mackeben, 1999) and are sometimes attributed to effects of attention, though studies which have involved manipulating visual attention have shown that performance fields are similarly modulated across isoeccentric locations, leading to a uniform boost in performance without affecting the overall shape of the performance field (Purokayastha et al., 2021; Roberts et al., 2018). In the following chapter, stimuli will be presented at various locations around the visual field, including locations along the vertical and horizontal meridians. This will allow for comparison of OKR characteristics on and off the cardinal meridians to be assessed, and allow examination of whether OKR gain, frequency and amplitude are enhanced in response to stimuli presented along the horizontal meridian. Additionally, the influence of attentional manipulation on OKR parameters will be assessed across the visual field to examine the uniformity of its impact on the OKR. The results of Experiment 2 revealed a greater effect of attention on OKR in response to a peripheral stimulus. It is anticipated that, rather than seeing a uniform boost in performance as has been reported in the performance field

literature, a correlation between the effect of attention on OKR and eccentricity will be observed.

In agreement with past research (e.g. Valmaggia et al., 2005), Experiment 1 showed that gain in response to central vertical motion was lower than that in response to horizontal motion. In the following chapter, horizontal and vertical motion will be presented across the visual field, allowing the difference in response to the two axes of motion to be assessed as a function of stimulus eccentricity. In this way, it will be possible to ascertain whether this difference in response to vertical and horizontal motion is limited to any particular region of the visual field.

Experiment 2 showed that peripheral OKR was reduced compared to central stimulation, and although attention was able to enhance the response, it was not sufficient to improve it to the level of the centre. From this, it was inferred that lower gain OKR in response to peripheral stimuli is largely a result of anatomical differences between the centre and the periphery. However, eccentricity was not precisely manipulated in Experiment 2, therefore inferences about eccentricity beyond a centre-periphery distinction were not made. In the following chapter, eccentricity will be manipulated by presenting stimuli to various visual field locations while asking participants to hold fixation at the centre of the display. This will allow the impact of attention to be assessed as a function of eccentricity. In this way, it will be possible to investigate whether more eccentric regions are associated with a greater performance boost as a consequence of attention.

5.2 Methods

5.2.1 Participants

This experiment used nine participants (four female, five male) with an age range of 23-55 years old (M = 32.89 years). Participants were staff and students at the University of Nottingham. All participants had normal vision.

5.2.2 Stimuli

Stimuli were random-dot kinematograms presented with gaussian windows (Figure 5.1) presenting against a grey (94.8lm) background. Gaussians were 10 deg in diameter and had a standard deviation of 0.5. Dots were 11 pixels in size (diameter ~4 pixels) and had an overall density of 1.17 dots/deg^2. During counting task trials, black (0.38lm) (task-irrelevant) dots had a density of 0.94 dots/deg^2 while coloured (task-relevant) dots had a density of 0.23 dots/deg^2. Dots drifted at a velocity of 15 deg/s and were presented for a duration of 20 seconds. Dot motion was either vertical (up/down) or horizontal (left/right). Stimuli were presented at 27 locations across the visual field. With the centre of the display as x = 0 deg, y = 0 deg, stimuli were presented at horizontal (x) locations of ±18.81, ±14.11, ±9.41, ±4.70 and 0 deg, and at vertical (y) locations of ±8.26, ±4.13 and 0 deg. Stimuli were therefore displayed at the following distances from the centre: 0.00, 4.13, 4.70, 6.26, 6.27, 8.26, 9.40, 12.52, 14.70, 18.81 and 20.54 deg. The locations at which stimuli were displayed are illustrated in

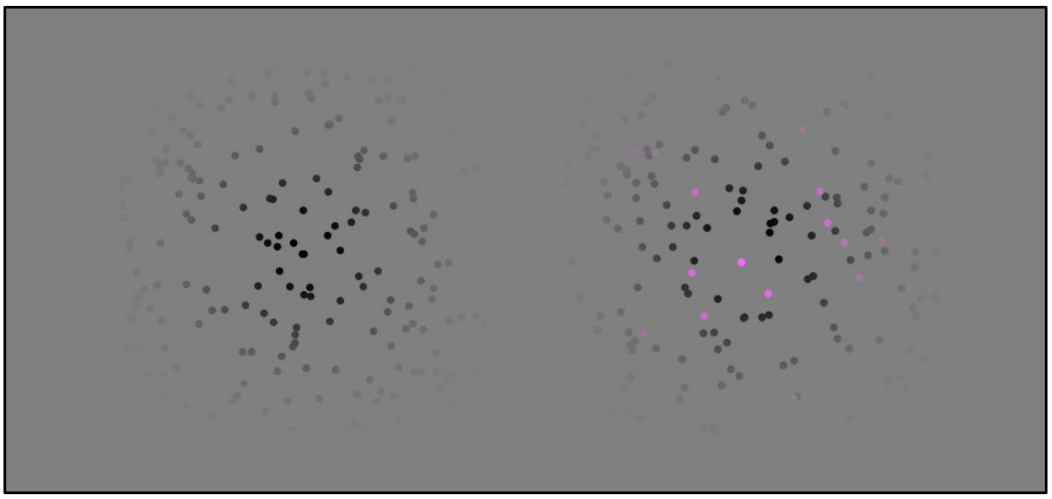

Figure 5.1: Examples of stimuli used in non-counting task (left) and counting task (right) trials. Gaussian windows had a diameter of 10 deg of visual angle (σ = 0.5). Dots drifted vertically or horizontally with 100% coherency and at a velocity of 15 deg/s. Dots were 11 pixels in size (diameter: ~4 pixels). Overall dot density was 1.17 dots/deg^2. During trials using the counting task, coloured task dots had a density of 0.23 dots/deg^2 and black dots had a density of 0.94 dots/deg^2.

Figure 5.2. A higher density of locations was used towards the centre; this was due to a dramatic drop-off in OKR measures around the centre, necessitating a denser sampling distribution in order to effectively quantify the drop in OKR.

5.2.3 Design

All observers participated in every condition, and each viewed a total of 216 stimuli. Counting task and non-task trials were presented in separate blocks. Vertical and horizontal motion were also presented in separate blocks. The 27 locations at which stimuli were presented were split across separate blocks: 15 locations (x = ±18.81, ±9.41 and 0 deg, y = ±8.26 and 0 deg) forming a 5x3 grid (Figure 5.2, grey circles) were presented in one block, 12 locations (x = ±14.11, ±4.70 and 0 deg, y = ±4.13 and 0 deg) forming a 4x2 grid with additional

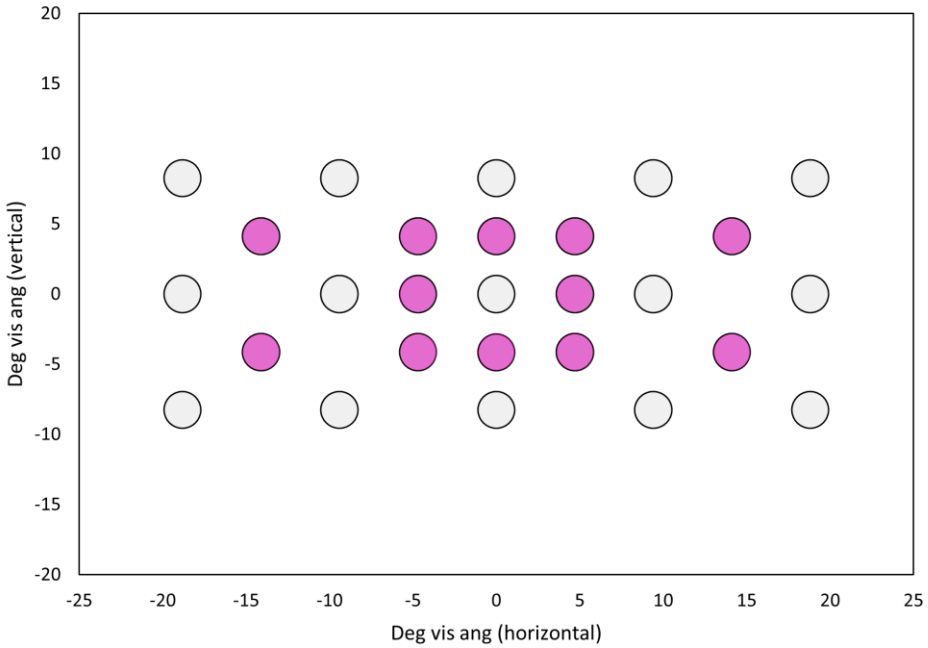

Figure 5.2: Locations at which stimuli were presented, with 0,0 representing the centre of the display. Stimuli were presented at horizontal (x) locations of ±18.81, ±14.11, ±9.41, ±4.70 and 0 deg, and at vertical (y) locations of ±8.26, ±4.13 and 0 deg. A total of 27 locations was used. Locations coloured in grey and pink were presented in separate blocks.

locations around the centre, resulting in a vertically distributed 5-2-5 layout rather than a uniform grid (Figure 5.2, pink circles), were presented in another block. As each orientation of motion (vertical/horizontal) used both directions (up/down, left/right), this meant that the blocks presented 30 (5x3 layout block) and 24 (5-2-5 layout block) stimuli. There were eight blocks in total: horizontal motion without counting task, 5x3 block and 5-2-5 block; horizontal motion with counting task, 5x3 block and 5-2-5 block; vertical motion without counting task, 5x3 block and 5-2-5 block; vertical motion with counting task, 5x3 block and 5-2-5 block. The order of blocks, and of stimuli within each block, was randomised.

Gaze monitoring was used to ensure that participants viewed the correct region of the display. As this experiment involved presenting stimuli to different locations on the visual field, maintaining central gaze was desirable; however, flexibility was required due to the nature of the experiment, as the designated viewing area should not restrict the natural OKR eye movements. The designated viewing area matched the size of the stimulus: a circle 10 deg in diameter. Participants were therefore required to maintain gaze within 5 deg of the centre of the display at all times. Gaze shifts away from this region for over 100ms resulted in a warning, reading 'LOOK AT THE MIDDLE', being displayed at the centre of the display in red text for 1000ms; an additional 1000ms was added to the stimulus duration to account for this disruption.

5.2.4 Procedure

Participants were initially shown example stimuli to familiarise them with the stimuli and with the task. When they stated that they understood the task, the experiment was initiated. Instructions were displayed at the centre of the screen in black text, reading '*Please look towards the centre of the screen. Press the SPACE KEY to continue to the task.*' Prior to the presentation of each stimulus, a white fixation cross with a height of 1 deg was presented at the centre of the screen for four seconds; this served to provide participants with a reference for the centre, where they were asked to maintain gaze throughout the trial. The stimulus was then presented for 20 seconds. During non-counting task blocks, the next trial was immediately presented once the previous trial had ended; during blocks using the counting task, text was then presented on screen reading

'How many different colours did you see? Using the number pad, provide a response between 1 and 9'. Participants had an unlimited amount of time in which to provide their response. The next trial was initiated only once a response had been provided. At the end of each block, an on-screen message reading *'End of block. Thank you for your participation'* was presented to inform the participant that the block had ended. They were then given the opportunity to continue to the next block or to terminate the session.

5.3 Results

It should be noted that the eccentricities reported are approximate due to the nature of the experiment; as participants generated optokinetic eye movements throughout each trial, the exact stimulus eccentricity varied throughout the trial. Participants were required to maintain gaze within a ±5 deg window, which puts a constraint of the accuracy of reported eccentricity values. The average eye position was recorded for each trial. Across the entire experiment, the mean eye position recorded was x = -0.119 deg (SD = 1.049 deg), y = 0.336 deg (SD = 0.825 deg), indicating that there was no systematic bias towards a particular location over the duration of the experiment. The average vertical and horizontal eye position was also examined separately for stimuli presented in the upper, lower, left and right visual fields to assess whether gaze drifted towards the stimulus position. During stimuli presented to the upper visual field, gaze took a mean position 0.101 deg (SD = 1.044) above the centre; during stimuli presented to the lower visual field, gaze took a mean position of 0.106 deg (SD = 0.998) above the centre. During stimuli presented to the right visual field, gaze took a mean position 0.362 deg (SD = 1.006) to the left of the centre; during stimuli presented to the left visual field, mean gaze position was 0.177 deg (SD = 1.017) to the right of the centre. This suggests that, with the exception of stimuli presented to the upper visual field, true eccentricities may be slightly elevated compared to what is reported. However, as these mean positions are less than 1 deg from the centre of the display, participants successfully maintained approximately central gaze. Example traces from stimulation at various eccentricities can be seen in Figure 5.15, showing an approximately central average gaze position throughout.

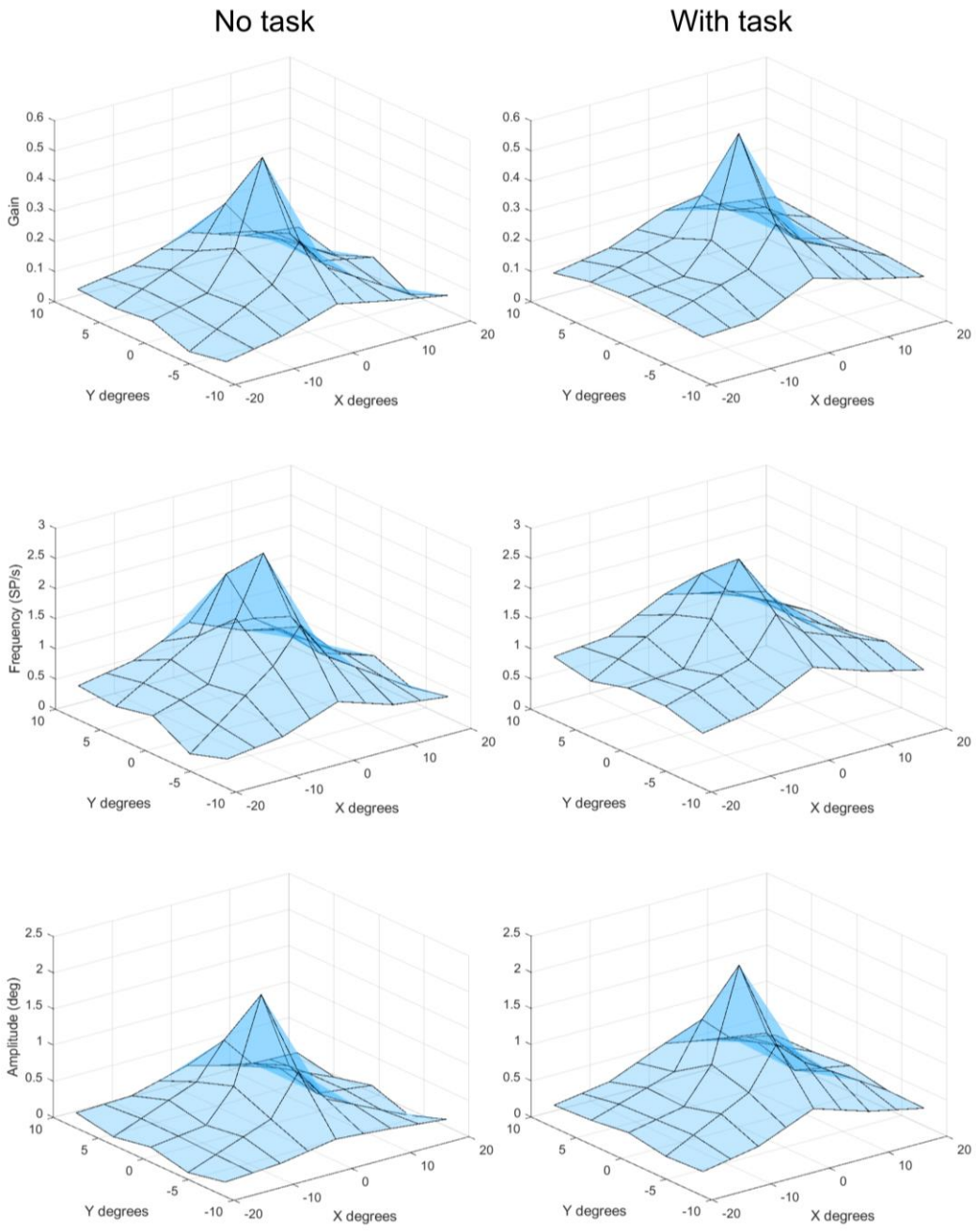

Figure 5.3: N = 9. Surface plots showing gain (upper), frequency (middle) and amplitude (lower) of OKR across vertical and horizontal eccentricity, where 0,0 represents the centre of the visual field, in conditions without (left) and with (right) the counting task. Linear interpolation was used to fill missing values that resulted from the irregular sampling distribution. 'X deg' indicates horizontal eccentricity while 'Y deg' indicates vertical eccentricity. On the X deg axis, positive numbers indicate the right half of the display; on the Y deg axis, positive numbers indicate the lower half of the display. Near the centre, note the more severe drop-off in OKR measures horizontally compared to vertically.

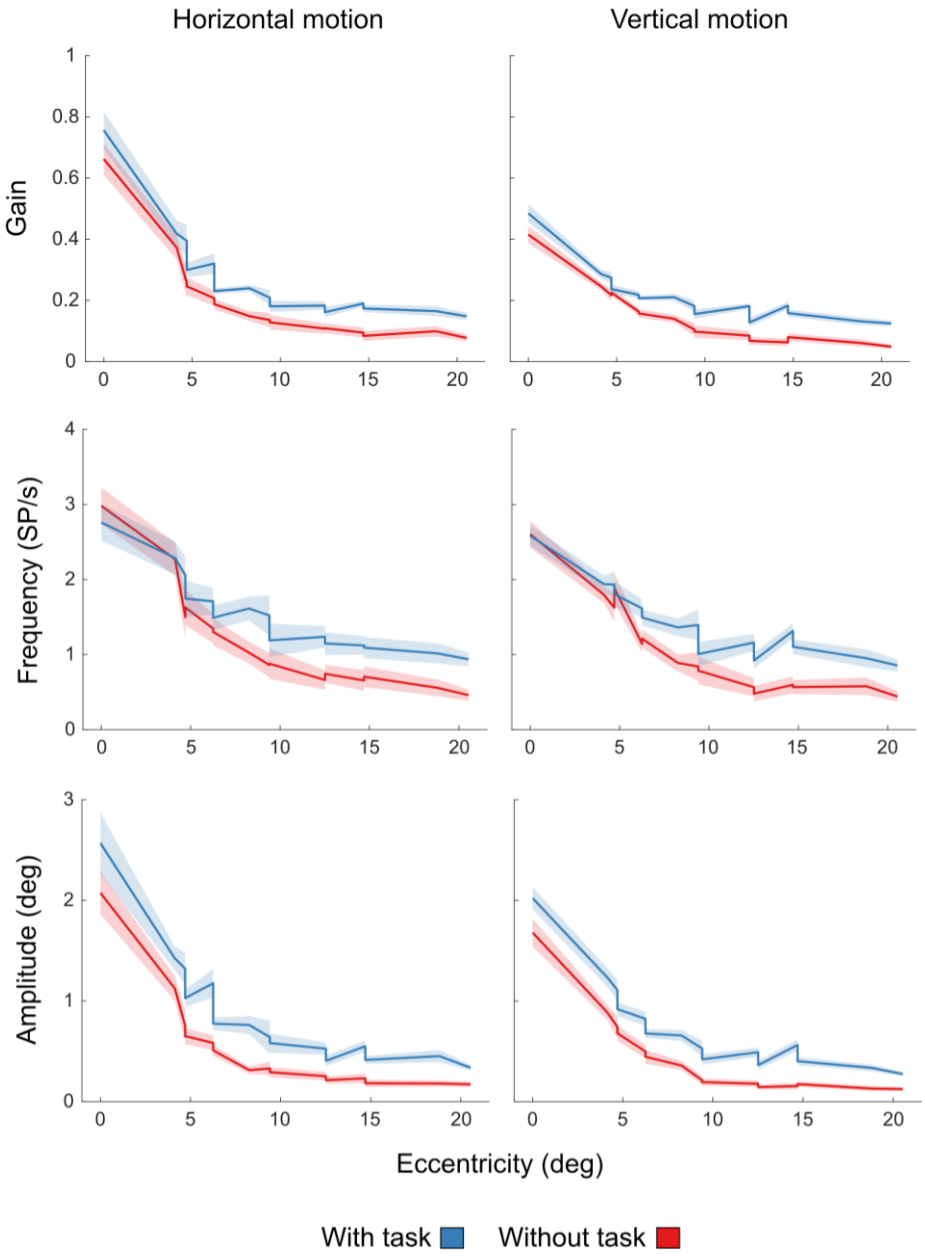

Figure 5.4: N = 9. Mean gain (upper), frequency (middle) and amplitude (lower) in response to horizontal (left) and vertical (right) motion by stimulus eccentricity. Means obtained during trials using the counting task are shown in blue, with means from non-counting task trials shown in red. The shaded area indicates the SEM.

Gain, frequency and amplitude of the OKR by eccentricity are shown in Figure 5.4 and Figure 5.3. Three linear regression models were used to assess the roles eccentricity, upper versus lower visual field stimulus presentation,

orientation of motion (horizontal or vertical), meridian or within-quadrant stimulus presentation, and counting task condition (with or without task). Analyses were run on central stimulus locations (within 10 deg of centre) and peripheral stimulus locations (beyond 10 deg of centre). To further assess the role of presentation along the meridians, an analysis was run using all stimulus locations except foveal (x = 0 deg, y = 0 deg) presentation to assess whether presentation of stimuli on the vertical and horizontal midlines of the display significantly predicted the OKR when foveal presentation was excluded; this involved analysis of all stimuli presented beyond 4 deg of the centre.

Table 5.1

Results of linear regression analysis to predict the gain, frequency and amplitude of OKR in the centre (<10 deg eccentricity) based on four predictor variables (meridian or within-quadrant, eccentricity, orientation of motion and counting task condition)

Gain	β	SE	F	*p*
Intercept	0.3124	0.018	17.200	< .001*
Meridian	0.0426	0.008	5.212	< .001*
Eccentricity	-0.0271	0.003	-10.328	< .001*
Orientation of motion	0.2143	0.020	10.892	< .001*
Task condition	0.0571	0.020	2.899	.004*
Eccentricity*Orientation	-0.0242	0.003	-7.975	< .001*
Eccentricity*Task cond.	0.0010	0.003	0.318	.751
Frequency	β	SE	F	*p*
Intercept	2.4869	0.134	18.525	< .001*
Meridian	0.1816	0.060	3.009	.003*
Eccentricity	-0.1954	0.019	-10.064	< .001*
Orientation of motion	0.1685	0.145	1.159	.247
Task condition	-0.1129	0.145	-0.776	.438
Eccentricity*Orientation	-0.0319	0.022	-1.424	.155
Eccentricity*Task cond.	0.0661	0.022	2.952	.003*
Amplitude	β	SE	F	*p*
Intercept	1.3603	0.076	17.816	< .001*
Meridian	0.1496	0.034	4.361	< .001*
Eccentricity	-0.1433	0.011	-12.982	< .001*
Orientation of motion	0.2580	0.083	3.119	.002*
Task condition	0.3943	0.083	4.767	< .001*
Eccentricity*Orientation	-0.0292	0.013	-2.293	.022*
Eccentricity*Task cond.	-0.0089	0.013	-0.703	.482

Linear regression analyses were run to assess the prediction of the gain, frequency and amplitude of the OKR in response to central (within 10 deg of centre) stimuli, using eccentricity, orientation of motion (horizontal or vertical), meridian or within-quadrant stimulus presentation, and counting task condition (with or without task) as predictors. Interactions between counting task condition and eccentricity, and between orientation of motion and eccentricity, were also assessed. Significant regression equations were found in the prediction of OKR gain ($F(6, 935) = 152.920$, $p < .001$), frequency ($F(6, 935) = 51.013$, $p < .001$) and amplitude ($F(6, 935) = 135.580$, $p < .001$), with adjusted R^2s of .494, .243 and .463, respectively. The results of these analyses are shown in Table 5.1.

In the prediction of gain, whether the stimulus was presented along the vertical/horizontal meridian ($\beta = 0.0426$), stimulus eccentricity ($\beta = -0.0271$), orientation of motion ($\beta = 0.2143$) and task condition ($\beta = 0.0571$) were all found to be significant predictors (Table 5.1). There was also a significant interaction between eccentricity and orientation of motion ($\beta = -0.0242$). Orientation of motion was found to be the largest predictor of gain in the centre, with horizontal motion (M = 0.280, SD = 0.196) producing higher gain than vertical motion (M = 0.211, SD = 0.108). Gain was higher when stimuli were presented along a meridian (vertical or horizontal midline), when eccentricity was lower, and when the counting task was presented. To examine the interaction between eccentricity and orientation of motion, the difference between horizontal and vertical gain was calculated and correlated across eccentricity. This showed a significant

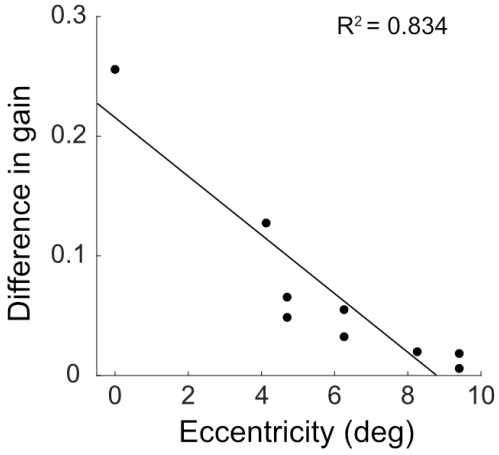

Figure 5.5: N = 9. Scatterplot showing the negative correlation between eccentricity and mean difference between horizontal and vertical gain.

negative correlation ($R^2 = 0.834$, $p < .001$) whereby the difference between horizontal and vertical gain diminished with increasing eccentricity. A scatterplot illustrating this relationship is shown in Figure 5.5.

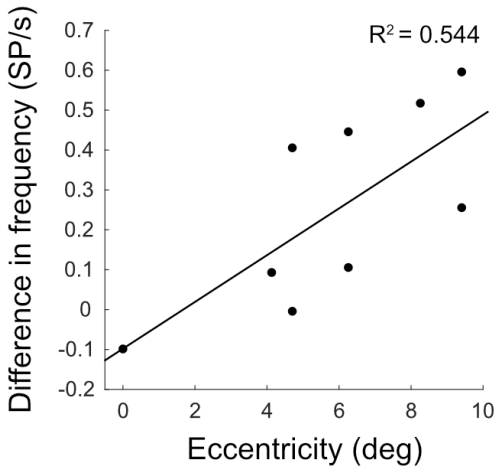

Figure 5.6: N = 9. Scatterplot showing the positive correlation between eccentricity and mean difference between counting task and non-task frequency.

Only stimulus eccentricity and whether the stimulus was presented along a meridian were significant predictors of OKR frequency in response to a centrally presented stimulus, and there was a significant interaction between eccentricity and task condition (Table 5.1). Frequency was higher in response to stimuli presented on the horizontal or vertical meridian ($\beta = 0.1816$) and reduced as stimulus eccentricity increased ($\beta = -0.1954$). To examine the interaction between eccentricity and task condition, the difference in frequency between task and non-task conditions was calculated and correlated across eccentricity. This revealed a significant positive correlation whereby the difference in frequency between task and non-task conditions increased with eccentricity ($R^2 = 0.544$, $p = .023$) (Figure 5.6), with a t-test showing no significant difference between counting task and non-task frequency in response to a stimulus presented at the fovea (x = 0 deg, y = 0 deg) ($t(35) = 1.088$, $p = .284$) whereas higher eccentricities were associated with significantly higher OKR frequency during counting task trials ($t(431) = -8.538$, $p < .001$).

Amplitude of OKR in response to centrally presented stimuli was significantly predicted by every predictor variable (Table 5.1), and there was a significant interaction between eccentricity and orientation of motion. Amplitude was increased by presenting a stimulus on a cardinal meridian (β = 0.1496), by presenting horizontal rather than vertical motion (β = 0.2580) and by presenting the counting task (β = 0.3943). Increasing eccentricity resulted in lower slow phase amplitude (β = -0.1433). T-tests were carried out to examine the interaction between eccentricity and orientation of motion, finding that the slow phase amplitude in response to a stimulus presented at 0,0 deg (foveal presentation) was significantly higher in response to horizontal (M = 2.226, SD = 0.910) compared to vertical (M = 1.841, SD = 0.645) motion ($t(70) = -2.070$, $p = .042$), however, greater eccentricities were not associated with a significant difference between horizontal and vertical amplitude ($t(862) = -1.589$, $p = .113$). A scatterplot showing the negative correlation between the two variables is shown in Figure 5.7.

These analyses were repeated to examine gain, frequency and amplitude in response to peripheral stimuli (beyond 10 deg of the centre). Linear regression models were calculated to predict the gain, frequency and amplitude of the OKR in response to peripheral stimuli using eccentricity, orientation of motion (horizontal or vertical), counting task condition (with or without task) and upper or lower visual field presentation as predictors. Interactions between eccentricity and orientation of motion and between eccentricity and task condition were also

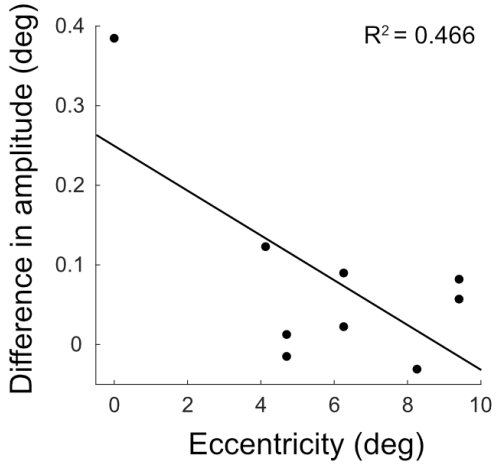

Figure 5.7: N = 9. Scatterplot showing the negative correlation between eccentricity and mean difference between vertical and horizontal amplitude.

assessed. Significant regression equations were found in the prediction of gain ($F(6, 863) = 39.795$, $p < .001$), frequency ($F(6, 863) = 22.117$, $p < .001$) and amplitude ($F(6, 863) = 40.357$, $p < .001$) of OKR, with adjusted R^2s of .212, .128 and .215, respectively. The results of these analyses are shown in Table 5.2.

Table 5.2

Results of linear regression analysis to predict the gain, frequency and amplitude of OKR in the periphery (>10 deg eccentricity) based on four predictor variables (eccentricity, orientation of motion, counting task condition and upper or lower visual field)

Gain	β	SE	F	*p*
Intercept	0.1278	0.024	5.412	< .001*
Eccentricity	-0.0035	0.001	-2.417	.016*
Orientation of motion	0.0176	0.027	0.651	.515
Task condition	0.0915	0.027	3.379	< .001*
Upper or lower VF	-0.0087	0.006	-1.546	.123
Eccentricity*Orientation	-0.0001	0.002	-0.101	.920
Eccentricity*Task cond.	-0.0006	0.002	-0.390	.697
Frequency	β	SE	F	*p*
Intercept	0.8791	0.198	4.450	< .001*
Eccentricity	-0.0156	0.012	-1.295	.196
Orientation of motion	0.0783	0.226	0.346	.730
Task condition	0.6624	0.226	2.925	.004*
Upper or lower VF	-0.0690	0.047	-1.463	.144
Eccentricity*Orientation	-0.0104	0.014	-0.744	.457
Eccentricity*Task cond.	-0.0102	0.014	-0.735	.463
Amplitude	β	SE	F	*p*
Intercept	0.2929	0.070	3.771	< .001*
Eccentricity	-0.0064	0.005	-1.496	.135
Orientation of motion	0.0029	0.080	0.036	.971
Task condition	0.4713	0.080	5.897	< .001*
Upper or lower VF	0.0028	0.017	0.171	.864
Eccentricity*Orientation	0.0008	0.005	0.157	.876
Eccentricity*Task cond.	-0.0147	0.005	-2.997	.003*

Stimulus eccentricity and counting task condition were found to significantly predict the gain of peripheral OKR (Table 5.2). Gain was increased by presenting stimuli at lower eccentricities ($\beta = -0.0035$) and by using the counting task ($\beta = 0.0915$). Only the counting task condition was found to significantly predict frequency (Table 5.2), with the counting task being associated with

higher frequency ($\beta = 0.6624$). OKR amplitude was predicted by task condition ($\beta = 0.4713$) with use of the counting task associated with higher amplitude (Table 5.2). Eccentricity and counting task condition also significantly interacted in the prediction of peripheral OKR amplitude. To examine this interaction, t-tests were used to compare the difference in amplitude caused by the counting task in response to the most eccentric stimulus versus all other stimuli, finding that the counting task had a significantly larger impact on amplitude in response to the less eccentric stimuli ($t(358) = 3.315$, $p = .001$). However, the difference between task and non-task amplitude did not correlate significantly across eccentricity ($R^2 = 0.252$, $p = .309$).

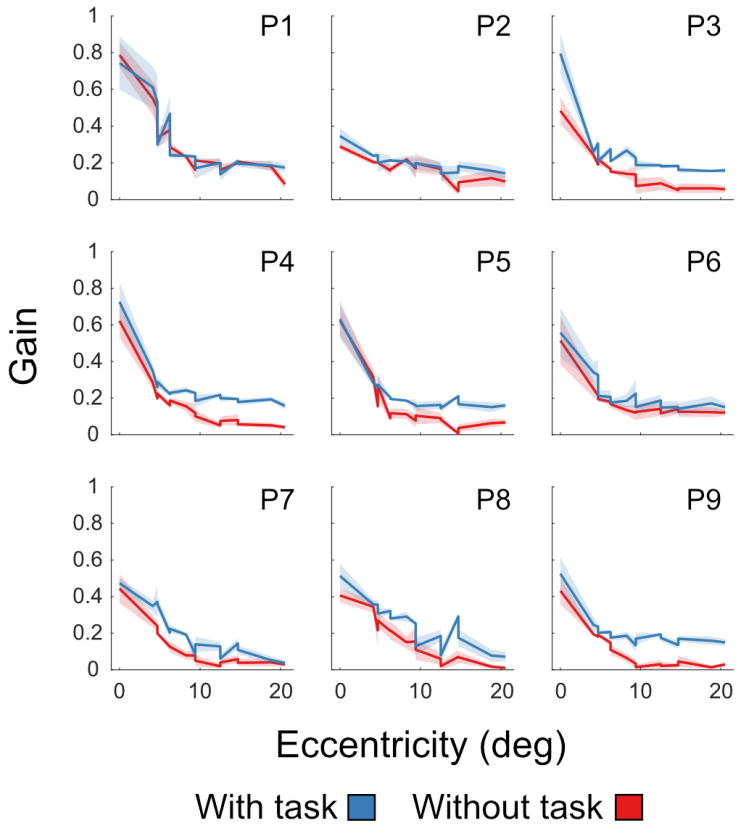

Figure 5.8: Individual mean gain by stimulus eccentricity in response to trials without the counting task (red) and with the counting task (blue), with all directions of motion combined. The shaded area indicates the SEM. Participant numbers are indicated in the upper right corner of each plot.

Finally, a linear regression model was calculated to predict gain, frequency and amplitude of OKR across the visual field excluding the fovea. This was primarily to assess the impact of presenting stimuli to the vertical and horizontal meridian when foveal stimuli have been excluded, and to highlight the presence of interactions that may have been missed in the previous two analyses due to the separation of central and peripheral visual field regions. Linear regression models were calculated to predict the gain, frequency and amplitude of the OKR in response to a non-foveal stimulus using meridian or within-quadrant presentation, stimulus eccentricity, orientation of motion, counting task condition and upper or lower visual field presentation as predictors. Interactions were also examined between eccentricity and meridian presentation, eccentricity and orientation of motion, and eccentricity and counting task condition. Significant regression equations were found in the prediction of OKR gain ($F(8, 1439) = 115.560$, $p < .001$), frequency ($F(8, 1439) = 64.134$, $p < .001$) and amplitude ($F(8, 1439) = 131.540$, $p < .001$) with adjusted R^2s of .389, .260 and .421, respectively. The results of these analyses are shown in Table 5.3.

Gain of non-foveal OKR was significantly predicted by all predictor variables except upper or lower visual field presentation (Table 5.3). Gain was significantly increased by presenting stimuli along the vertical or horizontal meridian ($\beta = 0.2096$), by presenting stimuli at less eccentric locations ($\beta = -0.0061$), by presenting horizontal motion instead of vertical motion ($\beta = 0.0884$) and by using the counting task ($\beta = 0.0536$). There were also significant interactions between the effects of eccentricity and meridian presentation and between eccentricity and orientation of motion. The interaction between eccentricity and orientation of motion is likely that described in the analysis of centrally presented stimuli, where the difference in gain between horizontal and vertical OKR drops with increasing eccentricity. As the results of the peripheral analysis showed no such interaction, this effect is probably limited to central (<10 deg eccentricity) visual field regions. Examining the interaction between meridian and eccentricity, this effect appears to be a result of meridian presentation including stimuli with lower eccentricities than those in the within-quadrant presentation group; meridian group included three eccentricities of ~4–5 deg, whereas the lowest

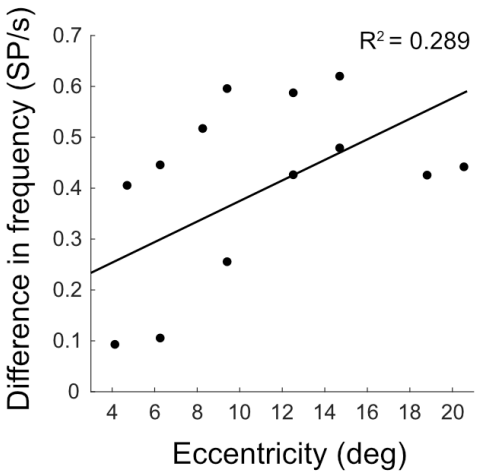

Figure 5.9: N = 9. Scatterplot showing the correlation between stimulus eccentricity and the difference between counting task and non-task mean frequency.

eccentricity available in the within-quadrant stimulus group was 6.26 deg. Once eccentricities of <5 deg were excluded from the analysis, leaving only the more comparable eccentricities, a t-test found that there was no significant difference in gain between meridian and within-quadrant presentation ($t(1582) = 1.290$, $p = .197$). This indicates that the significant effects of meridian presentation in the centre may instead simply be effects of low stimulus eccentricity. However, it should be noted that direct comparison between meridian and within-quadrant presentation is not possible due to the different range of eccentricities used in each group. Individual gain by stimulus eccentricity is shown in Figure 5.8.

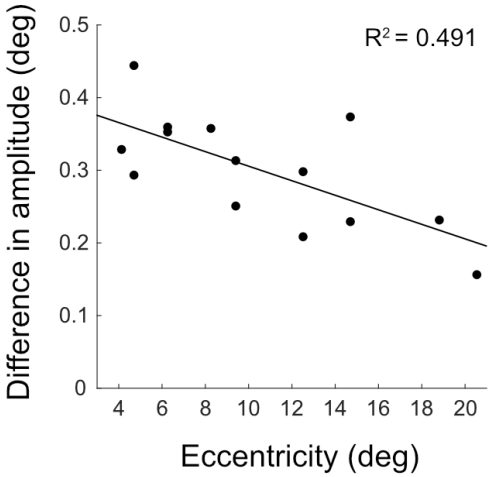

Figure 5.10: N = 9. Scatterplot showing the correlation between stimulus eccentricity and the difference in mean amplitude between counting task and non-task

Meridian, stimulus eccentricity, counting task condition and upper or lower visual field presentation were all found to significantly predict the frequency of non-foveal OKR (Table 5.3). There was also a significant interaction between eccentricity and meridian presentation, and between eccentricity and task condition. As stated in the analysis of the gain model for non-foveal OKR, effects of meridian may in fact be effects of low stimulus eccentricity due to the different ranges of eccentricities used in either group, therefore effects of meridian stimulus presentation are assumed to be a result of this lower eccentricity presentation. As with gain, once eccentricities of <5 deg were excluded, a t-test found no significant difference in frequency between meridian and within-quadrant stimulus presentation ($t(1582) = 1.145$, $p = .252$). The frequency of non-

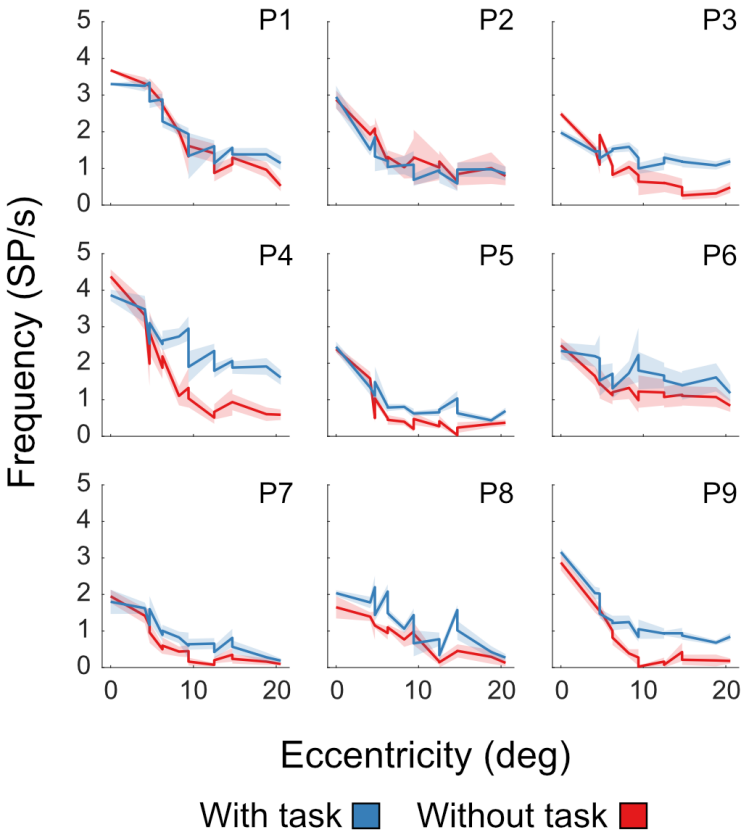

Figure 5.11: Mean frequency of OKR across stimulus eccentricity in trials using the counting task (blue) and trials without the counting task (red) in nine participants, with all directions of stimulus motion combined. The shaded area indicates the SEM.

foveal OKR was increased by presenting stimuli at lower eccentricities (β = -0.0509, $p < .001$), by presenting the counting task (β = 0.2511, $p = .010$) and by presenting stimuli to the lower visual field (β = -0.0887, $p = .028$). To examine the interaction between eccentricity and task condition, the difference in mean frequency between task and non-task trials was calculated and correlated across eccentricity, revealing a significant positive correlation ($R^2 = 0.289$, $p = .048$) whereby the difference in frequency between counting task and non-task conditions increased with eccentricity (Figure 5.9). Individual frequency across stimulus eccentricity is shown in Figure 5.11.

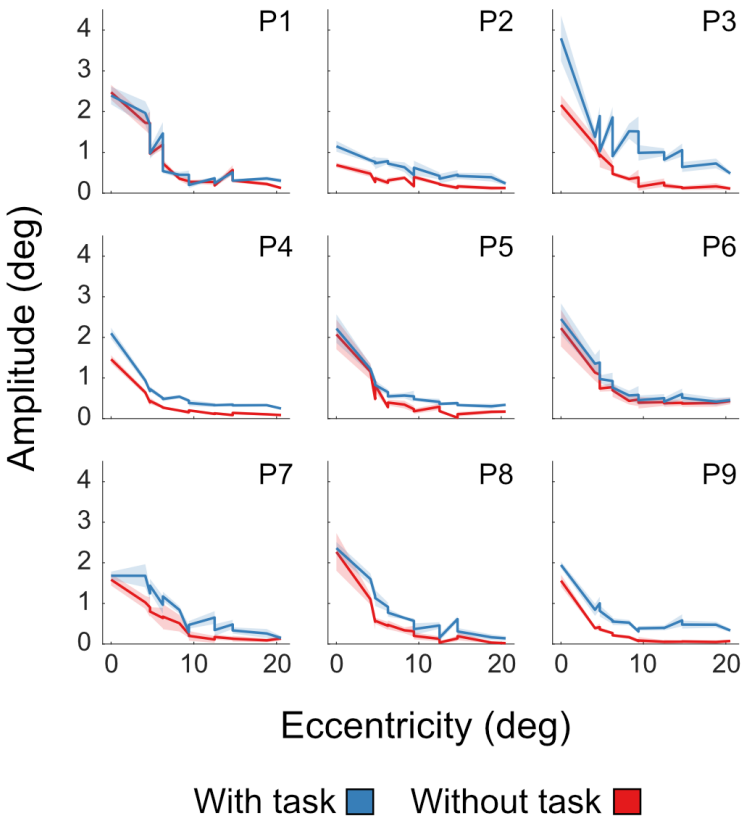

Figure 5.12: Mean amplitude of OKR across stimulus eccentricity in trials using the counting task (blue) and trials without the counting task (red) in nine participants, with all directions of stimulus motion combined. The shaded area indicates the SEM.

Table 5.3

Results of linear regression analysis to predict the gain, frequency and amplitude of non-foveal OKR (>4 deg eccentricity) based on five predictor variables (meridian or within-quadrant presentation, eccentricity, orientation of motion, counting task condition and upper or lower visual field)

Gain	β	SE	F	*p*
Intercept	0.1712	0.012	14.340	< .001*
Meridian	0.2096	0.019	10.769	< .001*
Eccentricity	-0.0061	0.001	-7.155	< .001*
Orientation of motion	0.0884	0.012	7.311	< .001*
Task condition	0.0536	0.012	4.436	< .001*
Upper or lower VF	-0.0047	0.005	-0.942	.347
Eccentricity*Meridian	-0.0248	0.003	-8.940	< .001*
Eccentricity*Orientation	-0.0045	0.001	-4.919	< .001*
Eccentricity*Task cond.	0.0016	0.001	1.781	.075
Frequency	β	SE	F	*p*
Intercept	1.4897	0.095	15.607	< .001*
Meridian	1.2277	0.156	7.887	< .001*
Eccentricity	-0.0509	0.007	-7.504	< .001*
Orientation of motion	0.1104	0.097	1.142	.254
Task condition	0.2511	0.097	2.597	.010*
Upper or lower VF	-0.0887	0.040	-2.206	.028*
Eccentricity*Meridian	-0.1501	0.022	-6.759	< .001*
Eccentricity*Orientation	-0.0127	0.007	-1.733	.083
Eccentricity*Task cond.	0.0145	0.007	1.995	.046*
Amplitude	β	SE	F	*p*
Intercept	0.5353	0.045	12.024	< .001*
Meridian	0.9702	0.073	13.363	< .001*
Eccentricity	-0.0228	0.003	-7.194	< .001*
Orientation of motion	0.0972	0.045	2.156	.031*
Task condition	0.4122	0.045	9.139	< .001*
Upper or lower VF	0.0212	0.019	1.132	.258
Eccentricity*Meridian	-0.1207	0.010	-11.652	< .001*
Eccentricity*Orientation	-0.0051	0.003	-1.473	.141
Eccentricity*Task cond.	-0.0111	0.003	-3.261	.001*

The amplitude of non-foveal OKR was significantly predicted by meridian or within-quadrant presentation, stimulus eccentricity, orientation of stimulus motion and counting task condition (Table 5.3). There were significant interactions between eccentricity and meridian presentation and between eccentricity and counting task condition. Again, the effect of meridian or within-quadrant presentation, and its interaction with eccentricity, were assumed to result from meridian locations including lower eccentricities; confirming this, a t-test

excluding eccentricities below 5 deg found no difference in amplitude between meridian and within-quadrant presentation ($t(1582) = 0.279$, $p = .781$). The amplitude of non-foveal OKR was increased by presenting stimuli at lower eccentricities ($\beta = -0.0228$, $p < .001$), by presenting horizontal motion instead of

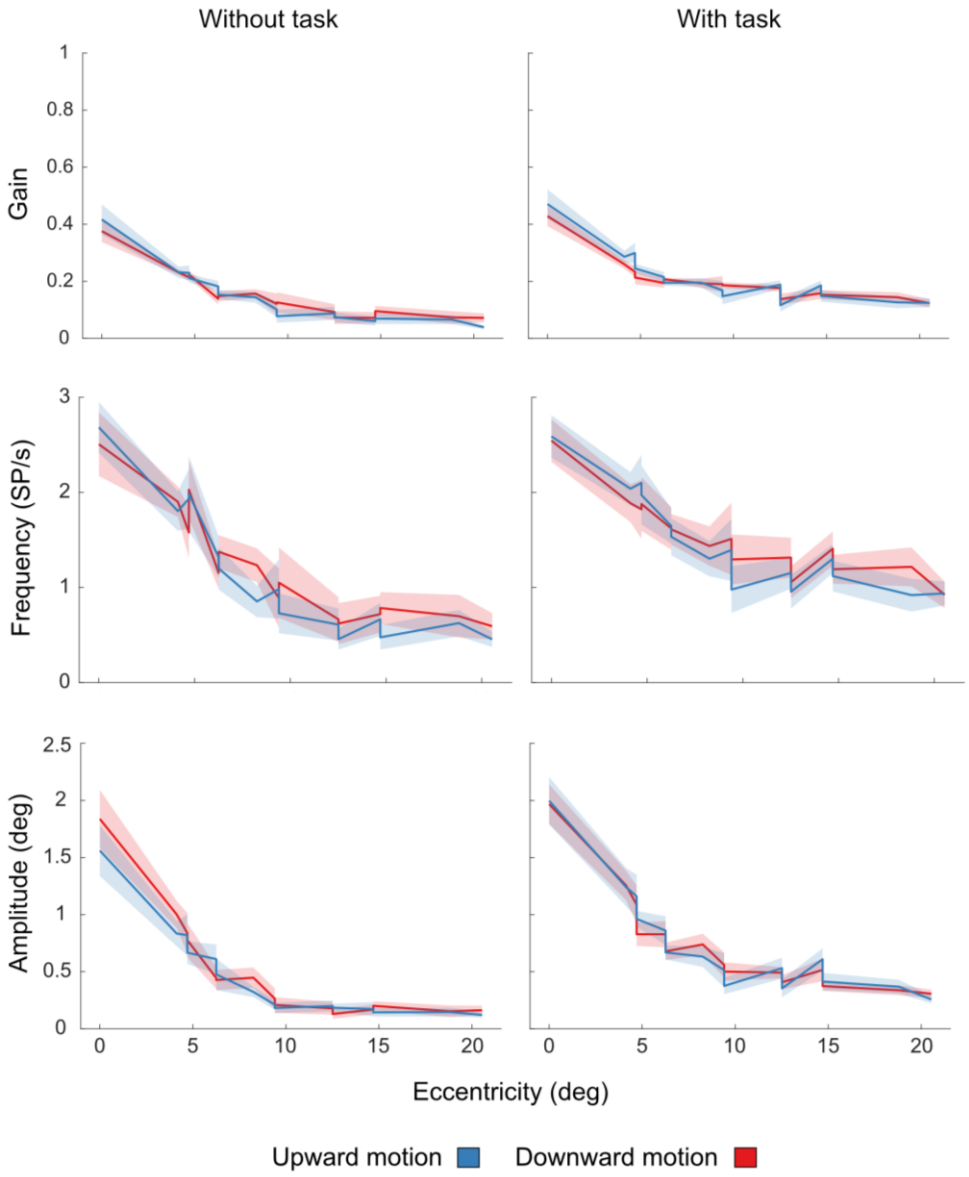

Figure 5.13: N = 9. Mean gain (upper), frequency (middle) and amplitude (lower) in response to vertical motion drifting in an upward (blue) or downward (red) direction during trials using the counting task (right) and not using the counting task (left). The shaded area indicates the SEM.

vertical motion ($\beta = 0.0972$, $p = .031$) and by presenting the counting task ($\beta = 0.4122$, $p < .001$). To investigate the interaction between eccentricity and counting task condition ($\beta = -0.0111$, $p = .001$), the difference between task and non-task amplitude was calculated and correlated across stimulus eccentricity, revealing a significant negative correlation ($R^2 = 0.491$, $p = .005$) whereby the difference between task and non-task amplitude declines with increasing eccentricity (Figure 5.10). Individual amplitude across eccentricity is shown in Figure 5.12.

Finally, t-tests were carried out to assess whether the counting task had a significantly larger effect in the upper or lower visual field. Results showed that the impact of the counting task on gain ($t(359) = -0.829$, $p = .408$) and frequency ($t(359) = -0.372$, $p = .711$) did not differ between the upper and lower hemifields, but the effect on amplitude was significantly larger in the upper visual field (M = +0.307 deg, SD = 0.426) compared to the lower visual field (M = +0.250 deg, SD = 0.345) ($t(359) = -2.297$, $p = .022$).

5.3.1 Individual analyses

To address concerns of individual differences in performance, regression models were calculated for each participant in response to stimuli presented within 10 deg of the centre, beyond 10 deg of the centre, and beyond the fovea (> 4 deg). These analyses focused on gain as the variable of primary interest in this experiment. As group-level analyses highlighted that effects of meridian presentation were caused solely by the inclusion of foveal stimuli, meridian presentation was removed as a variable for individual analyses.

Regression models were calculated for all participants to investigate the impact of stimulus eccentricity, orientation of motion (vertical or horizontal), counting task condition and the interaction between eccentricity and task condition on the gain of OKR in response to stimuli presented within the central (< 10 deg eccentricity) visual field. Significant regression equations were found for all participants (P1: ($F(4, 103) = 47.922$, $p < .001$, adjusted $R^2 = .646$); P2: ($F(4, 103) = 11.374$, $p < .001$, adjusted $R^2 = .287$); P3: ($F(4, 103) = 30.290$, $p < .001$, adjusted $R^2 = .532$); P4: ($F(4, 103) = 40.637$, $p < .001$, adjusted $R^2 = .606$); P5: ($F(4, 103) = 40.399$, $p < .001$, adjusted $R^2 = .605$); P6: ($F(4, 103) = 31.723$, $p <$

.001, adjusted $R^2 = .544$); P7: ($F(4, 103) = 47.015$, $p < .001$, adjusted $R^2 = .641$); P8: ($F(4, 103) = 28.717$, $p < .001$, adjusted $R^2 = .518$); P9: ($F(4, 103) = 43.207$, $p < .001$, adjusted $R^2 = .621$)). The results of these analyses are presented in Table AC.1 (Appendix C). Stimulus eccentricity was found to significantly predict central OKR gain in every participant, with more eccentric stimuli being associated with significantly lower gain. β-coefficients for this variable ranged from -0.0077 to -0.0650. Orientation of motion significantly predicted gain in six participants, five of whom showed significantly higher gain in response to horizontal motion. Counting task condition predicted gain in just three participants (P2, P3, P7), with the task being associated with significantly higher gain. There were no significant interactions between eccentricity and task condition.

Regression analyses were then conducted to assess gain in response to peripheral (>10 deg eccentricity) stimuli. Stimulus eccentricity, orientation of motion, counting task condition and lower versus upper visual field presentation were used as predictors. The interaction between eccentricity and task condition was also assessed. Significant regression equations were found for all but one (P2: ($F(5, 95) = 1.905$, $p = .101$, adjusted $R^2 = .046$)) participant: P1 ($F(5, 95) = 6.609$, $p < .001$, adjusted $R^2 = .228$), P3 ($F(5, 95) = 15.036$, $p < .001$, adjusted $R^2 = .425$), P4 ($F(5, 95) = 31.217$, $p < .001$, adjusted $R^2 = .614$), P5 ($F(5, 95) = 15.401$, $p < .001$, adjusted $R^2 = .431$), P6 ($F(5, 95) = 7.666$, $p < .001$, adjusted $R^2 = .260$), P7 ($F(5, 95) = 8.623$, $p < .001$, adjusted $R^2 = .286$), P8 ($F(5, 95) = 6.835$, $p < .001$, adjusted $R^2 = .235$) and P9 ($F(5, 95) = 29.512$, $p < .001$, adjusted $R^2 = .600$). The results of these analyses are presented in Table AC.2 (Appendix C). Stimulus eccentricity predicted peripheral OKR gain in just one participant (P1: $\beta = -0.0137$, $p < .001$). Orientation of motion significantly predicted gain in five participants (P1, P4, P6, P7, P9); of these five, three showed higher gain in response to horizontal motion (P1, P6, P9) whereas two showed higher gain in response to vertical motion (P4, P7). Counting task condition also significantly predicted gain in five participants (P1, P4, P7, P8, P9), with the counting task being associated with higher gain in all but one (P1) of these five participants. Whether the stimulus was presented to the upper or lower visual field did not significantly predict gain in any participant. There was an interaction between stimulus eccentricity and counting task condition in P1 only. T-testing was used to examine this interaction, finding that, at the lowest eccentricity tested, there

was no significant difference in gain between task and non-task conditions ($t(15) = -0.333$, $p = .744$), whereas at the highest eccentricity tested, gain was significantly higher during the counting task ($t(15) = 3.056$, $p = .008$). The effect of the counting task therefore increased with eccentricity during peripheral stimulation in this participant only.

Finally, regression analyses were conducted to assess the effect of stimulus eccentricity, orientation of motion, counting task condition, upper versus lower visual field presentation, and the interaction between eccentricity and task condition, on the gain of OKR in each participant in response to non-foveal OKR (> 4 deg eccentricity). Significant regression equations were found for each participant (P1: ($F(5, 159) = 27.717$, $p < .001$, adjusted $R^2 = .457$); P2: ($F(5, 159) = 8.479$, $p < .001$, adjusted $R^2 = .190$); P3: ($F(5, 159) = 38.397$, $p < .001$, adjusted $R^2 = .540$); P4: ($F(5, 159) = 45.066$, $p < .001$, adjusted $R^2 = .581$); P5: ($F(5, 159) = 19.735$, $p < .001$, adjusted $R^2 = .371$); P6: ($F(5, 159) = 17.971$, $p < .001$, adjusted $R^2 = .348$); P7: ($F(5, 159) = 36.319$, $p < .001$, adjusted $R^2 = .526$); P8: ($F(5, 159) = 34.762$, $p < .001$, adjusted $R^2 = .515$); P9: ($F(5, 159) = 34.469$, $p < .001$, adjusted $R^2 = .457$)). The results of these analyses can be viewed in Table AC.3 (Appendix C). Stimulus eccentricity significantly predicted gain in every participant, with an increase in eccentricity causing a decrease in gain (β-coefficient range: -0.0053 to -0.2120). Orientation of motion significantly predicted gain in five participants (P1, P2, P3, P6, P8), with horizontal motion producing higher gain. Counting task condition also predicted gain in five participants (P3, P4, P7, P8, P9), with trials using the counting task producing higher gain. In four participants (P4, P5, P7, P9) there was a significant interaction between stimulus eccentricity and counting task condition, despite there being no effect at the group level. T-testing was used to compare the difference in gain between task and non-task conditions at the lowest and highest non-foveal eccentricity tested, finding that the counting task caused a significantly larger increase in gain at a higher stimulus eccentricity in P4 ($t(15) = -2.451$, $p = .027$) and P9 ($t(15) = -3.242$, $p = .006$) and at a lower stimulus eccentricity in P7 ($t(15) = -2.451$, $p = .027$). In P5, there was no significant difference in the impact of counting task on eccentricity between the lowest and highest eccentricities, however, t-testing showed that the difference between task and non-task conditions was significant at the highest

eccentricity ($t(15) = 4.449$, $p < .001$) but not at the lowest eccentricity ($t(15) = 0.392$, $p = .701$).

Summary of key findings

- Gain, frequency and amplitude of the OKR drop off dramatically within 5-10 deg of the centre of vision
- Attention increases the gain, frequency and amplitude of the OKR across the visual field
- The difference in gain between responses to horizontal and vertical motion declines with increasing eccentricity
- After controlling for stimulus eccentricity, OKR measures were not higher in response to stimuli presented on the cardinal meridians
- OKR gain did not show a lower hemifield advantage
- Analyses of individual participants highlighted between-subject variation in these effects

5.3.2 Vertical OKR symmetry across the visual field

The up-down symmetry of vertical OKR across the visual field was examined (Figure 5.13). T-tests were carried out to assess for significant difference in OKR gain. Results showed that within 5 deg of the centre (parafoveal region), a significant difference between upward and downward gain can be observed ($t(89) = -2.471$, $p = .015$) whereby upward motion elicited higher OKR gain (M = 0.291, SD = 0.126) than downward motion (M = 0.267, SD = 0.097). Beyond 5 deg eccentricity, no significant difference was seen between upward and downward gain ($t(395) = 1.050$, $p = .294$). However, t-tests conducted to assess up-down symmetry of OKR within 5 deg of the centre in each participant showed that this significant effect of asymmetry at the centre was only present in three participants (P1: ($t(9) = 2.989$, $p = .015$); P4: ($t(9) = 3.287$, $p = .009$); P7: ($t(9) = -8.423$, $p < .001$)), with others showing no significant up-down gain asymmetry.

The symmetry of frequency was also examined (Figure 5.13), with t-tests showing no significant difference in upward and downward frequency in response to a stimulus within 5 deg of the centre ($t(89) = -1.139$, $p = .258$). However, there was a significant difference in the upward and downward frequency of OKR beyond 5 deg eccentricity ($t(395) = 2.198$, $p = .027$), indicating that OKR frequency in response to upward drifting stimuli (M = 0.953, SD = 0.786) was significantly lower than to downward drifting stimuli (M = 1.068, SD = 0.878). T-tests were used to examine these effects in individual participants, finding that both within and beyond 5 deg eccentricity, the majority of participants showed no significant up-down asymmetry of frequency. Within 5 deg eccentricity, P4 ($t(9) = 2.312$, $p = .046$) and P9 ($t(9) = 2.495$, $p = .034$) had significantly higher upward frequency whereas P5 ($t(9) = -5.699$, $p < .001$) had higher downward frequency. Beyond 5 deg, P3 ($t(43) = 6.914$, $p < .001$) had higher upward frequency and P6 ($t(43) = -21.352$, $p < .001$) had higher downward frequency.

Finally, slow phase amplitude was examined for its up-down symmetry (Figure 5.13), finding no significant difference between upward and downward amplitude in response to stimuli within 5 deg of the centre ($t(89) = 0.989$, $p = .325$) nor in response to stimuli presented at an eccentricity beyond 5 deg ($t(89) = 0.309$, $p = .758$). T-tests carried out to test for up-down asymmetry in individual participants showed that, within 5 deg of the centre, one participant produced higher upward amplitude (P1 ($t(9) = 2.974$, $p = .016$)), three participants produced higher downward amplitude (P5 ($t(9) = -3.209$, $p = .011$), P6 ($t(9) = -3.284$, $p = .010$), P8 ($t(9) = -2.831$, $p = .020$)) and the remaining five participants showed no significant up-down asymmetry. Beyond 5 deg of the centre, higher upward amplitude was observed in four participants (P3 ($t(43) = 3.743$, $p < .001$), P4 ($t(43) = 4.351$, $p < .001$), P7 ($t(43) = 2.785$, $p = .008$), P9 ($t(43) = 3.439$, $p = .001$)) whereas higher downward amplitude was observed in two participants (P5 ($t(43) = -3.536$, $p < .001$), P6 ($t(43) = -20.194$, $p < .001$)). The remaining three participants showed no significant effect.

Summary of key findings

- Vertical OKR gain is significantly asymmetrical in response to central, but not peripheral, motion
- OKR frequency is higher in response to downward motion presented beyond 5 deg of the centre
- OKR amplitude is vertically symmetrical across the visual field
- Individual analyses show that these effects are not fully consistent across participants

5.3.3 Effect of eccentricity along the meridians

Linear modelling was used to assess whether the decline in gain, frequency and amplitude with increasing eccentricity was different for vertical and horizontal distance from the centre (Figure 5.14). This analysis used stimuli presented on the vertical and horizontal midlines of the display. As the vertical extent of the display was less than the horizontal extent of the display, only stimuli presented at less than 10 deg eccentricity were included. Stimuli presented to the centre of the display (x = 0 deg, y = 0 deg) were also excluded, as the fovea exists at the intersection of both cardinal meridians. It should be noted that direct comparison between stimuli along the horizontal and vertical meridians is not possible due to using slightly different stimulus eccentricities; the analysis includes stimuli presented along the horizontal meridian at positions 4.70 and 9.41 deg from the centre and stimuli presented along the vertical meridian at positions 4.13 and 8.26 deg from the centre. This slight discrepancy in vertical and horizontal eccentricities should be considered while interpreting the results of these models.

Linear regression models were calculated to predict the gain, frequency and amplitude of the OKR in response to stimuli with eccentricities 4-10 deg presented along the vertical and horizontal midline of the display (i.e. vertical and horizontal meridian) using stimulus eccentricity, orientation of motion (vertical or horizontal), task condition (with or without counting task) and vertical

or horizontal meridian stimulus presentation as predictors. Interactions between vertical or horizontal meridian and stimulus eccentricity, between vertical or horizontal meridian and orientation of motion, and between vertical or horizontal meridian and counting task condition were also assessed. Significant regression equations were found in the prediction of the gain ($F(7, 575) = 41.119$, $p < .001$), frequency ($F(7, 575) = 21.151$, $p < .001$) and amplitude ($F(7, 575) = 51.337$, $p < .001$) of the OKR with adjusted R^2s of .328, .197 and .380, respectively. The results of these analyses are shown in Table 5.4, with corresponding data displayed in Figure 5.14.

Table 5.4

Results of linear regression analysis to predict the gain, frequency and amplitude of OKR along the vertical and horizontal meridians based on four predictor variables (eccentricity, orientation of motion, task condition and vertical or horizontal meridian)

Gain	β	SE	F	*p*
Intercept	0.3301	0.023	14.530	< .001*
Eccentricity	-0.0247	0.003	-8.856	< .001*
Orientation of motion	0.0346	0.013	2.638	.009*
Task condition	0.0618	0.013	4.714	< .001*
Ver/Hor meridian	0.0523	0.032	1.628	.104
Eccentricity*Ver/Hor m.	-0.0076	0.004	-1.806	.071
Orientation*Ver/Hor m.	0.0391	0.018	2.107	.036*
Task* Ver/Hor m.	-0.0013	0.018	-0.069	.945
Frequency	β	SE	F	*p*
Intercept	2.4521	0.177	13.883	< .001*
Eccentricity	-0.1561	0.022	-7.198	< .001*
Orientation of motion	-0.1847	0.102	-1.811	.071
Task condition	0.3132	0.102	3.071	.002*
Ver/Hor meridian	0.1909	0.250	0.764	.445
Eccentricity*Ver/Hor m.	-0.0440	0.033	-1.338	.181
Orientation*Ver/Hor m.	0.3010	0.144	2.087	.037*
Task* Ver/Hor m.	-0.0080	0.144	-0.055	.956
Amplitude	β	SE	F	*p*
Intercept	1.2175	0.089	13.681	< .001*
Eccentricity	-0.1075	0.012	-9.838	< .001*
Orientation of motion	0.0342	0.051	0.666	.506
Task condition	0.3254	0.051	6.333	< .001*
Ver/Hor meridian	0.3588	0.126	2.851	.005*
Eccentricity*Ver/Hor m.	-0.0440	0.017	-2.660	.008*
Orientation*Ver/Hor m.	0.0118	0.073	0.163	.871
Task* Ver/Hor m.	0.0177	0.073	0.244	.808

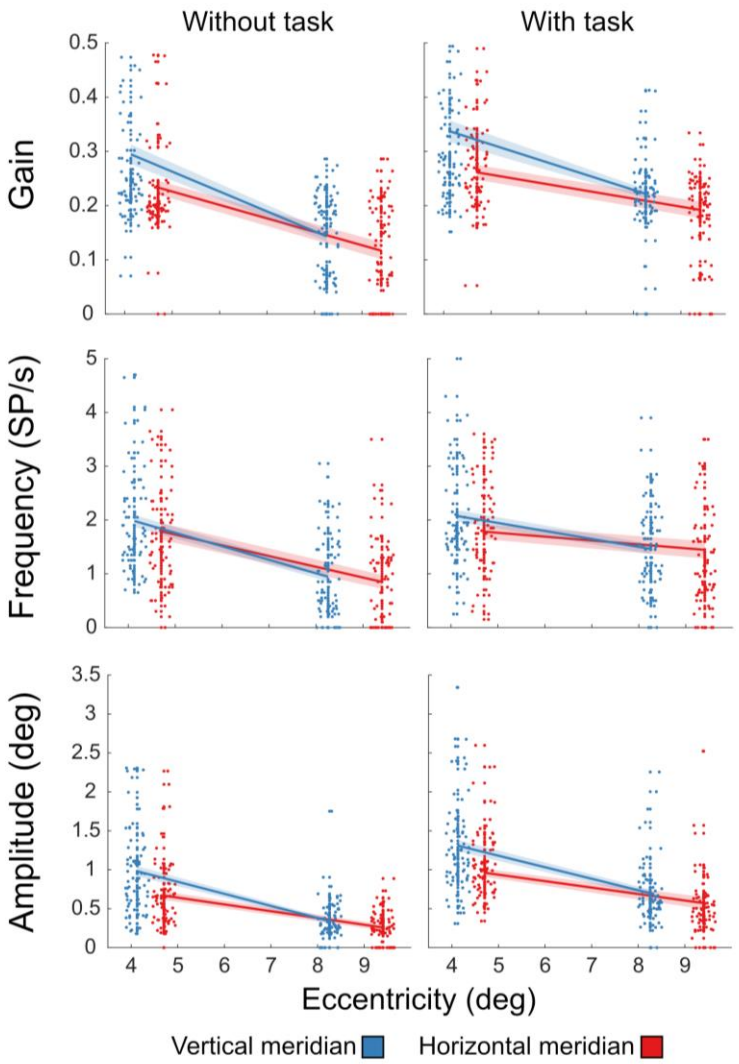

Figure 5.14: N = 9. Mean gain (upper), frequency (middle) and amplitude (lower) by stimulus eccentricity along the vertical (blue) and horizontal (red) meridian, during trials without (left) and with (right) the counting task. Data points show the mean obtained in that trial, with the shaded area indicating the SEM. A horizontal jitter of up to 0.5 deg has been applied to improve the visibility of data points.

The gain of OKR in response to stimuli presented 4–10 deg from the centre along the vertical and horizontal meridian was significantly predicted by the stimulus eccentricity (β = -0.0247, $p < .001$), orientation of motion (β = 0.0346, $p = .009$) and counting task condition (β = 0.0618, $p < .001$). OKR gain was increased by presenting stimuli at lower eccentricities, by presenting horizontal

motion rather than vertical motion and by presenting the counting task. Whether a stimulus was presented along the vertical or horizontal meridian did not significantly predict gain ($p = .104$), however, there was a significant interaction between orientation of motion and vertical/horizontal meridian presentation. T-tests were used to examine this interaction. Horizontal motion was found to produce significantly higher gain than vertical motion on both the horizontal ($t(143) = -3.175$, $p = .002$) and vertical ($t(143) = -5.764$, $p < .001$) meridians, and both vertical motion ($t(143) = 3.553$, $p < .001$) and horizontal motion ($t(143) = 5.503$, $p < .001$) produced significantly higher gain on the vertical meridian than the horizontal meridian. However, the difference between vertical and horizontal gain was found to be significantly larger in response to stimuli presented on the vertical meridian (M = 0.074, SD = 0.153) compared to the horizontal meridian (M = 0.035, SD = 0.131) ($t(143) = 2.918$, $p = .004$).

These regression models were then calculated at the individual level for each participant to assess the consistency of the identified effects across participants. Models to predict OKR gain were significant in eight out of nine participants (P1 ($F(7, 63) = 15.408$, $p < .001$, adjusted $R^2 = .616$), P3 ($F(7, 63) = 5.361$, $p = < .001$, adjusted $R^2 = .326$), P4 ($F(7, 63) = 10.785$, $p = < .001$, adjusted $R^2 = .521$), P5 ($F(7, 63) = 7.214$, $p = < .001$, adjusted $R^2 = .408$), P6 ($F(7, 63) = 9.038$, $p < .001$, adjusted $R^2 = .472$), P7 ($F(7, 63) = 16.001$, $p < .001$, adjusted $R^2 = .625$), P8 ($F(7, 63) = 8.622$, $p < .001$, adjusted $R^2 = .459$), P9 ($F(7, 63) = 10.477$, $p < .001$, adjusted $R^2 = .513$)). The results of these analyses are presented in Tables AC.4 through to AC.12 (Appendix C). Gain was significantly reduced by increasing stimulus eccentricity in each of these eight participants. Though the group level analysis showed a significant effect of orientation of stimulus motion, this was only found to significantly predict gain in two participants (P1 and P6). The use of the counting task significantly increased gain in each of these eight participants, whereas whether stimuli were presented on the vertical or horizontal meridian did not predict gain in any participant. At the individual level, the interaction between orientation of motion and vertical/horizontal meridian presentation was not found to be significant in any participant. However, there was a significant interaction between stimulus eccentricity and vertical/horizontal meridian presentation in P1 only. T-tests were used to examine this interaction, finding that the difference in gain between vertical and horizontal meridian

presentation was significant only at a lower eccentricity ($t(15) = 2.830$, $p = .013$) but not at a higher eccentricity ($t(15) = 2.074$, $p = .056$).

The frequency of the OKR was significantly predicted by stimulus eccentricity ($\beta = -0.1561$, $p < .001$) and counting task condition ($\beta = .3132$, $p = .002$), but not by vertical or horizontal meridian presentation ($p = .445$). This indicates that frequency was higher when stimuli were less eccentric and when the counting task was used. There was a significant interaction between orientation of motion and vertical/horizontal meridian presentation; on the vertical meridian, there was no significant difference between frequency in response to vertical or horizontal motion ($t(143) = -1.620$, $p = .107$), but on the horizontal meridian, frequency in response to vertical motion (M = 1.508, SD = 0.987) was significantly higher than frequency in response to horizontal motion (M = 1.323, SD = 0.911) ($t(143) = 2.318$, $p = .022$).

Analyses were again repeated at the individual level to investigate the consistency of the effects of these variables on the frequency of OKR across participants. Significant regression models were calculated for every participant (P1 ($F(7, 63) = 17.276$, $p < .001$, adjusted $R^2 = .644$), P2 ($F(7, 63) = 2.494$, $p = .027$, adjusted $R^2 = .142$), P3 ($F(7, 63) = 2.626$, $p = .020$, adjusted $R^2 = .153$), P4 ($F(7, 63) = 8.438$, $p = .020$, adjusted $R^2 = .452$), P5 ($F(7, 63) = 9.640$, $p < .001$, adjusted $R^2 = .490$), P6 ($F(7, 63) = 3.573$, $p = .003$, adjusted $R^2 = .222$), P7 ($F(7, 63) = 11.302$, $p < .001$, adjusted $R^2 = .534$), P8 ($F(7, 63) = 6.512$, $p < .001$, adjusted $R^2 = .380$), P9 ($F(7, 63) = 19.309$, $p < .001$, adjusted $R^2 = .670$)). The results of these analyses can be viewed in Tables AC.4 through to AC.12 (Appendix C). Increasing stimulus eccentricity significantly lowered OKR frequency in all but one participant (P6). Using the counting task significantly increased frequency in five participants (P4, P5, P6, P8 and P9) and had no effect on the remaining four participants (P1, P2, P3 and P7). Whether the stimulus was presented on the vertical or horizontal meridian significantly predicted frequency in P5 only, who produced a higher OKR frequency in response to stimuli on the vertical meridian. Orientation of motion significantly predicted gain in five participants: P4, P7, P8 and P9 produced higher frequency in response to vertical motion, whereas P6 produced higher frequency in response to horizontal motion. The significant interaction between orientation of motion and vertical/horizontal meridian

presentation shown at the group level was found to be driven by just two participants (P4 and P9).

Finally, the amplitude of the OKR was significantly predicted by stimulus eccentricity (β = -0.1705, $p < .001$), counting task condition (β = 0.3254, $p < .001$), and vertical/horizontal meridian presentation (β = 0.3588, $p = .005$), and there was a significant interaction between eccentricity and vertical/horizontal meridian presentation (β = -0.0440, $p = .008$). Amplitude was higher when stimuli were less eccentric, when the counting task was used, and when stimuli were presented along the vertical meridian. T-tests were used to examine the interaction between eccentricity and vertical/horizontal meridian presentation, finding that although vertical meridian presentation produced higher amplitude across the visual field, the difference in amplitude between horizontal and vertical meridian presentation was significantly larger in response to stimuli closer to the centre (<5 deg eccentricity, parafoveal region) compared to stimuli further from the centre (>5 deg eccentricity) ($t(143) = -2.075$, $p = .040$).

These analyses were repeated at the individual level to assess the consistency of the effects across participants. Significant regression equations were calculated for prediction of slow phase amplitude in all participants (P1 ($F(7, 63) = 26.764$, $p < .001$, adjusted $R^2 = .741$), P2 ($F(7, 63) = 8.965$, $p < .001$, adjusted $R^2 = .470$), P3 ($F(7, 63) = 6.052$, $p < .001$, adjusted $R^2 = .360$), P4 ($F(7, 63) = 28.627$, $p < .001$, adjusted $R^2 = .754$), P5 ($F(7, 63) = 11.923$, $p < .001$, adjusted $R^2 = .548$), P6 ($F(7, 63) = 7.293$, $p < .001$, adjusted $R^2 = .411$), P7 ($F(7, 63) = 13.043$, $p < .001$, adjusted $R^2 = .572$), P8 ($F(7, 63) = 20.357$, $p < .001$, adjusted $R^2 = .683$), P9 ($F(7, 63) = 15.601$, $p < .001$, adjusted $R^2 = .619$)). The results of these analyses are shown in Tables AC.4 through to AC.12 (Appendix C). The effect of stimulus eccentricity was found to be significant in all but one (P2) participant, with higher stimulus eccentricity being associated with lower amplitude. Orientation of motion predicted amplitude in just one participant (P2), who produced higher horizontal amplitude. The effect of the counting task was significant in seven participants, with only P6 and P1 showing no effect. The significant effect of vertical/horizontal meridian stimulus presentation identified at the group level was found to be driven by three participants (P4, P5 and P6), all of whom produced higher amplitude in response to stimuli on the vertical

meridian. The significant interaction between stimulus eccentricity and vertical/horizontal meridian presentation seen at the group level was also reflected in four individual participants (P1, P4, P5 and P8) with the remaining five participants showing no significant interaction. Finally, a significant interaction between orientation of motion and vertical/horizontal meridian presentation was identified in P1 only. A t-test showed that this interaction was due to the difference in amplitude between responses to horizontal and vertical motion being significantly higher in response to stimuli presented along the vertical meridian ($t(15) = 2.814$, $p = .013$) compared to the horizontal meridian.

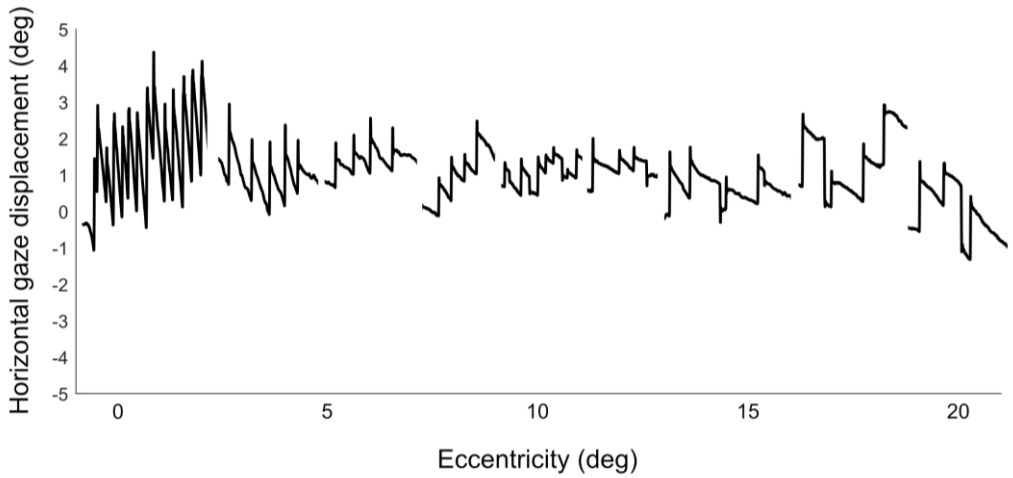

Figure 5.15: Horizontal gaze displacement traces obtained from a single participant (P1) in response to leftward drifting (temporonasal) stimuli during conditions using the counting task, across eccentricity of stimulus presentation. Traces are obtained in response to stimuli presented at eccentricities of 0.00, 4.70, 6.26, 8.26, 9.41, 12.52, 14.70, 18.81 and 20.54 deg to demonstrate the variation in the OKR waveform by stimulus eccentricity. On the Y axis, 0 indicates the vertical midline of the display: positive numbers indicate the right side of the display and negative numbers indicate the left. To create this plot, individual traces are first plotted as horizontal gaze displacement over time; on the X axis, 1 deg corresponds to 1 second.

Summary of key findings

- Gain and frequency of the OKR did not differ between the vertical and horizontal meridians
- OKR amplitude was higher in response to stimuli on the vertical meridian overall, with individual analyses finding this effect in three participants
- This horizontal-vertical meridian anisotropy of slow phase amplitude was more pronounced <5 deg from the centre; this interaction effect was shown in four participants

5.3.4 Accuracy during the counting task

The percentage of incorrect counting task responses was calculated for each stimulus eccentricity and correlated across eccentricity, revealing a significant positive correlation ($R^2 = 0.859$, $p < .001$): the proportion of incorrect responses increased with stimulus eccentricity (Figure 5.16).

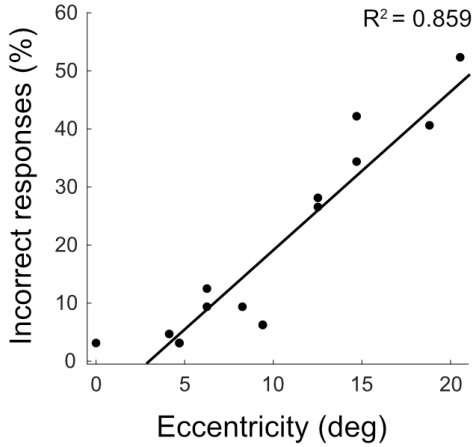

Figure 5.16: Proportion of incorrect responses during counting task trials across stimulus eccentricity

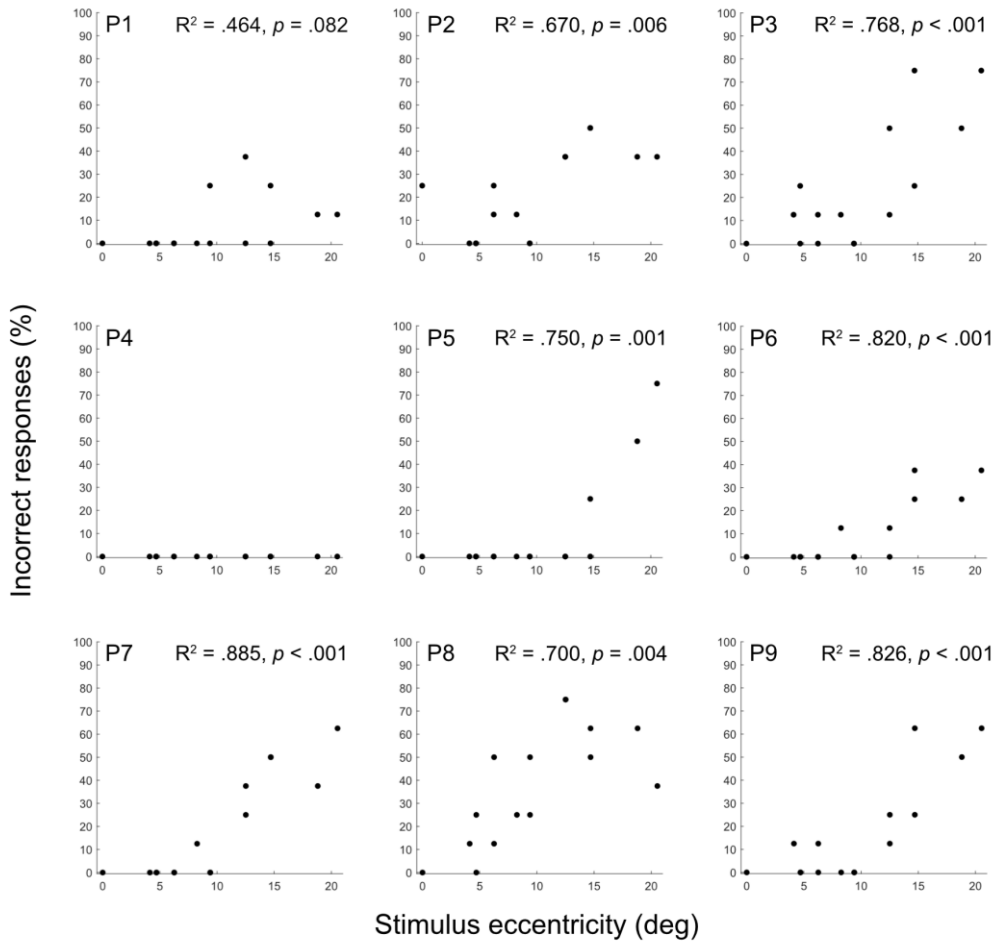

Figure 5.17: Proportion of incorrect responses during counting task trials across stimulus eccentricity in each individual participant. Participant numbers are indicated in the upper left corner of each plot; correlation coefficients and p-values are shown at the upper right of each plot.

Correlations were also carried out at the individual level; corresponding scatterplots are shown in Figure 5.17. All except P1 and P4 had a significant positive correlation between stimulus eccentricity and error rate, with R^2 ranging from 0.670 to 0.885. While P1 did make some errors that did not significantly correlate across eccentricity, P4 made no errors at all, resulting in no correlation.

Trials in which OKR was produced, but an incorrect response was provided for the counting task, were compared to those in which a correct response was provided to assess whether incorrect responses were associated with lower OKR measures. Only gain in response to stimuli beyond 10 deg eccentricity was

found to differ significantly based on response accuracy ($t(371) = 2.121$, $p = .035$): mean gain increased from 0.173 (SD = 0.068) when the task response was incorrect to 0.187 (SD = 0.051) when the task response was correct.

5.4 Discussion

It was expected that a slight drift of gaze position towards the location of the stimulus would be observed as participants attempted to best complete the counting task; the use of colour in this task makes it inherently difficult to perform in peripheral regions due to inferior colour sensitivity in the visual periphery (Hansen et al., 2009; Mullen, 1991; Newton & Eskew, 2003). However, this does not appear to have been the case. With the exception of stimuli presented to the upper visual field, average gaze position tended to be pushed away from the stimulus location. Participants were told to maintain central gaze and not to look directly at a non-central stimulus. This effect of mean gaze position drifting away from the stimulus location may have been caused by participants over-compensating due to this request. During a trial, the only available cue for the display centre was the edges of the display; the precise location of the centre was thus uncertain for the participant. This may have caused a repulsion effect which pushed fixation away from the stimulus location. However, these drifts away from the stimulus location were only slight, amounting to less than 1 deg away from the true centre.

As shown in Figure 5.4 and Figure 5.3, the mean gain, frequency and amplitude of the OKR fell sharply between 0 and 5 deg eccentricity, then declined less sharply beyond this point. This finding of a dramatic drop-off in OKR measures towards the centre and a less dramatic drop-off in the periphery is in keeping with photoreceptor and ganglion cell topography in the human retina (Curcio et al., 1990; Curcio & Allen, 1990), with a high density of photoreceptors and ganglion cells at the fovea which dramatically drops off between the fovea and the edge of the perifoveal area. This high density of photoreceptors (cones) at the fovea is mirrored in the retinotopic maps in visual cortex including the motion-sensitive MT+ complex (Amano et al., 2009). Therefore, OKR properties appear to reflect this superior central sensitivity caused by increased retinal cell density and cortical magnification in visual cortex.

Horizontal motion was found to produce an OKR with significantly higher gain and amplitude than vertical motion during stimulation of the central visual field (<10 deg eccentricity). This difference in gain and amplitude between responses to horizontal and vertical motion declined with eccentricity. Orientation of motion (horizontal versus vertical) was the largest predictor of gain in the centre (<10 deg eccentricity). In the periphery (>10 deg eccentricity), attentional modulation via the colour counting task became the largest predictor of gain, though it should be noted that this variable was not a significant predictor of gain in periphery in three of the nine participants. The finding of higher horizontal gain is consistent with previous OKR research (Valmaggia et al., 2005) and suggests an advantage in the processing of horizontal compared to vertical motion which, like the oblique effect (where orientation discrimination is superior for the cardinal axes) (Cohen & Zaidi, 2007; Furmanski & Engel, 2000; Li & Westheimer, 1997), is often attributed to the prevalence of certain orientations within the natural environment (Pilz & Papadaki, 2019). For example, horizontal motion is frequently perceived due to horizontal scanning of the environment via both eye movements and yaw rotation of the head. Group level analysis found no significant effect of orientation of motion on OKR frequency; however, individual analyses of frequency in response to stimuli between 4-10 deg eccentricity showed that four participants produced higher vertical frequency whereas one participant produced higher horizontal frequency. At the group level, the only orientation effect of frequency was observed in response to stimuli presented along the horizontal meridian.

The impact of increasing attention towards the stimulus caused a boost of OKR gain that was invariant to stimulus eccentricity; rather than seeing an increasing effect of attention towards the periphery, a uniform increase in performance was observed across the visual field. This is reminiscent of studies which have reported that attention causes a uniform boost in performance without distorting the shape of the performance field (Purokayastha et al., 2021); this is argued to indicate that such performance fields are not attentional in origin. However, a different effect was seen in the frequency of the OKR; within the centre (<10 deg eccentricity), the counting task had a greater effect on OKR frequency with increasing eccentricity, but beyond 10 deg eccentricity the effect of the counting task no longer continued to increase. It may be the case that the

effect of eccentricity on the frequency of OKR is partially caused by reduced visual attention in more eccentric visual field regions, however, attention is limited in its ability to compensate for low frequency due to other limiting factors, such as anatomy. For example, due to anatomical differences across the visual field, peripheral vision suffers particularly from visual crowding, which some have argued to be the main cause of reduced visual quality in the periphery (Rosenholtz, 2016). These factors may have simply posed a greater issue to OKR beyond 10 deg eccentricity, limiting the impact of increased attention on the response. Such effects have been previously reported, with attentional cueing reducing, but not eliminating, eccentricity effects seen in other visual domains such as visual search (Carrasco & Yeshurun, 1998). Wolfe et al. (1998) proposed that eccentricity effects in vision are caused by attentional biases in favour of the centre, as evidenced by the reduction of some eccentricity effects following attentional manipulation. That the counting task was not sufficient to bring OKR measures to the level of the centre is indicative of anatomical contributions to such eccentricity effects. The frequency of the OKR has been reported to be related to the level of attention of the observer (Frattini & Wibble, 2021), with the results of Experiment 2 (Chapter 3) providing evidence for attentional influence on OKR frequency. The coefficients produced by the regression analyses in Experiment 3 show that the counting task condition was more predictive of frequency than gain, however, in response to central visual field stimulus presentation, slow phase amplitude, not frequency, was best predicted by whether the counting task was used. This indicates that amplitude may be more strongly related to attention during central viewing, despite attention best predicting frequency during peripheral stimulation.

A lower visual hemifield advantage has been reported across a range of vision parameters, including a report of higher OKR gain in response to stimuli presented in the lower visual hemifield (Murasugi & Howard, 1989a). This effect was not replicated in the present study. Gain and amplitude did not differ between upper and lower visual field presentation, though the frequency of OKR was found to be higher in the lower visual hemifield. Despite reports of a higher attentional increase in performance in response to stimuli presented in the upper visual hemifield (Kristjánsson & Sigurdardottir, 2008), there was no difference in the effect of the counting task in either the upper or lower hemifield in terms of

gain or frequency, however, the impact of attention on amplitude was found to be higher in the upper visual hemifield. Thus, while the result of Murasugi and Howard (1989a) was not replicated, these results do offer some support for the notion of differences in OKR responses in the upper and lower visual hemifields and a greater impact of attention in the upper visual hemifield. This is partially in keeping with reports of superior visual performance in the lower hemifield such as motion discrimination (Levine & McAnany, 2005) and a corresponding asymmetry in cortical representations of the upper and lower visual hemifields at multiple levels of visual processing (Maunsell & van Essen, 1987; Tootell et al., 1998). However, whereas OKR gain provides an objective measure of the quality of the response due to describing how well slow phase velocity matched stimulus velocity, the meaning of frequency in this regard is less clear and does not necessarily indicate 'superior' performance. Further, while past research has shown that the lower visual field offers superior visual performance in many domains (Lakha & Humphreys, 2005; Levine & McAnany, 2005; Millodot & Lamont, 1974; Payne, 1967; Rossit et al., 2013; Tyler, 1987), there is evidence that this may not apply in the same way to pursuit eye movements. In monkeys, Lisberger and Pavelko (1989) found that target motion in the upper and lower visual hemifields was equally effective in initiating pursuit; they suggested that the topography of cortical maps is smoothed when the visual signals are transferred to the pursuit system, reducing the lower hemifield advantage. Given the proximity of SPEM and OKR in humans, it is entirely possible that the lower hemifield advantage is diminished in OKR.

In agreement with many past studies (e.g. Howard & Simpson, 1989; Murasugi & Howard, 1989b), a vertical asymmetry was observed whereby upward motion elicited an OKR with higher gain compared to downward motion. However, at the group level, this effect only applied to stimuli presented at less than 5 deg eccentricity; beyond 5 deg, no up-down asymmetry was observed. This finding contradicts Murasugi and Howard (1989b), who found that occlusion of the central visual field produced a vertically asymmetrical OKR. They argued that this provided evidence that the asymmetry only applies to peripheral visual field regions. In contrast, the present experiment found that only stimuli presented within the fovea and parafoveal area produced a vertical OKR asymmetry, indicating that the asymmetry exists within central vision. However, there

appears to be substantial individual differences in vertical OKR symmetry: up-down gain asymmetry was only present in three participants, whereas six participants showed no effect of the direction of vertical motion in the centre on gain. Further research is thus required to clarify the roles of the central and peripheral visual fields in vertical OKR asymmetry. This will be addressed in further detail in the General Discussion (Chapter 6). Methodological differences between the present study and that of Murasugi and Howard (1989b) must be taken into account. For example, while they used a scleral search coil to record eye movements, the present study used a video-based eye tracker (EyeLink 1000), which is less invasive and more comfortable for the participant, potentially facilitating the emergence of more natural eye movement patterns. The present study also used more participants than Murasugi and Howard (1989b), employing nine individuals compared to their seven. This is particularly relevant when considering the individual differences observed in OKR symmetry in the present study; larger samples may be required to accurately capture vertical asymmetry effects. Murasugi and Howard (1989b) used monocular stimulus viewing, whereas in the present study, stimuli were viewed binocularly. It is therefore possible that the discrepancy in results also reflects monocular versus binocular processing. Finally, the stimuli used in the two studies were different. While Murasugi and Howard (1989b) created peripheral stimuli by obstructing the centre of a full-field dot stimulus with a black occluding band, which may have acted as a stationary object within the moving field, the present study used dot stimuli presented with a circular Gaussian aperture at a variety of eccentricities, without stationary objects placed within the moving field.

Due to the arrangement of stimulus locations chosen for this experiment, there were slight discrepancies in the eccentricities along the vertical and horizontal meridians. Additionally, the aspect ratio of the display meant that more horizontal locations were included than vertical locations. To assess horizontal-vertical meridian anisotropy (HVA), stimuli between 4–10 deg eccentricity were selected from the horizontal and vertical meridians that had the closest, and thus most comparable, eccentricities (horizontal: 4.70 and 9.41 deg; vertical: 4.13 and 8.26 deg). Whether a stimulus was presented on the vertical or horizontal meridian did not significantly predict the gain or frequency of the OKR, and this was found to be highly consistent across participants. However, gain and

frequency did show a significant interaction between orientation of motion and vertical/horizontal meridian presentation. Though horizontal motion produced significantly higher gain than vertical motion regardless of whether the stimulus was presented on the vertical or horizontal meridian, the difference in gain between the response to vertical and horizontal motion was found to be significantly larger when stimuli were presented on the vertical meridian. Upon examining the mean gain in response to both orientations of motion on each cardinal meridian, t-tests indicated that the gain was slightly higher in response to stimuli presented on the vertical meridian. The difference in gain between horizontal and vertical meridian presentation was larger for horizontal motion, demonstrating that the response to horizontal motion particularly benefitted from vertical meridian presentation. Amplitude was found to be higher in response to stimuli presented on the vertical meridian, and this effect interacted with stimulus eccentricity: the extent of horizontal-vertical anisotropy (HVA) decreased with eccentricity. Similarly, some other aspects of HVA have been reported to decline with eccentricity; for example, Barbot et al. (2021) showed that the HVA effect on visual acuity (measured as orientation discrimination performance as a function of SF) reduced with distance from the vertical meridian. However, in the case of the present study, there was a benefit of vertical meridian presentation over horizontal meridian presentation, which is in conflict with the consistent evidence of superior performance along the horizontal meridian (e.g. Barbot et al., 2021) and higher photoreceptor density along the horizontal meridian (Curcio et al., 1990). It is possible that the slightly reduced eccentricity of vertical meridian stimuli has contributed to this unexpected effect. For example, Essig et al. (2022) showed that, while OKR amplitude was not significantly affected by stimulus SF or grating type, it was significantly affected by stimulus contrast, with higher contrast stimuli yielding a larger slow phase amplitude. As contrast sensitivity is known to decline with eccentricity (e.g. Thibos et al., 1996), this may contribute towards sensitivity of OKR amplitude to stimulus eccentricity. The contribution of eccentricity to this finding of superior vertical meridian performance can be investigated simply by presenting cardinal meridian stimuli with identical eccentricities.

Compared to Experiment 2, the error rate seen during the counting task in response to peripheral stimuli was higher in the present experiment. Error

rate and eccentricity showed a strong positive correlation with an R^2 of 0.859, and this relationship was found to be significant in seven participants. This effect indicates that the counting task became more difficult to carry out accurately as eccentricity increased. This is likely due to a combination of reduced colour sensitivity in more peripheral visual field regions (Hansen et al., 2009; Mullen, 1991; Newton & Eskew, 2003) and greater difficulty in allocating visual attention to more eccentric stimuli. Compared to Experiment 2, the stimuli used in the present experiment had a smaller area and were each limited to one 78.54 deg^2 patch rather than using an annular ring. This smaller stimulated area and restriction to a single region may have contributed to the higher error rate compared to Experiment 2. Beyond 10 deg eccentricity, the frequency and amplitude of the OKR were not found to differ depending on whether the counting task response was correct. The gain, however, was found to be higher during trials in which the counting task response was correct, though this only accounted for a modest increase in gain of 0.014. Overall, the difference in the OKR between correct and incorrect response trials appears to be negligible, indicating that reduced gain, frequency and amplitude with increasing eccentricity was not a consequence of an inability to engage with the task. The success of the counting task in increasing OKR measures across the visual field regardless of whether or not the response was correct suggests that participants did actively attempt to engage with the task despite occasional difficulty in providing an accurate response.

In sum, the present study provides evidence for a decline in gain, frequency and amplitude of the OKR across stimulus eccentricity and interactions between eccentricity and orientation of motion. The difference in response to horizontal and vertical motion declines with eccentricity. A vertical asymmetry was observed: gain in response to upward motion was higher than that in response to downward motion. Two different patterns of OKR enhancement were seen as a consequence of increased attention towards the stimulus: a uniform boost in gain across the visual field and a frequency boost that increased with eccentricity up to 10 deg. Overall, the evidence suggests that while attention is able to reduce some eccentricity effects and improve performance of the OKR, performance does decline with eccentricity, an effect that is likely caused by anatomical differences between the central and peripheral visual fields.

Chapter 6

General Discussion

6.1 Summary of key findings

Experiment 1 investigated look and stare OKR and OKAN in response to a drifting sinusoidal luminance grating with three stimulus velocities (10, 20 and 40 deg/s) and eight directions of motion, evenly spaced in polar coordinates. Results showed that increasing stimulus velocity resulted in reduced OKR gain. The highest gains were obtained in response to horizontal motion. The further the orientation of motion from this axis, the lower the gain. Vertical look, but not stare, OKR was found to be asymmetric with higher upward gain. Horizontal motion produced an OKR with higher gain than that of vertical motion; oblique motion produced an OKR that more closely resembled horizontal OKR than vertical OKR. Neither look nor stare OKR were more associated with occurrence of OKAN. OKAN reversal was more likely to follow an OKR with low accuracy in terms of slow phase velocity and direction; this was interpreted as offering support for the hypothesis that OKAN reversal is caused by adaptation to motion.

Experiment 2 investigated OKR in response to central and peripheral motion presented in isolation, or together with different directions of stimulus motion. A counting task was used to increase attention towards the stimulus. The results showed that increasing attention to the stimulus increased the gain, frequency and amplitude of the OKR, with responses to peripheral motion seeing a particular benefit. Increasing the area of a stimulus that included central stimulation increased the gain in response to the stimulus. Interestingly, in the absence of central stimulation, increasing peripheral stimulus area did not increase gain. During centre-surround stimuli presenting different directions of motion, the presence of this incongruent motion suppressed gain in response to both regions. Importantly, during centre-surround motion with opposite directions of motion, directing attention to the surround stimulus was sufficient to cause the

surround stimulus to drive the OKR, demonstrating that central motion is not necessarily prioritised in the OKR.

Experiment 3 aimed to more precisely manipulate stimulus eccentricity in order to elaborate on the findings of Experiment 2, using both horizontal and vertical stimulus motion. This involved selectively stimulating 27 locations across the visual field while manipulating attention using a counting task. Results showed that, across the visual field, directing attention towards the stimulus increased the gain, frequency and amplitude of the OKR. The increase in gain was uniform across eccentricity. Increasing stimulus eccentricity decreased each of these measures, with the most dramatic decrease in gain, frequency and amplitude observed within 5 deg of the centre. Interestingly, vertical asymmetry with higher upward gain was observed only in response to central (<5 deg eccentricity) motion, though this effect was only present in some participants.

In this final chapter, these findings will be discussed in terms of the wider research context, unresolved issues will be highlighted, and future directions for research will be proposed.

6.2 Vertical OKR asymmetry

Past literature has produced mixed reports regarding the vertical symmetry of the OKR in normal human adults. Some studies have reported no asymmetry (Kanari et al., 2017; Knapp et al., 2008), some have reported higher upward gain (Garbutt, Han, Kumar, Harwood, Rahman, et al., 2003; Koerner & Schiller, 1972; Murasugi & Howard, 1989b; van den Berg & Collewijn, 1988) and some have reported higher downward gain (Schor & Narayan, 1981). To further complicate matters, some authors have argued that this asymmetry is velocity dependent, reporting that it emerges at a stimulus speed of ~15-20 deg/s (Murasugi & Howard, 1989b). In contrast, others have reported asymmetry across a range of stimulus speeds, including those as low as 10 deg/s (Garbutt, Han, Kumar, Harwood, Harris, et al., 2003). Additionally, it has been suggested that this asymmetry is not uniform across the visual field: Murasugi and Howard (1989b) showed that stimulation of the central retina with a small (6x10 deg) stimulus produced a vertically symmetrical OKR whereas stimulation of the periphery

with the centre occluded produced an asymmetrical response. From this, they argued that the asymmetry of vertical OKR is caused by peripheral stimulation and resides within the LOKR system.

In Experiment 1, an asymmetrical OKR with higher upward gain was observed in response to look, but not stare, OKR conditions. This effect was not tied to velocity within the range tested (10-40 deg/s) and did not apply to oblique OKR. It is acknowledged that individual analyses showed vertical stare OKR asymmetry in some participants, however, these participants had a higher gain and amplitude stare OKR and many were unaffected by instruction type, indicating that they may have produced a more 'look-like' OKR during stare conditions. Experiment 3 also showed asymmetric vertical OKR with higher upward gain in response to stimuli presented less than 5 deg from the centre; beyond this eccentricity, vertical OKR was largely symmetrical. Taken together, these findings appear to point towards an asymmetry of pursuit. Many researchers have suggested that OKR, particularly look OKR, involves smooth pursuit due to similarities both in behaviour (Pola & Wyatt, 1985) and in activation regions shown in fMRI research (Kashou et al., 2010), with Kashou et al. (2010) arguing based on fMRI evidence that look OKR represents an alternating series of smooth pursuit eye movements (SPEM) and saccades rather than being a 'true' optokinesis. Given the evidence of SPEM involvement in look OKR, it is possible that the asymmetry observed here in responses to central stimuli and look OKR conditions reflect an asymmetry of OKR when the smooth pursuit system is more involved in the response. In assessing this possibility, it is important to consider the characteristics of SPEM. Similar to the findings regarding up-down symmetry of OKR, reports on the vertical symmetry of adult SPEM are mixed. Asymmetry has been reported in some studies, though this has been shown with both upward (Baloh et al., 1983, 1988; Rottach et al., 1996) and downward (in monkeys: Akao et al., 2007; in humans: Ke et al., 2013) preference. This mixed evidence leaves open the possibility that vertical OKR asymmetry is associated with involvement of SPEM, but firm conclusions cannot be drawn based on this.

To further consider the role of SPEM in OKR asymmetry, the symmetry of OKR should be considered in the absence of SPEM. In afoveate mammals such as mice that do not exhibit SPEM, OKR has been reported to be asymmetrical with a superior response to upward motion (Harris & Dunn, 2023). This indicates

that there is an asymmetry in the optokinetic system of such mammals, as they lack a smooth pursuit system. However, OKR is known to differ between species. For example, in non-primate mammals, retinal slip is encoded by on-direction selective ganglion cells (oDSGCs) in the retina (Dhande et al., 2013, 2015). In mice and rabbits, different types of oDSGC have been shown to respond to different directions of motion (Oyster, 1968; Oyster & Barlow, 1967; Sabbah et al., 2017). oDSGCs responding to upward and downward motion show differences in their response properties; oDCGCs responding to upward motion have broader tuning curves and higher spike rates (Harris & Dunn, 2023). This asymmetry in oDSGC response is thought to contribute to the upward asymmetry seen in the OKR of such mammals (Harris & Dunn, 2023, mouse). The primate retina is not thought to contain oDSGCs, though recent studies have identified candidate cells in the macaque retina. For example, Wang et al. (2023) identified pRGC10 cells, which show speed and direction tuning consistent with properties of oDSGCs, and Kim et al. (2022) identified potential on-off DSGCs in macaque retina. However, this research is very recent and the presence of oDSGCs in primate retina has not been established. The OKR of primates is known to be different to that of lower mammals: it shows a rapid build-up of slow phase velocity and horizontal symmetry which are thought to be due to involvement of a cortical OKR pathway and smooth pursuit (Garbutt & Harris, 1999; Leigh & Zee, 2015). It therefore seems likely that vertical asymmetry in primate OKR could arise from a different source than that of afoveate mammals such as mice and rabbits. For example, there is evidence from monkeys of reduced responses in MT to stimuli with a downward direction (Maunsell & Van Essen, 1983). It may be the case that asymmetries in directional responses in visual cortex regions contribute towards vertical OKR asymmetry in primates.

Vertical SPEM and OKR asymmetries have been reported in patients with ocular abnormalities such as strabismus. Individuals with early onset strabismus have asymmetrical vertical OKR and SPEM with reduced response to downward motion (Garbutt, Han, Kumar, Harwood, Rahman, et al., 2003; Tychsen et al., 1984; Tychsen & Lisberger, 1986). Garbutt, Han, Kumar, Harwood, Rahman, et al. (2003) demonstrated that participants with normal vision and with strabismus both showed asymmetrical vertical OKR that usually involved superior response to upward motion, though participants with strabismus

tracked vertical motion diagonally. Across these studies, the authors have suggested that the asymmetries present in individuals with strabismus may be caused by abnormal visual motion processing. As these disruptions to early visual development are associated with asymmetries in both OKR and SPEM, it is possible that these asymmetries have the same origin. Like the reports of vertical OKR and SPEM in adults with normal vision, reports in those with abnormal vision also vary in whether upward or downward motion is found to produce superior tracking. For example, while Tychsen and Lisberger (1986) found that individuals with normal vision had symmetrical vertical SPEM and those with strabismus showed an upward preference, González et al. (2018) found that individuals with central vision loss caused by macular degeneration exhibited a preference for downward motion. Given that these studies look at different patient populations, it is possible that there are multiple causes of asymmetry that vary between conditions.

The suggestion that these asymmetries are associated with abnormalities in visual motion processing (Garbutt, Han, Kumar, Harwood, Rahman, et al., 2003; Tychsen & Lisberger, 1986) is supported by evidence showing asymmetries in motion perception. In individuals with normal vision, Ono et al. (2019) showed that directional asymmetries in initial horizontal SPEM acceleration were consistent with an asymmetric bias in visual motion reaction time to different directions of motion; they argued that these asymmetries may underpin perceptual biases. In adults with early onset strabismus, Tychsen et al. (1996) showed evidence of asymmetries in the perception of visual motion direction which were not present in those with normal vision or later strabismus onset. That conditions such as strabismus are associated with asymmetry in vertical OKR and SPEM indicates that these asymmetries may be related. Unfortunately, there has been a focus on horizontal OKR and SPEM in the study of asymmetries, the result of which is that the causes of horizontal asymmetry are better understood. Additionally, the study of vertical OKR and SPEM asymmetries is complicated by the mixed reports regarding the existence and direction of the asymmetry. It may be the case that this inconsistency of reports reflects individual differences in vertical asymmetry, potentially arising from multiple sources, particularly in the case of different patient populations.

Given the evidence of asymmetry in the pursuit system of primates, and the proposed involvement of SPEM in primate OKR, it is possible that the OKR asymmetry observed here in response to central stimuli (Experiment 3) and look OKR (Experiment 1) reflects an asymmetry in the pursuit system. This pursuit asymmetry may arise from asymmetry in directional responses of neurons in visual cortex (Maunsell & Van Essen, 1983) and directional biases in the perception of motion (Ono et al., 2019; Tychsen et al., 1996). A role of SPEM and cortical responses to visual motion in asymmetry of look OKR is in keeping with fMRI data reported by Kashou et al. (2010), who found greater cortical activation during look compared to stare OKR which overlapped with activation during SPEM, with significant activation of several occipital areas including MT/V5 during look, but not stare, OKR. This indicates that these visual cortical areas are more involved in SPEM and look OKR compared to stare OKR. However, due to evidence of asymmetry of OKR in non-foveate mammals that lack a smooth pursuit system, the possibility of asymmetry within the optokinetic system cannot be ruled out.

6.3 The effect of attention on the OKR

Directing attention towards an optokinetic stimulus increases the gain, frequency and amplitude in response to the stimulus, regardless of its eccentricity. Peripheral stimuli saw a greater benefit of attention compared to central stimuli, indicating an attentional contribution to the eccentricity effect seen in the OKR. When two stimuli with opposite directions of motion were simultaneously presented in a centre-surround configuration (Experiment 2), directing attention to the peripheral (surround) stimulus was sufficient to override the central motion and produce an OKR consistent with the peripheral motion. However, attention was not sufficient to raise the peripheral response to the level of the centre. This inability to fully compensate for eccentricity indicates that anatomical factors, such as cortical magnification, play a role in eccentricity effects in OKR. Even with attention actively guided towards the periphery, slow phase velocity remained less than half the stimulus velocity.

Attention may affect responses to visual stimuli by modulating activity in neural populations responding to the available stimuli. This has been shown

to occur in area MT in response to visual motion. In monkeys, Treue and Martinez Trujillo (1999) showed that during feature-based attention the gain of direction-selective cells in MT increased without narrowing their tuning curves. The response amplitude of a neuron increased by 10% when attention was directed to a stimulus within its receptive field (RF). Attending to a motion stimulus enhanced the responses of neurons selective for that direction of motion and attenuated the responses of neurons selective for the opposite direction of motion. This was a spatially extensive effect, applying to stimuli presented 20 deg apart and in opposite visual hemifields. It therefore seems likely that such effects could apply over the stimulus area used in Experiment 2 and the eccentricities used in Experiment 3. In a similar monkey study, Treue and Maunsell (1996) showed that the response of an MT neuron decreased when attention was directed to a stimulus outside of its RF. When two stimuli were presented within the RF, the influence of the distractor stimulus was reduced, even when it was a powerful sensory stimulus. This demonstrates that responses to attended stimuli can be enhanced relative to competing stimuli within the same RF. The size and shape of a cell's RF may also be affected by attention: in monkeys, Anton-Erxleben et al. (2009) showed that attention directed toward an MT neuron's RF caused the RF to shrink, whereas directing attention outside of the RF caused the RF to expand. Attentional effects on cortical activity have also been shown in humans using fMRI; activity in the human homologue of the MT-MST complex was found to be higher when participants attended to a moving dot stimulus (O'Craven et al., 1997).

The available evidence indicates that visual attention allows neural responses to attended stimuli to be enhanced while responses to distractors are suppressed. It may be through this process that attention enhanced responses to optokinetic stimuli and allowed a peripheral stimulus to override a central stimulus and drive the response in Experiment 2. Responses of neurons selective for the direction of motion at the centre may have been suppressed while responses of neurons selective for the direction of peripheral motion were enhanced, causing a sufficient reweighting of neural responses to allow the peripheral stimulus to take precedence in driving the OKR. The fluctuating OKR that was sometimes observed in response to centre-surround stimuli during Experiment 2 either represented a state in which the responses to the two regions had become

approximately equally weighted, potentially producing rivalry between the stimuli, or a situation in which the participant's locus of attention fluctuated between the two stimuli.

The way in which attentional modulation is exerted over visual regions has been studied, and the FEF has been identified as a source of these modulating signals. The FEF, which has been shown to be active during look OKR in humans (Ruehl et al., 2019), has direct axonal projections to areas V4 and MT, shown in macaque monkeys (Anderson et al., 2011; Ninomiya et al., 2012; Stanton et al., 1995). During allocation of voluntary attention to visual stimuli in monkeys, the FEF causes activation changes in downstream visual areas (Buschman & Miller, 2007; Gregoriou et al., 2009, 2012). In a more recent study using monkeys, Hüer et al. (2024) showed evidence that the FEF is involved in exerting attentional influence over visual cortex regions. Optogenetic inhibition of the FEF input reduced attentional modulation in MT neurons by approximately one third, without impacting the sensory response component of the neuron. During attention, input from the FEF increased neuronal firing rates when attention was directed inside the neuron's RF and decreased their firing rates when attention was directed outside of the RF, demonstrating target enhancement and distractor suppression. This thus describes an effect similar to that observed by Treue and Maunsell (1996) in MT, indicating that signals from the FEF may have been responsible for the reported attentional modulation of MT neuron activity. Studies of V4 in monkeys and humans have also shown modulation of neuronal responses to attended and unattended stimuli resulting from an FEF signal (Armstrong & Moore, 2007; Gregoriou et al., 2009, 2012, 2014; Marshall et al., 2015; Moore & Armstrong, 2003; Veniero et al., 2021), indicating that attentional signals from the FEF modulate activity in several visual areas. It may be possible to study this in the context of the OKR using methods similar to those used in the above studies; for example, in monkeys, Hüer et al. (2024) inhibited the FEF and measured the way in which this impacted attentional modulation of MT neurons, and Treue and Martinez Trujillo (1999) recorded from MT neurons to investigate the effects of allocating attention to different motion stimuli on the cell's response. By employing such methods and applying a stimulus similar to those used in Experiment 2 and eye tracking methods, one can investigate how inhibition of the FEF impacts both activity in visual neurons responding to

optokinetic stimuli and the driving stimulus for the OKR, as well as the way in which allocating attention to different stimulus regions impacts the response of visual neurons during OKR.

Attention may thus exert its effects on the OKR by modulating responses in visual areas responsible for processing visual motion under the direction of mediating signals generated in the FEF. The extent to which neuronal responses to the available stimuli are enhanced or suppressed may determine whether the activity in response to the peripheral stimulus is sufficient to override the OKR in response to the central stimulus. The manner in which neural responses to attended and unattended stimuli are modulated by attention can be described by divisive normalisation models; this will be discussed in further detail in the following section.

6.4 Centre-surround interactions

The use of stimuli with a centre-surround (C/S) configuration presenting different directions of motion to the centre and to the surround showed that gain in response to the centre was slightly reduced by the presence of incongruent motion in the surround in some participants. More so, gain in response to the surround was reduced by the presence of incongruent motion in the centre in all participants. The presence of motion with a different direction in the centre or in the surround thus had a suppressive effect on the gain of the OKR, with responses to the surround being particularly affected by central motion. This effect occurred regardless of whether the incongruent motion was coherent or Brownian. These results indicate a suppressive interaction between the centre and surround stimulus regions, which may be accounted for by effects such as surround suppression.

Area MT/V5 contains neurons with large RFs. For example, in owl monkeys, Felleman and Kaas (1984) reported that MT RF size ranged from 4 to 25 deg in width. As in other visual areas, these RF sizes become larger and more elongated with eccentricity, as demonstrated by Hangen et al. (2022) in marmosets. Stimuli outside of the RF of an MT neuron do not trigger a response in the neuron; however, they are able to normalise the responses to stimuli within the

cell's RF (Britten & Heuer, 1999). This normalisation occurs over large regions that extend beyond the RF of the cell. In monkeys, Britten and Heuer's (1999) reported that the largest RF was ~9 deg, while stimuli divisively interacted over a distance of at least 20 deg. When more than one moving stimulus is available, researchers have suggested that MT neurons average inputs via divisive operations (Recanzone et al., 1997). The suppressive effects seen as a result of C/S stimuli during Experiment 2 may be partly caused by divisive normalisation being performed by cells in visual cortex responding to the stimulus motion.

Surround suppression is usually discussed in the context of a centre and a surround that contain motion drifting in the same direction. It explains why increasing the area of a stimulus beyond a certain size can sometimes reduce responses to that stimulus, as responses are suppressed when a stimulus exceeds the classical RF (Jones et al., 2001). These centre-surround interactions have been reported in macaque monkeys in MT (Anton-Erxleben et al., 2009) and MST (Eifuku & Wurtz, 1998). Using rabbits, some visual neurons have been found to possess an extra-classical RF that surrounds the classical RF, where stimuli presented in the extra-classical RF do not trigger a response in the cell but can have a modulating effect, either excitatory or inhibitory, on the activity of the neuron (Barlow & Levick, 1965). In monkey MT, stimuli presented outside of the classical RF have been shown to modulate responses to stimuli within the RF (Albright & Stoner, 2002; Allman et al., 1985b; Xiao et al., 1997). In this way, motion presented to the centre or surround of the C/S stimulus may have a modulating influence on visual neurons responding to motion in each direction, resulting in a suppressed response. In the context of directionally selective cells responding to visual motion, these centre-surround interactions are usually reported to be antagonistic (e.g. Allman et al., 1985a), often with surround motion in the centre's preferred direction inhibiting the response; however, a facilitatory effect is seen in some neurons whereby the preferred motion in the surround reinforces the activity of the neuron (Barlow & Levick, 1965; Zarei Eskikand et al., 2020). Using monkeys, Huang et al. (2007) showed that the dominance of antagonistic surrounds in the literature is related to the stimulus characteristics used in these studies: there is evidence that the centre-surround interaction varies with stimulus factors such as contrast (Huang et al., 2007; Zarei Eskikand et

al., 2020). Such facilitatory effects may contribute to the increases in OKR gain observed as the size of a central stimulus is increased.

The responses of some visual neurons are affected by the presence of more than one stimulus in the RF. In macaque monkeys, Recanzone et al. (1997) showed that two stimuli within an MT or MST RF interact, producing either an increase or a decrease in the neural response. They found that when one of the two present stimuli drifted in the null (opposite, non-preferred) direction, the response in the cell was smaller than when only the preferred stimulus was present. The response to the preferred stimulus is thus normalised with respect to the non-preferred stimulus. They argued that their results show that the responses of MT and MST neurons are predicted by a vector average of the responses to the component stimuli. Similarly, in macaque monkeys, Rust et al. (2002) showed that when grating stimuli drifting in the cell's preferred direction were paired with stimuli drifting in the non-preferred direction, the presence of the non-preferred grating had a suppressive effect on the response. This effect was stronger when stimuli were presented at the same location and weaker when they were separated in space. From this, they concluded that non-preferred stimuli inhibit responses when they are proximal to the preferred stimulus. The effect of the presence of multiple moving stimuli has also been assessed in the context of oculomotor control. Groh et al. (1997) used microstimulation of MT neurons in monkeys, finding that the pursuit and saccadic systems use a vector average of the available stimuli to calculate planned eye movement velocity.

Suppressive effects of motion within and beyond the classical RF may partly account for the results obtained in Experiment 2. MT has a retinotopic organisation with an expanded foveal representation: in macaque monkeys, Van Essen et al. (1981) reported that the central 15 deg of vision occupies more than half of its surface area. More eccentric RFs are also larger in size (in marmosets: Hangen et al., 2022). Centre stimuli thus likely occupy more RFs and RF centres compared to more eccentric regions of surround stimuli, while having smaller RFs that may be less likely to extend into the surround motion. The presence of incongruent motion in one region of the stimulus may have a suppressive effect through modulating responses of neurons responding to the motion in areas such as MT; the incongruent motion appears to have a normalising effect on the response. That central motion has a larger suppressive effect on surround motion

than the reverse may be a consequence of central stimuli occupying more RFs and RF centres, and neurons responding to more eccentric motion having larger RFs that may be more likely to overlap with a region of incongruent motion. Cells with RFs located at regions of the visual field where the centre and surround stimuli meet will have more than one direction of motion present within the RF. Through vector averaging, this may result in a reduced response to the stimulus (Recanzone et al., 1997) and a lower velocity estimate being used in oculomotor planning (Groh et al., 1997).

Centre-surround interactions between stimuli may also be modulated by attention. There is evidence that attention can impact the shape and size of MT neuron RFs. In the context of C/S Opposing stimuli in Experiment 2, this indicates that directing attention to the central stimulus shrinks the RF size of cells responding to that central stimulus; this may reduce the suppressive impact of the surround motion. Attention also influences the extent of surround suppression: in macaque monkeys, surround suppression has been shown to be stronger when attention is directed to a surround rather than a centre stimulus (Sundberg et al., 2009). This may also account for why directing attention to the surround region of a C/S Opposing stimulus had such a dramatic effect on gain in response to the centre: by directing attention to the surround, the suppression of responses to the central motion may have increased. Similarly, while applying a divisive normalisation model of attention (Reynolds & Heeger, 2009) to such effects, Kınıklıoğlu and Boyaci (2022) reported that the suppression was stronger during a 'wide attention' condition (humans observers asked to attend to the surround) compared to a 'narrow attention' condition (observers asked to attend to the centre). An effect such as this may contribute towards central motion having a greater effect on responses to the surround compared to the effect of surround motion on the centre: the widening of the attention field that occurs when attention is directed to the annular stimulus in the surround may have selectively strengthened the effects of suppression.

In the normalisation model of attention, both the stimulus drive and the suppressive drive contribute to the response of a neuron (Reynolds & Heeger, 2009). This model describes a 'stimulus drive' which represents a neuron's response to the stimulation field in the absence of attention or normalisation (Reynolds & Heeger, 2009). In the context of C/S stimuli, this may represent a

neuron's response to a given direction of stimulus motion, for example motion in the centre. In contrast, the suppression field includes the features and locations that contribute to suppression. The 'suppressive drive' describes the amount of suppression contributing to a neuron's response; this suppression divisively normalises the stimulus drive and is pooled over a broader range of locations and features compared to the stimulus drive. Importantly, this model includes an 'attention field' which is multiplied by the stimulus drive prior to normalisation by the suppressive drive. This calculation determines the output firing rate of a neuron. This model is thus able to account for effects described earlier in this chapter, such as the findings of Treue and Martinez Trujillo (1999) showing that responses of monkey MT neurons are affected by the allocation of visual attention, while also incorporating effects such as surround suppression. In the context of Experiment 2, central motion may be particularly detrimental to responses to the surround stimulus due to providing a stronger suppressive drive to cells responding to the surround motion, or due to more eccentric motion providing a weaker stimulus drive than central motion. In this way, the extent to which motion in the centre of the C/S stimulus normalises responses to the surround region may be greater. These differences between the excitatory and inhibitory drives provided by each region may be exacerbated by differences in the attention field between the two conditions, such as the effect reported by Kınıklıoğlu and Boyaci (2022), where a wider attention field resulting from directing attention to the surround of a C/S stimulus resulted in a greater suppressive effect. However, that attention provided a greater boost to OKR gain in the peripheral response could be interpreted as an indication that the multiplication of the stimulus drive by the attention field was larger during conditions of surround attention compared to conditions of centre attention.

6.5 Stimulus area and eccentricity

Experiments 2 and 3 confirmed that peripheral motion can drive the OKR. In contrast with the report of Dubois and Collewijn (1979), directing attention to the peripheral stimulus was not required to induce a peripheral OKR. However, directing attention to the peripheral stimulus enhanced the OKR by increasing its gain, frequency and amplitude. In Experiment 2, increasing

stimulus area significantly increased OKR gain when the fovea was stimulated. When foveal stimulation was removed, increasing the area of the stimulus did not increase OKR gain. Though gain in response to a non-foveal stimulus was largely invariant to stimulus area, achieving a gain of ~1.0 appeared to depend on the inclusion of peripheral stimulation. Therefore, in normal adult observers, stimulation of the fovea is crucial for producing high-gain OKR. Removing even the central 19.63 deg^2 (i.e. a central patch 5 deg in diameter) markedly lowered gain; this gain reduction was largely invariant to the size of the central occlusion. In other words, increasing stimulus area only increased gain when foveal stimulation was included, and during foveal stimulation, extending stimulation into the peripheral retina was necessary for the slow phase to match the stimulus velocity at the velocities tested (15 and 30 deg/s). Further demonstrating the importance of foveal stimulation, the results of Experiment 3 showed that moving the stimulus away from the central field dramatically reduced OKR gain. Beyond 5 deg eccentricity, further increases in stimulus eccentricity had a smaller effect on the OKR, indicating that each deg of eccentricity is more impactful towards the centre.

The importance of central stimulation in driving the OKR has been disputed in the literature. Previous studies have reported that central stimulation is a more effective driver of the OKR (Abadi et al., 2005; Cheng & Outerbridge, 1975), in agreement with the results presented here. However, in contrast, Cheng and Outerbridge (1975) reported that deletion of the central 5 deg had little effect on the OKR. Similarly, in a study using patients with central scotoma, Valmaggia et al. (2001) reported that OKR was only affected when a scotoma was larger than 20 deg and the stimulus velocity was above 30 deg/s. Conversely, van Die and Collewijn (1982) found that deletion of the central 5 deg dramatically reduced the gain of the OKR in a manner similar to that seen in Experiment 2. These differences across studies may result from variations in methods to remove central stimulation. For example, artificial occlusions and real scotoma may impact the OKR in different ways, with artificial occlusions having a more detrimental effect, though van Die and Collewijn (1982) reported that the impact of removal of the centre on the OKR was comparable across real and artificial scotoma. Experiments using artificial occlusions vary in the types of masks used to occlude the centre. Cheng and Outerbridge (1975) removed the centre using a

square mask with hard edges, whereas Experiment 2 used a circular mask with blurred edges. The mask used by Cheng and Outerbridge (1975) therefore did not simulate the appearance of a scotoma; to the observer, the square mask may have appeared as a stationary object within the moving field. Differences such as this may contribute to the dramatic differences in outcomes between studies of the effects of removal of central stimulation on the OKR.

The processing and perception of motion may differ between central and peripheral visual field regions, contributing to eccentricity effects in the OKR. For example, drifting gratings in the visual periphery are perceived to move more slowly (Johnston & Wright, 1986), indicating that stimulus velocity may be underestimated with increasing eccentricity. Temporal summation times have also been shown to differ between central and peripheral regions: Melcher et al. (2004) demonstrated longer temporal summation in response to central stimuli and showed that attention was able to reduce the difference in temporal summation time between central and peripheral visual field regions. This evidences a difference in motion processing between the central and peripheral visual fields and demonstrates that attention may improve perception of motion in eccentric visual field regions by extending the duration of temporal summation. De Bruyn (1997) showed that while transparent moving textures are segregated in central vision, they are blended in the periphery, creating the perception of motion corresponding to the average of the composite stimuli. They argued that this provides evidence of distinct motion processing mechanisms in the periphery. Mareschal et al. (2008) reported higher motion discrimination thresholds in the peripheral visual field which were not caused by reduced visibility in the periphery. This eccentric deterioration of motion discrimination was instead attributed to an increase in local directional uncertainty caused by internal noise. They argued that this result was a reflection of the properties of motion detectors in the visual periphery. For example, in monkeys, direction selectivity in V1 has been shown to decrease with eccentricity (Orban et al., 1986). The outcomes of these studies indicate that peripheral motion may be perceived less accurately in terms of its speed and direction, and may be associated with different processing mechanisms compared to central vision. Upon finding higher OKR gain in response to centrally presented stimuli in humans, Abadi et al. (2005) suggested that central gain was higher due to RFs for detection of motion being smaller at less

eccentric regions, resulting in superior sensitivity to low velocity retinal motion that occurs during relatively high-gain OKR (Barnes, 1993; Smith & Snowden, 1994). In this way, the slow phase velocity may be better 'fine-tuned' in response to central stimulation due to enhanced sensitivity to small amounts of residual motion. Differences in the perception of motion across the visual field may contribute towards differences in gain across the visual field. This can be assessed by testing whether thresholds for visual motion perception are correlated with the gain of the OKR, or by having participants perceptually match the perceived speed of stimuli at different eccentricities and assessing whether OKR gain follows the actual or perceived velocity.

In addition to eccentricity, the size of a stimulus is known to impact the perception of that stimulus. For example, thresholds for determining the direction of motion reduce as stimulus size increases (Hutchinson & Ledgeway, 2010; Watamaniuk & Sekuler, 1992). As mentioned previously, studies involving non-human animals have shown that some visual neuron RFs have facilitatory surrounds where surround motion in the preferred direction increases the response of the neuron (Barlow & Levick, 1965; Zarei Eskikand et al., 2020). Increasing the size of a stimulus beyond the RF centre thus increases the activity of such neurons. The enhanced OKR gain associated with increased stimulus size may partly result from increased activity in visual neurons with facilitatory surrounds.

Eye movements are also known to affect the perception of motion in humans, and this too may vary with stimulus size and location. Using a pursue and fixate method with drifting grating stimuli, Turano and Heidenreich (1999) showed that eye movements affect the perceived speed of distal stimuli. When eye movements moved in the opposite direction to the stimulus motion, small stimuli (8 deg) were associated with increased perceived speed whereas larger (18 deg) stimuli were associated with decreased perceived speed. They argued that the way in which eye movement velocity is represented is influenced by stimulus size, causing eye velocity to be either under- or over-represented when the speed of the stimulus is estimated. In a similar study, Brenner and van den Berg (1994) reported that estimates of target velocity during pursuit are affected by an underestimation of eye velocity when the eyes move in the same direction as background motion; when moving in the opposite direction to the background

motion, perceived target speed was based on retinal slip. In reference to C/S Opposing stimuli used in Experiment 2, results such as these indicate that errors in estimates of eye movement velocity impact perceived speed in a way that may be modulated both by the size of the stimulus and by whether the direction of stimulus motion matches the slow phase direction. This may affect the gain of the OKR by causing motion speed in each region to be perceived differently.

'Pursuit cells' of the superior temporal sulcus (STS) of MT have been shown to have preferences for different stimulus sizes and to change their response level based on stimulus size. Komatsu and Wurtz (1988) recorded from pursuit cells in monkeys in response to dot field stimuli. Cells that preferred large field stimulation showed changes in their responses as stimulus size was increased. For example, one cell with a very large (80x80 deg) RF was shown to increase its spike rate as stimulus size was increased from 10x10 deg to 73x73 deg, with the most dramatic increase seen between 10x10 deg and 40x40 deg. Interestingly, the increase in stimulus area also caused the preferred direction of motion of the cell to reverse; at below 30x30 deg stimulus size, the cell showed a preference for downward motion, however, above this size, a preference for upward motion was demonstrated. This result demonstrates that the activity of pursuit cells preferentially responding to large field motion, such as that typically used to induce OKR, is affected by stimulus size. The reversal of the cell's preferred motion direction with an increase in stimulus size highlights that the relationship between stimulus area and neural responses to visual motion is highly complex and impacted by a number of different factors.

The available evidence indicates that motion perception thresholds are affected by stimulus area (Hutchinson & Ledgeway, 2010; Watamaniuk & Sekuler, 1992) and eccentricity (Mareschal et al., 2008; Melcher et al., 2004); these effects of stimulus factors on perception thresholds may contribute to changes in OKR gain. Though Experiment 2 found that, in the absence of foveal stimulation, increasing peripheral stimulus area did not increase the gain of the OKR, it is possible that this was due to the range of stimulus sizes used; it cannot be ruled out that a more dramatic increase of peripheral stimulation, for example by full-field stimulation, might produce an effect. Approaching the fovea, each deg of eccentricity appears to become more impactful on the OKR; this may be due to factors such as smaller RF sizes towards the centre (Hangen et al., 2022), over-

representation of the fovea in visual areas such as MT (Van Essen et al., 1981) and differences in the perception of motion at the centre compared to the periphery (Johnston & Wright, 1986; Melcher et al., 2004; De Bruyn, 1997; Mareschal et al., 2008). If estimates of visual motion features obtained from the centre are more accurate than those of the periphery, this information may simply be more heavily weighted when determining the required slow phase velocity.

6.6 OKAN reversal as an adaptation effect

Reversed OKAN (OKAN-II) is difficult to study in human observers: human OKAN data are noisy, and OKAN-II is not observed in every individual (Gygli et al., 2021). For this reason, the cause of OKAN reversal is not well understood. Stimulus velocity has been proposed to contribute, with slower stimuli producing OKAN-I and faster stimuli causing OKAN to reverse (Clément et al., 1981; Collewijn, 1985). Experiment 1 showed that reversal of OKAN was indeed predicted by stimulus velocity; however, stimulus velocity and OKR gain were collinear, as increasing stimulus velocity significantly reduced gain. With velocity controlled for, OKR gain was found to significantly predict OKAN reversal. This confirms that lower OKR gain is associated with OKAN-II, leaving a question mark over the role of stimulus velocity in reversal of OKAN.

Adaptation to motion has been hypothesised to be a cause of OKAN reversal. Some researchers have proposed that OKAN-I and OKAN-II should be considered to result from separate mechanisms. For example, Gygli et al. (2021) argued that they are independent exponential functions with opposite sign: OKAN-II opposes OKAN-I. They showed that participants who produced OKAN-II had reduced OKAN-I velocity compared to individuals who only produced OKAN-I, and that OKAN-II was associated with longer exposure times up to three minutes. They interpreted the reduced OKAN-I velocity as being caused by the opposing impact of the OKAN-II component. Their results agree with the proposal of Brandt et al. (1974) that reversal of OKAN is caused by adaptation to motion during the preceding optokinetic stimulus. This adaptation was described as being a negative velocity command which summates with OKAN-I activity but decays over a longer time period (Gygli et al., 2021). In this way, different patterns of OKAN can be observed depending on the intensity of

each component. Chen et al. (2014) also produced evidence of a link between motion adaptation and OKAN reversal. Following suppression of OKR using a fixation point, reversed OKAN occurred when an observer experienced motion after-effect induced eye movements and retinal afterimages. The finding of a relationship between low OKR gain and OKAN reversal in Experiment 1 can be interpreted as offering support for a link between motion adaptation and OKAN-II, as it indicates that the greater relative retinal motion resulting from lower OKR gain was associated with reversal of the OKAN direction.

Oblique motion was exploited to investigate this hypothesis. In response to oblique motion, an OKAN which was reversed only in the vertical component was sometimes observed. For example, following stimulation with a stimulus drifting in the down-right 45° direction, an OKAN with a slow phase in the up-right 45° direction was seen. The properties of the preceding OKR were investigated, showing that this vertical reversal was predicted by a shift of the OKR slow phase direction towards the horizontal axis. During such an OKR, the gain of the horizontal component would be greater than the gain of the vertical component, resulting in net vertical motion across the retina as an oblique stimulus is tracked horizontally. That this resulted in vertical, but not horizontal, OKAN reversal thus provides support for the motion adaptation hypothesis. In the two-component model that views OKAN-I and OKAN-II as separate, opposing forces, this vertical reversal might be explained by the horizontal OKAN component being a result of discharge of VSM activity stored during the preceding OKR (OKAN-I component) being greater than any adaptation to horizontal motion during stimulation (OKAN-II component), and the vertical OKAN component being reversed due to the discharge of VSM activity (OKAN-I component) being opposed and overpowered by the greater adaptation effect (OKAN-II component) caused by reduced vertical gain. By extension, this indicates a separation between vertical and horizontal OKAN components, possibly associated with separate VSMs.

6.7 Considerations for OKR as a no-report measure

The findings of this project have highlighted a number of variables that impact the OKR and should be considered when endeavouring to use OKR as an

objective no-report measure in clinical and research settings. For no-report measures such as the induction method used in OKR-based acuity testing (Aleci et al., 2018; Shin et al., 2006) which use the absence or presence of an OKR to make assumptions about the visibility of a stimulus or stimulus feature, the main consideration is use of a stimulus that will definitely invoke and OKR when visible. In Experiment 1, one participant produced no downward stare OKR in response to a grating drifting at 40 deg/s despite producing a rigorous response under different conditions. This absence of a response was not a consequence of an inability to perceive the stimulus. This indicates that visibility of the stimulus is not the only factor determining whether an OKR will be induced; there may be individual differences in the velocity at which OKR, particularly vertical stare OKR, breaks down. Such limitations must be considered in methods associating the presence or absence of an OKR with visual function.

No-report measures that attempt to make assumptions about visual function based on the characteristics of the induced OKR, such as its gain, may suffer from a lack of consideration for other factors affecting the OKR. For example, it has been proposed that OKR may serve to provide an estimation of the extent of visual field loss (VFL) due to a correlation between the extent of simulated visual field loss (SVFL) and the gain of the OKR (Doustkouhi et al., 2020b). Doustkouhi et al. (2020b) used observers with normal vision and varied the extent of SVFL, reporting that as the percentage of the stimulus that was masked increased, the gain of the OKR in response to the stimulus decreased. The stimulus used in their study (see Chapter 1: General Introduction, Figure 1.13) included a spared circular patch of stimulation over the fovea (5 deg); beyond this central patch, the extent of peripheral stimulation was varied using a mask. However, the findings of the present project indicate that this central 5 deg of stimulation is the most critical region for producing high-gain OKR, and that the effect of stimulus area on gain may be reliant on the presence of this foveal stimulation. Upon removal of this region in Experiment 2, increasing peripheral stimulus area did not significantly increase gain. The correlations reported by Doustkouhi et al. (2020b) between the gain of the OKR and the extent of SVFL may therefore be dependent on the presence of a spared circular 5 deg patch of stimulation centred over the fovea; if a different pattern of central visual sparing was tested, or SVFL with the centre masked, the outcome may not be the same. The results of Experiment 2

indicate that removal of this central stimulation may result in no correlation between stimulated area and gain. Such outcomes would limit the clinical usefulness of this measure, as attempts to measure the extent of VFL should not be reliant on the presence of a specific VFL topography.

Results obtained in studies using artificial occlusions and pathological scotoma are often very different; this poses a threat to the generalisability of findings obtained using SVFL. In Experiment 2, removal of the central 5 deg by masking dramatically reduced the gain of the OKR; this effect was also reported by van Die and Collewijn (1982), whereas Valmaggia et al. (2001) reported that central scotoma patients' OKR gain was unaffected if the scotoma was less than 20 deg in size. Similarly, Abadi and Pantazidou (1997) examined OKR in individuals with age-related macular degeneration (AMD) and age-matched controls in response to stimuli drifting at 30, 50 and 70 deg/s, finding no difference in gain between participants with AMD and controls. This surprising preservation of the OKR in the presence of maculopathy may be related to the ability to 'fill in' the stimulus at the location of the scotoma, in addition to a preference for central vision (Gloriani & Schütz, 2019). Cohen et al. (2003) reported that bilateral scotoma was associated with filling in whereas unilateral scotoma was not, and Valmaggia and Gottlob (2002) found that OKR was elicited by filling in of the scotoma in individuals with AMD, resulting in an OKR of similar gain to that of age-matched controls. These findings indicate that scotoma may be less detrimental to the OKR than artificial occlusions, that the OKR may be unaffected by central scotoma below a certain size, and that 'filling in' of bilateral scotoma may facilitate the OKR. Attempts to develop methods of quantifying visual field loss based on OKR gain should thus focus on using participants with real visual field loss, as results obtained using SVFL may exaggerate the effects of central field loss on the OKR.

The impact of attention on the OKR should also be considered in the development of methods to quantify VFL using OKR gain. In the absence of central stimulation, gain in response to the periphery was approximately doubled by directing attention to the peripheral motion. A measure that relies on an association between VFL and gain, such as the correlation reported by Doustkouhi et al. (2020b), may therefore be unduly affected by the attention of the observer. Inconsistencies in the allocation of attention throughout testing may disrupt the

correlation between extent of VFL and OKR gain, particularly in the absence of central stimulation.

The location of a scotoma in relation to the slow phase direction may also affect the OKR. Studies of SPEM indicate that eye movements are affected depending on whether they are made towards or away from the location of the scotoma. Shanidze et al. (2016) reported that the gain of pursuit was significantly lower in response to targets moving towards the scotoma compared to those moving away from it. Given the similarities between OKR slow phases and SPEM, it is possible that such an effect will also apply to the OKR. In this way, the direction of motion of an OKR stimulus being used to assess VFL may impact the gain obtained in response to the stimulus. However, further research is required to assess the way in which scotoma location affects the symmetry of the OKR. It may be possible to incorporate this information into methods of OKR-based VFL assessment in order to obtain some topographical information about VFL.

Gain is not the only aspect of the OKR that is affected by stimulus eccentricity. Including frequency and amplitude in addition to gain may provide a more robust measure in the context of VFL assessment. The coefficients obtained in regression analyses during Experiment 3 indicate that, compared to the gain, the frequency and amplitude of the OKR can be even more sensitive to stimulus eccentricity. Figure 5.16 (Chapter 5: Experiment 3) shows how the OKR waveform varies dramatically with eccentricity; this effect is not well captured by relying only OKR gain. There is often a focus on gain in the OKR literature, but incorporating other characteristics of the OKR may improve the diagnostic potential of OKR-based measures of visual function. However, due to the focus on gain, may studies of OKR do not report frequency or amplitude measures (e.g. Doustkouhi et al., 2020b; Knapp et al., 2008; Rubinstein & Abel, 2011; Williams et al., 2016), the result of which is that the effect of many variables, such as stimulus appearance or ocular disease, on the frequency and amplitude of the OKR is less well understood.

Beyond the clinical applications of the OKR, it has been proposed that the OKR could be used as a measure of attention (Frattini & Wibble, 2021; Rubinstein & Abel, 2011; Williams et al., 2006). The results of Experiment 2 indicate that attention can be used to change which available motion stimulus drives the

OKR. However, attention is not the only determining factor. Even with the surround attended, the centre region of the C/S Opposing stimulus sometimes elicited an OKR, though it is noted that this may be related to difficulty in maintaining visual attention on the peripheral stimulus. There were individual differences in the extent to which an attended peripheral stimulus drove the OKR in the presence of a competing central stimulus. For example, in Experiment 2, one participant (P6) did not produce any OKR consistent with the direction of motion in the surround during this condition, despite accurately responding to the counting task presented to the surround. This shows that despite actively engaging in the peripheral attention task, the central, 'unattended' stimulus drove the response. An alternative explanation for this finding is that this participant divided their attention between the central and peripheral stimuli, with sufficient attention being reserved in the centre for that stimulus to drive the response while the task was carried out in the surround. In this participant, the gain and frequency of the response to the centre was reduced as a result of attending to the surround; this indicates that attending to the surround motion did affect the OKR despite the surround not driving the direction of the response. If it is the case that this outcome was an effect of divided attention, this result could be interpreted as offering further support for the use of OKR as a measure of attention as it may demonstrate the effect of multiple levels of attention on the OKR.

Further investigation of the impact of attention on the OKR with a focus on more naturalistic stimuli and stimuli including depth cues would be of benefit to the application of OKR as a measure of attention; this information could improve the versatility of such a measure. For example, OKR could be used to provide an indication of the locus of visual attention in a context such as driving research in order to better understand the way in which drivers direct their visual attention while navigating different environments. In the present project, artificial stimuli such as random-dot kinematograms have been used; these stimuli present first-order motion, with different directions of motion in different regions being presented to the same depth plane in the form of C/S stimuli. It may be the case that the results obtained here do not fully transfer to more complex, naturalistic stimuli that include depth information. The availability of stimuli at different depths may complicate the way in which attention and retinal location affect the OKR. Kanari and Kaneko (2019) showed that when attention is directed

to a central stimulus while vergence is maintained on a peripheral stimulus, the central stimulus drives the OKR. However, when vergence is on the central stimulus and attention on the peripheral stimulus, the OKR is driven equally by both stimuli, producing an alternating response similar to that seen in response to some C/S Opposing stimuli during Experiment 2. This indicates that the attended stimulus does not necessarily drive the OKR when attention and vergence are at different loci, and that the relationship between these factors depends on which stimulus is central or peripheral. Though it seems unlikely that vergence and attention would be directed towards different stimuli under normal viewing conditions, these results nonetheless highlight that in a natural environment with stimuli available at different depth planes, other factors outside of attention and retinal location impact the driving stimulus of the OKR. Applying OKR-based measures in such contexts will thus rely on further research being carried out using more complex stimuli.

OKR offers the potential of a promising no-report measure that may widen the participant pool in research and increase accessibility to testing of visual function for disabled individuals and very young children. It offers the possibility of accommodating the inclusion of individuals, such as those who are non-speaking or non-compliant due to disability, to be tested in clinical settings and to be involved in research as participants. The inclusion of such individuals in research will ultimately aid in better understanding these populations. However, factors highlighted here indicate that successful application of OKR-based methods relies on consideration of a wide range of exogenous and endogenous variables, such as the attention of the observers and the velocity and direction of stimulus motion, in the development of such measures.

6.8 Unresolved issues and future directions

6.8.1 The role of smooth pursuit in OKR asymmetry

Due to the finding of vertically asymmetric OKR mainly in response to look OKR (Experiment 1) and central stimuli (Experiment 3), it was argued that this asymmetry may be related to smooth pursuit asymmetry. However, as with the OKR literature, the smooth pursuit literature reports outcomes in adults with

normal vision varying from no asymmetry (Tychsen et al., 1984; Tychsen & Lisberger, 1986) to upward preference (Baloh et al., 1983, 1988; Rottach et al., 1996) to downward preference (in monkeys: Akao et al., 2007; in humans: Ke et al., 2013). Many studies report that vertical SPEM asymmetry does vary between individuals (Baloh et al., 1988; Tychsen & Lisberger, 1986), an effect that has also been reported in vertical OKR asymmetry (Knapp et al., 2008) and that has been observed in the present study, leaving open the possibility that vertical asymmetry in OKR and SPEM is idiosyncratic. This may explain the varied results reported across the literature. In order to assess whether these vertical asymmetries are related, they could be investigated within individuals to test for consistency. The vertical symmetry of both OKR and SPEM could be assessed across a range of individuals to determine whether asymmetries in both eye movement types are internally consistent: this would indicate that they arise from a common source that varies between individuals. Additionally, as it has been suggested that such asymmetries are associated with asymmetry in visual motion perception (Ono et al., 2019), it would be useful to also assess whether these OKR and SPEM asymmetries, when present, are associated with biases in motion perception thresholds for different directions of motion. Such an outcome would provide support for the assertion that vertical tracking asymmetries are a consequence of anisotropies in visual motion processing that vary between individuals.

6.8.2 The effect of attention on the OKR

Difficulty in directing attention to the visual periphery, particularly in the context of a colour-based task, may have caused the role of attention in response to more eccentric stimuli to be underestimated. During Experiment 2, error rate in response to surround stimuli was higher than that of centre stimuli, and analysis in Experiment 3 showed a strong positive correlation ($R^2 = 0.859$) between eccentricity and error rate in the counting task. This finding indicates that participants experienced greater difficulty in completing the task at more eccentric locations; this is likely a consequence of reduced colour sensitivity in the peripheral retina causing difficulty in detecting or discriminating the coloured task dots (Hansen et al., 2009; Mullen, 1991; Newton & Eskew, 2003).

However, difficulty in allocating attention to these more eccentric stimuli may have also contributed. To disentangle these factors, a task that does not involve colour could be used to assess whether this impacts the effect of the task on the OKR, or peripheral stimuli could be scaled to improve visibility. In this way, it will be possible to delineate whether the difficulty experienced here reflects a visual or an attentional effect, and to better quantify the role of attention in the OKR.

C/S Opposing stimuli sometimes produced a direction-changing OKR. This result led to two alternative interpretations: equal weighting of neural responses being achieved between central and peripheral stimuli due to the allocation of attention to the periphery and the natural prioritisation of the centre; a difficulty in fully directing and maintaining peripheral attention in the presence of a compelling central stimulus, resulting in attention fluctuating between the two stimuli. The first interpretation implies that the centre is more heavily weighted in driving the OKR, and that sufficient attention has been allocated to the periphery to match that weighting. In this case, neither the central stimulus nor the attended stimulus necessarily drive the OKR, though the central stimulus carries a higher weighting under neutral attention conditions. The second interpretation implies that the driving stimulus for the OKR is determined by attention. A more precise manipulation of attention is required to delineate this. A similar task could be carried out before and after training observers to better direct their spatial attention; if the training results in greater dominance of the peripheral stimulus in driving the OKR, this would suggest that changes in OKR slow phase direction were caused by attention. Alternatively, tasks in each region (centre and surround) could be used to divide attention between the two stimuli at varying ratios to assess the way in which this modulates the driving region of the OKR. By varying the difficulty or demands of tasks in each region, it may be possible to more precisely manipulate the allocation of attentional resources in order to better understand the role played by attention in determining the driving stimulus for the OKR.

6.8.3 Reversal of OKAN

Experiment 1 showed an association between low OKR accuracy (low gain and directional inaccuracy) and OKAN with a reversed direction. This was interpreted as providing support for the hypothesis that reversal of OKAN results from an adaptation to motion during optokinetic stimulation (Brandt et al., 1974; Chen et al., 2014; Gygli et al., 2021). To further investigate the link between motion adaptation and OKAN reversal, stimuli producing different strengths of motion after-effects (MAEs) could be used to induce OKR/OKAN in order to assess whether the propensity to induce MAEs is related to the occurrence of reversed OKAN and whether the strength or duration of the MAE is correlated with OKAN reversal. Another possibility is assessing whether methods of influencing motion adaptation affect the reversal of OKAN in tandem. For example, studies have shown that applying TMS over sites at which adaptation to visual motion occurs, such as MT/V5, affects the duration of the MAE (Stewart et al., 1999; Théoret et al., 2002). By applying methods to impact the adaptation to visual motion during optokinetic stimulation, it should be possible to assess whether manipulating the extent of motion adaptation has an influence on OKAN-II.

Stimulus velocity was also found to predict OKAN reversal, however, due to collinearity with gain it is unclear whether this is an effect of stimulus velocity or simply a consequence of the association between high stimulus velocity and low OKR gain. Low gain was confirmed as a predictor of OKAN reversal when velocity was controlled for, however, vast differences in gain between the tested stimulus velocities made controlling for gain while testing velocity very difficult. It may be possible to overcome this issue. For example, one could train observers to increase their gain (Boman & Hotson, 1987) so that similar gains can be achieved across a range of stimulus velocities. The role of velocity could then be assessed while gain is held relatively constant. Alternatively, as there are individual differences in OKR gain, it may be possible to group participants based on their gains in response to different stimulus velocities and assess the way in which velocity impacts OKAN in each group. For example, participants could be split into 'low', 'medium' and 'high' gain groups before viewing a range of stimulus velocities. If the low gain group experiences more OKAN-II than the high gain group, independent of stimulus velocity, this would indicate that the effect

is of gain; if increasing the stimulus velocity causes a comparable increase in OKAN-II across every group, this would indicate that velocity also plays a role.

6.9 Concluding statement

The goal of this project has been to better understand the human OKR and the way in which it is impacted by numerous bottom-up and top-down factors including attention, stimulus characteristics and retinal location. A greater understanding of the OKR is critical to the successful implementation of the OKR as a no-report measure in clinical and research settings. This has the potential to allow inclusion of patient populations in research who would often be excluded from traditional experiments; it is the opinion of this researcher that inclusion of such individuals in research is of paramount importance. This project has successfully furthered the knowledge of the effects of stimulus area, stimulus eccentricity, stimulus velocity, multiple directions of motion, and the attention of the observer on the OKR. However, as is common in research, for each answer provided new questions have arisen. The quest to understand the optokinetic responses is thus far from over.

References

Abadi, R. V., Howard, I. P., & Ohmi, M. (1999). Gaze orientation during full-field and peripheral field passive optokinesis. *Ophthalmic and Physiological Optics*, *19*(3), 261–265. https://doi.org/10.1016/S0275-5408(98)00067-2

Abadi, R. V., Howard, I. P., Ohmi, M., Howard, T., Lee, E. E., & Wright, M. J. (1994). The rise time and steady-state gain of the human optokinetic response (OKR). *Investigative Ophthalmology & Visual Science*, *35*, 2035.

Abadi, R. V., Howard, I. P., Ohmi, M., & Lee, E. E. (2005). The effect of central and peripheral field stimulation on the rise time and gain of human optokinetic nystagmus. *Perception*, *34*(8), 1015–1024. https://doi.org/10.1068/p5251b

Abadi, R. V., & Pantazidou, M. (1997). Monocular optokinetic nystagmus in humans with age-related maculopathy. *British Journal of Ophthalmology*, *81*(2), 123–129. https://doi.org/10.1136/bjo.81.2.123

Abadi, R. V., & Pascal, E. (1991). The effects of simultaneous central and peripheral field motion on the optokinetic response. *Vision Research*, *31*(12), 2219–2225. https://doi.org/10.1016/0042-6989(91)90174-4

Akao, T., Kumakura, Y., Kurkin, S., Fukushima, J., & Fukushima, K. (2007). Directional asymmetry in vertical smooth-pursuit and cancellation of the vertical vestibulo-ocular reflex in juvenile monkeys. *Experimental Brain Research*, *182*(4), 469–478. https://doi.org/10.1007/S00221-007-1005-1/FIGURES/4

Albright, T. D., & Stoner, G. R. (2002). Contextual influences on visual processing. *Annual Review of Neuroscience*, *25*, 339–379. https://doi.org/10.1146/ANNUREV.NEURO.25.112701.142900/CITE/REFWORKS

Aleci, C., Scaparrotti, M., Fulgori, S., & Canavese, L. (2018). A novel and cheap method to correlate subjective and objective visual acuity by using the optokinetic response. *International Ophthalmology*, *38*(5), 2101–2115. https://doi.org/10.1007/S10792-017-0709-X/TABLES/6

Aleshin, S., Ziman, G., Kovács, I., & Braun, J. (2019). Perceptual reversals in binocular rivalry: Improved detection from OKN. *Journal of Vision*, *19*(3), 5–5. https://doi.org/10.1167/19.3.5

Allman, J., Miezin, F., & McGuinness, E. (1985a). Direction- and velocity-specific responses from beyond the classical receptive field in the middle temporal visual area (MT). *Perception*, *14*(2), 105–126. https://doi.org/10.1068/p140105

Allman, J., Miezin, F., & McGuinness, E. (1985b). Stimulus specific responses from beyond the classical receptive field: Neurophysiological mechanisms for local-global comparisons in visual neurons. *Annual Review of Neuroscience*, *8*, 407–430. https://doi.org/10.1146/ANNUREV.NE.08.030185.002203

Altpeter, E., Mackeben, M., & Trauzettel-Klosinski, S. (2000). The importance of sustained attention for patients with maculopathies. *Vision Research*, *40*(10–12), 1539–1547. https://doi.org/10.1016/S0042-6989(00)00059-6

Amano, K., Wandell, B. A., & Dumoulin, S. O. (2009). Visual field maps, population receptive field sizes, and visual field coverage in the human MT+ complex. *Journal of Neurophysiology*, *102*(5), 2704. https://doi.org/10.1152/JN.00102.2009

Anderson, J. C., Kennedy, H., & Martin, K. A. C. (2011). Pathways of attention: synaptic relationships of frontal eye field to V4, lateral intraparietal cortex, and area 46 in macaque monkey. *The Journal of Neuroscience*, *31*(30), 10872–10881. https://doi.org/10.1523/JNEUROSCI.0622-11.2011

Anstis, S. (1998). Picturing peripheral acuity. *Perception*, *27*(7), 817–825. https://doi.org/10.1068/p270817

Anton-Erxleben, K., Stephan, V. M., & Treue, S. (2009). Attention reshapes center-surround receptive field structure in macaque cortical area MT. *Cerebral Cortex*, *19*(10), 2466–2478. https://doi.org/10.1093/CERCOR/BHP002

Armstrong, K. M., & Moore, T. (2007). Rapid enhancement of visual cortical response discriminability by microstimulation of the frontal eye field. *Proceedings of the National Academy of Sciences of the United States of America*, *104*(22), 9499–9504. https://doi.org/10.1073/PNAS.0701104104

Azzopardi, P., & Cowey, A. (1996). The overrepresentation of the fovea and adjacent retina in the striate cortex and dorsal lateral geniculate nucleus of the macaque monkey. *Neuroscience*, *72*(3), 627–639. https://doi.org/10.1016/0306-4522(95)00589-7

Baloh, R. W., Honrubia, V., & Sills, A. (1977). Eye-tracking and optokinetic nystagmus: Results of quantitative testing in patients with well-defined nervous system lesions. *Annals of Otology, Rhinology & Laryngology*, *86*(1), 108–114. https://doi.org/10.1177/000348947708600119

Baloh, R. W., Richman, L., Yee, R. D., & Honrubia, V. (1983). The dynamics of vertical eye movements in normal human subjects. *Aviation, Space and Environmental Medicine*, *54*(1), 32–38.

Baloh, R. W., Yee, R. D., & Honrubia, V. (1980a). Optokinetic asymmetry in patients with maldeveloped foveas. *Brain Research*, *186*(1), 211–216. https://doi.org/10.1016/0006-8993(80)90268-1

Baloh, R. W., Yee, R. D., & Honrubia, V. (1980b). Optokinetic nystagmus and parietal lobe lesions. *Annals of Neurology*, *7*, 269–276.

Baloh, R. W., Yee, R. D., & Honrubia, V. (1982). Clinical abnormalities of optokinetic nystagmus. In G. Lennerstrand, D. S. Zee, & E. L. Keller (Eds.), *Functional basis of ocular motility disorders* (pp. 311–320). Pergamon Press.

Baloh, R. W., Yee, R. D., Honrubia, V., & Jacobson, K. (1988). A comparison of the dynamics of horizontal and vertical smooth pursuit in normal human subjects. *Aviation, Space, and Environmental Medicine*, *59*(2), 121–124.

Bao, Y., Lei, Q., Fang, Y., Tong, Y., Schill, K., Pöppel, E., & Strasburger, H. (2013). Inhibition of return in the visual field: The eccentricity effect is independent of cortical magnification. *Experimental Psychology*, *60*(6), 425–431. https://doi.org/10.1027/1618-3169/A000215

Barbot, A., Xue, S., & Carrasco, M. (2021). Asymmetries in visual acuity around the visual field. *Journal of Vision*, *21*(1), 2–2. https://doi.org/10.1167/JOV.21.1.2

Barlow, H. B. (1958). Temporal and spatial summation in human vision at different background intensities. *The Journal of Physiology*, *141*(2), 337–350. https://doi.org/10.1113/JPHYSIOL.1958.SP005978

Barlow, H. B., & Levick, W. R. (1965). The mechanism of directionally selective units in rabbit's retina. *The Journal of Physiology*, *178*(3), 477–504. https://doi.org/10.1113/JPHYSIOL.1965.SP007638

Barnes, G. R. (1993). Visual-vestibular interaction in the control of head and eye movement: The role of visual feedback and predictive mechanisms. *Progress in Neurobiology*, *41*(4), 435–472. https://doi.org/10.1016/0301-0082(93)90026-O

Barnes, G. R., & Crombie, J. W. (1985). The interaction of conflicting retinal motion stimuli in oculomotor control. *Experimental Brain Research*, *59*(3), 548–558. https://doi.org/10.1007/BF00261346

Barratt, H. J., & Hood, J. D. (1988). Transfer of optokinetic activity to vestibular nystagmus. *Acta Oto-Laryngologica*, *105*(3–4), 318–327. https://doi.org/10.3109/00016488809097014

Bartlett, L. K., Graf, E. W., Hedger, N., & Adams, W. J. (2019). Motion adaptation and attention: A critical review and meta-analysis. *Neuroscience & Biobehavioral Reviews*, *96*, 290–301. https://doi.org/10.1016/J.NEUBIOREV.2018.10.010

Bedell, H. E., Tong, J., & Aydin, M. (2010). The perception of motion smear during eye and head movements. *Vision Research*, *50*(24), 2692–2701. https://doi.org/10.1016/J.VISRES.2010.09.025

Berens, P. (2009). CircStat: A MATLAB Toolbox for Circular Statistics. *Journal of Statistical Software*, *31*(10), 1–21. https://doi.org/10.18637/JSS.V031.I10

Bertolini, G., Romano, F., Straumann, D., Keller, K., Palla, A., & Feddermann-Demont, N. (2021). Measuring optokinetic after-nystagmus: potential for detecting patients with signs of visual dependence following concussion. *Journal of Neurology*, *268*(5), 1747–1761. https://doi.org/10.1007/s00415-020-10359-8

Bi, K., Zhang, Y., & Zhang, Y. Y. (2022). Central-peripheral dichotomy: Color-motion and luminance-motion binding show stronger top-down feedback in central vision. *Attention, Perception, and Psychophysics*, *84*(3), 861–877. https://doi.org/10.3758/S13414-022-02465-8/FIGURES/5

Blanke, O., Spinelli, L., Thut, G., Michel, C. M., Perrig, S., Landis, T., & Seeck, M. (2000). Location of the human frontal eye field as defined by electrical cortical stimulation: Anatomical, functional and electrophysiological characteristics. *NeuroReport*, *11*(9), 1907–1913.

Boman, D. K., & Hotson, J. R. (1987). Smooth pursuit training and disruption: Directional differences and nystagmus. *Neuro-Ophthalmology*, *7*(4), 185–194. https://doi.org/10.3109/01658108709007451

Braddick, O., Atkinson, J., Hood, B., Harkness, W., Jackson, G., & Vargha-Khademt, F. (1992). Possible blindsight in infants lacking one cerebral hemisphere. *Nature*, *360*(6403), 461–463. https://doi.org/10.1038/360461a0

Brainard, D. H. (1997). The Psychophysics Toolbox. *Spatial Vision*, *10*(4), 433–436. https://doi.org/10.1163/156856897X00357

Brandt, T., Dichgans, J., & Buchele, W. (1974). Motion habituation: Inverted self motion perception and optokinetic after-nystagmus. *Experimental Brain Research*, *21*, 337–352.

Brantberg, K. (1992). Human optokinetic after-nystagmus: variability in serial test results. *Acta Oto-Laryngologica*, *112*(1), 7–13. https://doi.org/10.3109/00016489209100776

Brenner, E., & van den Berg, A. V. (1994). Judging object velocity during smooth pursuit eye movements. *Experimental Brain Research, 99*(2), 316–324. https://doi.org/10.1007/BF00239598

Britten, K. H., & Heuer, H. W. (1999). Spatial summation in the receptive fields of MT neurons. *Journal of Neuroscience, 19*(12), 5074–5084. https://doi.org/10.1523/JNEUROSCI.19-12-05074.1999

Brotchie, P. R., Lee, M. B., Chen, D.-Y., Lourensz, M., Jackson, G., & Bradley, W. G. (2003). Head position modulates activity in the human parietal eye fields. *Neuroimage, 18*, 178–184. https://doi.org/10.1006/nimg.2002.1294

Büchel, C., Josephs, O., Rees, G., Turner, R., Frith, C. D., & Friston, K. J. (1998). The functional anatomy of attention to visual motion A functional MRI study. *Brain, 121*, 1281–1294.

Burr, D. C. (1980). Motion smear. *Nature, 284*(5752), 164–165. https://doi.org/10.1038/284164A0

Buschman, T. J., & Miller, E. K. (2007). Top-down versus bottom-up control of attention in the prefrontal and posterior parietal cortices. *Science, 315*(5820), 1860–1864. https://doi.org/10.1126/SCIENCE.1138071

Büttner-Ennever, J. A., Cohen, B., Horn, A. K. E., & Reisine, H. (1996). Efferent pathways of the nucleus of the optic tract in monkey and their role in eye movements. *The Journal of Comparative Neurology, 373*, 90–107. https://doi.org/10.1002/(SICI)1096-9861(19960909)373:1

Carandini, M., & Heeger, D. J. (2011). Normalization as a canonical neural computation. *Nature Reviews Neuroscience 2011 13:1, 13*(1), 51–62. https://doi.org/10.1038/nrn3136

Cardin, V., & Smith, A. T. (2011). Sensitivity of human visual cortical area V6 to stereoscopic depth gradients associated with self-motion. *Journal of Neurophysiology, 106*, 1240–1249. https://doi.org/10.1152/jn.01120.2010.-The

Carpenter, R. H. S. (1988). *Movements of the Eyes* (2nd ed.). Pion.

Carrasco, M., & Barbot, A. (2019). Spatial attention alters visual appearance. *Current Opinion in Psychology, 29*, 56–64. https://doi.org/10.1016/j.copsyc.2018.10.010

Carrasco, M., Ling, S., & Read, S. (2004). Attention alters appearance. *Nature Neuroscience, 7*(3), 308–313. https://doi.org/10.1038/nn1194

Carrasco, M., & Yeshurun, Y. (1998). The contribution of covert attention to the set-size and eccentricity effects in visual search. *Journal of Experimental Psychology: Human Perception and Performance, 24*(2), 673–692. https://doi.org/DOI: 10.1037//0096-1523.24.2.673

Çetinkaya, A., Oto, S., Akman, A., & Akova, Y. A. (2008). Relationship between optokinetic nystagmus response and recognition visual acuity. *Eye*, *22*(1), 77–81. https://doi.org/10.1038/sj.eye.6702529

Chaudhuri, A. (1990). Modulation of the motion aftereffect by selective attention. *Nature*, *344*, 60–62. https://doi.org/10.1038/344060A0

Chen, C. C., Huang, M. Y. Y., Weber, K. P., Straumann, D., & Bockisch, C. J. (2014). Afternystagmus in darkness after suppression of optokinetic nystagmus: An interaction of motion aftereffect and retinal afterimages. *Experimental Brain Research*, *232*(9), 2891–2898. https://doi.org/10.1007/S00221-014-3971-4

Cheng, M., & Outerbridge, J. S. (1975). Optokinetic nystagmus during selective retinal stimulation. *Experimental Brain Research*, *23*(2), 129–139. https://doi.org/10.1007/BF00235455

Clément, G. R., Courjon, J. H., Jeannerod, M., & Schmid, R. (1981). Unidirectional habituation of vestibulo-ocular responses by repeated rotational or optokinetic stimulations in the cat. *Experimental Brain Research*, *42*(1), 34–42. https://doi.org/10.1007/BF00235726

Cohen, B., Henn, V., Raphan, T., & Dennett, D. (1981). Velocity storage, nystagmus, and visual-vestibular interactions in humans. *Annals of the New York Academy of Sciences*, *374*(1), 421–433. https://doi.org/10.1111/j.1749-6632.1981.tb30888.x

Cohen, B., Matsuo, V., & Raphan, T. (1977). Quantitative analysis of the velocity characteristics of optokinetic nystagmus and optokinetic after-nystagmus. *The Journal of Physiology*, *270*(2), 321–344. https://doi.org/10.1113/JPHYSIOL.1977.SP011955

Cohen, B., Schiff, D., & Buettner, J. (1990). Contribution of the nucleus of the optic tract to optokinetic nystagmus and optokinetic afternystagmus in the monkey: clinical implications. *Research Publications - Association for Research in Nervous and Mental Disease*, *67*, 233–255.

Cohen, B., Uemura, T., & Takemori, S. (1973). Effects of labyrinthectomy on optokinetic nystagmus (OKN) and optokinetic after-nystagmus (OKAN). *International Journal of Equilibrium Research*, *3*(1), 88–93.

Cohen, E. H., & Zaidi, Q. (2007). The oblique effect and three-dimensional shape. *Visual Cognition*, *15*(1), 80. /pmc/articles/PMC2971682/

Cohen, S. Y., Lamarque, F., Saucet, J.-C., Provent, P., Langram, C., & Le-Gargasson, J.-F. (2003). Filling-in phenomenon in patients with age-related macular degeneration: differences regarding uni- or bilaterality of central scotoma. *Graefe's Archive for Clinical and Experimental Ophthalmology*, *241*(10), 785–791. https://doi.org/10.1007/s00417-003-0744-3

Collewijn, H. (1972). An analog model of the rabbit's optokinetic system. *Brain Research*, *36*(1), 71–88. https://doi.org/10.1016/0006-8993(72)90767-6

Collewijn, H. (1985). Integration of adaptive changes of the optokinetic reflex, pursuit and the vestibulo-ocular reflex. *Reviews of Oculomotor Research*, *1*, 51–69.

Collewijn, H., & Tamminga, E. P. (1984). Human smooth and saccadic eye movements during voluntary pursuit of different target motions on different backgrounds. *The Journal of Physiology*, *351*(1), 217. https://doi.org/10.1113/JPHYSIOL.1984.SP015242

Cornelissen, F. W., Peters, E. M., & Palmer, J. (2002). The Eyelink Toolbox: Eye tracking with MATLAB and the Psychophysics Toolbox. *Behavior Research Methods, Instruments, and Computers*, *34*(4), 613–617. https://doi.org/10.3758/BF03195489

Costa, A. C. S. (2011). An assessment of optokinetic nystagmus (OKN) in persons with down syndrome. *Experimental Brain Research*, *214*(3), 381–391. https://doi.org/10.1007/s00221-011-2834-5

Curcio, C. A., & Allen, K. A. (1990). Topography of ganglion cells in human retina. *Journal of Comparative Neurology*, *300*(1), 5–25. https://doi.org/10.1002/cne.903000103

Curcio, C. A., Sloan, K. R., Kalina, R. E., & Hendrickson, A. E. (1990). Human photoreceptor topography. *Journal of Comparative Neurology*, *292*(4), 497–523. https://doi.org/10.1002/cne.902920402

Dakin, S. C., Doustkouhi, S. M., Kersten, H., Turnbull, P. R. K., Yoon, J., & Danesh-Meyer, H. (2019). Measuring visual field loss in glaucoma using involuntary eye movements. *Investigative Ophthalmology and Visual Science*, *60*. https://iovs.arvojournals.org/article.aspx?articleid=2746218

Dakin, S. C., & Turnbull, P. R. K. (2016). Similar contrast sensitivity functions measured using psychophysics and optokinetic nystagmus. *Scientific Reports*, *6*. https://doi.org/10.1038/SREP34514

Das, V. E., Economides, J. R., Ono, S., & Mustari, M. J. (2001). Information processing by parafoveal cells in the primate nucleus of the optic tract. *Experimental Brain Research*, *140*(3), 301–310. https://doi.org/10.1007/s002210100816

Dayton, G. O., & Jones, M. H. (1964). Analysis of characteristics of fixation reflex in infants by use of direct current electrooculography. *Neurology*, *14*(12), 1152–1156. https://doi.org/10.1212/WNL.14.12.1152/ASSET/D8BB6766-601A-45C8-BB0F-FAB8966298DB/ASSETS/WNL.14.12.1152.FP.PNG

Dayton, G. O., Jones, M. H., Aiu, P., Rawson, R. A., Steele, B., & Rose, M. (1964). Developmental study of coordinated eye movements in the human infant: I. Visual acuity in the newborn human: A study based on induced optokinetic nystagmus recorded by electro-oculography. *Archives of Ophthalmology*, *71*(6), 865–870.

Dayton, G. O., Jones, M. H., Steele, B., & Rose, M. (1964). Developmental study of coordinated eye movements in the human infant: II. An electro-oculographic study of the fixation reflex in the newborn. *Archives of Ophthalmology*, *71*(6), 871–875. https://doi.org/10.1001/archopht.1964.00970010887018

De Bruyn, B. (1997). Blending transparent motion patterns in peripheral vision. *Vision Research*, *37*(5), 645–648. https://doi.org/10.1016/S0042-6989(96)00117-4

Desimone, R. (1998). Visual attention mediated by biased competition in extrastriate visual cortex. *Philosophical Transactions of the Royal Society of London. Series B, Biological Sciences*, *353*(1373), 1245–1255. https://doi.org/10.1098/RSTB.1998.0280

Desimone, R., & Duncan, J. (1995). Neural mechanisms of selective visual attention. *Annual Review of Neuroscience*, *18*, 193–222. https://doi.org/10.1146/ANNUREV.NE.18.030195.001205

Deubel, H., & Schneider, W. X. (1996). Saccade target selection and object recognition: Evidence for a common attentional mechanism. *Vision Research*, *36*(12), 1827–1837. https://doi.org/10.1016/0042-6989(95)00294-4

Dhande, O. S., Estevez, M. E., Quattrochi, L. E., El-Danaf, R. N., Nguyen, P. L., Berson, D. M., & Huberman, A. D. (2013). Genetic dissection of retinal inputs to brainstem nuclei controlling image stabilization. *Journal of Neuroscience*, *33*(45), 17797–17813. https://doi.org/10.1523/JNEUROSCI.2778-13.2013

Dhande, O. S., Stafford, B. K., Lim, J.-H. A., & Huberman, A. D. (2015). Contributions of retinal ganglion cells to subcortical visual processing and behaviors. *Annual Review of Vision Science*, *1*, 291–328. https://doi.org/10.1146/ANNUREV-VISION-082114-035502

Dichgans, J. (1977). Optokinetic nystagmus as dependent on the retinal periphery via the vestibular nucleus. In R. G. Baker & A. Berthoz (Eds.), *Control of gaze by brain stem neurones, developments in neuroscience* (Vol. 1). Elsevier North-Holland.

Dieterich, M., Bense, S., Stephan, T., Yousry, T. A., & Brandt, T. (2003). fMRI signal increases and decreases in cortical areas during small-field optokinetic stimulation and central fixation. *Experimental Brain Research*, *148*, 117–127. https://doi.org/10.1007/s00221-002-1267-6

Distler, C., & Hoffmann, K. P. (2001). Cortical input to the nucleus of the optic tract and dorsal terminal nucleus (NOT-DTN) in macaques: A retrograde tracing study. *Cerebral Cortex*, *11*(6), 572–580. https://doi.org/10.1093/cercor/11.6.572

Distler, C., Mustari, M. J., & Hoffmann, K. P. (2002). Cortical projections to the nucleus of the optic tract and dorsal terminal nucleus and to the dorsolateral pontine nucleus in macaques: A dual retrograde tracing study. *Journal of Comparative Neurology*, *444*(2), 144–158. https://doi.org/10.1002/cne.10127

Donaghy, M. (1980). The contrast sensitivity, spatial resolution and velocity tuning of the cat's optokinetic reflex. *The Journal of Physiology*, *300*(1), 353–365. https://doi.org/10.1113/jphysiol.1980.sp013166

Doustkouhi, S. M., Turnbull, P. R. K., & Dakin, S. C. (2020a). The effect of refractive error on optokinetic nystagmus. *Scientific Reports*, *10*(20062), 1–14. https://doi.org/10.1038/s41598-020-76865-x

Doustkouhi, S. M., Turnbull, P. R. K., & Dakin, S. C. (2020b). The effect of simulated visual field loss on optokinetic nystagmus. *Translational Vision Science & Technology*, *9*(3), 25. https://doi.org/10.1167/tvst.9.3.25

Dubois, M. F. W., & Collewijn, H. (1979). Optokinetic reactions in man elicited by localized retinal motion stimuli. *Vision Research*, *19*(10), 1105–1115. https://doi.org/10.1016/0042-6989(79)90005-1

Eifuku, S., & Wurtz, R. H. (1998). Response to motion in extrastriate area MSTI: Center-surround interactions. *Journal of Neurophysiology*, *80*(1), 282–296. https://doi.org/10.1152/JN.1998.80.1.282/ASSET/IMAGES/LARGE/JNP.JU35F11.JPEG

Engbert, R., & Kliegl, R. (2003). Microsaccades uncover the orientation of covert attention. *Vision Research*, *43*(9), 1035–1045. https://doi.org/10.1016/S0042-6989(03)00084-1

Engbert, R., & Mergenthaler, K. (2006). Microsaccades are triggered by low retinal image slip. *Proceedings of the National Academy of Sciences of the United States of America*, *103*(18), 7192–7197. https://doi.org/10.1073/PNAS.0509557103/ASSET/FE70BFAA-0256-41BD-BFAC-D9FB33E8126B/ASSETS/GRAPHIC/ZPQ01806-1988-M02.JPEG

Essig, P., Müller, J., & Wahl, S. (2022). Parameters of optokinetic nystagmus are influenced by the nature of a visual stimulus. *Applied Sciences (Switzerland)*, *12*(23). https://doi.org/10.3390/APP122311991

Everling, S. (2007). Where do I look? From attention to action in the frontal eye field. *Neuron*, *56*(3), 417–419. https://doi.org/10.1016/J.NEURON.2007.10.026

Felleman, D. J., & Kaas, J. H. (1984). Receptive-field properties of neurons in middle temporal visual area (MT) of owl monkeys. *Journal of Neurophysiology*, *52*(3), 488–513. https://doi.org/10.1152/JN.1984.52.3.488

Frattini, D., & Wibble, T. (2021). Alertness and visual attention impact different aspects of the optokinetic reflex. *Investigative Ophthalmology & Visual Science*, *62*(13), 1–7.

Fuchs, A. F., & Mustari, M. J. (1993). The optokinetic response in primates and its possible neuronal substrate. In F. A. Miles & J. Wallman (Eds.), *Visual motion and its role in the stabilisation of gaze* (pp. 343–369). Elsevier Science.

Furmanski, C. S., & Engel, S. A. (2000). An oblique effect in human primary visual cortex. *Nature Neuroscience 2000 3:6*, *3*(6), 535–536. https://doi.org/10.1038/75702

Garbutt, S., Han, Y., Kumar, A. N., Harwood, M., Harris, C. M., & Leigh, R. J. (2003). Vertical optokinetic nystagmus and saccades in normal human subjects. *Investigative Ophthalmology and Visual Science*, *44*(9), 3833–3841. https://doi.org/10.1167/IOVS.03-0066

Garbutt, S., Han, Y., Kumar, A. N., Harwood, M., Rahman, R., & Leigh, R. J. (2003). Disorders of vertical optokinetic nystagmus in patients with ocular misalignment. *Vision Research*, *43*(3), 347–357. https://doi.org/10.1016/S0042-6989(02)00387-5

Garbutt, S., & Harris, C. M. (1999). A review of optokinetic nystagmus (OKN) in infants and children. *British Orthoptic Journal*, *56*, 1–10.

Garbutt, S., Harwood, M. R., & Harris, C. M. (2001). Comparison of the main sequence of reflexive saccades and the quick phases of optokinetic nystagmus. *British Journal of Ophthalmology*, *85*, 1477–1483. http://bjo.bmj.com/

Ghasia, F. F., & Shaikh, A. G. (2015). Uncorrected myopic refractive error increases microsaccade amplitude. *Investigative Ophthalmology & Visual Science*, *56*(4), 2531–2535. https://doi.org/10.1167/IOVS.14-15882

Gloriani, A. H., & Schütz, A. C. (2019). Humans trust central vision more than peripheral vision even in the dark. *Current Biology*, *29*(7), 1206-1210.e4. https://doi.org/10.1016/J.CUB.2019.02.023

Gobell, J., & Carrasco, M. (2005). Attention alters the appearance of spatial frequency and gap size. *Psychological Science*, *16*(8), 644–651. https://doi.org/10.1111/J.1467-9280.2005.01588.X/FORMAT/EPUB

González, E. G., Tarita-Nistor, L., Mandelcorn, E., Mandelcorn, M., & Steinbach, M. J. (2018). Mechanisms of image stabilization in central vision loss: Smooth pursuit. *Optometry and Vision Science*, *95*(1), 60–69. https://doi.org/10.1097/OPX.0000000000001161

Gorman, J. J., Cogan, D. G., & Gellis, S. S. (1957). An apparatus for grading the visual acuity of infants on the basis of opticokinetic nystagmus. *Pediatrics*, *19*, 1088–1092.

Grasse, K. L., Cynader, M. S., & Douglas, R. M. (1984). Alterations in response properties in the lateral and dorsal terminal nuclei of the cat accessory optic system following visual cortex lesions. *Experimental Brain Research*, *55*(1), 69–80. https://doi.org/10.1007/BF00240499

Gregoriou, G. G., Gotts, S. J., & Desimone, R. (2012). Cell-type-specific synchronization of neural activity in FEF with V4 during attention. *Neuron*, *73*(3), 581–594. https://doi.org/10.1016/J.NEURON.2011.12.019

Gregoriou, G. G., Gotts, S. J., Zhou, H., & Desimone, R. (2009). High-frequency, long-range coupling between prefrontal and visual cortex during attention. *Science*, *324*(5931), 1207–1210. https://doi.org/10.1126/SCIENCE.1171402

Gregoriou, G. G., Rossi, A. F., Ungerleider, L. G., & Desimone, R. (2014). Lesions of prefrontal cortex reduce attentional modulation of neuronal responses and synchrony in V4. *Nature Neuroscience*, *17*(7), 1003–1011. https://doi.org/10.1038/nn.3742

Gresty, M., & Halmagyi, M. (1979). Following eye movements in the absence of central vision. *Acta Oto-Laryngologica*, *87*(3–6), 477–483. https://doi.org/10.3109/00016487909126455

Groh, J. M., Born, R. T., & Newsome, W. T. (1997). How is a sensory map read out? Effects of microstimulation in visual area MT on saccades and smooth pursuit eye movements. *Journal of Neuroscience*, *17*(11), 4312–4330. https://doi.org/10.1523/JNEUROSCI.17-11-04312.1997

Gygli, J., Romano, F., Bockisch, C. J., Feddermann-Demont, N., Straumann, D., & Bertolini, G. (2021). Effect of the stimulus duration on the adaptation of the optokinetic afternystagmus. *Frontiers in Neurology*, *12*, 408. https://doi.org/10.3389/FNEUR.2021.518133/BIBTEX

Hainline, L., Lemerise, E., Abramov, I., & Turkel, J. (1984). Orientational asymmetries in small-field optokinetic nystagmus in human infants. *Behavioural Brain Research*, *13*(3), 217–230. https://doi.org/10.1016/0166-4328(84)90164-5

Han, S. B., Han, E. R., Hyon, J. Y., Seo, J. M., Lee, J. H., & Hwang, J. M. (2011). Measurement of distance objective visual acuity with the computerized optokinetic nystagmus test in patients with ocular diseases. *Graefe's Archive for Clinical and Experimental Ophthalmology*, *249*(9), 1379–1385. https://doi.org/10.1007/S00417-011-1705-X

Hangen, H., Coop, S., & Mitchell, J. (2022). Laminar organization and diversity of area MT receptive fields in the marmoset. *Journal of Vision*, *22*(14), 3791–3791. https://doi.org/10.1167/JOV.22.14.3791

Hanning, N. M., & Deubel, H. (2019). Unlike saccades, quick phases of optokinetic nystagmus (OKN) are not preceded by shifts of attention. *Journal of Vision*, *19*(10), 53c–53c. https://doi.org/10.1167/19.10.53C

Hansen, T., Pracejus, L., & Gegenfurtner, K. R. (2009). Color perception in the intermediate periphery of the visual field. *Journal of Vision*, *9*(4), 26–26. https://doi.org/10.1167/9.4.26

Harris, C. M., Jacobs, M., Shawkat, F. S., & Taylor, D. S. I. (1993). Human ocular motor neural integrator failure. *Neuro-Ophthalmology*, *13*(I), 25–34.

Harris, C. M., Jacobs, M., & Taylor, D. S. I. (1994). The development of binocular and monocular optokinetic gain from 1 to 7 months. *Investigative Ophthalmology and Visual Science (Supplement)*, *35*(4), 1829.

Harris, C. M., Kriss, A., Shawkat, F. S., Taylor, D. S. I., & Russell-Eggitt, I. (1996). Delayed visual maturation in infants: A disorder of figure-ground separation? *Brain Research Bulletin*, *40*(5–6), 365–369. https://doi.org/10.1016/0361-9230(96)00128-1

Harris, C. M., Shawkat, F. S., Russell-Eggitt, I., Wilson, J., & Taylor, D. S. I. (1996). Intermittent horizontal saccade failure ('ocular motor apraxia') in children. *British Journal of Ophthalmology*, *80*, 151–158.

Harris, C. M., Walker, J., Shawkat, F. S., Wilson, J., & Russell-Eggitt, I. (1993). Movements in a familial vestibulocerebellar disorder. *Neuropediatrics*, 117–122.

Harris, L. R., & Smith, A. T. (1992). Motion defined exclusively by second-order characteristics does not evoke optokinetic nystagmus. *Visual Neuroscience*, *9*(6), 565–570. https://doi.org/10.1017/S0952523800001802

Harris, L. R., & Smith, A. T. (2000). Interactions between first- and second-order motion revealed by optokinetic nystagmus. *Experimental Brain Research*, *130*(1), 67–72. https://doi.org/10.1007/s002219900232

Harris, S. C., & Dunn, F. A. (2023). Asymmetric retinal direction tuning predicts optokinetic eye movements across stimulus conditions. *ELife*, *12*, 81780. https://doi.org/10.7554/ELIFE.81780

Henn, V., Young, L. R., & Finley, C. (1974). Vestibular nucleus units in alert monkeys are also influenced by moving visual fields. *Brain Research*, *71*(1), 144–149. https://doi.org/10.1016/0006-8993(74)90198-X

Henriksson, N. G., Pyykko, I., Schalen, L., & Wennmo, C. (1980). Velocity patterns of rapid eye movements. *Acta Oto-Laryngologica*, *89*(3–6), 504–512. https://doi.org/10.3109/00016488009127168

Hoffmann, K. P. (1982). Cortical versus subcortical contributions to the optokinetic reflex in the cat. In G. Lennerstrand, D. S. Zee, & E. L. Keller (Eds.), *Functional basis of ocular motility disorders* (pp. 303–311). Pergamon Press.

Hoffmann, K. P. (1989). Control of the optokinetic reflex by the nucleus of the optic tract in primates. *Progress in Brain Research*, *80*(C), 173–182. https://doi.org/10.1016/S0079-6123(08)62211-6

Hoffmann, K. P., & Distler, C. (1986). The role of direction selective cells in the nucleus of the optic tract of cat and monkey during OKN. In E. L. Keller & D. S. Zee (Eds.), *Adaptive Processes in Visual and Oculomotor Systems: Proceedings of a Conference Held in Asolimar, California, USA, 16-20 June 1985* (pp. 261–267).

Hoffmann, K. P., & Huber. (1983). Responses to visual stimulation in single cells in the nucleus of the optic tract (NOT) during optokinetic nystagmus (OKN) in the awake cat. *Society for Neuroscience (Abstracts)*, *9*, 1048.

Honrubia, V., Downey, W. L., Mitchell, D. P., & Ward, P. H. (1968). Experimental studies on optokinetic nystagmus II. Normal humans. *Acta Oto-Laryngologica*, *65*(1–6), 441–448. https://doi.org/10.3109/00016486809120986

Hood, J. D. (1967). Observations upon the neurological mechanism of optokinetic nystagmus with especial reference to the contribution of peripheral vision. *Acta Oto-Laryngologica*, *63*(2–3), 208–215. https://doi.org/10.3109/00016486709128751

Hood, J. D. (1975). Observations upon the role of the peripheral retina in the execution of eye movements. *ORL*, *37*(2), 65–73. https://doi.org/10.1159/000275208

Hood, J. D., & Leech, J. (1974). The significance of peripheral vision in the perception of movement. *Acta Oto-Laryngologica*, *77*(1–6), 72–79.

Howard, I. P., & Gonzalez, G. (1987). Human optokinetic nystagmus in response to moving binocularly disparate stimuli. *Vision Research*, *27*(10), 1807–1816.

Howard, I. P., & Ohmi, M. (1984). The efficiency of the central and peripheral retina in driving human optokinetic nystagmus. *Vision Research*, *24*(9), 969–976. https://doi.org/10.1016/0042-6989(84)90072-5

Howard, I. P., & Simpson, W. A. (1989). Human optokinetic nystagmus is linked to the stereoscopic system. *Experimental Brain Research*, *78*(2), 309–314. https://doi.org/10.1007/BF00228902

Huang, X., Albright, T. D., & Stoner, G. R. (2007). Adaptive surround modulation in cortical area MT. *Neuron*, *53*(5), 761–770. https://doi.org/10.1016/J.NEURON.2007.01.032

Hubert-Wallander, B., Green, C. S., Sugarman, M., & Bavelier, D. (2011). Changes in search rate but not in the dynamics of exogenous attention in action videogame players. *Attention, Perception, and Psychophysics*, *73*(8), 2399–2412. https://doi.org/10.3758/S13414-011-0194-7/TABLES/2

Hüer, J., Saxena, P., & Treue, S. (2024). Pathway-selective optogenetics reveals the functional anatomy of top-down attentional modulation in the macaque visual cortex. *Proceedings of the National Academy of Sciences of the United States of America*, *121*(3). https://doi.org/10.1073/PNAS.2304511121

Hutchinson, C. V., & Ledgeway, T. (2010). Spatial summation of first-order and second-order motion in human vision. *Vision Research*, *50*(17), 1766–1774. https://doi.org/10.1016/J.VISRES.2010.05.032

Ireland, D. J., & Jell, R. M. (1982). Optokinetic after-nystagmus in man after loss or reduction of labyrinthine function: A preliminary report. *Journal of Otolaryngology*, *11*(2), 86–90. https://europepmc.org/article/med/6978946

Jacobs, M., Harris, C. M., Shawkat, F. S., & Taylor, D. S. I. (1997). Smooth pursuit development in infants. *Australian and New Zealand Journal of Ophthalmology*, *25*(3), 199–206. https://doi.org/10.1111/j.1442-9071.1997.tb01392.x

Johnston, A., & Wright, M. J. (1986). Matching velocity in central and peripheral vision. *Vision Research*, *26*(7), 1099–1109.

Jones, H. E., Grieve, K. L., Wang, W., & Sillito, A. M. (2001). Surround suppression in primate V1. *Journal of Neurophysiology*, *86*(4), 2011–2028. https://doi.org/10.1152/JN.2001.86.4.2011/ASSET/IMAGES/LARGE/9K1011938016.JPEG

Kanari, K., & Kaneko, H. (2019). Effect of visual attention and horizontal vergence in three-dimensional space on occurrence of optokinetic nystagmus. *Journal of Eye Movement Research*, *12*(1). https://doi.org/10.16910/jemr.12.1.2

Kanari, K., Sakamoto, K., & Kaneko, H. (2017). Effect of visual attention on the properties of optokinetic nystagmus. *PLoS ONE*, *12*(4). https://doi.org/10.1371/JOURNAL.PONE.0175453

Kashou, N. H., Leguire, L. E., Roberts, C. J., Fogt, N., Smith, M. A., & Rogers, G. L. (2010). Instruction dependent activation during optokinetic nystagmus (OKN) stimulation: An FMRI study at 3 T. *Brain Research*, *1336*, 10–21. https://doi.org/10.1016/j.brainres.2010.04.017

Kato, I., Harada, K., Hasegawa, T., & Ikarashi, T. (1988). Role of the nucleus of the optic tract of monkeys in optokinetic nystagmus and optokinetic after-nystagmus. *Brain Research*, *474*(1), 16–26. https://doi.org/10.1016/0006-8993(88)90665-8

Katz, E., Vianney de Jong, J. M. B., Buettner-Ennever, J., & Cohen, B. (1991). Effects of midline medullary lesions on velocity storage and the vestibulo-ocular reflex. *Experimental Brain Research 1991 87:3*, *87*(3), 505–520. https://doi.org/10.1007/BF00227076

Ke, S. R., Lam, J., Pai, D. K., & Spering, M. (2013). Directional asymmetries in human smooth pursuit eye movements. *Investigative Ophthalmology and Visual Science*, *54*(6), 4409–4421. https://doi.org/10.1167/IOVS.12-11369

Khan, S. G., Chen, K. F. C., & Frenkel, M. (1976). Subjective and objective visual acuity testing techniques. *Archives of Ophthalmology*, *94*(12), 2086–2091. https://doi.org/10.1001/archopht.1976.03910040746009

Kim, Y. J., Peterson, B. B., Crook, J. D., Joo, H. R., Wu, J., Puller, C., Robinson, F. R., Gamlin, P. D., Yau, K.-W., Viana, F., Troy, J. B., Smith, R. G., Packer, O. S., Detwiler, P. B., & Dacey, D. M. (2022). Origins of direction selectivity in the primate retina. *Nature Communications*. https://doi.org/10.1038/s41467-022-30405-5

Kirsch, W., Pfister, R., & Kunde, W. (2020). On why objects appear smaller in the visual periphery. *Psychological Science*, *31*(1), 88–96. https://doi.org/10.1177/0956797619892624

Kınıklıoğlu, M., & Boyaci, H. (2022). Increasing the spatial extent of attention strengthens surround suppression. *Vision Research*, *199*, 108074. https://doi.org/10.1016/J.VISRES.2022.108074

Knapp, C. M., Gottlob, I., McLean, R. J., & Proudlock, F. A. (2008). Horizontal and vertical look and stare optokinetic nystagmus symmetry in healthy adult volunteers. *Investigative Ophthalmology and Visual Science*, *49*(2), 581–588. https://doi.org/10.1167/iovs.07-0773

Knapp, C. M., Gottlob, I., McLean, R. J., Rafelt, S., & Proudlock, F. A. (2009). Effect of distance upon horizontal and vertical look and stare OKN. *Journal of Vision*, *9*(12), 23–23. https://doi.org/10.1167/9.12.23

Knapp, C. M., Proudlock, F. A., & Gottlob, I. (2013). OKN asymmetry in human subjects: A literature review. *Strabismus*, *21*(1), 37–49. https://doi.org/10.3109/09273972.2012.762532

Koenig, E., & Dichgans, J. (1981). Aftereffects of vestibular and optokinetic stimulation and their interaction. *Annals of the New York Academy of Sciences*, *374*(1), 434–445. https://doi.org/10.1111/J.1749-6632.1981.TB30889.X

Koerner, F., & Schiller, P. H. (1972). The optokinetic response under open and closed loop conditions in the monkey. *Experimental Brain Research*, *14*(3), 318–330. https://doi.org/10.1007/BF00816166

Komatsu, H., & Wurtz, R. H. (1988). Relation of cortical areas MT and MST to pursuit eye movements. III. Interaction with full-field visual stimulation. *Journal of Neurophysiology*, *60*(2), 621–644. https://doi.org/10.1152/JN.1988.60.2.621

Konen, C. S., Kleiser, R., Seitz, R. J., & Bremmer, F. (2005). An fMRI study of optokinetic nystagmus and smooth-pursuit eye movements in humans. *Experimental Brain Research*, *165*, 203–216. https://doi.org/10.1007/s00221-005-2289-7

Kremenitzer, J. P., Vaughan, H. G., Kurtzberg, D., & Dowling, K. (1979). Smooth-pursuit eye movements in the newborn infant. *Child Development*, *50*(2), 442. https://doi.org/10.2307/1129421

Kristjánsson, Á., & Sigurdardottir, H. M. (2008). On the benefits of transient attention across the visual field. *Perception*, *37*(5), 747–764. https://doi.org/10.1068/P5922

Kröller, J., & Behrens, F. (1995). Investigation of the horizontal, vertical, and oblique optokinetic nystagmus and afternystagmus in squirrel monkeys. *Journal of Vestibular Research*, *5*(3), 171–186.

Kustov, A. A., & Robinson, D. L. (1996). Shared neural control of attentional shifts and eye movements. *Nature*, *384*(6604), 74–77. https://doi.org/10.1038/384074A0

Lafortune, S., Ireland, D. J., Jell, R. M., & Duval, L. (1986a). Human optokinetic afternystagmus: Charging characteristics and stimulus exposure time dependence in the two-component model. *Acta Oto-Laryngologica*, *101*(5–6), 353–360. https://doi.org/10.3109/00016488609108619

Lafortune, S., Ireland, D. J., Jell, R. M., & Duval, L. (1986b). Human optokinetic afternystagmus: Stimulus velocity dependence of the two-component decay model and involvement of pursuit. *Acta Oto-Laryngologica*, *101*(3–4), 183–192. https://doi.org/10.3109/00016488609132826

Lakha, L., & Humphreys, G. (2005). Lower visual field advantage for motion segmentation during high competition for selection. *Spatial Vision*, *18*(4), 447–460. https://doi.org/10.1163/1568568054389570

Lankheet, M. J. M., & Verstraten, F. A. J. (1995). Attentional modulation of adaptation to two-component transparent motion. *Vision Res*, *35*(10), 1401–1412.

Lee, K. A., Foeller, P., Bradley, D. C., Tychsen, L., & Wong, A. M. F. (2009). Defining the critical period for smooth pursuit development in infant primates: Effects of binocular decorrelation. *Investigative Ophthalmology & Visual Science*, *50*(13), 1208. https://iovs.arvojournals.org/article.aspx?articleid=2363286

Leigh, J. R., & Zee, D. S. (2015). *The Neurology of Eye Movements* (5th ed.). Oxford University Press.

Levine, M. W., & McAnany, J. J. (2005). The relative capabilities of the upper and lower visual hemifields. *Vision Research*, *45*(21), 2820–2830. https://doi.org/10.1016/J.VISRES.2005.04.001

Li, H. H., Rankin, J., Rinzel, J., Carrasco, M., & Heeger, D. J. (2017). Attention model of binocular rivalry. *Proceedings of the National Academy of Sciences of the United States of America*, *114*(30), E6192–E6201. https://doi.org/10.1073/PNAS.1620475114

Li, W., & Westheimer, G. (1997). Human discrimination of the implicit orientation of simple symmetrical patterns. *Vision Research*, *37*(5), 565–572. https://doi.org/10.1016/S0042-6989(96)00166-6

Lindsay, G. W. (2020). Attention in psychology, neuroscience, and machine learning. *Frontiers in Computational Neuroscience*, *14*, 29. https://doi.org/10.3389/FNCOM.2020.00029

Lisberger, S. G., Miles, F. A., Optican, L. M., & Eighmy, B. B. (1981). Optokinetic response in monkey: underlying mechanisms and their sensitivity to long-term adaptive changes in vestibuloocular reflex. *Journal of Neurophysiology*, *45*(5), 869–890. https://doi.org/10.1152/jn.1981.45.5.869

Lisberger, S. G., & Pavelko, T. A. (1989). Topographic and directional organization of visual motion inputs for the initiation of horizontal and vertical smooth-pursuit eye movements in monkeys. *Journal of Neurophysiology*, *61*(1), 173–185. https://doi.org/10.1152/JN.1989.61.1.173

Logothetis, N. K., Leopold, D. A., & Sheinberg, D. L. (1996). What is rivalling during binocular rivalry? *Nature*, *380*(6575), 621–624. https://doi.org/10.1038/380621A0

Mackeben, M. (1999). Sustained focal attention and peripheral letter recognition. *Spatial Vision*, *12*(1), 51–72. https://doi.org/10.1163/156856899X00030

Magnusson, M., Pyykkö, I., & Jäntti, V. (1985). Effect of alertness and visual attention on optokinetic nystagmus in humans. *American Journal of Otolaryngology--Head and Neck Medicine and Surgery*, *6*(6), 419–425. https://doi.org/10.1016/S0196-0709(85)80020-X

Mareschal, I., Bex, P. J., & Dakin, S. C. (2008). Local motion processing limits fine direction discrimination in the periphery. *Vision Research*, *48*(16), 1719–1725. https://doi.org/10.1016/J.VISRES.2008.05.003

Marshall, T. R., O'shea, J., Jensen, O., Bergmann, T. O., O'shea, J., & Bergmann, T. O. (2015). Frontal eye fields control attentional modulation of alpha and gamma oscillations in contralateral occipitoparietal cortex. *The Journal of Neuroscience*, *35*(4), 1638–1647. https://doi.org/10.1523/JNEUROSCI.3116-14.2015

Martínez-Trujillo, J. C., & Treue, S. (2002). Attentional modulation strength in cortical area MT depends on stimulus contrast. *Neuron*, *35*(2), 365–370. https://doi.org/10.1016/S0896-6273(02)00778-X

Maruyama, M., Kobayashi, T., Katsura, T., & Kuriki, S. (2003). Early behavior of optokinetic responses elicited by transparent motion stimuli during depth-based attention. *Experimental Brain Research*, *151*, 411–419. https://doi.org/10.1007/s00221-003-1497-2

Matsuo, V., & Cohen, B. (1984). Vertical optokinetic nystagmus in the monkey: Up-down asymmetry effects of gravity. *Experimental Brain Research*, *53*, 197–216.

Maunsell, J. H. R., & Van Essen, D. C. (1983). Functional properties of neurons in middle temporal visual area of the macaque monkey. I. Selectivity for stimulus direction, speed, and orientation. *Journal of Neurophysiology*, *49*(5), 1127–1147. https://doi.org/10.1152/JN.1983.49.5.1127

Maunsell, J. H. R., & van Essen, D. C. (1987). Topographic organization of the middle temporal visual area in the macaque monkey: Representational biases and the relationship to callosal connections and myeloarchitectonic boundaries. *The Journal of Comparative Neurology*, *266*(4), 535–555. https://doi.org/10.1002/CNE.902660407

Melcher, D., Crespi, S., Bruno, A., & Morrone, M. C. (2004). The role of attention in central and peripheral motion integration. *Vision Research*, *44*(12), 1367–1374. https://doi.org/10.1016/J.VISRES.2003.11.023

Millodot, M., & Lamont, A. (1974). Peripheral visual acuity in the vertical plane. *Vision Research*, *14*(12), 1497–1498. https://doi.org/10.1016/0042-6989(74)90031-5

Montarolo, P. G., Precht, W., & Strata, P. (1981). Functional organisation of the mechanisms subserving the optokinetic nystagmus in the cat. *Neuroscience*, *6*, 231–246. https://doi.org/https://doi.org/10.1016/0306-4522(81)90059-2

Moore, T., & Armstrong, K. M. (2003). Selective gating of visual signals by microstimulation of frontal cortex. *Nature*, *421*(6921), 370–373. https://doi.org/10.1038/NATURE01341

Moran, J., & Desimone, R. (1985). Selective attention gates visual processing in the extrastriate cortex. *Science*, *229*, 782–784.

Morgan, M. (2013). Sustained attention is not necessary for velocity adaptation. *Journal of Vision*, *13*(8). https://doi.org/10.1167/13.8.26

Mullen, K. T. (1991). Colour vision as a post-receptoral specialization of the central visual field. *Vision Research*, *31*(1), 119–130. https://doi.org/10.1016/0042-6989(91)90079-K

Murasugi, C. M., & Howard, I. P. (1989a). Human horizontal optokinetic nystagmus elicited by the upper versus the lower visual fields. *Visual Neuroscience*, *2*(1), 73–79. https://doi.org/10.1017/S095252380000434X

Murasugi, C. M., & Howard, I. P. (1989b). Up-down asymmetry in human vertical optokinetic nystagmus and afternystagmus: contributions of the central and peripheral retinae. *Experimental Brain Research*, *77*(1), 183–192. https://doi.org/10.1007/BF00250580

Murasugi, C. M., Howard, I. P., & Ohmi, M. (1986). Optokinetic nystagmus: The effects of stationary edges, alone and in combination with central occlusion. *Vision Research*, *26*(7), 1155–1162. https://doi.org/10.1016/0042-6989(86)90049-0

Mustari, M. J., Fuchs, A. F., Kaneko, C. R. S., & Robinson, F. R. (1994). Anatomical connections of the primate pretectal nucleus of the optic tract. *Journal of Comparative Neurology*, *349*(1), 111–128. https://doi.org/10.1002/cne.903490108

Mustari, M. J., Fuchs, A. F., Langer, T. P., Kaneko, C., & Wallman, J. (1988). Chapter 11: The role of the primate lateral terminal nucleus in visuomotor behavior. *Progress in Brain Research*, *75*(C), 121–128. https://doi.org/10.1016/S0079-6123(08)60471-9

Newton, J. R., & Eskew, R. T. (2003). Chromatic detection and discrimination in the periphery: A postreceptoral loss of color sensitivity. *Visual Neuroscience*, 511521. https://doi.org/DOI:10.1017/S0952523803205058

Ninomiya, T., Sawamura, H., Inoue, K. ichi, & Takada, M. (2012). Segregated pathways carrying frontally derived top-down signals to visual areas MT and V4 in macaques. *The Journal of Neuroscience*, *32*(20), 6851–6858. https://doi.org/10.1523/JNEUROSCI.6295-11.2012

Nooij, S. A. E., Pretto, P., & Bülthoff, H. H. (2018). More vection means more velocity storage activity: a factor in visually induced motion sickness? *Experimental Brain Research 2018 236:11*, *236*(11), 3031–3041. https://doi.org/10.1007/S00221-018-5340-1

O'Craven, K. M., Rosen, B. R., Kwong, K. K., Treisman, A., & Savoy, R. L. (1997). Voluntary attention modulates fMRI activity in human MT-MST. *Neuron*, *18*(4), 591–598. https://doi.org/10.1016/S0896-6273(00)80300-1

Ono, S., Miura, K., Kawamura, T., & Kizuka, T. (2019). Asymmetric smooth pursuit eye movements and visual motion reaction time. *Physiological Reports*, *7*(14). https://doi.org/10.14814/PHY2.14187

Orban, G. A., Kennedy, H., & Bullier, J. (1986). Velocity sensitivity and direction selectivity of neurons in areas V1 and V2 of the monkey: influence of eccentricity. *Journal of Neurophysiology*, *56*(2), 462–480. https://doi.org/10.1152/JN.1986.56.2.462

Owsley, C., & Sloane, M. E. (1987). Contrast sensitivity, acuity, and the perception of "real-world" targets. *British Journal of Ophthalmology*, *71*, 791–796.

Oyster, C. W. (1968). The analysis of image motion by the rabbit retina. *The Journal of Physiology*, *199*(3), 613–635. https://doi.org/10.1113/JPHYSIOL.1968.SP008671

Oyster, C. W., & Barlow, H. B. (1967). Direction-selective units in rabbit retina: Distribution of preferred directions. *Science*, *155*(3764), 841–842. https://doi.org/10.1126/SCIENCE.155.3764.841

Paffen, C. L. E., & Alais, D. (2011). Attentional modulation of binocular rivalry. *Frontiers in Human Neuroscience*, *5*, 1–10. https://doi.org/10.3389/FNHUM.2011.00105

Paffen, C. L. E., Alais, D., & Verstraten, F. A. J. (2006). Attention speeds binocular rivalry. *Association for Psychological Science*, *17*(9), 752–756.

Paige, G. D. (1983). Vestibuloocular reflex and its interactions with visual following mechanisms in the squirrel monkey. I. Response characteristics in normal animals. *Journal of Neurophysiology*, *49*(1), 134–151. https://doi.org/10.1152/JN.1983.49.1.134

Pashler, H. E. (1998). *The Psychology of Attention*. The MIT Press.

Pasik, P., Pasik, T., Valciukas, J. A., & Bender, M. B. (1971). Vertical optokinetic nystagmus in the split-brain monkey. *Experimental Neurology*, *30*(1), 162–171. https://doi.org/10.1016/0014-4886(71)90230-5

Payne, W. H. (1967). Visual reaction times on a circle about the fovea. *Science*, *155*(3761), 481–482. https://doi.org/10.1126/SCIENCE.155.3761.481

Pham, N. C., Kim, Y. G., Kim, S. J., & Kim, C. H. (2021). Efficacy of spaced learning in adaptation of optokinetic response. *Brain and Behavior*, *11*(1). https://doi.org/10.1002/BRB3.1944

Pierrot-Deseilligny, C., Èri, R. M. M., Ploner, C. J., Gaymard, B., Demeret, S., & Rivaud-Pechoux, S. (2004). Decisional role of the dorsolateral prefrontal cortex in ocular motor behaviour. *Brain*, *126*(6), 1460–1473. https://doi.org/10.1093/brain/awg148

Pilz, K. S., & Papadaki, D. (2019). An advantage for horizontal motion direction discrimination. *Vision Research*, *158*, 164–172. https://doi.org/10.1016/J.VISRES.2019.03.005

Pitzalis, S., Sereno, M. I., Committeri, G., Fattori, P., Galati, G., Patria, F., & Galletti, C. (2010). Human V6: The Medial Motion Area. *Cerebral Cortex*, *20*(2), 411. https://doi.org/10.1093/CERCOR/BHP112

Pola, J., & Wyatt, H. J. (1985). Active and passive smooth eye movements: Effects of stimulus size and location. *Vision Research*, *25*(8), 1063–1076. https://doi.org/10.1016/0042-6989(85)90094-X

Purokayastha, S., Roberts, M., & Carrasco, M. (2021). Voluntary attention improves performance similarly around the visual field. *Attention, Perception, and Psychophysics*, *83*(7), 2784–2794. https://doi.org/10.3758/S13414-021-02316-Y

Qian, S. C., & Brascamp, J. W. (2019). The attentional modulation of binocular rivalry: An OKN approach. *Journal of Vision*, *19*(10), 131a–131a. https://doi.org/10.1167/19.10.131A

Raphan, T., & Cohen, B. (1988). Organizational principles of velocity storage in three dimensions: The effect of gravity on cross-coupling of optokinetic after-nystagmus. *Annals of the New York Academy of Sciences*, *545*, 74–92.

Recanzone, G. H., Wurtz, R. H., & Schwarz, U. (1997). Responses of MT and MST neurons to one and two moving objects in the receptive field. *Journal of Neurophysiology*, *78*(6), 2904–2915. https://doi.org/10.1152/JN.1997.78.6.2904/ASSET/IMAGES/LARGE/JNP.DE31F9.JPEG

Reed, M. J., Steinbach, M. J., Anstis, S. M., Gallie, B., Smith, D. S., & Kraft, S. (1991). The development of optokinetic nystagmus in strabismic and monocularly enucleated subjects. *Behavioural Brain Research*, *46*(1), 31–42. https://doi.org/10.1016/S0166-4328(05)80094-4

Rees, G., Frith, C. D., & Lavie, N. (1997). Modulating irrelevant motion perception by varying attentional load in an unrelated task. *Science*, *278*(5343), 1616–1619. https://doi.org/10.1126/SCIENCE.278.5343.1616/ASSET/047FC6B8-3F2C-49EF-B815-1337D0928B53/ASSETS/GRAPHIC/SE4876022001.JPEG

Reynolds, J. H., & Heeger, D. J. (2009). The Normalization Model of Attention. *Neuron*, *61*(2), 168–185. https://doi.org/10.1016/J.NEURON.2009.01.002

Reynolds, J. H., Pasternak, T., & Desimone, R. (2000). Attention increases sensitivity of V4 neurons. *Neuron*, *26*, 703–714.

Roberts, M., Ashinoff, B. K., Castellanos, F. X., & Carrasco, M. (2018). When attention is intact in adults with ADHD. *Psychonomic Bulletin & Review*, *25*(4), 1423–1434. https://doi.org/10.3758/S13423-017-1407-4

Roelofs, C. O. (1954). Optokinetic nystagmus. *Documenta Ophthalmologica*, *7–8*(1), 579–650. https://doi.org/10.1007/BF00238148

Rosenholtz, R. (2016). Capabilities and limitations of peripheral vision. *Annual Review of Vision Science*, *2*, 437–457. https://doi.org/10.1146/ANNUREV-VISION-082114-035733/CITE/REFWORKS

Rossit, S., McAdam, T., Mclean, D. A., Goodale, M. A., & Culham, J. C. (2013). fMRI reveals a lower visual field preference for hand actions in human superior parieto-occipital cortex (SPOC) and precuneus. *Cortex*, *49*(9), 2525–2541. https://doi.org/10.1016/J.CORTEX.2012.12.014

Rottach, K. G., Zivotofsky, A. Z., Das, V. E., Averbuch-Heller, L., Discenna, A. O., Poonyathalang, A., & Leigh, J. R. (1996). Comparison of horizontal, vertical and diagonal smooth pursuit eye movements in normal human subjects. *Vision Research*, *36*(14), 2189–2195. https://doi.org/10.1016/0042-6989(95)00302-9

Rubinstein, N. J., & Abel, L. A. (2011). Optokinetic nystagmus suppression as an index of the allocation of visual attention. *Investigative Opthalmology & Visual Science*, *52*(1), 462. https://doi.org/10.1167/IOVS.10-6016

Ruehl, R. M., Hoffstaedter, F., Reid, A., Eickhoff, S., & zu Eulenburg, P. (2019). Functional hierarchy of oculomotor and visual motion subnetworks within the human cortical optokinetic system. *Brain Structure and Function*, *224*, 567–582. https://doi.org/10.1007/s00429-018-1788-9

Rust, N. C., Simoncelli, E. P., & Movshon, J. A. (2002). Inhibitory interactions in MT receptive fields. *Journal of Vision*, *2*(7), 413–413. https://doi.org/10.1167/2.7.413

Sabbah, S., Gemmer, J. A., Bhatia-Lin, A., Manoff, G., Castro, G., Siegel, J. K., Jeffery, N., & Berson, D. M. (2017). A retinal code for motion along the gravitational and body axes. *Nature*, *546*(7659), 492–497. https://doi.org/10.1038/nature22818

Sasser, M. (1994). Vestibular-optokinetic eye movements. In K. J. Ciuffreda & B. Tannen (Eds.), *Eye movement basics for clinicians* (pp. 102–126). Mosby-Yearbook.

Schor, C. M., & Narayan, V. (1981). The influence of field size upon the spatial frequency response of optokinetic nystagmus. *Vision Research*, *21*(7), 985–994. https://doi.org/10.1016/0042-6989(81)90002-X

Schwartz, O., & Coen-Cagli, R. (2013). Visual attention and flexible normalization pools. *Journal of Vision*, *13*(1), 25–25. https://doi.org/10.1167/13.1.25

Shanidze, N., Fusco, G., Potapchuk, E., Heinen, S., & Verghese, P. (2016). Smooth pursuit eye movements in patients with macular degeneration. *Journal of Vision*, *16*(3), 1. https://doi.org/10.1167/16.3.1

Shin, Y. J., Park, K. H., Hwang, J. M., Wee, W. R., Lee, J. H., & Lee, I. B. (2006). Objective measurement of visual acuity by optokinetic response determination in patients with ocular diseases. *American Journal of Ophthalmology*, *141*(2), 327–332. https://doi.org/10.1016/j.ajo.2005.09.025

Smith, A. T., Greenlee, M. W., Singh, K. D., Kraemer, F. M., & Hennig, J. (1998). The processing of first- and second-order motion in human visual cortex assessed by functional magnetic resonance imaging (fMRI). *Journal of Neuroscience*, *18*(10), 3816–3830. https://doi.org/10.1523/jneurosci.18-10-03816.1998

Smith, A. T., & Snowden, R. J. (1994). *Visual Detection of Motion*. Academic Press.

Souto, D., & Kerzel, D. (2021). Visual selective attention and the control of tracking eye movements: A critical review. *Journal of Neurophysiology*, *125*(5), 1552–1576. https://doi.org/10.1152/JN.00145.2019

Sperling, G., & Melchner, M. J. (1978). The attention operating characteristic: Examples from visual search. *Science*, *202*(4365), 315–318.

Stanton, G. B., Bruce, C. J., & Goldberg, M. E. (1995). Topography of projections to posterior cortical areas from the macaque frontal eye fields. *The Journal of Comparative Neurology*, *353*(2), 291–305. https://doi.org/10.1002/CNE.903530210

Staugaard, C. F., Petersen, A., & Vangkilde, S. (2016). Eccentricity effects in vision and attention. *Neuropsychologia*, *92*, 69–78. https://doi.org/10.1016/j.neuropsychologia.2016.06.020

Steinman, R. M., Skavenski, A. A., & Sansbury, R. V. (1969). Voluntary control of smooth pursuit velocity. *Vision Research*, *9*(9), 1167–1171. https://doi.org/10.1016/0042-6989(69)90054-6

Stewart, L., Battelli, L., Walsh, V., & Cowey, A. (1999). Motion perception and perceptual learning studied by magnetic stimulation. *Electroencephalography and Clinical Neurophysiology*, *51*, 334–350.

Sundberg, K. A., Mitchell, J. F., & Reynolds, J. H. (2009). Spatial attention modulates center-surround interactions in macaque visual area V4. *Neuron*, *61*(6), 952–963. https://doi.org/10.1016/J.NEURON.2009.02.023

Takemura, A., Inoue, Y., & Kawano, K. (2002). Visually driven eye movements elicited at ultra-short latency are severely impaired by MST lesions. *Annals of the New York Academy of Sciences*, *956*, 456–459.

Takemura, A., & Kawano, K. (2002). Sensory-to-motor processing of the ocular-following response. *Neuroscience Research*, *43*(3), 201–206. https://doi.org/10.1016/S0168-0102(02)00044-5

Taore, A., Lobo, G., Turnbull, P. R., & Dakin, S. C. (2022). Diagnosis of colour vision deficits using eye movements. *Scientific Reports*, *12*(7734), 1–14. https://doi.org/10.1038/s41598-022-11152-5

Tauber, E. S., & Atkin, A. (1968). Optomotor responses to monocular stimulation: Relation to visual system organization. *Science*, *160*(3834), 1365–1367.

Ter Braak, J. W. G. (1936). Untersuchungen ueber optokinetischen nystagmus. *Archives de Physiologie*, 310–376.

Ter Braak, J. W. G., Schenk, V. W. D., & van Vliet, A. G. M. (1971). Visual reactions in a case of long-lasting cortical blindness. *Journal of Neurology, Neurosurgery & Psychiatry*, *34*(2), 140–147. https://doi.org/10.1136/jnnp.34.2.140

Théoret, H., Kobayashi, M., Ganis, G., Di Capua, P., & Pascual-Leone, A. (2002). Repetitive transcranial magnetic stimulation of human area MT/V5 disrupts perception and storage of the motion aftereffect. *Neuropsychologia*, *40*(13), 2280–2287. https://doi.org/10.1016/S0028-3932(02)00112-4

Thibos, L. N., Still, D. L., & Bradley, A. (1996). Characterization of spatial aliasing and contrast sensitivity in peripheral vision. *Vision Research*, *36*(2), 249–258. https://doi.org/10.1016/0042-6989(95)00109-D

Tootell, R. B. H., Hadjikhani, N. K., Vanduffel, W., Liu, A. K., Mendola, J. D., Sereno, M. I., & Dale, A. M. (1998). Functional analysis of primary visual cortex (V1) in humans. *Proceedings of the National Academy of Sciences of the United States of America*, *95*(3), 811–817.

Treue, S., & Martinez Trujillo, J. C. (1999). Feature-based attention influences motion processing gain in macaque visual cortex. *Nature*, *399*(6736), 575–579.

Treue, S., & Maunsell, J. H. R. (1996). Attentional modulation of visual motion processing in cortical areas MT and MST. *Nature*, *382*, 539–541.

Turalba, A. V., & Grosskreutz, C. (2010). A review of current technology used in evaluating visual function in glaucoma. *Seminars in Ophthalmology*, *25*(5–6), 309–316. https://doi.org/10.3109/08820538.2010.518898

Turano, K. A., & Heidenreich, S. M. (1999). Eye movements affect the perceived speed of visual motion. *Vision Research*, *39*(6), 1177–1187. https://doi.org/10.1016/S0042-6989(98)00174-6

Turatto, M., Vescovi, M., & Valsecchi, M. (2007). Attention makes moving objects be perceived to move faster. *Vision Research*, *47*(2), 166–178. https://doi.org/10.1016/J.VISRES.2006.10.002

Tychsen, L., Hurtig, R. R., & Thalacker, J. A. (1984). Defective downward smooth pursuit in infantile strabismus. *Investigative Ophthalmology and Visual Science, Supplement*, *25*, 74.

Tychsen, L., & Lisberger, S. G. (1986). Maldevelopment of visual motion processing in humans who had strabismus with onset in infancy. *Journal of Neuroscience*, *6*(9), 2495–2508. https://doi.org/10.1523/jneurosci.06-09-02495.1986

Tychsen, L., Rastelli, A., Steinman, S., & Steinman, B. (1996). Biases of motion perception revealed by reversing gratings in humans who had infantile-onset strabismus. *Developmental Medicine & Child Neurology*, *38*(5), 408–422. https://doi.org/10.1111/J.1469-8749.1996.TB15099.X

Tyler, C. W. (1987). Analysis of visual modulation sensitivity. III. Meridional variations in peripheral flicker sensitivity. *JOSA A, Vol. 4, Issue 8, Pp. 1612-1619*, *4*(8), 1612–1619. https://doi.org/10.1364/JOSAA.4.001612

Tynan, P. D., & Sekuler, R. (1982). Motion processing in peripheral vision: Reaction time and perceived velocity. *Vision Research*, *22*, 61–68.

Valmaggia, C., Charlier, J., & Gottlob, I. (2001). Optokinetic nystagmus in patients with central scotomas in age related macular degeneration. *British Journal of Ophthalmology*, *85*(2), 169–172. https://doi.org/10.1136/bjo.85.2.169

Valmaggia, C., & Gottlob, I. (2002). Optokinetic nystagmus elicited by filling-in in adults with central scotoma. *Investigative Ophthalmology and Visual Science*, *43*, 1804–1808.

Valmaggia, C., Proudlock, F. A., & Gottlob, I. (2003). Optokinetic nystagmus in strabismus: Are asymmetries related to binocularity? *Investigative Ophthalmology and Visual Science*, *44*(12), 5142–5150. https://doi.org/10.1167/iovs.03-0322

Valmaggia, C., Proudlock, F. A., & Gottlob, I. (2005). Look and stare optokinetic nystagmus in healthy subjects and in patients with no measurable binocularity. A prospective study. *Klinische Monatsblatter Fur Augenheilkunde*, *222*(3), 196–201. https://doi.org/10.1055/s-2005-858013

Valsecchi, M., Toscani, M., & Gegenfurtner, K. R. (2013). Perceived numerosity is reduced in peripheral vision. *Journal of Vision*, *13*(13), 7–7. https://doi.org/10.1167/13.13.7

van den Berg, A. V., & Collewijn, H. (1988). Directional asymmetries of human optokinetic nystagmus. *Experimental Brain Research*, *70*(3), 597–604. https://doi.org/10.1007/BF00247608

van Die, G. C., & Collewijn, H. (1982). Optokinetic nystagmus in man. Role of central and peripheral retina and occurrence of asymmetries. *Human Neurobiology*, *1*(2), 111–119. https://pubmed.ncbi.nlm.nih.gov/7185785/

van Die, G. C., & Collewijn, H. (1986). Control of human optokinetic nystagmus by the central and peripheral retina: Effects of partial visual field masking, scotopic vision and central retinal scotomata. *Brain Research*, *383*(1–2), 185–194. https://doi.org/10.1016/0006-8993(86)90019-3

Van Essen, D. C., Maunsell, J. H. R., & Bixby, J. L. (1981). The middle temporal visual area in the macaque: Myeloarchitecture, connections, functional properties and topographic organization. *Journal of Comparative Neurology*, *199*(3), 293–326. https://doi.org/10.1002/CNE.901990302

Van Hof-Van Duin, J., & Mohn, G. (1983). Optokinetic and spontaneous nystagmus in children with neurological disorders. *Behavioural Brain Research*, *10*, 163–175.

Veniero, D., Gross, J., Morand, S., Duecker, F., Sack, A. T., & Thut, G. (2021). Top-down control of visual cortex by the frontal eye fields through oscillatory realignment. *Nature Communications*, *12*(1). https://doi.org/10.1038/S41467-021-21979-7

Ventre-Dominey, J., & Luyat, M. (2009). Asymmetry of visuo-vestibular mechanisms contributes to reversal of optokinetic after-nystagmus. *Experimental Brain Research*, *193*(1), 55–67. https://doi.org/10.1007/s00221-008-1595-2

Virsu, V., & Rovamo, J. (1979). Visual resolution, contrast sensitivity, and the cortical magnification factor. *Experimental Brain Research*, *37*(3), 475–494. https://doi.org/10.1007/BF00236818

Von Hofsten, C., & Rosander, K. (1997). Development of smooth pursuit tracking in young infants. *Vision Research*, *37*(13), 1799–1810. https://doi.org/10.1016/S0042-6989(96)00332-X

Waespe, W., & Henn, V. (1977). Brain neuronal activity in the vestibular nuclei of the alert monkey during vestibular and optokinetic stimulation. *Experimental Brain Research*, *27*, 523–538.

Waespe, W., & Schwarz, U. (1986). Characteristics of eye velocity storage during periods of suppression and reversal of eye velocity in monkeys. *Experimental Brain Research*, *65*(1), 49–58. https://doi.org/10.1007/BF00243829

Wang, A. Y. M., Kulkarni, M. M., McLaughlin, A. J., Gayet, J., Smith, B. E., Hauptschein, M., McHugh, C. F., Yao, Y. Y., & Puthussery, T. (2023). An ON-type direction-selective ganglion cell in primate retina. *Nature 2023 623:7986*, *623*(7986), 381–386. https://doi.org/10.1038/s41586-023-06659-4

Watamaniuk, S. N. J., & Sekuler, R. (1992). Temporal and spatial integration in dynamic random-dot stimuli. *Vision Research*, *32*(12), 2341–2347.

Wen, W., Wu, S., Wang, S., Zou, L., Liu, Y., Liu, R., Zhang, P., He, S., & Liu, H. (2018). A novel dichoptic optokinetic nystagmus paradigm to quantify interocular suppression in monocular amblyopia. *Investigative Ophthalmology & Visual Science*, *59*(12), 4775–4782. https://doi.org/10.1167/IOVS.17-23661

Wester, S. T., Rizzo, J. F., Balkwill, M. D., & Wall, C. (2007). Optokinetic nystagmus as a measure of visual function in severely visually impaired patients. *Investigative Ophthalmology and Visual Science*, *48*(10), 4542–4548. https://doi.org/10.1167/iovs.06-1206

Williams, I. M., Mulhall, L., Mattingley, J., Lueck, C., & Abel, L. (2006). Optokinetic nystagmus as an assessment of visual attention to divided stimuli. *Journal of Clinical Neuroscience*, *13*(8), 828–833. https://doi.org/10.1016/J.JOCN.2005.10.010

Williams, I. M., Schofield, P., Khade, N., & Abel, L. A. (2016). Divided visual attention: A comparison of patients with multiple sclerosis and controls, assessed with an optokinetic nystagmus suppression task. *Journal of Clinical Neuroscience*, *34*, 187–192. https://doi.org/10.1016/j.jocn.2016.06.015

Winterson, B. J., & Steinman, R. M. (1978). The effect of luminance on human smooth pursuit of perifoveal and foveal targets. *Vision Research*, *18*(9), 1165–1172. https://doi.org/10.1016/0042-6989(78)90100-1

Wolfe, J. M., O'Neill, P., & Bennett, S. C. (1998). Why are there eccentricity effects in visual search? Visual and attentional hypotheses. *Perception & Psychophysics*, *60*(1), 140–156.

Wright, K. W. (1996). Clinical optokinetic nystagmus asymmetry in treated esotropes. *Journal of Pediatric Ophthalmology and Strabismus*, *33*(3), 153–155. https://doi.org/10.3928/0191-3913-19960501-06

Wyatt, H. J., & Pola, J. (1984). A mechanism for suppression of optokinesis. *Vision Research*, *24*(12), 1931–1945. https://doi.org/10.1016/0042-6989(84)90027-0

Xiao, D.-K., Marcar, V. L., Raiguel, S. E., & Orban, G. A. (1997). Selectivity of macaque MT/V5 neurons for surface orientation in depth specified by motion. *European Journal of Neuroscience*, *9*(5), 956–964. https://doi.org/10.1111/J.1460-9568.1997.TB01446.X

Zarei Eskikand, P., Kameneva, T., Burkitt, A. N., Grayden, D. B., & Ibbotson, M. R. (2020). Adaptive surround modulation of MT neurons: A computational model. *Frontiers in Neural Circuits*, *14*. https://doi.org/10.3389/FNCIR.2020.529345

Zee, D. S., Yee, R. D., Cogan, D. G., Robinson, D. A., & Engel, W. K. (1976). Ocular motor abnormalities in hereditary cerebellar ataxia. *Brain*, *99*(2), 207–234. https://doi.org/10.1093/brain/99.2.207

Appendix A

Professional Internship for PhD Students (PIPS) Reflective Statement: Open Science Tools Ltd.

Note to examiners:

This statement is included as an appendix to the thesis in order that the thesis accurately captures the PhD training experienced by the candidate as a BBSRC Doctoral Training Partnership student.

The Professional Internship for PhD Students is a compulsory 3-month placement which must be undertaken by DTP students. It is usually centred on a specific project and must not be related to the PhD project. This reflective statement is designed to capture the skills development which has taken place during the student's placement and the impact on their career plans it has had.

Reflective statement:

During my PIPS, I worked for Open Science Tools Ltd., a company that makes open-source software for researchers including the software *PsychoPy*. I was already somewhat familiar with PsychoPy, having learned it as an undergrad before teaching it as a postgrad. Working with PsychoPy during my PIPS thus seemed ideal, as it wasn't completely new ground, but there was still plenty left to learn.

PsychoPy is written in Python, whereas I am a MATLAB user with very little experience of Python. For this reason, it was initially decided that I would work on improving documentation; as a fairly naïve observer, since I don't routinely use PsychoPy, I am in an ideal position to identify issues with their current documentation. We decided that I would set up an experiment in PsychoPy 'Builder' (PsychoPy's GUI for building experiments using pre-programmed modules) and attempt to integrate the experiment with eye tracking hardware (EyeLink 1000). We also decided that I would do this without input from the PsychoPy team, as we wanted to see how easy it would be for me to do using only the available documentation. Through this process, we identified issues with

the existing documentation. I eventually wrote new documentation to more accurately reflect the current status of PsychoPy hardware integration.

Two weeks into my PIPS with Open Science Tools, they held an event that they call the 'code sprint'. This is an annual event in which people – researchers, software developers, students, etc. – travel to Nottingham to work on PsychoPy-related problems together. For example, one person was a researcher from Indiana, USA, who wanted to develop her own plugin; another was a man from Germany who had created his own eye tracker and wanted to integrate it with PsychoPy. There was even a Welsh BBSRC DTP student who, like me, was doing his PIPS. I appreciated the opportunity to talk to individuals from a range of different backgrounds about their work.

During the code sprint, I continued with my project of setting up a successful eye tracking experiment in PsychoPy. I found that running an unencumbered experiment with the available hardware was near impossible; there was a bug in our midst preventing the calibration process from functioning. Despite having very little Python experience, I combed through some very dense codes, and with the patient assistance of the PsychoPy team, the issue was found. We could see another problem, but we unfortunately declared that particular bug to be an 'easy fix'. Fate clearly punished us for our arrogance, as that bug remained a frustrating mystery for over two weeks.

Once we had fixed the bugs identified during the code sprint, more came up, of course. So, those were also addressed. I was then pointed towards some issues that users were reporting in the forum, to have a look into those as well. Many of the issues we found were around the same theme, such as the wrong units being inherited somewhere so that stimuli are drawn too small. This meant that they were easy to resolve, thankfully.

Once I had run out of bugs to fix, I turned my attention back to improving documentation and improving navigation between docs. The documentation was written in RST (restructured text) which meant that once again, there was something new to learn. For the most part it was easy to simply follow guides online and look at the formatting of existing docs. This wasn't without hiccups, though. For example, I wanted to add a hyperlink to the documentation so that people could easily navigate to the correct place. Unfortunately, it took several iterations to get this right, as every time the updated documentation went live, the hyperlink was broken. My Github account has become a monument to this mistake, as a list of pull requests labelled 'attempt to fix hyperlink' document my many failed attempts.

Overall, I have found working with Open Science Tools Ltd. to be a pleasant experience. The team are very supportive and create a fun working environment, facilitated by a never-ending stream of coffee. I have picked up skills in Python, RST and Github. I feel that I have gained an insight into the world of

software development, which in some ways feels like endlessly falling up an infinite flight of stairs as things are serially improved, but somehow there is never a single unifying moment in which everything *'just works'*. Though any contributions that I have made in the form of bug fixes or docs written were contingent on the support of the rest of the team, I still feel a sense of pride in knowing that I have played a small role in helping to improve the user experience, ultimately making carrying out research more accessible, which is something I value greatly.

Appendix B

Individual analyses: Experiment 1

Table AB.1

Results of linear regression analysis to predict the gain of OKR using three predictor variables (velocity, orientation of motion, instruction type)

P1 Gain	β	SE	F	*p*
Intercept	1.2340	0.035	35.631	< .001*
Velocity	-0.0130	0.001	-13.637	< .001*
Orientation (vertical)	-0.2385	0.034	-7.098	< .001*
Orientation (oblique)	0.0131	0.029	0.452	.654
Instruction type	-0.0405	0.024	-1.706	.095
P2 Gain	β	SE	F	*p*
Intercept	0.9666	0.043	22.588	< .001*
Velocity	-0.0154	0.001	-13.061	< .001*
Orientation (vertical)	-0.0975	0.042	-2.348	.024*
Orientation (oblique)	-0.0138	0.036	-0.385	.702
Instruction type	-0.3443	0.029	-11.728	< .001*
P3 Gain	β	SE	F	*p*
Intercept	1.1934	0.043	27.59	< .001*
Velocity	-0.0228	0.001	-19.134	< .001*
Orientation (vertical)	-0.2341	0.042	-5.577	< .001*
Orientation (oblique)	-0.0524	0.036	-1.442	.156
Instruction type	-0.1339	0.030	-4.512	< .001*
P4 Gain	β	SE	F	*p*
Intercept	1.2152	0.044	27.814	< .001*
Velocity	-0.0229	0.001	-19.035	< .001*
Orientation (vertical)	-0.1588	0.042	-3.746	< .001*
Orientation (oblique)	-0.0492	0.037	-1.341	.187
Instruction type	-0.0520	0.030	-1.735	.090
P5 Gain	β	SE	F	*p*
Intercept	1.7463	0.067	26.144	< .001*
Velocity	-0.0324	0.002	-17.654	< .001*
Orientation (vertical)	-0.2496	0.065	-3.852	< .001*
Orientation (oblique)	-0.0779	0.056	-1.388	.172
Instruction type	-0.1194	0.046	-2.605	.013*
P6 Gain	β	SE	F	*p*
Intercept	1.4664	0.047	30.972	< .001*
Velocity	-0.0276	0.001	-21.224	< .001*
Orientation (vertical)	-0.2058	0.046	-4.481	< .001*
Orientation (oblique)	-0.0773	0.040	-1.943	.059
Instruction type	-0.0525	0.032	-1.617	.113
P7 Gain	β	SE	F	*p*
Intercept	1.3930	0.047	29.599	< .001*
Velocity	-0.0206	0.001	-15.903	< .001*
Orientation (vertical)	-0.3120	0.046	-6.833	< .001*
Orientation (oblique)	-0.0757	0.040	-1.914	.062
Instruction type	-0.0688	0.032	-2.133	.039*
P8 Gain	β	SE	F	*p*
Intercept	1.4046	0.062	22.678	< .001*
Velocity	-0.0246	0.002	-14.469	< .001*
Orientation (vertical)	-0.2523	0.060	-4.199	< .001*
Orientation (oblique)	-0.0334	0.052	-0.641	.525
Instruction type	-0.0999	0.042	-2.351	.023*

Note: 'Orientation' uses horizontal motion as a reference variable

Table AB.2

Results of linear regression analysis to predict the frequency of OKR using three predictor variables (velocity, orientation of motion, instruction type)

P1 Frequency	β	SE	F	*p*
Intercept	1.9290	0.216	8.950	< .001*
Velocity	-0.0131	0.006	-2.204	.033*
Orientation (vertical)	-0.4583	0.209	-2.192	.033*
Orientation (oblique)	0.1442	0.181	0.796	.430
Instruction type	0.2883	0.148	1.950	.058
P2 Frequency	β	SE	F	*p*
Intercept	2.0381	0.167	12.183	< .001*
Velocity	-0.0117	0.005	-2.552	.014*
Orientation (vertical)	-0.5512	0.162	-3.399	.001*
Orientation (oblique)	0.0175	0.141	0.125	.901
Instruction type	-0.4417	0.115	-3.849	< .001*
P3 Frequency	β	SE	F	*p*
Intercept	1.5235	0.199	7.664	< .001*
Velocity	-0.0120	0.005	-2.190	.034*
Orientation (vertical)	-0.3783	0.193	-1.962	.056
Orientation (oblique)	0.1175	0.167	0.704	.486
Instruction type	0.1583	0.136	1.161	.252
P4 Frequency	β	SE	F	*p*
Intercept	1.4023	0.136	10.285	< .001*
Velocity	-0.0139	0.004	-3.717	< .001*
Orientation (vertical)	-0.0800	0.132	-0.605	.548
Orientation (oblique)	-0.0125	0.115	-0.109	.914
Instruction type	-0.0008	0.094	-0.009	.993
P5 Frequency	β	SE	F	*p*
Intercept	1.3837	0.160	8.643	< .001*
Velocity	0.0029	0.004	0.661	.512
Orientation (vertical)	-0.3033	0.155	-1.953	.057
Orientation (oblique)	0.0117	0.135	0.087	.931
Instruction type	-0.7700	0.110	-7.011	< .001*
P6 Frequency (non-sig)	β	SE	F	*p*
Intercept	1.6712	0.132	12.620	< .001*
Velocity	-0.0027	0.004	-0.740	.463
Orientation (vertical)	-0.0467	0.128	-0.363	.718
Orientation (oblique)	-0.0033	0.111	-0.030	.976
Instruction type	0.2467	0.091	2.715	.009*
P7 Frequency (non-sig)	β	SE	F	*p*
Intercept	1.5981	0.208	7.687	< .001*
Velocity	0.00002	0.006	0.005	.996
Orientation (vertical)	-0.2467	0.202	-1.223	.228
Orientation (oblique)	0.0592	0.175	0.339	.736
Instruction type	-0.0908	0.143	-0.637	.528
P8 Frequency	β	SE	F	*p*
Intercept	1.7042	0.199	8.560	< .001*
Velocity	-0.0081	0.005	-1.478	.147
Orientation (vertical)	-0.1200	0.193	-0.621	.538
Orientation (oblique)	0.1058	0.167	0.633	.530
Instruction type	-0.3842	0.137	-2.813	.007*

Note: 'Orientation' uses horizontal motion as a reference variable

Table AB.3

Results of linear regression analysis to predict the amplitude of OKR using three predictor variables (velocity, orientation of motion, instruction type)

P1 Amplitude	β	SE	F	*p*
Intercept	3.5443	0.605	5.858	< .001*
Velocity	0.1753	0.017	10.534	< .001*
Orientation (vertical)	-0.5989	0.587	-1.020	.313
Orientation (oblique)	0.1041	0.508	0.205	.839
Instruction type	-2.1493	0.415	-5.178	< .001*
P2 Amplitude	β	SE	F	*p*
Intercept	4.4436	0.480	9.255	< .001*
Velocity	0.0042	0.013	0.317	.753
Orientation (vertical)	-0.1052	0.466	-0.226	.822
Orientation (oblique)	-0.1888	0.403	-0.468	.642
Instruction type	-3.4731	0.329	-10.545	< .001*
P3 Amplitude	β	SE	F	*p*
Intercept	9.4428	0.891	10.593	< .001*
Velocity	-0.0891	0.025	-3.634	< .001*
Orientation (vertical)	-2.5349	0.865	-2.931	.005*
Orientation (oblique)	-1.8033	0.749	-2.408	.020*
Instruction type	-3.8943	0.611	-6.368	< .001*
P4 Amplitude	β	SE	F	*p*
Intercept	5.9687	0.562	10.615	< .001*
Velocity	-0.0179	0.015	-1.157	.254
Orientation (vertical)	-1.9677	0.545	-3.607	< .001*
Orientation (oblique)	-1.1931	0.472	-2.526	.015*
Instruction type	-0.7862	0.386	-2.038	.048*
P5 Amplitude	β	SE	F	*p*
Intercept	6.0318	0.556	10.847	< .001*
Velocity	-0.0197	0.015	-1.289	.204
Orientation (vertical)	-0.4766	0.539	-0.884	.382
Orientation (oblique)	-0.6731	0.467	-1.440	.157
Instruction type	-2.0080	0.381	-5.264	< .001*
P6 Amplitude	β	SE	F	*p*
Intercept	7.4858	0.774	9.676	< .001*
Velocity	-0.0427	0.021	-2.005	.051
Orientation (vertical)	-1.5676	0.751	-2.089	.043*
Orientation (oblique)	-1.1316	0.650	-1.741	.089
Instruction type	-0.9227	0.531	-1.739	.089
P7 Amplitude	β	SE	F	*p*
Intercept	6.7228	0.722	9.312	< .001*
Velocity	0.0546	0.020	2.747	.009*
Orientation (vertical)	-3.3732	0.700	-4.816	< .001*
Orientation (oblique)	-1.5732	0.607	-2.594	.013*
Instruction type	-1.1550	0.495	-2.332	.024*
P8 Amplitude	β	SE	F	*p*
Intercept	4.8054	0.446	10.776	< .001*
Velocity	-0.0196	0.012	-1.600	.117
Orientation (vertical)	-0.3809	0.433	-0.880	.384
Orientation (oblique)	-0.1991	0.375	-0.531	.598
Instruction type	-1.1916	0.306	-3.895	< .001*

Note: 'Orientation' uses horizontal motion as a reference variable

Table AB.4

Results of linear regression analysis to predict the occurrence of OKAN using five predictors (preceding stimulus velocity, motion orientation, instruction type, preceding OKR angular SP deviation and gain)

P1	β	SE	F	*p*
Intercept	38.8440	18.246	2.129	.033*
Velocity	-0.4074	0.194	-2.100	.036*
Orientation (vertical)	-1.3938	1.944	-0.717	.473
Orientation (up oblique)	3.5293	1.709	2.065	.039*
Orientation (down oblique)	0.1621	3.100	0.052	.958
Instruction type	-3.6752	1.630	-2.255	.024*
Angular SP deviation	0.3117	0.203	1.532	.126
Gain	-33.5010	16.033	-2.089	.037*
P2 (non-sig)	β	SE	F	*p*
Intercept	-5.6960	4.345	-1.311	.190
Velocity	0.1001	0.074	1.355	.175
Orientation (vertical)	1.9945	1.197	1.667	.096
Orientation (up oblique)	1.0261	0.983	1.044	.296
Orientation (down oblique)	-2.4870	1.635	-1.521	.128
Instruction type	2.6149	1.765	1.482	.138
Angular SP deviation	0.1285	0.078	1.646	.100
Gain	3.1134	3.975	0.783	.433
P4 (non-sig)	β	SE	F	*p*
Intercept	-0.1192	5.585	-0.021	.983
Velocity	-0.0161	0.109	-0.148	.883
Orientation (vertical)	0.9796	1.353	0.724	.469
Orientation (up oblique)	0.0984	1.063	0.093	.926
Orientation (down oblique)	1.5129	1.546	0.979	.328
Instruction type	0.4164	0.830	0.502	.616
Angular SP deviation	0.0148	0.090	0.165	.869
Gain	2.1654	4.679	0.463	.644
P6 (non-sig)	β	SE	F	*p*
Intercept	-2.9556	4.816	-0.614	.539
Velocity	0.0754	0.095	0.792	.429
Orientation (vertical)	1.4488	1.295	1.119	.263
Orientation (up oblique)	0.3212	0.921	0.349	.727
Orientation (down oblique)	0.0127	1.215	0.010	.992
Instruction type	-0.5187	0.681	-0.762	.446
Angular SP deviation	0.0402	0.052	0.779	.436
Gain	2.0333	3.243	0.627	.531
P7	β	SE	F	*p*
Intercept	18.154	6.653	2.729	.006*
Velocity	-0.2451	0.100	-2.448	.014*
Orientation (vertical)	-5.4408	1.899	-2.866	.004*
Orientation (up oblique)	-4.4299	2.416	-1.833	.067
Orientation (down oblique)	-2.5195	1.502	-1.678	.093
Instruction type	-1.1953	0.796	-1.502	.133
Angular SP deviation	0.1255	0.111	1.133	.257
Gain	-13.2890	4.788	-2.776	.006*
P8 (non-sig)	β	SE	F	*p*
Intercept	2.6523	3.624	0.732	.464
Velocity	-0.0242	0.059	-0.410	.682
Orientation (vertical)	-0.1196	1.114	-0.107	.915
Orientation (up oblique)	-0.1341	0.992	-0.135	.892
Orientation (down oblique)	2.1668	1.472	1.472	.141
Instruction type	0.4024	0.643	0.626	.531
Angular SP deviation	-0.1219	0.079	-1.545	.122
Gain	-1.7826	2.330	-0.765	.444

Note: 'Orientation' uses horizontal motion as a reference variable

Table AB.5

Results of linear regression analysis to predict the occurrence of OKAN using five predictors (preceding stimulus velocity, motion orientation, instruction type, preceding OKR angular SP deviation and frequency)

	β	SE	F	*p*
Intercept	-1.5648	0.465	-3.365	< .001*
Velocity	0.0094	0.009	1.099	.272
Orientation (vertical)	0.6944	0.303	2.292	.022*
Orientation (up oblique)	0.3535	0.306	1.155	.248
Orientation (down oblique)	0.0343	0.379	0.091	.928
Instruction type	0.0974	0.210	0.463	.643
Angular SP deviation	0.0148	0.017	0.871	.384
Frequency	0.6069	0.207	2.934	.003*

Note: Analysis of orientation uses horizontal motion as a reference variable

Table AB.6

Results of linear regression analysis to predict the reversal of OKAN using four predictors (preceding stimulus velocity, instruction type, preceding OKR angular slow phase (SP) deviation and gain)

P1	β	SE	F	*p*
Intercept	26.3110	10.483	2.510	.012*
Velocity	-0.4738	0.184	-2.576	.010*
Instruction type	-0.6543	1.393	-0.470	.638
Angular SP deviation	0.6073	0.222	2.736	.006*
Gain	-27.6250	10.451	-2.643	.008*
P2	β	SE	F	*p*
Intercept	9.3433	9.438	0.990	.322
Velocity	-0.1255	0.166	-0.754	.451
Instruction type	-1.4266	3.542	-0.403	.687
Angular SP deviation	0.1616	0.153	1.055	.292
Gain	-14.483	10.474	-1.383	.167
P4	β	SE	F	*p*
Intercept	19.3330	6.859	2.819	.005*
Velocity	-0.3565	0.139	-2.560	.010*
Instruction type	-1.0880	1.043	-1.043	.297
Angular SP deviation	0.1514	0.077	1.956	.050*
Gain	-19.6480	6.262	-3.138	.002*
P6	β	SE	F	*p*
Intercept	12.2350	6.703	1.826	.068
Velocity	-0.2573	0.144	-1.786	.074
Instruction type	-0.8296	1.036	-0.801	.423
Angular SP deviation	0.0429	0.051	0.846	.397
Gain	-11.1680	5.160	-2.164	.030*
P7 (non-sig)	β	SE	F	*p*
Intercept	1.4393	3.951	0.364	.715
Velocity	-0.0323	0.070	-0.461	.644
Instruction type	1.4408	1.052	1.370	.171
Angular SP deviation	0.0827	0.062	1.326	.185
Gain	-1.9395	3.125	-0.621	.535
P8	β	SE	F	*p*
Intercept	18.2650	9.959	1.834	.067
Velocity	-0.4854	0.232	-2.091	.037*
Instruction type	-3.9395	2.114	-1.864	.062
Angular SP deviation	0.2821	0.131	2.148	.032*
Gain	-14.4070	7.820	-1.842	.065

Appendix C

Individual analyses: Experiment 3

Table AC.1

Results of linear regression analysis to predict the gain of OKR in the centre (<10 deg eccentricity) based on three predictor variables (eccentricity, task condition, orientation of motion)

P1 Gain	β	SE	F	*p*
Intercept	0.6530	0.054	12.079	< .001*
Eccentricity	-0.0650	0.008	-8.091	< .001*
Orientation	-0.2274	0.028	8.063	< .001*
Task	0.0018	0.074	0.024	.981
Eccentricity*Task	0.0023	0.011	0.203	.840
P2 Gain	β	SE	F	*p*
Intercept	0.2159	0.232	9.319	< .001*
Eccentricity	-0.0077	0.003	-2.238	.027*
Orientation	0.0531	0.012	4.393	< .001*
Task	0.0640	0.032	2.022	.046*
Eccentricity*Task	-0.0060	0.005	-1.238	.219
P3 Gain	β	SE	F	*p*
Intercept	0.3883	0.039	9.988	< .001*
Eccentricity	-0.0354	0.006	-6.118	< .001*
Orientation	0.0339	0.020	1.672	.098
Task	0.1491	0.053	2.810	.006*
Eccentricity*Task	-0.0090	0.008	-1.100	.274
P4 Gain	β	SE	F	*p*
Intercept	0.4756	0.037	13.004	< .001*
Eccentricity	-0.0465	0.005	-8.548	< .001*
Orientation	0.0433	0.019	2.270	.025*
Task	0.0662	0.050	1.325	.188
Eccentricity*Task	0.0009	0.008	0.118	.906
P5 Gain	β	SE	F	*p*
Intercept	0.4868	0.038	12.880	< .001*
Eccentricity	-0.0531	0.006	-9.449	< .001*
Orientation	0.0479	0.020	2.432	.017*
Task	-0.0051	0.052	-0.099	.921
Eccentricity*Task	0.0102	0.008	1.280	.203
P6 Gain	β	SE	F	*p*
Intercept	0.3629	0.039	9.424	< .001*
Eccentricity	-0.0368	0.006	-6.426	< .001*
Orientation	0.1203	0.020	5.989	< .001*
Task	0.0562	0.053	1.068	.288
Eccentricity*Task	-0.0009	0.008	-0.111	.912
P7 Gain	β	SE	F	*p*
Intercept	0.4078	0.031	13.105	< .001*
Eccentricity	-0.0412	0.005	-8.913	< .001*
Orientation	0.0176	0.016	1.082	.282
Task	0.0857	0.042	2.017	.046*
Eccentricity*Task	0.0007	0.007	0.103	.918
P8 Gain	β	SE	F	*p*
Intercept	0.3887	0.033	11.684	< .001*
Eccentricity	-0.0320	0.005	-6.468	< .001*
Orientation	0.0685	0.017	3.947	< .001*
Task	0.0662	0.045	1.457	.148
Eccentricity*Task	0.0025	0.007	0.360	.720
P9 Gain	β	SE	F	*p*
Intercept	0.3799	0.0287	13.243	< .001*
Eccentricity	-0.0401	0.0043	-9.412	< .001*
Orientation	0.0118	0.0150	0.792	.431
Task	0.0295	0.0391	0.753	.453
Eccentricity*Task	0.0080	0.0060	1.327	.188

Note: 'Orientation' used horizontal motion as a reference level.

Table AC.2

Results of linear regression analysis to predict the gain of OKR in the periphery (>10 deg eccentricity) based on four predictor variables (eccentricity, task condition, orientation of motion, upper versus lower visual field)

P1 Gain	β	SE	F	*p*
Intercept	0.3459	0.052	6.681	< .001*
Eccentricity	-0.0137	0.003	-4.383	< .001*
Orientation	0.0485	0.015	3.246	.002*
Task	-0.1827	0.072	-2.548	.013*
Lower vis field	0.0050	0.015	0.334	.739
Eccentricity*Task	0.0131	0.004	2.984	.004*
P2 Gain (non-sig)	β	SE	F	*p*
Intercept	0.1599	0.072	2.228	.028*
Eccentricity	-0.0047	0.004	-1.090	.279
Orientation	0.0177	0.021	0.857	.394
Task	0.0121	0.099	0.121	.904
Lower vis field	0.0287	0.021	1.388	.169
Eccentricity*Task	0.0022	0.006	0.368	.713
P3 Gain	β	SE	F	*p*
Intercept	0.1055	0.044	2.407	.018*
Eccentricity	-0.0032	0.003	-1.197	.234
Orientation	0.0237	0.013	1.878	.064
Task	0.1013	0.061	1.670	.098
Lower vis field	-0.0002	0.013	-0.014	.989
Eccentricity*Task	0.0002	0.004	0.061	.952
P4 Gain	β	SE	F	*p*
Intercept	0.1184	0.037	3.206	.002*
Eccentricity	-0.0032	0.002	-1.460	.148
Orientation	-0.0214	0.011	-2.007	.048*
Task	0.1719	0.051	3.362	.001*
Lower vis field	0.0025	0.011	0.233	.817
Eccentricity*Task	-0.0028	0.003	-0.897	.372
P5 Gain	β	SE	F	*p*
Intercept	0.0643	0.045	1.443	.153
Eccentricity	-0.0004	0.003	-0.137	.891
Orientation	-0.0208	0.013	-1.618	.109
Task	0.1101	0.062	1.784	.078
Lower vis field	0.0205	0.013	1.599	.113
Eccentricity*Task	-0.0001	0.004	-0.020	.984
P6 Gain	β	SE	F	*p*
Intercept	0.1019	0.052	1.962	.053
Eccentricity	-0.0013	0.003	-0.409	.684
Orientation	0.0880	0.015	5.875	< .001*
Task	0.0325	0.072	0.452	.653
Lower vis field	0.0039	0.015	0.262	.794
Eccentricity*Task	-0.0003	0.004	-0.074	.941
P7 Gain	β	SE	F	*p*
Intercept	0.0651	0.040	1.638	.105
Eccentricity	-0.0007	0.002	-0.310	.758
Orientation	-0.0365	0.011	-3.189	.002*
Task	0.1782	0.055	3.237	.002*
Lower vis field	0.0012	0.011	0.109	.913
Eccentricity*Task	-0.0080	0.003	-2.372	.020*
P8 Gain	β	SE	F	*p*
Intercept	0.1140	0.073	1.571	.120
Eccentricity	-0.0050	0.004	-1.156	.251
Orientation	0.0022	0.021	0.106	.916
Task	0.2110	0.101	2.099	.039*
Lower vis field	0.0104	0.021	0.498	.620
Eccentricity*Task	-0.0066	0.006	-1.072	.286
P9 Gain	β	SE	F	*p*
Intercept	0.0090	0.039	0.230	.818
Eccentricity	0.0001	0.002	0.036	.971
Orientation	0.0332	0.011	2.932	.004*
Task	0.1892	0.054	3.485	< .001*
Lower vis field	0.0063	0.011	0.557	.579
Eccentricity*Task	-0.0036	0.003	-1.076	.284

Note: 'Orientation' used horizontal motion as a reference level.

Table AC.3

Results of linear regression analysis to predict the gain of non-foveal OKR (>4 deg eccentricity) based on four predictor variables (eccentricity, task condition, orientation of motion, upper versus lower visual field)

P1 Gain	β	SE	F	*p*
Intercept	0.4227	0.040	10.526	< .001*
Eccentricity	-0.0212	0.003	-7.558	< .001*
Orientation	0.1299	0.022	5.957	< .001*
Task	-0.0038	0.052	-0.072	.943
Lower vis field	0.0107	0.022	0.492	.623
Eccentricity*Task	0.0025	0.004	0.641	.522
P2 Gain	β	SE	F	*p*
Intercept	0.1993	0.025	7.958	< .001*
Eccentricity	-0.0070	0.002	-4.009	< .001*
Orientation	0.0304	0.014	2.236	.027*
Task	0.2405	0.033	0.736	.463
Lower vis field	0.0187	0.014	1.379	.170
Eccentricity*Task	0.0014	0.002	0.585	.559
P3 Gain	β	SE	F	*p*
Intercept	0.2256	0.018	12.614	< .001*
Eccentricity	-0.0098	0.001	-7.831	< .001*
Orientation	0.0210	0.010	2.164	.032*
Task	0.0584	0.023	2.500	.013*
Lower vis field	-0.0160	0.010	-1.648	.101
Eccentricity*Task	0.0029	0.002	1.667	.098
P4 Gain	β	SE	F	*p*
Intercept	0.2536	0.019	13.445	< .001*
Eccentricity	-0.0123	0.001	-9.380	< .001*
Orientation	0.0006	0.010	0.056	.956
Task	0.0487	0.025	1.979	.049*
Lower vis field	0.0156	0.010	1.523	.130
Eccentricity*Task	0.0044	0.002	2.362	.019*
P5 Gain	β	SE	F	*p*
Intercept	0.2010	0.022	8.945	< .001*
Eccentricity	-0.0092	0.002	-5.888	< .001*
Orientation	-0.0011	0.012	-0.090	.928
Task	0.0335	0.029	1.141	.256
Lower vis field	0.0186	0.012	1.525	.129
Eccentricity*Task	0.0046	0.002	2.070	.040*
P6 Gain	β	SE	F	*p*
Intercept	0.1575	0.024	6.659	< .001*
Eccentricity	-0.0053	0.002	-3.229	.002*
Orientation	0.0927	0.013	7.220	< .001*
Task	0.0540	0.031	1.749	.082
Lower vis field	0.0197	0.013	1.534	.127
Eccentricity*Task	-0.0017	0.002	-0.709	.479
P7 Gain	β	SE	F	*p*
Intercept	0.2191	0.022	10.140	< .001*
Eccentricity	-0.0101	0.002	-6.717	< .001*
Orientation	-0.0161	0.012	-1.374	.171
Task	0.1266	0.028	4.488	< .001*
Lower vis field	-0.0165	0.012	-1.405	.162
Eccentricity*Task	-0.0049	0.002	-2.302	.023*
P8 Gain	β	SE	F	*p*
Intercept	0.3096	0.029	10.607	< .001*
Eccentricity	-0.0171	0.002	-8.414	< .001*
Orientation	0.0340	0.016	2.147	.033*
Task	0.0818	0.038	2.147	.033*
Lower vis field	-0.0081	0.016	-0.511	.610
Eccentricity*Task	0.0012	0.003	0.411	.682
P9 Gain	β	SE	F	*p*
Intercept	0.1630	0.019	8.744	< .001*
Eccentricity	-0.0085	0.001	-6.510	< .001*
Orientation	0.0174	0.010	1.721	.087
Task	0.0594	0.024	2.441	.016*
Lower vis field	-0.0002	0.010	-0.020	.984
Eccentricity*Task	0.0041	0.002	2.235	.027*

Note: 'Orientation' used horizontal motion as a reference level.

Table AC.4

Results of linear regression analysis to predict the gain, frequency and amplitude of non-foveal OKR up to 10 deg eccentricity in P1

P1 Gain	β	SE	F	*p*
Intercept	0.5633	0.088	6.367	< .001*
Eccentricity	-0.0472	0.012	-4.343	< .001*
Orientation	0.1433	0.051	2.805	.007*
Task	0.0070	0.051	0.138	.891
Ver/Hor Meridian	0.2141	0.013	1.711	.093
Eccentricity*Ver/Hor m.	-0.0365	0.016	-2.216	.031*
Orientation*Ver/Hor m.	0.1216	0.072	1.683	.098
Task* Ver/Hor m.	0.0260	0.072	0.361	.720
P1 Frequency	β	SE	F	*p*
Intercept	4.5783	0.334	13.723	< .001*
Eccentricity	-0.3403	0.041	-8.307	< .001*
Orientation	0.3375	0.193	1.752	.085
Task	0.0125	0.193	0.065	.948
Ver/Hor Meridian	-0.1783	0.472	-0.378	.707
Eccentricity*Ver/Hor m.	0.0375	0.062	0.604	.548
Orientation*Ver/Hor m.	-0.0813	0.272	-0.298	.767
Task* Ver/Hor m.	-0.0063	0.272	-0.023	.982
P1 Amplitude	β	SE	F	*p*
Intercept	2.2748	0.245	9.281	< .001*
Eccentricity	-0.2194	0.030	-7.293	< .001*
Orientation	0.1727	0.142	1.221	.227
Task	0.0141	0.142	0.099	.921
Ver/Hor Meridian	0.6304	0.347	1.812	.074
Eccentricity*Ver/Hor m.	-0.1301	0.046	-2.853	.006*
Orientation*Ver/Hor m.	0.4281	0.200	2.139	.037*
Task* Ver/Hor m.	0.1527	0.200	0.763	.448

Table AC.5

Results of linear regression analysis to predict the gain, frequency and amplitude of non-foveal OKR up to 10 deg eccentricity in P2

P2 Gain (non-sig)	β	SE	F	*p*
Intercept	0.2032	0.039	5.266	< .001*
Eccentricity	-0.0052	0.005	-1.098	.277
Orientation	0.0518	0.022	2.325	.024*
Task	0.0125	0.022	0.562	.576
Ver/Hor Meridian	0.0023	0.055	0.043	.966
Eccentricity*Ver/Hor m.	0.0032	0.007	0.449	.655
Orientation*Ver/Hor m.	-0.0145	0.032	-0.461	.646
Task* Ver/Hor m.	-0.0011	0.032	-0.036	.971
P2 Frequency	β	SE	F	*p*
Intercept	2.8032	0.455	6.155	< .001*
Eccentricity	-0.1515	0.056	-2.710	.009*
Orientation	-0.1625	0.263	-0.618	.539
Task	-0.4125	0.263	-1.569	.122
Ver/Hor Meridian	-0.4220	0.644	-0.655	.515
Eccentricity*Ver/Hor m.	-0.0082	0.085	-0.096	.923
Orientation*Ver/Hor m.	0.3344	0.372	0.899	.372
Task* Ver/Hor m.	0.2344	0.372	0.630	.531
P2 Amplitude	β	SE	F	*p*
Intercept	0.3682	0.126	2.921	.005*
Eccentricity	-0.0269	0.015	-1.737	.088
Orientation	0.2433	0.073	3.343	.001*
Task	0.3405	0.073	4.679	< .001*
Ver/Hor Meridian	0.2004	0.178	1.124	.266
Eccentricity*Ver/Hor m.	-0.0060	0.023	-0.257	.798
Orientation*Ver/Hor m.	-0.1213	0.103	-1.179	.243
Task* Ver/Hor m.	-0.0458	0.103	-0.445	.658

Table AC.6

Results of linear regression analysis to predict the gain, frequency and amplitude of non-foveal OKR up to 10 deg eccentricity in P3

P3 Gain	β	SE	F	*p*
Intercept	0.2594	0.043	6.082	< .001*
Eccentricity	-0.0157	0.005	-3.005	.004*
Orientation	0.0134	0.025	0.545	.588
Task	0.0772	0.025	3.136	.003*
Ver/Hor Meridian	-0.0141	0.060	-0.233	.817
Eccentricity*Ver/Hor m.	0.0041	0.008	0.522	.604
Orientation*Ver/Hor m.	0.0224	0.035	0.644	.522
Task* Ver/Hor m.	-0.0048	0.035	-0.137	.892
P3 Frequency	β	SE	F	*p*
Intercept	1.9031	0.290	6.559	< .001*
Eccentricity	-0.1077	0.036	-3.022	.004*
Orientation	-0.0563	0.168	-0.336	.738
Task	0.1438	0.168	0.858	.394
Ver/Hor Meridian	-0.4625	0.410	-1.127	.264
Eccentricity*Ver/Hor m.	0.0638	0.054	1.181	.243
Orientation*Ver/Hor m.	0.2875	0.237	1.214	.230
Task* Ver/Hor m.	0.0938	0.237	0.396	.694
P3 Amplitude	β	SE	F	*p*
Intercept	1.2406	0.314	3.955	< .001*
Eccentricity	-0.0914	0.039	-2.373	.021*
Orientation	0.0018	0.181	0.010	.992
Task	0.7578	0.181	4.184	< .001*
Ver/Hor Meridian	0.0760	0.444	0.171	.864
Eccentricity*Ver/Hor m.	0.0074	0.058	0.127	.899
Orientation*Ver/Hor m.	-0.0709	0.256	-0.277	.783
Task* Ver/Hor m.	-0.0706	0.256	-0.276	.784

Table AC.7

Results of linear regression analysis to predict the gain, frequency and amplitude of non-foveal OKR up to 10 deg eccentricity in P4

P4 Gain	β	SE	F	*p*
Intercept	0.2912	0.041	7.084	< .001*
Eccentricity	-0.0179	0.005	-3.547	< .001*
Orientation	-0.0086	0.024	-0.364	.717
Task	0.0796	0.024	3.354	.001*
Ver/Hor Meridian	0.0774	0.058	1.332	.188
Eccentricity*Ver/Hor m.	-0.0105	0.008	-1.379	.173
Orientation*Ver/Hor m.	0.0637	0.034	1.897	.063
Task* Ver/Hor m.	-0.0044	0.034	-0.131	.896
P4 Frequency	β	SE	F	*p*
Intercept	3.4657	0.538	6.447	< .001*
Eccentricity	-0.1728	0.066	-2.618	.011*
Orientation	-0.9000	0.310	-2.900	.005*
Task	0.8250	0.310	2.658	.010*
Ver/Hor Meridian	0.7531	0.760	0.991	.326
Eccentricity*Ver/Hor m.	-0.1845	0.100	-1.844	.070
Orientation*Ver/Hor m.	1.3063	0.439	2.976	.004*
Task* Ver/Hor m.	0.0688	0.439	0.157	.876
P4 Amplitude	β	SE	F	*p*
Intercept	0.7010	0.084	8.321	< .001*
Eccentricity	-0.0562	0.010	-5.431	< .001*
Orientation	-0.0153	0.049	-0.314	.754
Task	0.2592	0.049	5.329	< .001*
Ver/Hor Meridian	0.3096	0.119	2.599	.012*
Eccentricity*Ver/Hor m.	-0.0466	0.016	-2.971	.004*
Orientation*Ver/Hor m.	0.1074	0.069	1.561	.124
Task* Ver/Hor m.	0.0596	0.069	0.866	.390

Table AC.8

Results of linear regression analysis to predict the gain, frequency and amplitude of non-foveal OKR up to 10 deg eccentricity in P5

P5 Gain	β	SE	F	*p*
Intercept	0.3133	0.052	5.995	< .001*
Eccentricity	-0.0245	0.006	-3.818	< .001*
Orientation	0.0205	0.030	0.678	.500
Task	0.0625	0.030	2.071	.043*
Ver/Hor Meridian	0.1103	0.074	1.492	.141
Eccentricity*Ver/Hor m.	-0.0122	0.010	-1.255	.215
Orientation*Ver/Hor m.	0.0154	0.043	0.362	.719
Task* Ver/Hor m.	-0.0413	0.043	-0.967	.338
P5 Frequency	β	SE	F	*p*
Intercept	1.5000	0.256	5.871	< .001*
Eccentricity	-0.1176	0.031	-3.749	< .001*
Orientation	-0.2345	0.148	-1.589	.118
Task	0.4094	0.148	2.775	.007*
Ver/Hor Meridian	0.8875	0.361	2.456	.017*
Eccentricity*Ver/Hor m.	-0.0898	0.048	-1.888	.064
Orientation*Ver/Hor m.	0.0094	0.209	0.045	.964
Task* Ver/Hor m.	-0.3281	0.209	-1.573	.121
P5 Amplitude	β	SE	F	*p*
Intercept	1.0157	0.182	5.567	< .001*
Eccentricity	-0.0845	0.022	-3.771	< .001*
Orientation	0.0193	0.105	0.184	.855
Task	0.2572	0.105	2.442	.017*
Ver/Hor Meridian	0.8666	0.258	3.358	.001*
Eccentricity*Ver/Hor m.	-0.0930	0.034	-2.739	.008*
Orientation*Ver/Hor m.	-0.0874	0.149	-0.587	.560
Task* Ver/Hor m.	-0.1118	0.149	-0.750	.456

Table AC.9

Results of linear regression analysis to predict the gain, frequency and amplitude of non-foveal OKR up to 10 deg eccentricity in P6

P6 Gain	β	SE	F	*p*
Intercept	0.2459	0.055	4.493	< .001*
Eccentricity	-0.0174	0.007	-2.586	.012*
Orientation	0.0798	0.032	2.526	.014*
Task	0.0657	0.032	2.079	.042*
Ver/Hor Meridian	0.0795	0.077	1.027	.309
Eccentricity*Ver/Hor m.	-0.0156	0.010	-1.532	.131
Orientation*Ver/Hor m.	0.0627	0.045	1.403	.166
Task* Ver/Hor m.	0.0048	0.045	0.106	.916
P6 Frequency	β	SE	F	*p*
Intercept	1.0188	0.491	2.076	.043*
Eccentricity	-0.0153	0.060	-0.254	.801
Orientation	0.7156	0.283	2.525	.014*
Task	0.6531	0.283	2.305	.025*
Ver/Hor Meridian	0.6562	0.694	0.945	.349
Eccentricity*Ver/Hor m.	-0.0801	0.091	-0.877	.384
Orientation*Ver/Hor m.	0.0906	0.401	0.226	.822
Task* Ver/Hor m.	-0.1781	0.401	-0.444	.658
P6 Amplitude	β	SE	F	*p*
Intercept	1.4921	0.250	5.960	< .001*
Eccentricity	-0.1215	0.031	-3.953	< .001*
Orientation	0.0724	0.145	0.501	.618
Task	0.1765	0.145	1.221	.227
Ver/Hor Meridian	0.2429	0.354	0.686	.496
Eccentricity*Ver/Hor m.	-0.0576	0.047	-1.237	.221
Orientation*Ver/Hor m.	0.2441	0.204	1.194	.237
Task* Ver/Hor m.	-0.0003	0.204	-0.002	.999

Table AC.10

Results of linear regression analysis to predict the gain, frequency and amplitude of non-foveal OKR up to 10 deg eccentricity in P7

P7 Gain	β	SE	F	*p*
Intercept	0.4454	0.050	8.962	< .001*
Eccentricity	-0.0434	0.006	-7.113	< .001*
Orientation	0.0042	0.029	0.145	.885
Task	0.0977	0.029	3.404	.001*
Ver/Hor Meridian	-0.0095	0.070	-0.136	.892
Eccentricity*Ver/Hor m.	0.0021	0.009	0.228	.821
Orientation*Ver/Hor m.	-0.0217	0.041	-0.534	.595
Task* Ver/Hor m.	0.0011	0.041	0.028	.978
P7 Frequency	β	SE	F	*p*
Intercept	2.0969	0.281	7.455	< .001*
Eccentricity	-0.1608	0.035	-4.657	< .001*
Orientation	-0.5625	0.162	-3.464	.001*
Task	0.3187	0.162	1.963	.055
Ver/Hor Meridian	0.3281	0.398	0.825	.413
Eccentricity*Ver/Hor m.	-0.0549	0.052	-1.049	.299
Orientation*Ver/Hor m.	0.2406	0.230	1.048	.299
Task* Ver/Hor m.	-0.02188	0.230	-0.095	.924
P7 Amplitude	β	SE	F	*p*
Intercept	1.7892	0.250	7.152	< .001*
Eccentricity	-0.1693	0.031	-5.513	< .001*
Orientation	-0.1183	0.144	-0.819	.416
Task	0.3258	0.144	2.256	.028*
Ver/Hor Meridian	0.2456	0.354	0.694	.490
Eccentricity*Ver/Hor m.	0.0051	0.047	0.110	.913
Orientation*Ver/Hor m.	-0.3811	0.204	-1.866	.067
Task* Ver/Hor m.	0.1663	0.204	0.184	.419

Table AC.11

Results of linear regression analysis to predict the gain, frequency and amplitude of non-foveal OKR up to 10 deg eccentricity in P8

P8 Gain	β	SE	F	*p*
Intercept	0.3644	0.055	6.587	< .001*
Eccentricity	-0.0266	0.007	-3.919	< .001*
Orientation	0.0219	0.032	0.687	.495
Task	0.0737	0.032	2.308	.025*
Ver/Hor Meridian	0.0302	0.078	0.386	.701
Eccentricity*Ver/Hor m.	-0.0050	0.010	-0.484	.630
Orientation*Ver/Hor m.	0.0757	0.045	1.677	.099
Task* Ver/Hor m.	0.0028	0.045	0.061	.951
P8 Frequency	β	SE	F	*p*
Intercept	2.0095	0.294	6.826	< .001*
Eccentricity	-0.1024	0.036	-2.832	.006*
Orientation	-0.4688	0.170	-2.760	.008*
Task	0.3813	0.170	2.243	.029*
Ver/Hor Meridian	0.2749	0.416	0.660	.512
Eccentricity*Ver/Hor m.	-0.0604	0.055	-1.102	.275
Orientation*Ver/Hor m.	0.0781	0.240	0.325	.746
Task* Ver/Hor m.	-0.0406	0.240	-0.169	.866
P8 Amplitude	β	SE	F	*p*
Intercept	1.1153	0.178	6.258	< .001*
Eccentricity	-0.1055	0.022	-4.823	< .001*
Orientation	0.0756	0.103	0.735	.465
Task	0.4041	0.103	3.927	< .001*
Ver/Hor Meridian	0.8908	0.252	3.534	< .001*
Eccentricity*Ver/Hor m.	-0.1031	0.033	-3.110	.003*
Orientation*Ver/Hor m.	-0.0661	0.146	-0.454	.651
Task* Ver/Hor m.	-0.0029	0.146	-0.020	.984

Table AC.12

Results of linear regression analysis to predict the gain, frequency and amplitude of non-foveal OKR up to 10 deg eccentricity in P9

P9 Gain	β	SE	F	*p*
Intercept	0.2845	0.039	7.247	< .001*
Eccentricity	-0.0244	0.005	-5.061	< .001*
Orientation	-0.0148	0.023	-0.654	.516
Task	0.0805	0.023	3.550	< .001*
Ver/Hor Meridian	-0.0196	0.056	-0.353	.725
Eccentricity*Ver/Hor m.	0.0016	0.007	0.222	.825
Orientation*Ver/Hor m.	0.0264	0.032	0.824	.413
Task* Ver/Hor m.	0.0053	0.032	0.166	.869
P9 Frequency	β	SE	F	*p*
Intercept	2.6938	0.266	10.137	< .001*
Eccentricity	-0.2366	0.033	-7.251	< .001*
Orientation	-0.3313	0.153	-2.159	.035*
Task	0.4875	0.153	3.177	.002*
Ver/Hor Meridian	-0.1188	0.376	-0.316	.753
Eccentricity*Ver/Hor m.	-0.0192	0.049	-0.389	.699
Orientation*Ver/Hor m.	0.4438	0.217	2.045	.046*
Task* Ver/Hor m.	0.1063	0.217	0.490	.626
P9 Amplitude	β	SE	F	*p*
Intercept	0.9602	0.130	7.385	< .001*
Eccentricity	-0.0927	0.016	-5.809	< .001*
Orientation	-0.1436	0.075	-1.913	.061
Task	0.3932	0.075	5.238	< .001*
Ver/Hor Meridian	-0.2329	0.184	-1.266	.211
Eccentricity*Ver/Hor m.	0.0275	0.024	1.136	.261
Orientation*Ver/Hor m.	0.0537	0.106	0.506	.615
Task* Ver/Hor m.	0.0122	0.106	0.115	.909